17639

NATIONAL LIBRARY
OTTAWA

CANADA

BIBLIOTHÈQUE NATIONALE
OTTAWA

NAME OF AUTHOR....JOHN FREDERICK NIXON

TITLE OF THESIS....THE CONSOLIDATION OF
.....THAWING SOILS.............
....

UNIVERSITY.......UNIVERSITY OF ALBERTA

DEGREE FOR WHICH THESIS WAS PRESENTED....PhD.............

YEAR THIS DEGREE GRANTED......1973.....................

Permission is hereby granted to THE NATIONAL LIBRARY OF CANADA to microfilm this thesis and to lend or sell copies of the film.

The author reserves other publication rights, and neither the thesis nor extensive extracts from it may be printed or otherwise reproduced without the author's written permission.

(Signed).....John F. Nixon

PERMANENT ADDRESS:

...DEPT. CIVIL ENGINEERING
..UNIVERSITY of ALBERTA
....EDMONTON, ALTA

DATED May 28........1973

NL-91 (10-68)

THE UNIVERSITY OF ALBERTA

THE CONSOLIDATION OF THAWING SOILS

by

©

JOHN FREDERICK NIXON

A THESIS
SUBMITTED TO THE FACULTY OF GRADUATE STUDIES
AND RESEARCH IN PARTIAL FULFILMENT OF THE
REQUIREMENTS FOR THE DEGREE OF
DOCTOR OF PHILOSOPHY

DEPARTMENT OF CIVIL ENGINEERING
EDMONTON, ALBERTA
FALL, 1973

THE UNIVERSITY OF ALBERTA

FACULTY OF GRADUATE STUDIES AND RESEARCH

The undersigned certify that they have read, and recommend to the Faculty of Graduate Studies and Research for acceptance, a thesis entitled "THE CONSOLIDATION OF THAWING SOILS" submitted by John Frederick Nixon in partial fulfilment of the requirements for the degree of Doctor of Philosophy in Civil Engineering.

N. R. Morgenstern, Supervisor

Z. Eisenstein

S Thomson
S. Thomson

G S H Lock
G. Lock

K. Anderson

G A Leonards
G. Leonards, External Examiner

Date: 22/5/73

ABSTRACT

When the thermal regime of permafrost is altered, melting of the frozen ground may be induced. Many civil engineering problems are concerned with the stability and deformation of such thawing soils. Some available solutions to the heat transfer problem are reviewed, which facilitate the calculation of the rate of melting. The physics of consolidation for thawing soils are formulated in terms of known equations for heat transfer and for linear consolidation. A moving boundary consolidation problem results, and analytical solutions are obtained for several cases of practical interest. The results are presented as normalised pore pressure distributions and settlement ratios, and it is demonstrated that both the pore pressures and settlements depend primarily on the thaw-consolidation ratio R.

An apparatus was fabricated to simulate the required stress and thermal conditions in the thawing soil. Samples of natural and reconstituted frozen soils were tested to determine the validity of the theoretical predictions, and extremely encouraging results were obtained. The concept of the residual stress is introduced, and its importance in thaw-consolidation and the undrained thaw strength is discussed.

The versatility of the theory is greatly increased by considering several theoretical extensions which permit the analysis of a wide range of practical problems. In particular, solutions for arbitrary movement of the thaw plane are obtained numerically, and some non-linear constitutive relationships for the soil skeleton are incorporated in the theory. The use of vertical sand drains for improving the conditions in a thawing foundation is discussed, and a typical case is analysed.

The excess pore pressures, settlements and rate of thaw in the foundation of a hot oil pipeline at Inuvik, N.W.T., are analysed within the context of the thaw-consolidation theory. Excellent agreement is obtained between theoretical predictions and the observed behaviour in this case study.

ACKNOWLEDGEMENTS

The research described in this thesis was carried out in the Civil Engineering Department, University of Alberta under the supervision of Professor N. R. Morgenstern. The author is deeply indebted to Professor Morgenstern for suggesting the topic and for his continued encouragement and enthusiastic discussion during the course of the work.

The many discussions with Dr. S. Thomson are greatly appreciated. The author wishes also to express his gratitude to his colleagues Dr. P. K. Chatterji and Mr. W. D. Roggensack for their many helpful discussions.

Research work carried out in the laboratory by Mr. Bruce Smith provided considerable stimulus at an early stage in this research, and the author is sincerely grateful to him for his assistance.

Many critical discussions with Mr. Ed. McRoberts have provided useful ideas concerning this research, and the assistance received in the preparation of Chapter 2 is particularly appreciated.

The author is grateful to Mr. D. Fielder of Canadian Gas Arctic Systems Ltd., and to Messrs. D. Hayley and L. B. Smith of E. W. Brooker and Associates Ltd., for the provision of permafrost samples.

Discussions with Dr. G. Watson of Mackenzie Valley Pipeline Research Ltd., concerning the Inuvik test pipeline installation are sincerely appreciated.

The financial assistance provided by the National Research Council of Canada and the University of Alberta is gratefully acknowledged.

Finally, the author wishes to acknowledge the support of his wife Sandie, whose Irish sense of humour helped on many occasions, and who did a magnificent job of typing the text.

TABLE OF CONTENTS

Page

Release Form (i)

Title Page (ii)

Approval Sheet (iii)

Abstract (iv)

Acknowledgements (vi)

Table of Contents (vii)

List of Tables (xii)

List of Figures (xiii)

CHAPTER I INTRODUCTION

1.1 Permafrost and associated geotechnical problems 1

1.2 Scope of the thesis 4

1.3 Review of the geotechnical literature concerning thawing soils 4

CHAPTER II THE ONE-DIMENSIONAL THAWING OF FROZEN SOILS

2.1 The thawing of a homogeneous soil subjected to a step increase in surface temperature 10

2.2 The thermal properties of soils 19

2.3 The temperature and phase dependence of thermal properties 32

2.4 The effect of thaw strain on the Neumann solution 41

2.5 The effect of water migration on the Neumann solution 46

TABLE OF CONTENTS (continued)

Page

CHAPTER II (continued)

2.6 Time dependent surface temperature 52

2.7 Thawing in a two layer profile 57

2.8 Thawing around a warm pipe in permafrost 61

CHAPTER III THE ONE-DIMENSIONAL CONSOLIDATION OF THAWING SOILS

3.1 Introduction 66

3.2 Formulation of the linear theory of thaw-consolidation 67

3.3 Solution of the linear equation of thaw-consolidation 73

3.4 Results of solution 85

3.5 Post-thawing conditions 92

3.6 Discussion and application of solution 99

CHAPTER IV LABORATORY TESTING OF THAWING SOILS

4.1 Thaw consolidation tests on remoulded soils 104

4.2 The design of an improved thaw-consolidation apparatus 108

4.3 Thaw-consolidation tests on undisturbed permafrost samples 111

4.4 The residual stress in thawed soil 123

4.5 The measurement of residual stress 129

4.6 Interpretation of laboratory test results 142

CHAPTER V EXTENSIONS TO THE THEORY OF CONSOLIDATION FOR THAWING SOILS

5.1 Introduction 151

5.2 Arbitrary movement of the thaw interface 152

TABLE OF CONTENTS (continued)

Page

CHAPTER V (Continued)

5.3 The non-linearity of the stress-strain relationship for the soil skeleton 163

5.4 Influence of a non-linear effective stress-strain relation 166

5.5 The thawing of ice-rich incompressible soils 176

5.6 The consolidation of a thawing soil with a layered profile 183

5.7 The analysis of a compressible soil with discrete ice lenses 192

CHAPTER VI ANALYSIS OF FIELD PROBLEMS

6.1 Introduction 208

6.2 Thawing under a hot pipeline 208

6.3 Thaw-consolidation with vertical sand-drains 213

6.4 Analysis of the performance of a hot oil test pipeline at Inuvik, N.W.T. 223

CHAPTER VII CONCLUDING REMARKS 250

LIST OF REFERENCES 253

APPENDIX A DETAILS OF FINITE DIFFERENCE PROCEDURES AND PROGRAM LISTINGS

A.1 Finite difference procedure for the one-dimensional thawing of soils 257

A.2 Program listing for one-dimensional heat conduction 259

A.3 Finite difference procedure for thaw-consolidation with arbitrary movement of the thaw plane 260

TABLE OF CONTENTS (continued)

Page

APPENDIX A (Continued)

A.4 Program listing for thaw-consolidation with arbitrary movement of the thaw plane 267

A.5 Numerical solution for thaw-consolidation in a two layer profile 269

A.6 Program listing for thaw-consolidation in a two layer profile 276

A.7 Finite difference scheme for thaw-consolidation with sand-drains 278

A.8 Program listing for thaw-consolidation with sand-drains 284

APPENDIX B LABORATORY RESULTS FOR THAW CONSOLIDATION TESTS 290

LIST OF TABLES

Table		Page
2.1	Hierarchy of solution methods	17
2.2	Comparison of one and two-dimensional calculations for thaw depth under a 48 inch hot pipe	65
4.1	Summary of soil properties	114
4.2	Summary of observations from thaw-consolidation tests	116
4.3	Laboratory results for residual stresses in undisturbed samples	141
6.1	Predicted and observed thaw penetration	229
6.2	Final effective stresses	231
6.3	Analysis of piezometer data	233
6.4	Observed and predicted settlements	239
6.5	Summary of data from pore pressure and settlement readings	243
6.6	Laboratory data for Inuvik clayey silt	244

LIST OF FIGURES

Figure		Page
2.1	The Neumann problem	12
2.2	Graphical solution of the Neumann equation	15
2.3	Solution of the Neumann equation with $T_g = 0$	18
2.4	Variation of α with ground temperature T_g	21
2.5	Thermal conductivity of fine grained soils	23
2.6	Variation of α with frozen conductivity k_f	24
2.7	Volumetric heat capacity of soils	29
2.8	Thermal diffusivity of fine-grained soils	30
2.9	Volumetric latent heats of soils	31
2.10	Unfrozen moisture content curves for numerical analysis	37
2.11	Effect of unfrozen moisture content curve on depth of thaw	38
2.12	Effect of unfrozen moisture content curve on temperature profile	39
2.13	Effect of melt water migration on normalised thaw rate	51
2.14	Thawing in a two-layer system	58
2.15	Thaw depth below pipe axis fitted to $X = Bt^{0.3}$	63
3.1	One-dimensional thaw-consolidation	68
3.2	Excess pore pressures for the applied loading condition, $W_r = 0$	87
3.3	Excess pore pressures for the self-weight loading condition, $W_r = \infty$	88
3.4	Variation of hydraulic gradient with R, $W_r = \infty$	89
3.5	Variation of S_t/S_{max} with R	90

LIST OF FIGURES (Continued)

Figure		Page
3.6	Excess pore pressures at the thaw front plotted against R	91
3.7	Excess pore pressure isochrones after completion of thawing, $W_r = \infty$	95
3.8	Base pore pressures after completion of thawing, $W_r = 0$	97
3.9	Degree of settlement after completion of thawing	98
4.1	Observed and predicted pore pressures and settlements for remoulded soils	106
4.2	Modified design of thaw-consolidation apparatus	110
4.3	Plan view of two samples of Noell Lake clay	113
4.4	Observed and predicted pore pressures for undisturbed permafrost	119
4.5	Observed and predicted settlement ratios for undisturbed permafrost	120
4.6	Thaw strains for undisturbed permafrost	122
4.7	Observed and predicted rates of thawing for undisturbed permafrost	124
4.8	Stress path in a closed system freeze-thaw cycle (schematic)	126
4.9	Apparatus for measurement of residual stress	131
4.10	The measurement of residual stress for reconstituted Athabasca clay	134
4.11	e versus σ_0' for reconstituted Athabasca clay	136
4.12	The measurement of residual stress for reconstituted Mountain River clay	138
4.13	e versus σ_0' for reconstituted Mountain River clay	139
4.14	Residual stresses for undisturbed Norman Wells silt	140
4.15	Variation of residual stresses with depth	143
4.16	Coefficient of consolidation with depth	144

LIST OF FIGURES (continued)

Figure		Page
4.17	Pore pressures in ice-rich samples interpreted using non-linear theory	148
5.1	Excess pore pressures at the thaw line	155
5.2	Excess pore pressures at the thaw line	155
5.3	Degree of settlement	156
5.4	Degree of settlement	156
5.5	Rate of thawing for sinusoidal surface temperature	160
5.6	Excess pore pressures for a sinusoidal surface temperature	161
5.7	Different void ratio - effective stress relationships	165
5.8	Pore pressures at the thaw line for non-linear theory	173
5.9	e - σ' curve on natural and logarithmic scales	175
5.10	Pore pressures from incompressible analysis	181
5.11	Thaw-consolidation in a two-layer profile	184
5.12	Excess pore pressures for 'silt over clay'	188
5.13	Excess pore pressures for 'clay over silt'	188
5.14	Excess pore pressures for 'peat over clay'	191
5.15	Thawing in a soil-ice profile	195
5.16	Pore pressures at a soil-ice interface	201
5.17	Sample solution for pore pressures at a soil-ice interface	206
6.1	Thawing under the centre-line of a hot pipeline (after Lachenbruch, 1970)	210
6.2	Pore pressures and settlements under the centre line of a hot pipeline	212
6.3	Thaw-consolidation with vertical sand-drains	215
6.4	Excess pore pressures at the effective radius	220

LIST OF FIGURES (Continued)

Figure		Page
6.5	Surface settlement profiles around a sand drain	220
6.6	Optimised use of sand drains in a thawing foundation	222
6.7	Configuration of the Inuvik test facility	224
6.8	Estimated latent heat with depth	227
6.9	Predicted and observed thawing at Inuvik	230
6.10	Final effective stresses	232
6.11	Settlement records in the thawing foundation	232
6.12	Observed and calculated transient settlements	241
6.13	Laboratory results for Inuvik clayey silt	246
6.14	Permeability calculated from observed pore pressures and settlements	247
A.1	Finite difference grid at the interface between two soil layers	
B.1-B.10	Laboratory results for thaw-consolidation tests	291-300

CHAPTER I

INTRODUCTION

1.1 Permafrost and Associated Geotechnical Problems.

Approximately one half of Canada is underlain by permafrost. Permafrost is more correctly termed "perennially frozen ground", and by definition refers to ground that remains frozen for more than one complete year. The thickness of permafrost may vary from a few feet at the southern boundary to greater than two thousand feet in the far north. The extent and many of the surface features associated with permafrost are described in detail by Brown (1970).

The delicate thermal equilibrium of permafrost is particularly sensitive to any natural or man-made changes in environmental conditions. The rate of construction of buildings, transportation and storage facilities necessary for the development of the north and the exploitation of its resources is increasing continually.

The problems in soil mechanics likely to be encountered in the Arctic are usefully subdivided into two sections, those involving a change of state, and those where no change of state takes place. The latter class of problems involves soil which remains continuously frozen or thawed. For geotechnical problems involving thawed soil, the conventional and well-established principles of soil mechanics are applicable.

If the region of soil under consideration is continuously frozen, the principal engineering problems are involved with the significant time-dependent deformation of frozen soils under constant stress. An engineering theory of creep for frozen soils has been established by Vialov (1963) and by Ladanyi (1972), based on a collection of rheological laws which are found to describe adequately the observed manifestations of creep at least in the laboratory. The theory as it presently stands seems perfectly capable of solving some specific soil engineering problems such as the bearing capacity of buried footings and anchors.

More dramatic problems arise when the geotechnical engineer is confronted with a soil whose water phase is actively freezing or thawing. Examples of soil freezing may be seen in frost penetration under highways, the long-term aggradation of permafrost, the annual freeze-back of the active layer, and in the freezing of soil around chilled pipes or cold gas pipelines. It is known that most saturated soils under low stresses exhibit an affinity for water during freezing, and the formation of lenses and layers of ice may occur. Coarse-grained soils under large stresses may also expel water on freezing if drainage is permitted (Mackay, 1971). If ice lensing is inhibited, substantial heaving pressures can result, or conversely, if the overburden stress at the frost plane is high enough, the growth of segregated ice is impeded. In reviewing the geotechnical properties of freezing ground, Anderson and Morgenstern (1973) have stated that ice lensing results when a soil has the ability to supply water to an active ice front for a sufficiently long time to grow an ice lens. The particle size of the soil influences the water flow to the ice front partly through its effect on the permeability of the unfrozen soil, and perhaps more importantly, by influencing the maximum stress difference that can be supported at the ice-water interface. This maximum stress difference is defined as the difference between the total and pore water stresses at the freezing plane, and has been the subject of much research, e.g. Williams (1966), Penner (1967).

The problems involving freezing soils might present themselves in two ways. If ice lensing occurs at low stress levels, and remains unrestrained, then serious deformations may occur in structures such as highways or chilled gas pipelines. On thawing of fine-grained soils containing segregated ice structures, serious stability and settlement problems may arise. If on the other hand, the ice lens growth is restrained during freezing, severe heaving pressures may arise which could cause damage to engineering structures.

Finally, of the important problems confronting the geotechnical engineer in the Arctic at the present time, probably the most common and potentially serious are those involving the thawing of frozen soil. Adverse conditions may disturb the delicate thermal equilibrium of permafrost sufficiently to induce melting. Examples of this are the burning or stripping of vegetation, the impounding of a reservoir, the construction of heated buildings or the thermal erosion adjacent to northern rivers. An extreme case of the melting of permafrost has been shown to exist around a hot oil pipeline buried in permafrost (Lachenbruch, 1970).

Severe conditions might be anticipated in a thawing foundation if the soil is rich in ice, or the soil is fine-grained and the rate of degradation is rapid.

1.2 Scope of the Thesis

In more northerly locations, the engineer is principally concerned with ground that is initially frozen (permafrost) and which is in danger of thawing. Thus, an analysis involving the stability and deformation of thawing soil appears to have the highest priority for the geotechnical engineer who is working in an Arctic area.

The analysis of deformation under stress, and the stability of the thawing soil against shear failure are both known to be intimately related to the effective stress in the thawing soil. Once the effective stresses are known, combination with a constitutive relation for the soil yields the deformations, and combination with the conventional strength parameters provides the available shear strength.

To the present time, no correct or coherent theory is available to accomplish the analysis mentioned above for thawing soils. With the recent accelerating development in Arctic regions, a rational analysis for the behaviour of thawing Arctic soils takes on a high priority indeed. It is to this end that the research work described in this thesis was carried out.

1.3 Review of the Geotechnical Literature Concerning Thawing Soils

At the time of the First International Permafrost Conference (1963) almost no North American geotechnical studies had been published on the behaviour of permafrost subjected to thawing. The general characteristics of high compressibility and low shear strength had been recognised in soils which were ice-rich and fine-grained prior to thawing. It was intuitively suspected that if the rate of generation of water in a thawing soil exceeded its drainage capacity, excess pore pressures would be generated, causing the reduction of the available shear resistance. This was the theme of a simplified analysis undertaken by Yao and Broms (1965), who recognised that the bearing capacity of a subgrade soil might be reduced by the incomplete dissipation of excess pore pressures during thawing. Their theoretical study did not, however, embrace fully the properties of fine-grained soils. An analysis for thawing and the subsequent total settlements under dikes at Kelsey, Manitoba was carried out by Brown and Johnston (1970). The total settlements were calculated on the basis of a visual estimation of the segregated ice conditions, but no analysis was undertaken for the transient settlements and excess pore pressure conditions. However, as no serious stability problems arose subsequent to thawing under the dikes, it was concluded in retrospect that adequate drainage was available to provide a stable foundation.

In the North American literature, physical descriptions of the processes involved in the consolidation of thawing soils were presented by Aldrich and Paynter (1953) and by Scott (1969), but no rigorous statement of the problem or solutions were obtained.

Considerable research has been continuing in the USSR since about 1930. Although many papers of a descriptive nature were published (Tsytovich, 1957; Kiselev et al, 1965; Tsytovich, 1965) little analysis of the problems of thawing soils was ever attempted. The first analytical solution to a problem in thaw-consolidation was apparently obtained by Tsytovich et al (1965). A situation was envisaged where the thaw front was penetrating into the soil at a rate proportional to the square root of time. The one-dimensional Terzaghi equation of consolidation was assumed to govern the dissipation of excess pore pressures. However, the analysis failed to describe the thaw-consolidation process in terms of previously defined geotechnical properties, because the excess pore pressure at the thaw line was assumed equal to a constant value. This constant pore pressure boundary condition was assumed to be equal to a fraction of the overburden stress on empirical grounds. This assumption necessarily required a laboratory test on thawing soil with pore pressure measurements, and was never related to other more easily recognised geotechnical parameters. This analysis, therefore, would be very difficult to use, and would probably only be applicable in practice to one set of soil, loading and thawing conditions.

Another analysis for thawing soils was carried out by Feldman (1965), who attempted to incorporate a non-linear constitutive relation for the soil skeleton. Although admirable in intention, the analysis failed completely by assuming the effective stress at the thaw line was continually equal to zero. Furthermore, it was incorrectly assumed that all settlement took place during thawing. Consequently, this analysis adds little to the general understanding of the subject.

A study by Malyshev (1966) incorporated a variation of total stress with depth, and although a sophisticated solution technique was required, no new physical statements were introduced to improve the behavioural description of thawing soils.

The first analysis which attempted to model realistically the boundary condition at the thaw line was proposed by Zaretskii (1968). Although the continuity of the pore phase at the thaw boundary was described mathematically in terms of recognisable soil parameters, errors were introduced in the formulation at this point. Even though the physical statement of the thaw front boundary condition was incorrect, this work provides the first valuable insight into the pore pressure and effective stress conditions in a thawing soil.

Considerable interest in North America has recently been concerned with the proposed construction of a hot oil pipeline through Arctic regions. Such a proposal has intensified the research effort on geotechnical problems in Arctic Canada and Alaska. The thermal disturbance caused by a warm oil pipeline on the underlying permafrost was estimated by Lachenbruch (1970) in one of the most significant studies carried out to date in this research area. This research established that a thawed area of some forty feet around the pipe was to be expected during its operating lifetime. Some of the implications were explored assuming that the thawed soil behaved like a viscous fluid, and it was demonstrated how this would be a serious impediment to the burial of a hot pipeline. This also provided a substantial incentive to develop a more realistic model for the behaviour of permafrost subjected to thawing.

More recently, various agencies have constructed test pipeline sections, to determine the effects of a hot pipeline on the foundation material. The observed field behaviour of a test section at Inuvik, N.W.T. was reported by Watson et al (1973). Settlements, pore pressures and thaw depths were reported, and these results constitute the first well documented field case history in North America on thawing permafrost that is available at this time. These observations are analysed in some detail in Chapter 6 of this thesis.

However, research on some of the geotechnical properties of thawing soils is still limited on this continent. Speer et al (1973) have reported the results of numerous thaw settlement tests on undisturbed permafrost samples exhibiting a wide variation of ground ice conditions. A statistical correlation was established between the total thaw settlement and the frozen bulk density of the material. The bulk density of the frozen soil appears to form a useful index to the quantity of total settlement in this instance, as it reflects the amount of ice and to a lesser extent the amount of air that is present in the soil pore spaces. A correlation such as this is useful in establishing a preliminary estimate of total settlement, but, of course, gives no indication of the transient pore pressure and settlement responses during thawing.

As can be seen, there is an extreme paucity of information to date on the geotechnical behaviour of thawing soils. Moreover, there is not available at the present time a complete, correct and succinct statement of the physics of thawing soils. In addition, there is no available solution which might be applied to solve the engineering problems involving the deformation and strength of thawing fine-grained soils. This is surprising in the light of recent developments in Arctic areas, and provides considerable stimulus to remedy the situation, at least in part.

This thesis develops solutions to some of the more obvious problems in permafrost soils confronting geotechnical engineers at the present, and indicates the manner in which problems of a more complex nature might be solved.

CHAPTER II

THE ONE-DIMENSIONAL THAWING OF FROZEN SOILS

2.1 The Thawing of a Homogeneous Frozen Soil Subjected to a Step Increase in Surface Temperature.

An analysis of the engineering behaviour of a thawing soil requires a knowledge of not only the extent of the thawed soil, but also the rate of melting. The functional relationship between the depth of thaw and time is required before any geotechnical study of thawing soil is attempted. Once this information is extracted from the solution to the problem in heat transfer, additional information such as the temperature profiles are considered to be of second order importance. Some of the assumptions involving the uncoupling of the thermal and consolidation problems in this manner, and their validity are discussed in subsequent sections. In the following paragraphs, some classical solutions to the melting problem are reviewed for soils where a sudden constant increase in surface temperature has been applied.

It is assumed that conduction is the chief mode of heat transfer within the soil mass. The mixture of soil particles and water is assumed to behave as a continuum, which is deemed valid considering that the scale of a soil particle is many orders of magnitude smaller than a representative mass of soil. Temperature boundary conditions are used exclusively in this study. Although it is quite feasible to include boundary conditions of the heat flux type in a numerical study, this approach is still the subject of much active research, and beyond the scope of this thesis.

As illustrated in Fig. 2.1, a uniform homogeneous frozen soil is subjected to a step increase in temperature from T_g initially in the ground to T_s at the surface. The properties of the frozen and thawed zone are considered to be homogeneous and independent of temperature. It is assumed further that the latent heat associated with the transformation from ice to water is liberated at a fixed melting point $T_f = 0$. The analytical solution for the movement of the thaw front and the associated temperature fields has been found by Neumann about 1860. A statement of the equations and boundary conditions is given in concise form by Carslaw and Jaegar (1947), where the solution is also derived. The movement of the interface between the thawed and frozen soil zones is expressed by

$$X = \alpha \sqrt{t} \tag{2.1}$$

where X is the depth of thaw

t is the time

and α is a constant which is determined as a root of the transcendental equation

$$\frac{e^{-\frac{\alpha^2}{4\kappa_u}}}{\operatorname{erf}\left(\frac{\alpha}{2\sqrt{\kappa_u}}\right)} - \frac{T_g}{T_s}\,\frac{k_f}{k_u}\,\sqrt{\frac{\kappa_u}{\kappa_f}}\;\frac{e^{-\frac{\alpha^2}{4\kappa_f}}}{\operatorname{erfc}\left(\frac{\alpha}{2\sqrt{\kappa_f}}\right)} = \frac{L\sqrt{\pi}\,\alpha}{2\sqrt{\kappa_u}\,c_u\,T_s} \tag{2.2}$$

Here, $\operatorname{erf}\left(\quad\right)$ is the error function,

$$\operatorname{erfc}\left(\quad\right) = 1 - \operatorname{erf}\left(\quad\right),$$

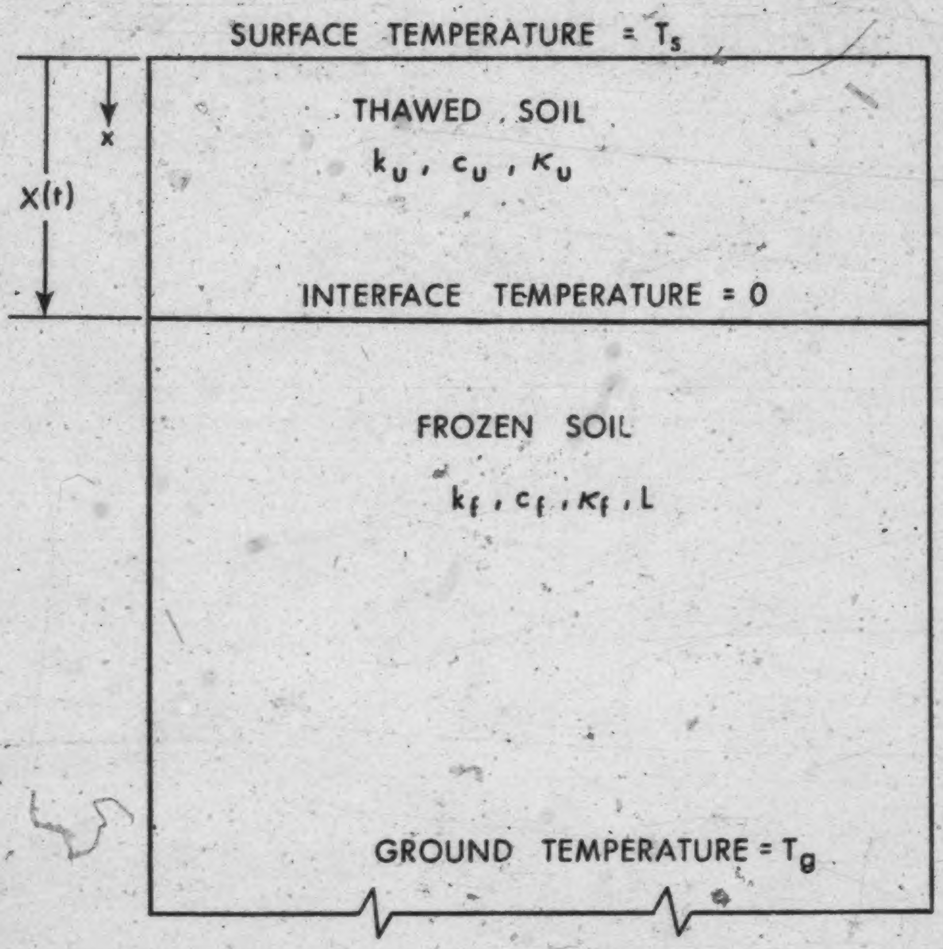
SURFACE TEMPERATURE = T_s
THAWED SOIL
k_u , c_u , κ_u
x
X(t)
INTERFACE TEMPERATURE = 0
FROZEN SOIL
k_f , c_f , κ_f , L
GROUND TEMPERATURE = T_g

Fig. 2.1 The Neumann problem

κ_u and κ_f are the diffusivities of unfrozen and frozen soil [cm^2/s],

k_u and k_f are the thermal conductivities of unfrozen and frozen soil [cal/°C cm s],

c_u and c_f are the volumetric heat capacities of unfrozen and frozen soil [$\mathrm{cal}/{}^{\circ}\mathrm{C}\ \mathrm{cm}^3$],

L is the volumetric latent heat of the soil [$\mathrm{cal}/\mathrm{cm}^3$ soil],

T_g is the (uniform) initial ground temperature difference [°C below freezing],

T_s is the applied constant surface temperature difference [°C above freezing].

As the diffusivity of a zone is simply the conductivity divided by the volumetric heat capacity for that zone, then the solution for α appears to be a function of the seven variables:

$$\alpha = f(k_u, k_f, c_u, c_f, T_g, T_s, \text{and } L) \qquad (2.3)$$

Their relative importance will be examined later.

Equation (2.2) may be rewritten in such a way that only three dimensionless parameters emerge.

$$\frac{e^{-\left(\frac{\alpha}{2\sqrt{\kappa_u}}\right)^2}}{\operatorname{erf}\left(\frac{\alpha}{2\sqrt{\kappa_u}}\right)} - \frac{T_g}{T_s}\,\frac{k_f}{k_u}\sqrt{\frac{\kappa_u}{\kappa_f}}\;\frac{e^{-\left(\frac{\kappa_u}{\kappa_f}\right)\left(\frac{\alpha}{2\sqrt{\kappa_u}}\right)^2}}{\operatorname{erfc}\left(\sqrt{\frac{\kappa_u}{\kappa_f}}\,\frac{\alpha}{2\sqrt{\kappa_u}}\right)}$$

$$= \frac{\alpha}{2\sqrt{\kappa_u}}\,\frac{\sqrt{\pi}}{\mathrm{Ste}} \qquad (2.4)$$

that is,

$$\frac{\alpha}{2\sqrt{\kappa_u}} = f\left\{\mathrm{Ste},\ -\frac{T_g}{T_s}\frac{k_f}{k_u}\sqrt{\frac{\kappa_u}{\kappa_f}}\ ,\ \sqrt{\frac{\kappa_u}{\kappa_f}}\right\} \tag{2.5}$$

and Ste is the so-called Stefan number, and is defined as the ratio of sensible heat to latent heat by

$$\mathrm{Ste} = \frac{c_u T_s}{L} \tag{2.6}$$

The seven variables in eq. (2.3) are absorbed into three dimensionless numbers. This makes a graphical presentation of the solution to eq. (2.4) feasible.

Equation (2.4) has been solved by the Newton-Raphson iteration scheme for finding the zeros of a function. It is of interest to note that the results are almost totally independent of the ratio $\sqrt{\kappa_u/\kappa_f}$. The results for the normalized thaw rate, $\alpha/2\sqrt{\kappa_u}$, are presented in Fig. 2.2 as a function of the two significant variables

$$\left(\mathrm{Ste}\right) \text{ and } \left(-\frac{T_g}{T_s}\frac{k_f}{k_u}\sqrt{\frac{\kappa_u}{\kappa_f}}\right).$$

Varying $\sqrt{\kappa_u/\kappa_f}$ over a reasonably wide range of values does not produce a measurable difference in the normalized thaw rate. A reasonable value of $\sqrt{\kappa_u/\kappa_f}$ for most soil conditions is 0.7, and this value was adopted for Fig. 2.2. This chart therefore represents a complete and accurate solution to the Neumann problem, with no assumptions other than those inherent in the original formulation.

Considerable simplifications to the rigorous Neumann solution have been made by various authors. It is possible to set up a table

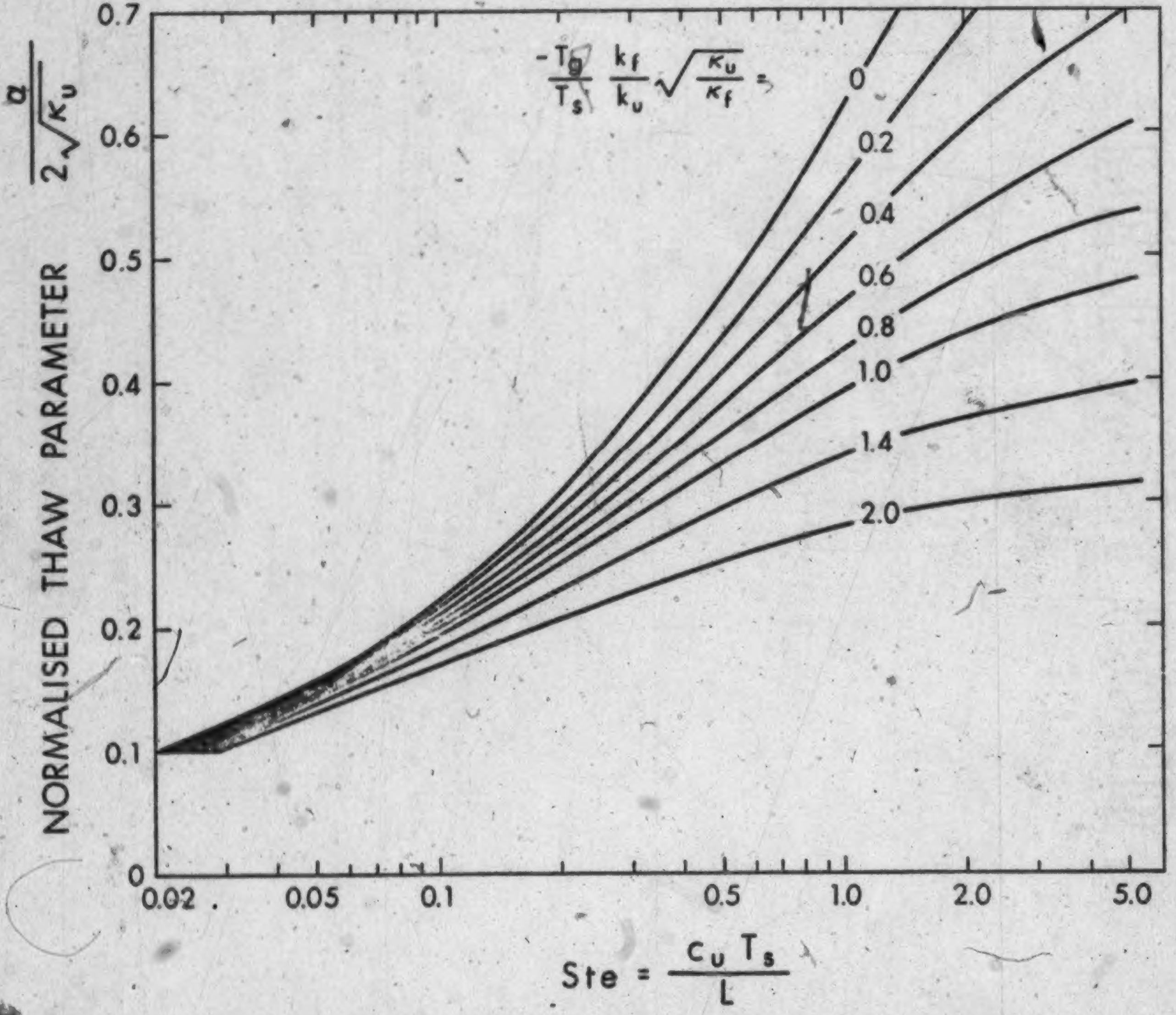

Fig. 2.2 Graphical solution of the Neumann equation.

of solutions in order of decreasing complexity and accuracy as in Table 2.1. This table applies only for the step increase in temperature at the surface. It appears that a formulation by Berggren (1943) has duplicated the earlier work of Neumann, and therefore is not discussed here.

After the solution proposed with $\sqrt{\kappa_u/\kappa_f} = 0.7$, the next simplification was made by Aldrich and Paynter (1953) in the so-called modified Berggren method, which assumes a slightly less realistic value of $\sqrt{\kappa_u/\kappa_f} = 1.0$. Moreover, slight errors are introduced by taking $c_f = c_u$, which by definition implies also that $k_f = k_u$.

The solution may be greatly reduced in complexity if we assume that the temperature distribution in the frozen zone does not affect the rate of thaw. As will be seen later, this is a reasonable simplification if T_g is close to the melting temperature. Setting $T_g = 0$ in eq. (2.2), we obtain

$$\sqrt{\pi}\,\frac{\alpha}{2\sqrt{\kappa_u}}\,e^{\frac{\alpha^2}{4\kappa_u}}\,\mathrm{erf}\left(\frac{\alpha}{2\sqrt{\kappa_u}}\right) = \mathrm{Ste} \qquad (2.7)$$

Now on a semi-empirical basis eq. (2.7) may be approximated to a high order of accuracy by

$$\frac{\alpha}{2\sqrt{\kappa_u}} = \sqrt{\frac{\mathrm{Ste}}{2}}\left(1 - \frac{\mathrm{Ste}}{8}\right) \qquad (2.8)$$

This equation is extremely simple to evaluate, and the results of eq. (2.7) and eq. (2.8) are plotted in Fig. 2.3.

If a linear temperature distribution is assumed in the thawed zone, and the temperature profile in the frozen zone is again ignored, a solution may be obtained which is often used and is originally due

TABLE 2.1 HIERARCHY OF SOLUTION METHODS

NAME	VARIABLES NEEDED	EQUATION	REMARKS
1. Neumann	k_u, k_f, c_u, c_f, L, T_s, T_g	See Eqn. 2	Rigorous analytical solution for a step temperature applied to homogeneous soil.
2. Proposed Solution #1	k_u, k_f, c_u, c_f, L, T_s, T_g	As Neumann	Solution of above insensitive to $\sqrt{\frac{\kappa_u}{\kappa_f}}$ Graphical solution given for $\sqrt{\frac{\kappa_u}{\kappa_f}} = 0.7$
3. Aldrich and Paynter (Modified Berggren)	k_u, k_f, c_u, c_f, L, T_s, T_g	As Neumann	Neumann solution with $\sqrt{\frac{\kappa_u}{\kappa_f}} = 1$ and $c_u = c_f$, therefore $k_u = k_f$ assumed.
4. Neumann with $T_g = 0$	k_u, c_u, T_s, L	$\frac{\alpha}{2\sqrt{\kappa_u}} e^{\frac{\alpha^2}{4\kappa_u}} \operatorname{erf} \frac{\alpha}{2\sqrt{\kappa_u}} = \sqrt{\pi}\, Ste$	Temperature distribution in frozen zone ignored.
5. Proposed Solution #2	k_u, c_u, T_s, L	$\frac{\alpha}{2\sqrt{\kappa_u}} = \sqrt{\frac{Ste}{2}}\left(1 - \frac{Ste}{8}\right)$	Semi-empirical approximation to 4. High accuracy if $Ste < 1$ and $T_g = 0$.
6. Stefan	k_u, c_u, T_s, L	$\frac{\alpha}{2\sqrt{\kappa_u}} = \sqrt{\frac{Ste}{2}}$	Linear temperature profile in thawed zone, and $T_g = 0$.

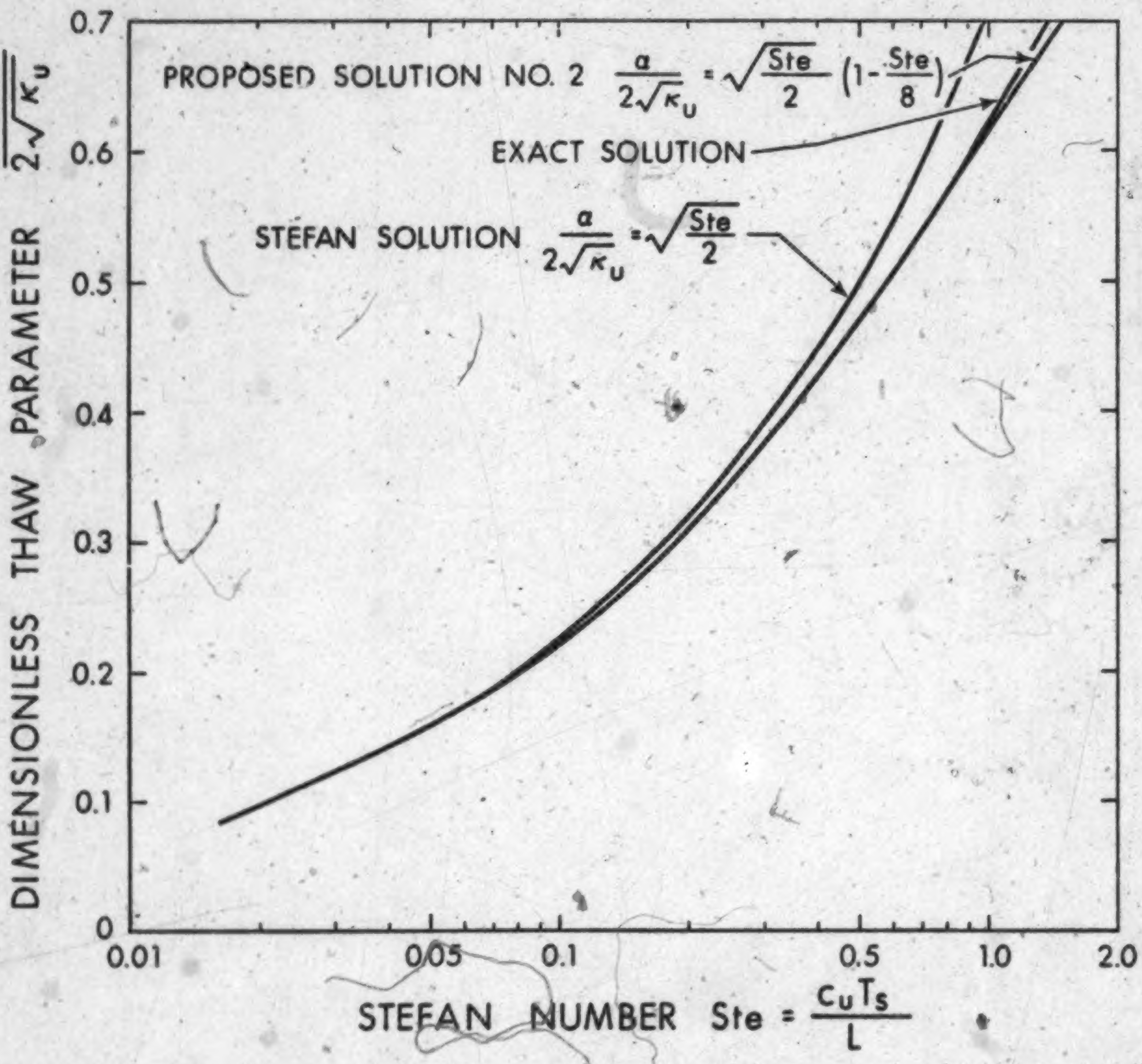

Fig. 2.3 Solution of the Neumann equation with $T_g = 0$

to Stefan.

$$X = \sqrt{\frac{2k_u T_s}{L}} \sqrt{t} \tag{2.9}$$

or writing in dimensionless form

$$\frac{\alpha}{2\sqrt{\kappa_u}} = \sqrt{\frac{Ste}{2}} \tag{2.10}$$

The results from eq. (2.10) are also plotted for comparison in Fig. 2.3.

The solution to the Neumann equation is presented in chart form in Fig. 2.2 and the α value can be extracted from it with a high degree of accuracy. If the ground temperatures are close to the melting point, then the simple function given by eq. (2.8) may be used to predict α, the relationship between depth of thaw and the square root of time.

Having established these analytical expressions for the thawing of frozen soils, it is desirable to examine the thermal parameters involved and their calculation.

2.2 The Thermal Properties of Soils.

The simplifications introduced by various authors in Table 2.1 suggest that some thermal properties may influence the thaw rate to a greater extent than others. For instance, the Stefan solution in eq. (2.9) depends only on k_u, L, and T_s. It is of interest therefore to assess the relative importance of the remaining four variables on the rate of thaw α. The Neumann solution will be used in combination with data for thermal conductivity for a saturated silt/clay soil taken from Kersten (1949). Now c_f, c_u, and L are also dependent on water content, and they are derived from the simple relationships given later. So k_u, k_f, c_u, c_f, and L can all be written as functions of the water content ω, and therefore the importance of each thermal property is assessed by plotting α against ω, for a given step temperature T_s. In examining each of these variables in turn, it has been assumed that the degree of saturation is 100%, and the specific gravity of soil solids is 2.7.

(a) Ground Temperature, T_g

The effect of the initial (uniform) ground temperature is determined over a range of values from 0 to -5°C. The effect of a change in ground temperature of 1°C is to change the rate of thaw parameter α by about 2.5% (see Fig. 2.4). These calculations are based on an example where $T_s = +10°C$. The effect of ground temperature on the rate of thaw can also be investigated by consulting the graphical solution of the Neumann problem in Fig. 2.2.

In problems where the ground temperatures are close to the melting point, it may often be reasonable to ignore them entirely. This will result in marginally overestimating α.

(b) Thermal Conductivity of Frozen Soil, k_f

It is well known that the thermal conductivity of frozen soil, k_f, is temperature dependent (Penner, 1970) and that this phenomenon is due to the presence of unfrozen water in fine grained soils below 0°C. Because k_{ice} is greater than k_{water} and, as there is only a slight temperature dependence of conductivity in soil minerals, Kersten (1949), it can be seen that k_f should be greater than k_u for soils. In fact, for high water contents the ratio k_f/k_u should approach the ratio of conductivities of ice to water of 3.7. Kersten has also presented

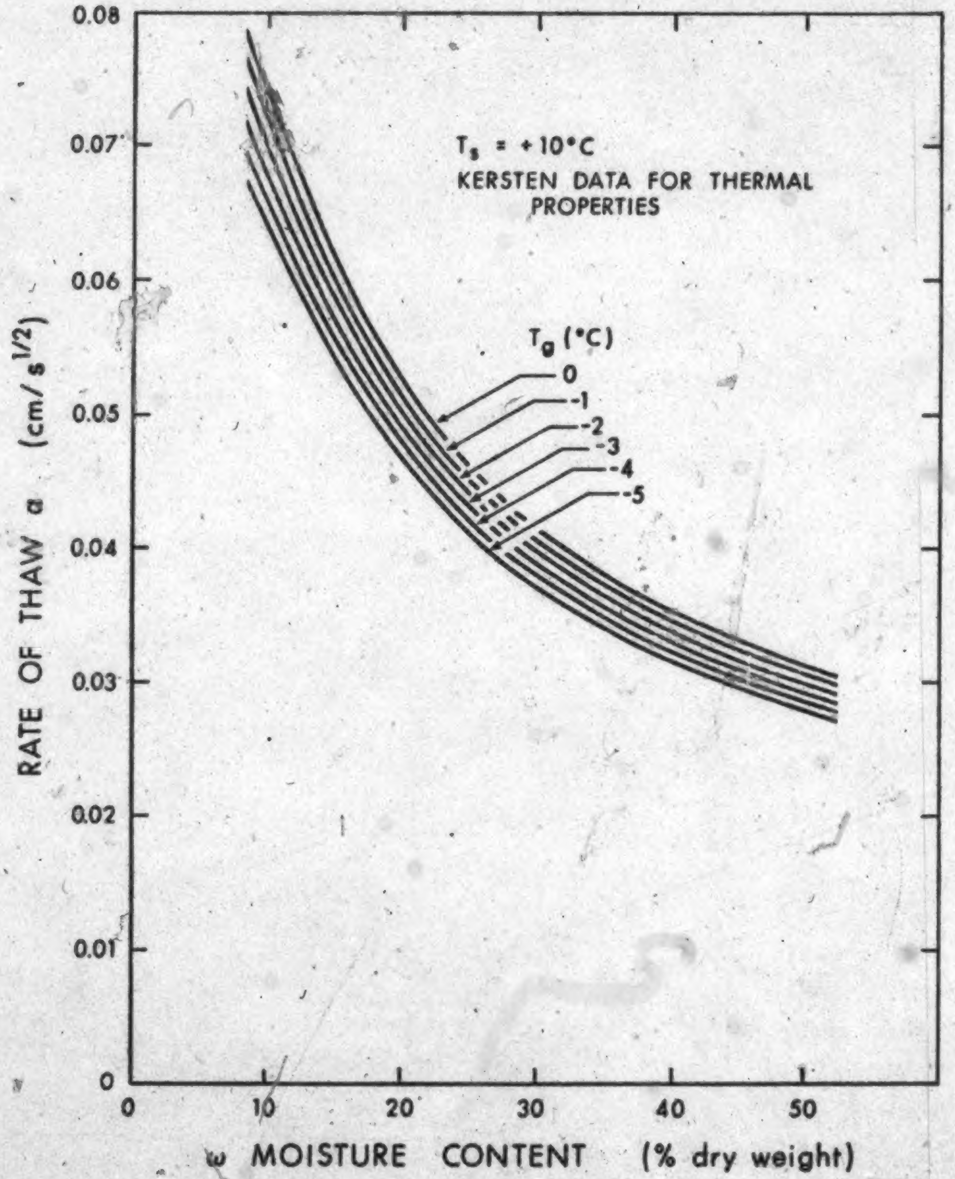

Fig. 2.4 Variation of α with ground temperature T_g

relationships for k_u and k_f for silt/clay soils and his results are presented in Fig. 2.5. It can be seen that the ratio k_f/k_u ranges from 1.1 to 3.7.

The effect of the absolute magnitude of k_f on α may be studied by varying k_f/k_u from 1.0 to 3.7. At a given water content, the value of k_u is used in the Neumann solution together with the k_f value as defined by the ratio k_f/k_u. This k_f is taken to be constant over the range $0^{\circ}C$ to T_g. The rather insignificant effect of absolute variations in k_f on α is readily apparent in Fig. 2.6.

It is suggested that for any thaw calculation the use of $k_f = k_{ice}$ = 5.3 mcal/$^{\circ}$C cm s will yield adequately accurate solutions to a thaw problem except for the most highly plastic clays. It should be noted that Kersten's data on k_f given in Fig. 2.5 approaches k_{ice} at a water content of 24% and then increases. This subsequent increase in k_f is felt to be incorrect and likely results from the function fitting method used.

Problems may be studied by numerical techniques where k_f is dependent on temperature and an example is presented in a later section. However, the effect of the temperature dependent k_f on α can be studied using the analytical results already obtained. As has been shown in Fig. 2.6, varying k_f from 1.0 k_u to 3.7 k_u has little effect on α. The effects of any intermediate relationship $k_f = k_f(\theta)$ on α will be bounded by the results already obtained for $k_f = 1.0\ k_u$ and $k_f = 3.7\ k_u$.

It may be concluded that neither the absolute magnitude nor the temperature dependence of the frozen conductivity k_f has any significant influence on the determination of the rate of thaw α. The calculations involved in Fig. 2.4 and Fig. 2.6 were provided by McRoberts (1972).

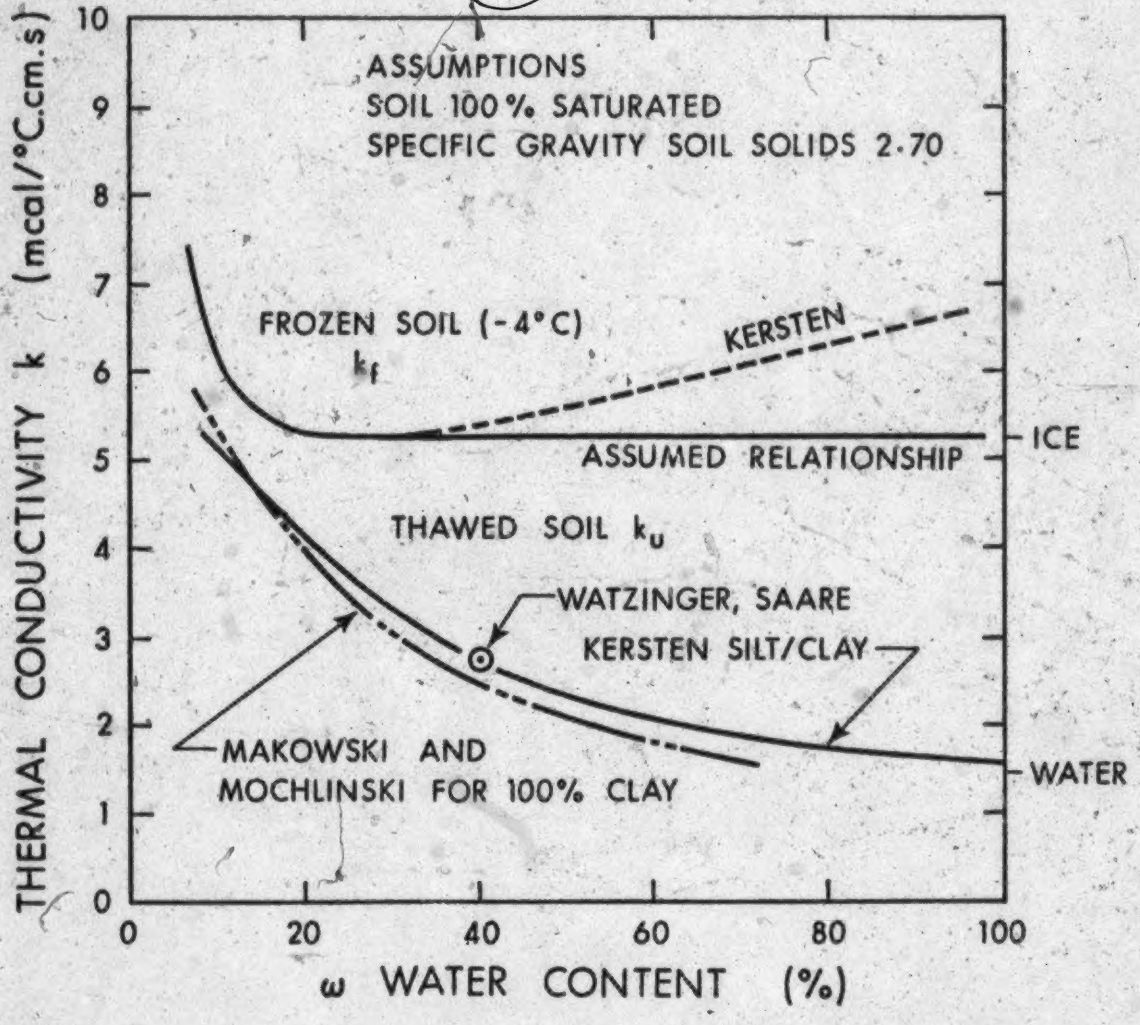

Fig. 2.5 Thermal conductivity of fine grained soils

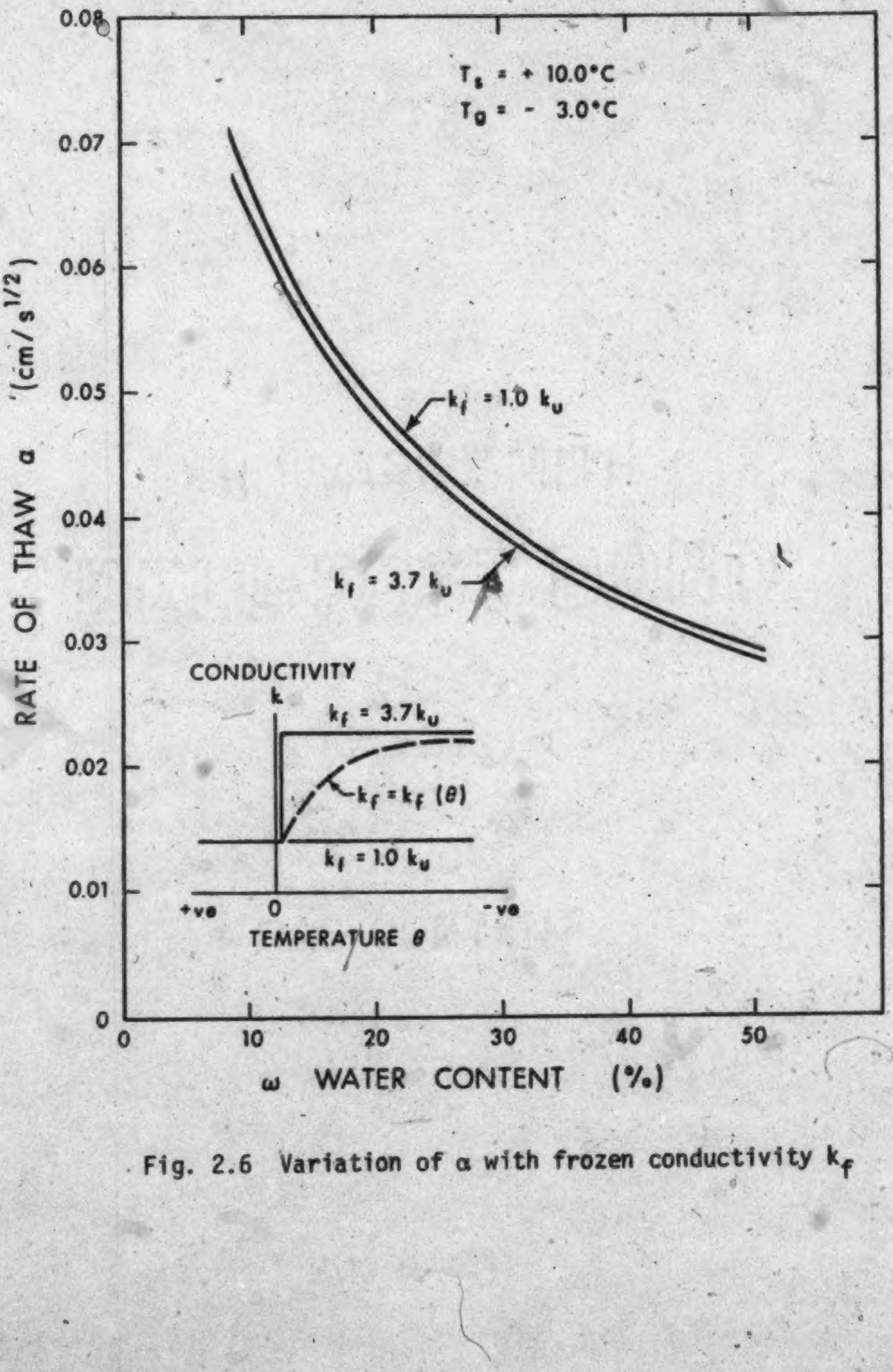

Fig. 2.6 Variation of α with frozen conductivity k_f

(c) Volumetric Heat Capacity of Frozen Soil, c_f

The volumetric heat capacity of soil is calculated by a simple mixture rule in which the relative heat capacity of the constituent materials are added together. That is

$$c_f = \gamma_d \left(c_m + 0.5\omega \right) \tag{2.11}$$

where γ_d denotes the dry density [g/cm^3],

c_m is the heat capacity of the soil grains [cal/g.$^\circ$C],

0.5 is the heat capacity of ice [cal/g.$^\circ$C],

ω denotes the water content [g/g].

As pointed out by Moulton (1969), there are some minor differences of opinion among some authors as to the correct value of c_m to use in eq. (2.11). Kersten (1949) finds that a value of 0.17 cal/g.°C represents an average value for soils close to their freezing point. Moulton refers to several sources that suggest a value of 0.20 cal/g.°C may be more representative.

For frozen soils containing unfrozen water, a modification to eq. (2.11) can be made to allow for the relative percentage of ice and water as follows:

$$c_f = \gamma_d \left\{ c_m + 0.5\ (1 + W_u)\omega \right\} \tag{2.12}$$

where W_u is the unfrozen water content [g. water/g. (ice + water)].

A value of c_f may be calculated based on the value of W_u at the ground temperature T_g of interest. However, as pointed out in the preceding sections, the effects of T_g and k_f on the rate of thaw α are small as well. For large ratios of T_g/T_s the role of c_f in the overall solution can become more significant, but these ratios are generally not encountered in geotechnical problems.

The effect of c_f can be inspected by considering the dimensionless variable

$$-\frac{T_g}{T_s} \cdot \frac{k_f}{k_u} \sqrt{\frac{\kappa_u}{\kappa_f}}$$

in Fig. 2.2. As κ_f may be replaced by k_f/c_f, it follows that α is related to $\sqrt{c_f}$. For an example with $\omega = 0.5$ and $W_u = 0.2$ at T_g, c_f is underestimated by 10% if eq. (2.11) is used. This error results in an underestimation of the rate of thaw of less than 2% for the usual range of 'Ste'.

If this error is considered to be significant, eq. (2.12) can be used to define c_f. The effect of the unfrozen moisture content-temperature relationship between T_g and 0^oC on c_f is completely insignificant with regard to predictions of the rate of thaw.

(d) Volumetric Heat Capacity of Thawed Soil, c_u

The parameter c_u plays an important role in thaw solutions. It is used in defining the Stefan number, Ste, which has been shown to be an important variable. The value of c_u can be determined, as was c_f, by the following:

$$c_u = \gamma_d \left(c_m + 1.0\omega\right) \tag{2.13}$$

where 1.0 = heat capacity of water [cal/g.^oC].

The comments in the preceding section on c_f apply equally to c_u. Variations in c_m have less effect on c_u than on c_f, as the specific heat of water has doubled from that of ice.

(e) Thermal Conductivity of Thawed Soil, k_u

The rate of thaw α is proportional to the square root of k_u and hence errors in k_u have serious consequences on α. For example an error of ± 25% in k_u results in an error in α of about ± 11%. The relationship given by Kersten (1949) for the thermal conductivity of thawed soil is

$$k_u = 3.446 \times 10^{-4} [0.9 \log_{10}(\omega) - 0.2] 10^{0.624\gamma_d} \tag{2.14}$$

where k_u is in cal/cm.°C.s,

ω is the water content (%),

γ_d is the dry density (g/cm^3).

Kersten's data on k_u have been used for the parametric studies presented. It is felt, furthermore, that the absolute magnitudes of the k_u values presented are entirely reasonable. Figure 2.5 indicates the comparison of Kersten's data with that presented by Makowski and Mochlinski (1956) and single determinations by Watzinger and Saare referenced by Skaven-Haug (1972).

(f) Latent heat and Water Content Effects

The water content of a soil is a dominant parameter in thermal calculations. As has been shown, the thermal conductivity and volumetric specific heats of both thawed and frozen saturated soil can be expressed as functions of the water content. Below 0°C it is recognised that some water exists in the liquid state as expressed by the unfrozen water content, W_u. It has been shown that this phenomenon has relatively minor effects on k_f and c_f in calculations for the rate of thaw.

The remaining variable in the thaw solution that has yet to be considered is the volumetric latent heat of the soil, L. This variable has a dominant role in thermal calculations and represents on a volume basis the amount of heat that must be supplied to a soil below 0^oC to change ice into water. Problems arise in defining the value of L to be used. Firstly at the temperature, T_g, applicable in a problem the percentage W_u must be known. Secondly, the effect of a gradual change of state of ice to water over the temperature range T_g to 0^oC must be considered.

The first approach that can be taken is to calculate the amount of ice per unit volume once the appropriate W_u is known. That is,

$$L = \gamma_d \, \omega(1 - W_u) \, L' \qquad (2.15)$$

where L' = 79.6 cal/gm the latent heat of water,

γ_d = dry density of soil (g/cm^3).

The rate of thaw can then be calculated from the Neumann formulation by using the total water content, ω, to define k_u, c_u, and c_f and taking k_f = 5.3 mcal/^oC cm s. This approach has the effect of "lumping" the total latent heat at 0^oC. That is, it is assumed that all the ice initially present in an unit volume of soil at T_g melts at 0^oC rather than over the range T_g to 0^oC.

The five thermal variables c_u, c_f, k_u, k_f and L are all functions solely of water content when the soil is saturated. The complete solution to the Neumann problem presented in Fig. 2.2 requires the two temperatures T_g and T_s, and the parameters c_u, k_u, k_f, κ_u, κ_f and L. As these six parameters are all functions of water content, it is convenient to plot them as shown in Figs. 2.7, 2.8 and 2.9. The conductivities k_u and k_f have already been given in Fig. 2.5. Therefore knowing T_s, T_g and the

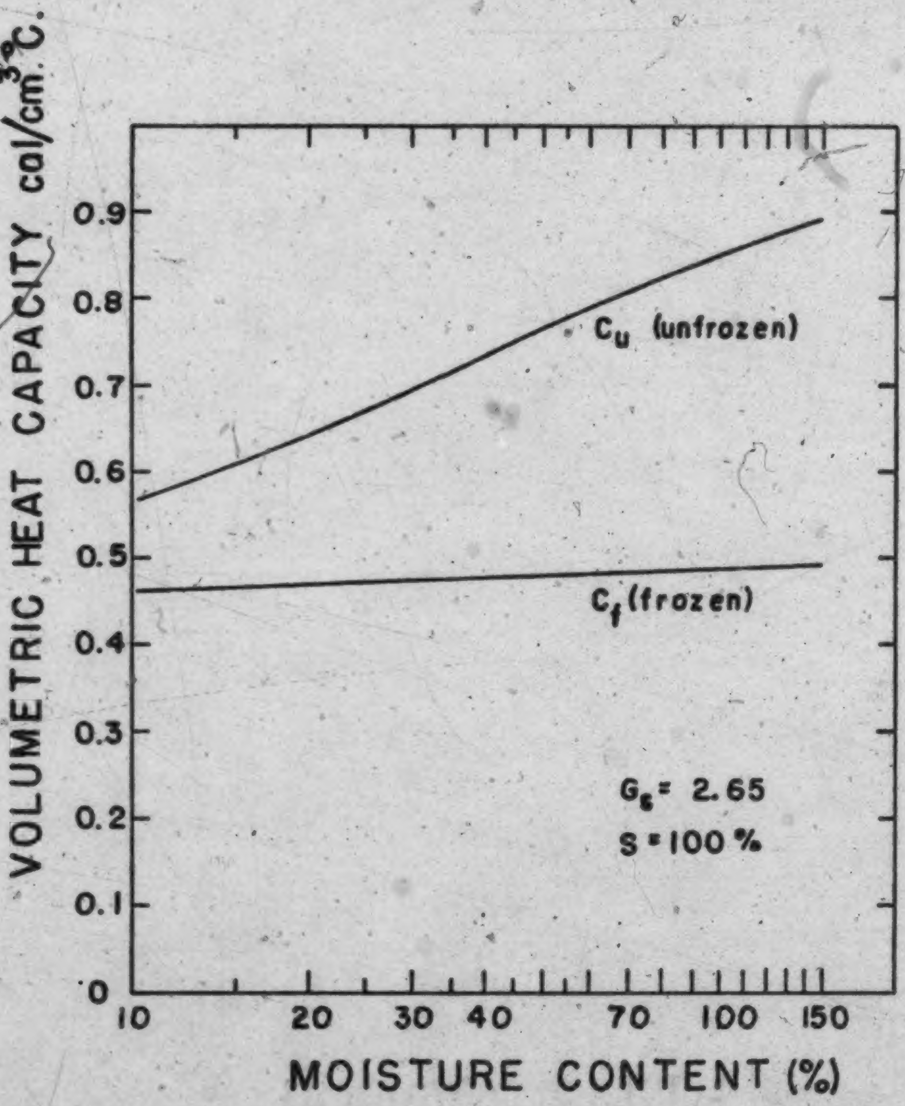

Fig. 2.7 Volumetric heat capacity of soils

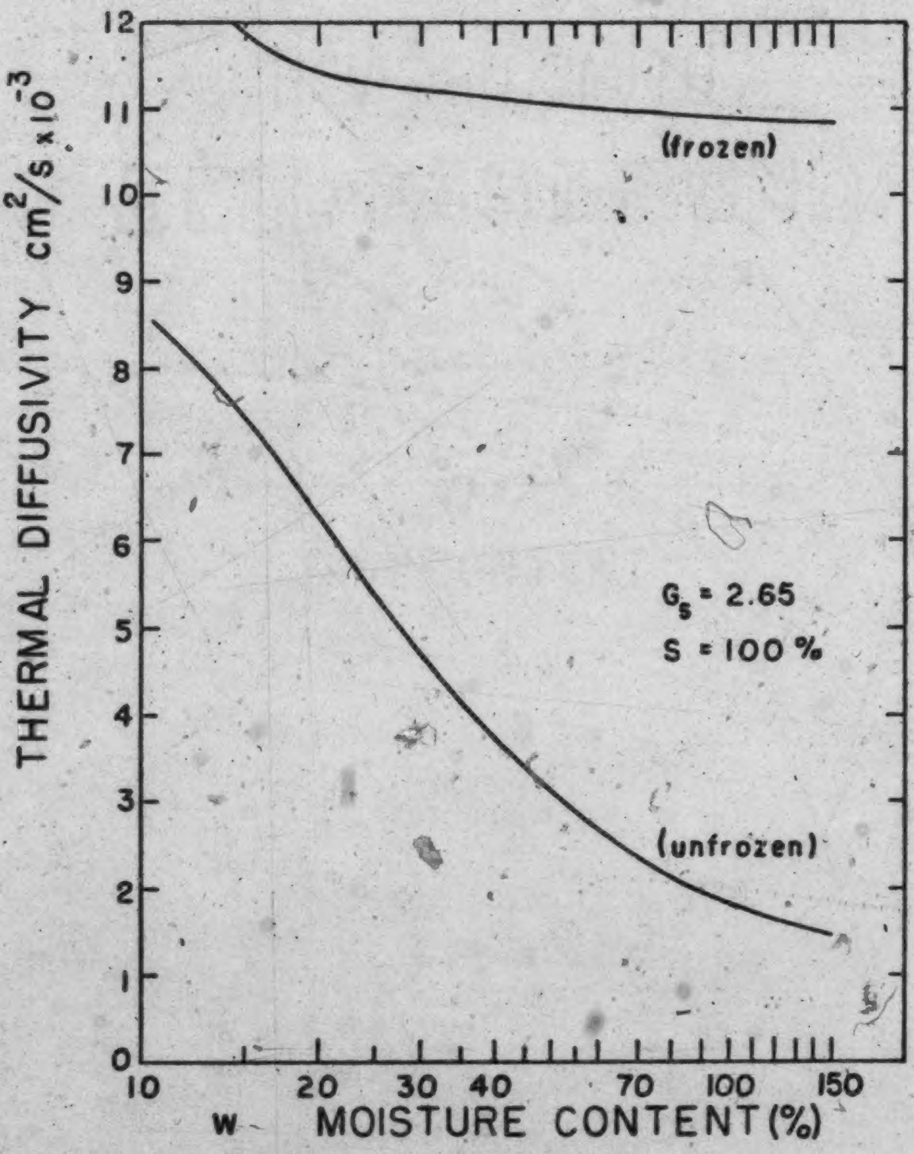

Fig. 2.8 Thermal diffusivity of fine-grained soils

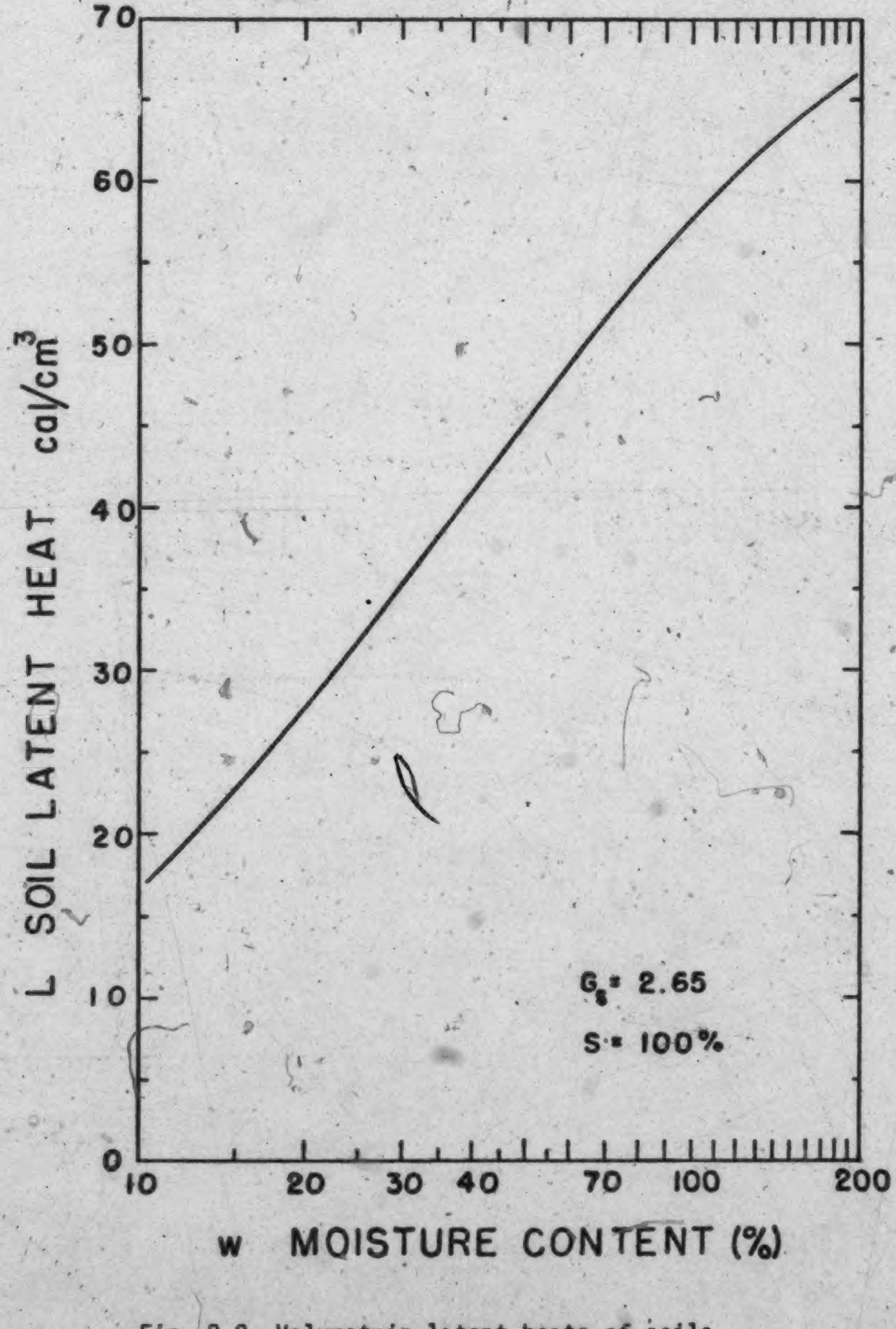

Fig. 2.9 Volumetric latent heats of soils

water content of a saturated soil, all the thermal parameters necessary for an accurate solution to the Neumann problem in Fig. 2.2 may be obtained from the charts included.

The effects of a gradual change of state from ice to water over the range T_g to 0^oC, and the accompanying effects of temperature or phase dependence of frozen conductivity and specific heat are investigated in the next section, as a numerical solution is required to solve the heat transfer problem.

2.3 The Temperature and Phase Dependence of Soil Thermal Properties.

In the previous section it was assumed that all ice melted at the 0^oC isotherm, and that the thawing soil could be divided into two discrete zones, each displaying a temperature-independent set of thermal properties. Since it has been well established that liquid water exists over a wide range of temperatures below 0^oC, it might well be argued that the thermal properties are dependent on temperature in the frozen soil, and that this should be accounted for more rigorously in the heat transfer formulation. Therefore, a more generalised equation for conductive heat transfer may be derived, and employed to establish the magnitude of any errors involved in the Neumann formulation described previously for soils.

Consider the thermal equilibrium of a small layer δx at a depth x. Taking heat flow as positive in the positive x-direction,

$$(\delta Q)_x = (Q)_x - (Q)_{x+\delta x} + (Q_\omega)_x \qquad (2.16)$$

where $(\delta Q)_x$ = change in heat of the layer,

$(Q)_x$ = heat flowing into the layer at x,

$(Q)_{x + \delta x}$ = heat flowing out of the layer at x

$(Q_\omega)_x$ = heat generated internally in δx by water changing phase.

In a time δt, the heat quantities in eq. (2.16) are replaced by their temperature dependent relationships giving

$$c_o\,(\theta)\;\delta\theta\;\delta x = -\left\{k\,(\theta)\,\frac{\partial\theta}{\partial x}\,\delta t\right\}_x - -\left\{k\,(\theta)\,\frac{\partial\theta}{\partial x}\,\delta t\right\}_{x + \delta x}$$

$$- L'\omega\,\gamma_d\;\delta W_u\;\delta x \qquad (2.17)$$

where

$c_o\,(\theta)$	is the volumetric heat capacity of the soil-ice-water mixture (cal/cm.^{3} ^{o}C),
$k\,(\theta)$	is the thermal conductivity (cal/^{o}C.cm.s),
L'	is the latent heat of fusion of ice (cal/gm water),
γ_d	is the dry unit weight of the soil (g/cm^3),
ω	is the total water content (g/g),
δW_u	is the fraction of ω which changes phase in time δt,
W_u	is the unfrozen moisture content defined as g.water/g.(ice + water).

Rearranging eq.(2.17) yields

$$c_o\,(\theta)\,\frac{\partial\theta}{\partial t} = \frac{\partial}{\partial x}\left\{k\,(\theta)\;\frac{\partial\theta}{\partial x}\right\} - L'\,\omega\gamma_d\;\frac{d\,W_u}{dt} \qquad (2.18)$$

As W_u is considered to be solely a function of the temperature θ, implying no hysteresis of the relationship, the following may be written

$$\frac{d\,W_u}{dt} = \frac{d\,W_u}{d\theta}\;\frac{\partial\theta}{\partial t} \qquad (2.19)$$

and bringing the last term on the right hand side of eq. (2.18) to the other side gives

$$\left\{c_o\ (\theta) + L'\omega\gamma_d \frac{d\ W_u}{d\theta}\right\} \frac{\partial\theta}{\partial t} = \frac{\partial}{\partial x} \left\{k\ (\theta) \frac{\partial\theta}{\partial x}\right\} \tag{2.20}$$

The term in braces on the left hand side is often referred to as the apparent heat capacity of the soil. This term contains the straightforward heat capacity of the soil-ice-water mixture, and the second part expresses the heat which is liberated or absorbed by the soil on freezing or melting. Hence the term

$$c_a\ (\theta) = c_o\ (\theta) + L'\omega\gamma_d \frac{d\ W_u}{d\theta} \tag{2.21}$$

is written as the apparent volumetric heat capacity of the soil. The quantity $c_o\ (\theta)$ is written in terms of W_u from eq. (2.12), and therefore $c_a\ (\theta)$ becomes solely a function of W_u, as follows

$$c_a\ (\theta) = \gamma_d \left\{0.17 + 0.5\omega\ (1 + W_u)\right\} + L\omega\gamma_d \frac{d\ W_u}{d\theta} \tag{2.22}$$

Using a method due to De Vries and described by Penner (1970), it may be shown that the temperature dependent conductivity may be well approximated by a linear dependence on W_u also, and hence

$$k\ (\theta) = k_f + W_u\ (k_t - k_f) \tag{2.23}$$

where k_t and k_f are the fully thawed and fully frozen conductivities respectively.

Therefore all temperature dependent coefficients appearing in eq. (2.20) may be written in terms of W_u. It remains now to establish the functional dependence of W_u on the temperature θ.

An exponential relationship between W_u and θ is adopted for the purpose of examining the effect of temperature dependent thermal properties on the rate of thaw. It should be noted, however, that any continuous function might be used to relate W_u to θ in this way. For example, Anderson et al., (1973) have expressed the unfrozen water content data versus temperature by the simple power equation

$$W_u = \alpha\, \theta^{\beta}$$

where α and β are constants which may be related to the specific surface area of the frozen soil. Dillon and Andersland (1966) have also provided a relationship for the terminal unfrozen moisture content at temperatures below -5°C. However, for the purpose of observing the sensitivity of the rate of thaw to the shape of the unfrozen moisture content curve, no regard need be given here to such correlations with more fundamental soil properties, and a simple empirical equation may be adopted. The unfrozen moisture is defined here in terms of three quantities P, Q and R which are capable of providing a wide variety of realistic relationships, that is

$$W_u = (P + e^{Q\theta + R})/100 \qquad (2.24)$$

This equation and its temperature derivative may now be substituted into the expressions for apparent heat capacity and conductivity in eq. (2.22) and (2.23). The governing differential equation (2.20) is written in finite difference form, and the details of the procedure for solving it are given in Appendix A1. The listing of the computer program and the accompanying function subprograms for conductivity and heat capacity are given in Appendix A2.

A set of unfrozen moisture curves covering a wide range are drawn in Fig. 2.10 by assigning values of P, Q and R to eq. (2.24). The values of P and R are constant for all the curves and are chosen so that W_u is unity at 0^oC and 0.3 at the ground temperature T_g. The value of Q is varied in order to produce the range of curves shown in Fig. 2.10. It is thought that this range of curves together with the Neumann solution (where all water melts at 0^oC) must bound the relationships that are physically possible for real soils.

The effect of these unfrozen moisture content curves on the movement of the 0^oC isotherm is studied. Temperature dependent thermal conductivity and specific heat functions are established for the frozen zone, and the necessary parameters entered as data in the computer program given in Appendix A2. A simple example is solved where a step increase in surface temperature of 10^oC is applied at the surface of a homogeneous soil exhibiting the three different W_u vs. temperature curves. The water content is 0.48, and therefore the conductivity of the thawed and fully frozen soils may be read from Fig. 2.5.

The depth to the 0^oC isotherm X is plotted for each case against the square root of time, and a straight line relationship is always obtained. Therefore, an α value may always be extracted from the solution. The results for X against $\sqrt{time}$ are shown in Fig. 2.11, and the α values for the different W_u - temperature curves are compared with a Neumann solution in which the latent heat L is calculated by eq. (2.15) and "lumped" at 0^oC. Another Neumann solution in which $W_u = 0$ is also included for comparison and is shown by the dotted line in Fig. 2.11.

It may be thought that the usual approach in dealing with the unfrozen moisture content relationship will underestimate the rate of

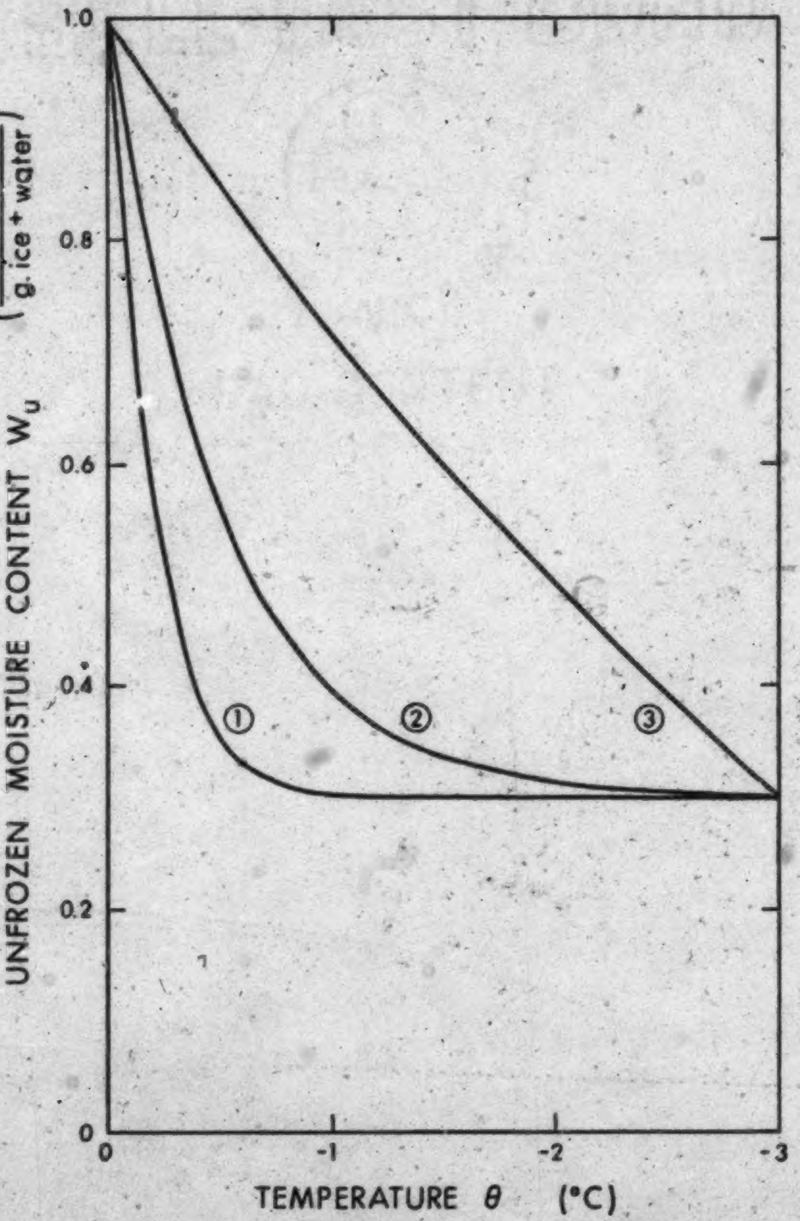

Fig. 2.10 Unfrozen moisture content curves for numerical analysis

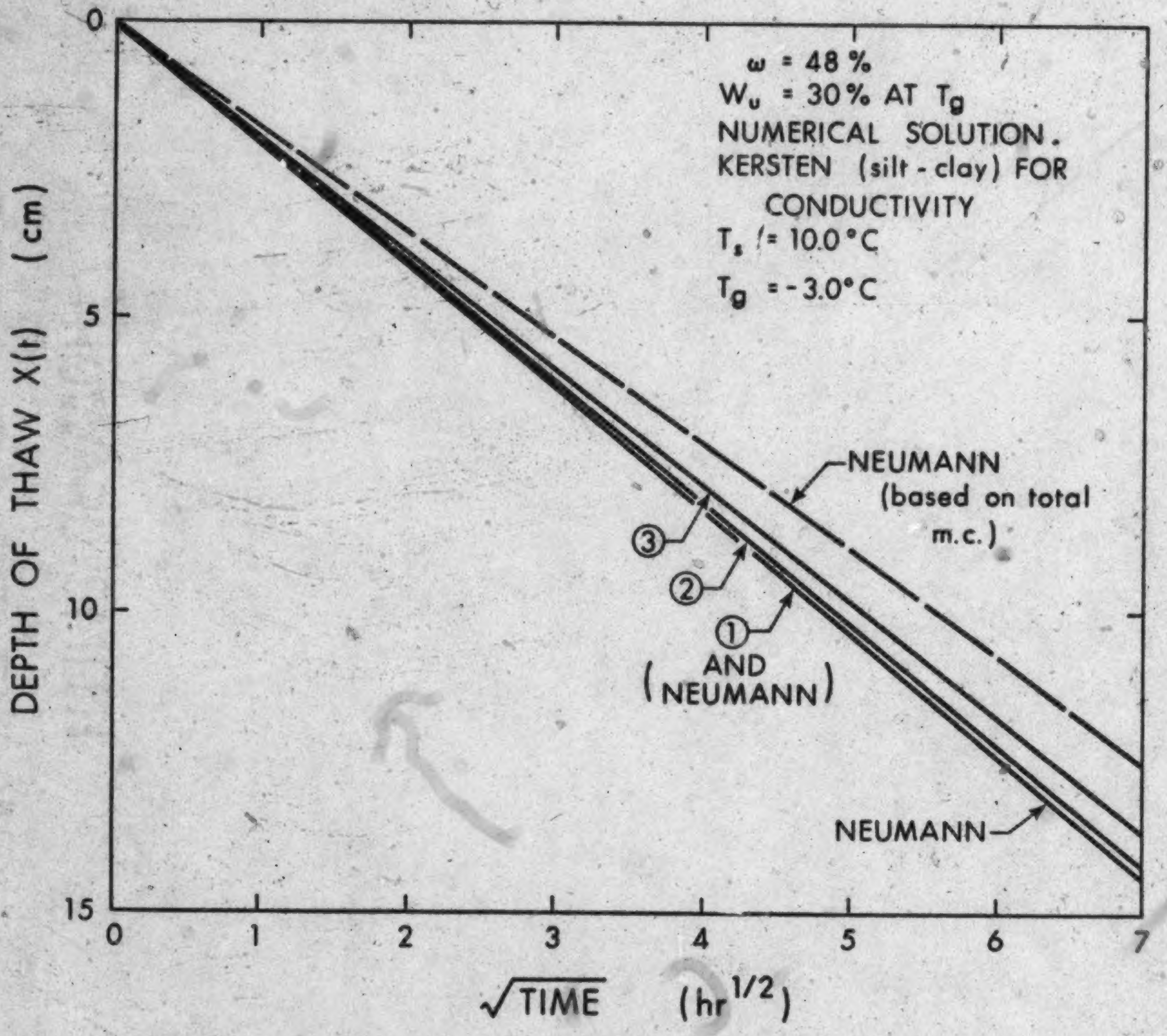

Fig. 2.11 Effect of unfrozen moisture content curve on depth of thaw

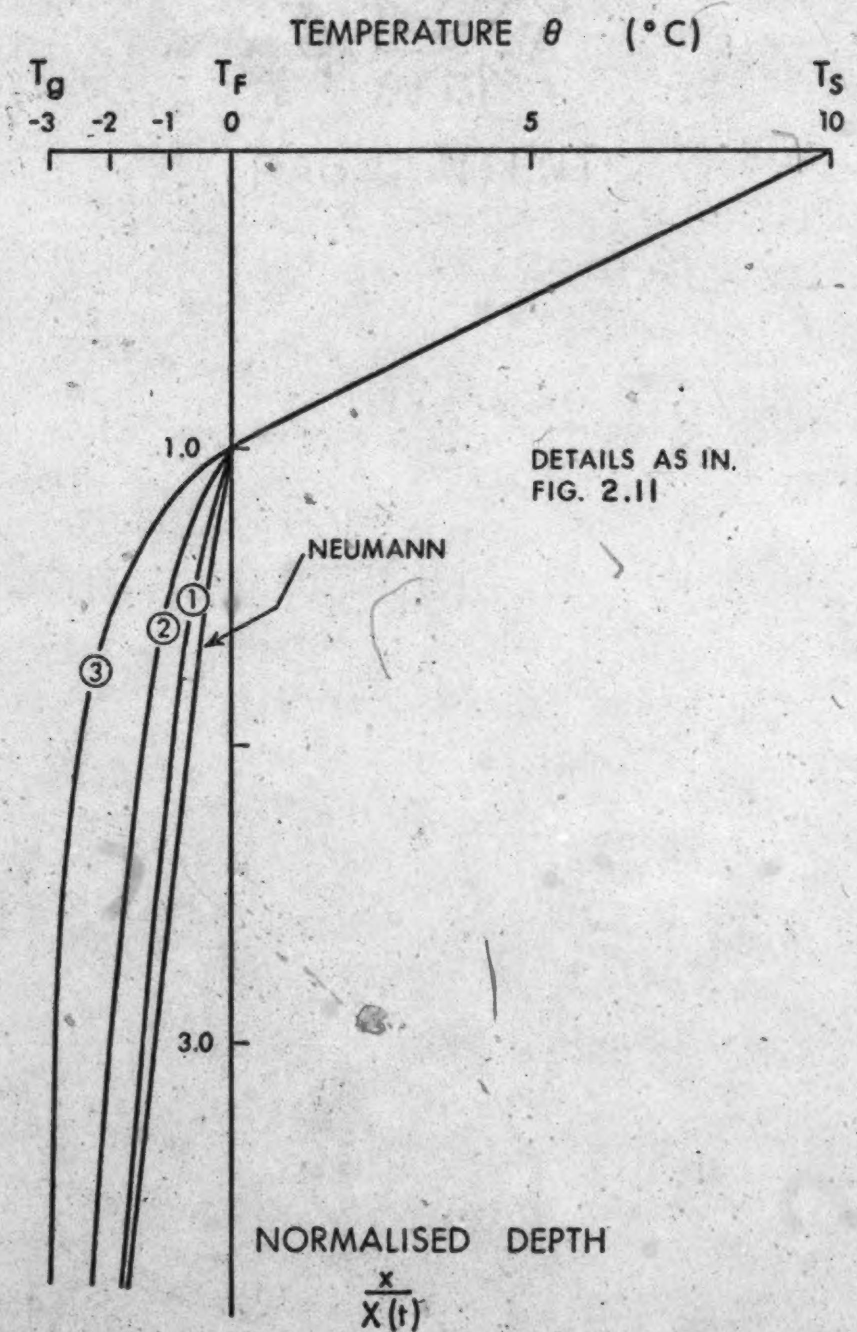

Fig. 2.12 Effect of unfrozen moisture content curve on temperature profile

thaw. This is true only if it is erroneously assumed that $W_u = 0$. It can be seen that the rate of thaw obtained by the Neumann analysis actually overestimates by an insignificant amount the α value calculated when the melting range is taken into account.

The agreement between a rigorously formulated model of heat conduction accounting for any reasonable phase dependence of conductivity and specific heat, and the Neumann solution presented on a single chart in Fig. 2.2 is remarkable, especially when the simplicity of the latter method is considered. There is no discernible difference between the α value calculated from the Neumann solution and that calculated from the first unfrozen moisture content curve in Fig. 2.10. The use of the second and third curves show very slight reduction in the α value.

Although there is little deviation in the rate of movement of the $0^{o}C$ isotherm, the temperature distributions in the frozen zone are certainly affected by the temperature dependent relationship. Temperature distributions for the same problems as solved in Fig. 2.11 are presented in Fig. 2.12.

The findings of this section might be usefully summarised at this point. In a problem involving the thawing of a frozen soil, the dominant variables are the ground surface temperature, the thermal properties of the thawed soil, and the total quantity of water that changes state in a unit volume of soil.

Two solutions are included for calculating an α value, the first being merely a graphical presentation of the Neumann solution in terms of three dimensionless variables. The second is a semi-empirical relationship which is accurate when the ground temperatures are close to zero.

The thermal properties of the frozen zone play an exceedingly minor role in the computation of thaw rates. It has been demonstrated that neither the absolute value nor the temperature dependence of the thermal conductivity of frozen ground is vital in calculating the depth or rate of thaw. For problems of geotechnical interest the use of the conductivity of ice equal to that of frozen soil will result in a sufficiently accurate solution. The volumetric heat capacity of frozen ground is easily estimated and small errors do not influence the thaw calculations significantly.

It has been found that when soils exhibit a range of melting temperature the depth to the $0^{o}C$ isotherm is still proportional to the square root of time for the boundary conditions of the Neumann problem. Moreover, it has been shown that there are no significant differences in the rate of thaw, α, calculated either by assuming that all ice involved in the change of state melts at $0^{o}C$, or by accounting for the melting range of ice in soil. In fact the melting range retards slightly the propagation of a $0^{o}C$ isotherm rather than accelerating it. A precise determination of the unfrozen water content - temperature curve is considered [illegible]necessary in a thawing problem provided that the correct quantity of water changing state is input to the analysis.

It can be concluded then that the solution obtained by lumping L as defined by eq. (2.14) is a satisfactory solution to rate of thaw problems. Ignoring temperature dependent latent heat effects introduces insignificant errors and, furthermore, is a mildly conservative assumption for soils.

2.4 The Effect of Thaw Strain on the Neumann Solution

As a thaw plane penetrates into a mass of frozen soil, considerable movements of the surface boundary may occur relative to the fixed frozen soil zone for a variety of reasons, the most important of which are dealt with in this section. When an element of frozen soil thaws, there is a volumetric contraction of approximately nine percent in the water phase of the soil. If the soil is saturated, this effect will be responsible for an instantaneous volumetric strain of nine percent of the volume fraction of water in the soil, or

$$S_{iw} = 0.09\ n\ X \tag{2.25}$$

where S_{iw} is the cumulative settlement due to the ice-water contraction,

n is the porosity of the thawed soil,

and X is the depth of thaw.

As the soil thaws, it may come under the influence of an externally applied stress, or perhaps just the influence of the self-weight of the soil itself. In either case, if pore water is present in excess of that normally in the soil pores under these stresses, the soil must consolidate by expelling excess pore fluids, causing a further strain on thawing. As will be shown in the next chapter, for many loading cases of practical interest, the degree of settlement, S/X, is a constant. It is considered useful then to combine the ice-water contraction and consolidation settlement in a relationship of the type

$$S = B\ X \tag{2.26}$$

where B is the total strain experienced by the soil in passing from a frozen to a thawed consolidated state.

This is done in order to assess the effect of thaw strains on the Neumann solution.

In general, the surface of application of the step increase in temperature moves relative to the frozen soil. This might also be the case in a situation where a hot pipeline was thawing the surrounding permafrost. If the bearing capacity of the soil were exceeded and the pipe were to sink into the soft thawed soil, the temperature source has moved closer to the thaw plane.

These effects are most easily examined by considering the plane of application of the surface temperature to be the zero point of the spacial co-ordinate x. This co-ordinate system places the frozen ground below in motion, with a velocity dS/dt which may be calculated from eq. (2.26) as

$$v = -\frac{dS}{dt} = -B\,\frac{dX}{dt} \tag{2.27}$$

The velocity v is negative if x is measured downwards.

A similar problem has been considered by Carslaw and Jaeger (1947) when accounting for the density change in the plane ice-water freezing problem. A solution is sought in which the position of the thaw line is given by

$$X = \alpha\sqrt{t} \tag{2.28}$$

and the temperature distribution in the thawed zone is given (as in the Neumann solution) by

$$\theta_1 = A\,\mathrm{erf}\left(\frac{x}{2\sqrt{\kappa_u t}}\right) \tag{2.29}$$

The equation of conduction of heat in the frozen zone moving with velocity v in the x-direction is derived for example by Carslaw and Jaeger (1947), and is

$$\frac{\partial\theta_2}{\partial t} = \kappa_u\,\frac{\partial^2\theta_2}{\partial x^2} - v\,\frac{\partial\theta_2}{\partial x} \tag{2.30}$$

Employing eq. (2.27) and (2.28) in eq. (2.30) yields

$$\frac{\partial \theta_2}{\partial t} = \kappa_u \frac{\partial^2 \theta_2}{\partial x^2} + B \frac{\alpha}{2\sqrt{t}} \frac{\partial \theta_2}{\partial x}, \qquad (2.31)$$

It may be verified that with the above value of X, eq. (2.31) is satisfied by

$$\theta_2 = C \operatorname{erfc} \left(\frac{x}{2\sqrt{\kappa_f t}} + \frac{\alpha B}{2\sqrt{\kappa_f}} \right) + D \qquad (2.32)$$

The constants C and D may be determined from the boundary conditions, and the temperature distributions for $\theta_1(x, t)$ and $\theta_2(x, t)$ may be shown to satisfy the governing equations and boundary conditions. The temperature distributions are not included here, but when substituted into the heat balance equation at the thaw interface, α may be determined as a root of the equation

$$\frac{e^{-\alpha^2/4\kappa_u}}{\operatorname{erf}\left(\frac{\alpha}{2\sqrt{\kappa_u}}\right)} - \frac{k_f}{k_u}\sqrt{\frac{\kappa_u}{\kappa_f}}\,\frac{T_g}{T_s}\,\frac{e^{-[\alpha(1+B)/2\sqrt{\kappa_f}]^2}}{\operatorname{erfc}\,[\alpha(1+B)/2\sqrt{\kappa_f}\,]}$$

$$= \frac{L\sqrt{\pi}\,\alpha}{2\sqrt{\kappa_u}\,c_u\,T_s} \qquad (2.33)$$

which is the same as the Neumann solution given by eq. (2.2), with the exception of the quantity (1 + B) appearing in the middle term.

The thaw strain number B only appears in a quantity which is known to have a minimal effect on α, (see Fig. 2.2) when the ground temperatures are close to zero. It is difficult to see how the effect of B on the rate of thaw α might be expressed generally in graphical form, so it is proposed to perform two sample calculations of α at two different ground temperatures in the range of interest. We assume the following typical set of properties.

$$T_s = +10^{\circ}C$$

$$\omega = 40\%$$

$$T_g = -3^{\circ}C \text{ and } -5^{\circ}C$$

$$B = 0.25.$$

A thaw strain of 25% is certainly a large value which is not encountered often in natural soils, and the ground temperature of $-5^{\circ}C$ represents a lower bound to many engineering field problems.

The calculations for α with a thaw strain of 25% and the specified ground temperatures were carried out using the revised equation (2.33), and the following results were obtained.

For $T_g = -3$; $\alpha = 0.0328 \text{ cm/s}^{1/2}$

and for $T_g = -5$; $\alpha = 0.0313 \text{ cm/s}^{1/2}$

The same calculations were carried out using the Neumann solution given in Fig. 2.2 which does not account for thaw strain, and these results were obtained.

For $T_g = -3$; $\alpha = 0.0329 \text{ cm/s}^{1/2}$

and for $T_g = -5$; $\alpha = 0.0314 \text{ cm/s}^{1/2}$

The deviation from the ordinary Neumann solution given in Fig. 2.2 when a large thaw strain is accounted for is, therefore, approximately 1 in 300, or 0.3%.

It is concluded that in the ground temperature range of interest, only negligible effects are observed when large thaw strains are accounted for theoretically. Consequently, provided the thaw depth, X, is measured from the point of application of the surface temperature, the effects of large strains in the thawing zone may be ignored completely.

This assumption was implicit in an analysis carried out by Brown and Johnston (1970) when calculating the depth of thaw under dikes constructed on permafrost at Kelsey, Manitoba. In this instance, the strains in the thawing soil were known to be approximately 30%. The analysis assumed a linear temperature profile in the thawed soil and ignored the temperature distribution in the frozen soil. On comparing the depth of thaw (measured from the ground surface) with observed thaw depths, excellent agreement was obtained using this simple analysis.

2.5 The Effect of Water Migration on the Neumann Solution.

In the previous section, the effects of large strains in the thawed zone were examined and found to be negligible. Although a considerable quantity of water must pass through the thawed soil to produce large thaw strains, the possible transfer of heat by the melt water migrating under an excess pore pressure gradient has not been considered. This component of heat transfer, which is sometimes known as advection, has not been incorporated in an analysis for thawing soils.

The equation of heat transfer in a thawed soil, including bulk motion of the pore fluid may be derived as follows. The derivation may be considered a coupling of the continuity of mass in the water phase and the equation of conductive heat transfer in a thawed saturated soil.

The conductive heat flux at x is

$$q = -k_u \frac{\partial \theta}{\partial x} \tag{2.34}$$

where $\theta(x, t)$ is the temperature distribution in the thawed soil.

The convective heat flux is

$$Q = c_\omega \theta \, v(x, t) \tag{2.35}$$

where c_ω is the volumetric heat capacity of water,

and $v(x, t)$ is the velocity of the pore fluid defined on the basis of total cross-sectional area.

The heat transfer equation may now be written as:

$$\frac{\partial}{\partial t}(c_u\,\theta) = -\frac{\partial Q}{\partial x} - \frac{\partial q}{\partial x} \qquad (2.36)$$

or

$$c_u\frac{\partial \theta}{\partial t} + \theta\frac{\partial c_u}{\partial t} = -\,c_\omega\,\theta\,\frac{\partial v}{\partial x} - c_\omega\,v\,\frac{\partial \theta}{\partial x} + \frac{\partial}{\partial x}\left(k_u\frac{\partial \theta}{\partial x}\right) \qquad (2.37)$$

Since

$$c_u = \gamma_d\,(0.17 + \frac{c_\omega}{\gamma_\omega}\,\omega)$$

then

$$\frac{\partial c_u}{\partial t} = \frac{\gamma_d}{\gamma\omega}\,c_\omega\,\frac{\partial \omega}{\partial t} = \frac{\gamma d}{\gamma\omega}\,\frac{c_\omega}{G_s}\,\frac{\partial e}{\partial t} \qquad (2.38)$$

where e is the void ratio,

ω is the water content,

G_s is the specific gravity of soil solids,

γ_d is the dry density = $G_s\gamma_\omega/(1 + e)$.

Replacing γ_d by its usual representation, we obtain from eq. (2.38)

$$\frac{\partial c_u}{\partial t} = c_\omega\,\frac{1}{1 + e}\,\frac{\partial e}{\partial t} \qquad (2.39)$$

Now the equation for continuity of fluids in a soil may be written as

$$\frac{1}{1 + e}\,\frac{\partial e}{\partial t} = -\,\frac{\partial v}{\partial x} \qquad (2.40)$$

and therefore from eq. (2.39)

$$\frac{\partial c_u}{\partial t} = c_\omega \frac{1}{1 + e} \frac{\partial e}{\partial t} = - c_\omega \frac{\partial v}{\partial x} \qquad (2.41)$$

Substituting this relationship in eq. (2.37), the terms in $\frac{\partial c_u}{\partial t}$ and $\frac{\partial v}{\partial x}$ cancel out, and we obtain

$$c_u \frac{\partial \Theta}{\partial t} = \frac{\partial}{\partial x} (k_u \frac{\partial \Theta}{\partial x}) - c_\omega v(x, t) \frac{\partial \Theta}{\partial x} \qquad (2.42)$$

and if k_u may be considered independent of position in the thawed soil, then

$$\frac{\partial \Theta}{\partial t} = \kappa_u \frac{\partial^2 \Theta}{\partial x^2} - \frac{c_\omega}{c_u} v(x, t) \frac{\partial \Theta}{\partial x} \qquad (2.43)$$

Equation (2.43) may be used to predict the thaw depth for an equation of consolidation in thawing soils, and in turn, the consolidation equation provides the pore fluid velocity v(x, t). Therefore, the heat transfer and consolidation equations might be solved numerically for arbitrary conditions of thawing, loading and drainage conditions in a thawing soil.

If an analytical solution to eq. (2.43) is desired for a step increase in temperature applied at x = 0, severe restrictions are placed on the form of the velocity function v(x, t). If a solution of the form

$$X = \alpha\sqrt{t} \qquad (2.44)$$

is sought, it appears to be possible only if

$$v(x, t) \propto \frac{dX}{dt} \qquad (2.45)$$

and it is doubtful if the case of a constant velocity might be solved.

Because of the obvious advantages in obtaining a solution in closed form, a velocity function of the type expressed by eq. (2.45) is adopted. It will be seen in succeeding chapters how these conditions for pore fluid velocity are achieved in many cases when a soil is thawing and expelling a constant quantity of excess pore fluid per unit depth. (See section 5.5 on the thawing of incompressible ice-rich soils).

Letting the excess ice content, expressed as a strain, be denoted by E_i, the pore water velocity is given by the product of excess pore fluid content and the velocity of the thaw front, that is

$$v(x, t) = - E_i \frac{dX}{dt} \tag{2.46}$$

where E_i is the constant thaw strain due to the expulsion of excess pore water.

Substituting eq. (2.46) into the governing eq. (2.43) provides

$$\frac{\partial\theta}{\partial t} = \kappa_u \frac{\partial^2\theta}{\partial x^2} + K_n \frac{dX}{dt} \frac{\partial\theta}{\partial x} \tag{2.47}$$

where $K_n = \frac{c_\omega}{c_u} E_i$ and is dimensionless.

A solution to the governing equation (2.47) in the thawed soil is sought in the form

$$\theta = A + B \operatorname{erf} \left(\frac{x}{2\sqrt{\kappa_u t}} + K_n \frac{\alpha}{2\sqrt{\kappa_u}}\right) \tag{2.48}$$

which ensures that the governing eq. (2.47) is satisfied. On obtaining the constants A and B from the boundary conditions of the thawed zone, the temperature distribution is given by

$$\theta = T_s - \frac{(T_s - T_f)\left\{\mathrm{erf}\left(\frac{x}{2\sqrt{\kappa_u t}} + K_n \frac{\alpha}{2\sqrt{\kappa_u}}\right) - \mathrm{erf}\left(K_n \frac{\alpha}{2\sqrt{\kappa_u}}\right)\right\}}{\mathrm{erf}\left(\frac{\alpha}{2\sqrt{\kappa_u}} + K_n \frac{\alpha}{2\sqrt{\kappa_u}}\right) - \mathrm{erf}\left(K_n \frac{\alpha}{2\sqrt{\kappa_u}}\right)} \qquad (2.49)$$

where T_s and T_f are the surface and freezing temperatures respectively.

The rate of thaw parameter, α, is determined as a root of the transcendental equation

$$\frac{e^{-\left(\frac{\alpha}{2\sqrt{\kappa_u}} + K_n \frac{\alpha}{2\sqrt{\kappa_u}}\right)^2}}{\mathrm{erf}\left(\frac{\alpha}{2\sqrt{\kappa_u}} + K_n \frac{\alpha}{2\sqrt{\kappa_u}}\right) - \mathrm{erf}\left(K_n \frac{\alpha}{2\sqrt{\kappa_u}}\right)} = \frac{\alpha L \sqrt{\pi}}{2\sqrt{\kappa_u}\, c_u (T_s - T_f)} \qquad (2.50)$$

The equation (2.50) has been derived ignoring the temperature distribution in the frozen ground. If T_g is not close to zero, then the middle term in eq. (2.33) may be included in eq. (2.50) to incorporate the effects of the temperature profile in the frozen zone. However, these effects have a minimal effect on α, and it is desired to isolate the effects of water migration in this study. Equation (2.50) is similar in form to the Neumann solution with $T_g = 0$, which has been discussed earlier. One new dimensionless quantity K_n is introduced however, which indicates the effect of the advective heat transfer in the thawed zone. The normalised thaw rate $\alpha/2\sqrt{\kappa_u}$ is shown plotted as a function of the Stefan number for two values of the ratio K_n in Fig. 2.13. The possible range of values for K_n must be between 0 and 0.5. As c_ω/c_u is usually around 1.4, then $K_n = 0.5$ implies that a thaw strain of 35% is occurring in the thawed soil due to the expulsion of excess pore fluids. As the value of α is affected so slightly in Fig. 2.13 by the possible ranges of K_n,

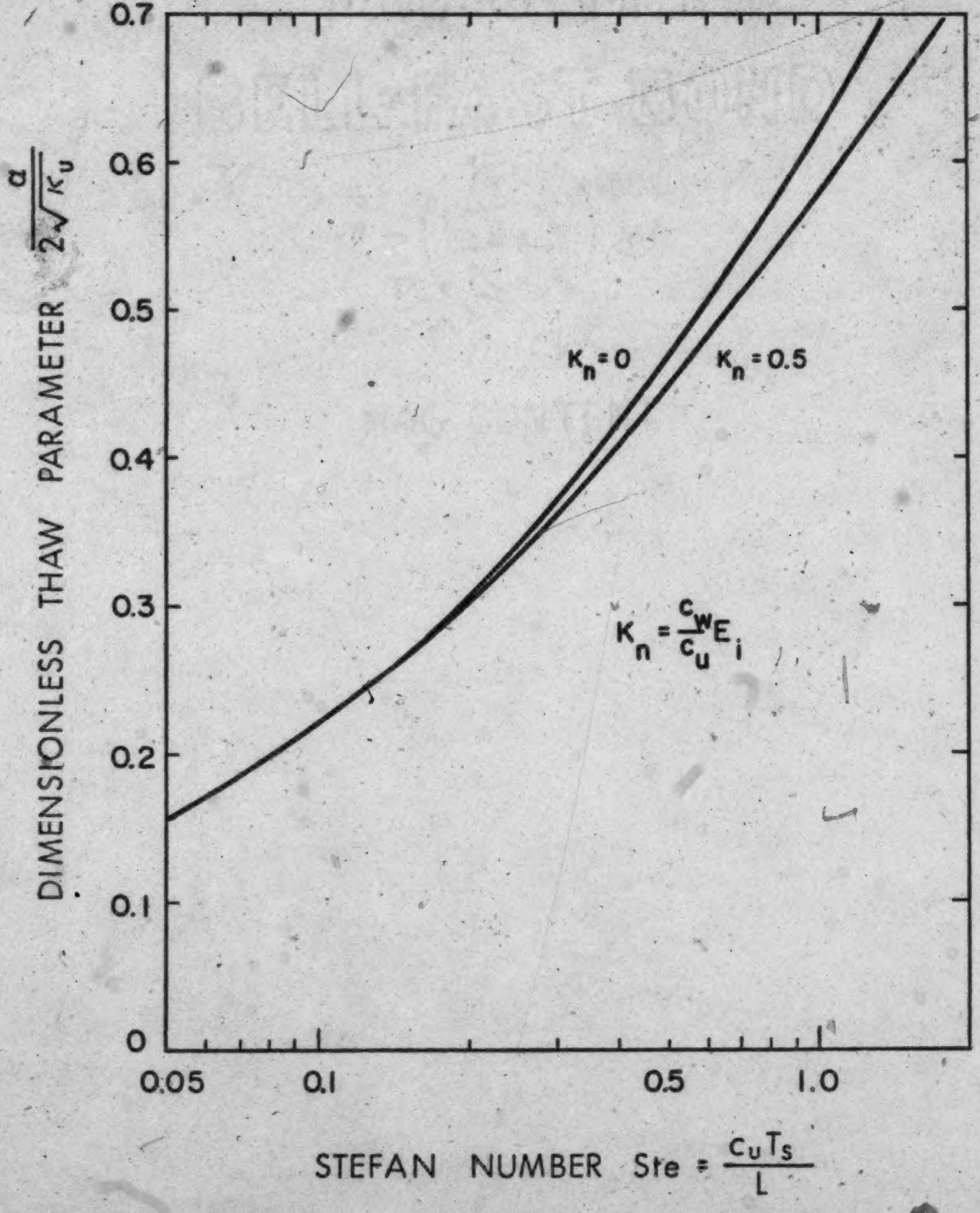

Fig. 2.13 Effect of melt water migration on normalised thaw rate

it is thought necessary to show only the two curves for $K_n = 0$, and $K_n = 0.5$. For lower values of the Stefan number, the effect of advective flow must be considered to be negligible. At extremely high values of Ste greater than unity, the effect of a large K_n value becomes noticable although still slight.

It may be concluded that from the results of the parametric study given in Fig. 2.13, that the effects of advective heat transfer in the thawed zone may be ignored in any practical analysis, without fear of incurring errors of greater than two or three percent. In addition, it may be noted that if the effects of water migration are ignored, then any errors incurred result in a slightly conservative estimation of the rate of thaw.

The other type of advective heat transfer which may be of concern is that due to lateral flow of water in a thawing slope or in the 'bulb' of thaw around a warm pipeline. If the flow is parallel to the slope of the ground, which is usually the case, then the flow of water in the thawed zone is parallel also to the temperature isotherms. Now, other than complex effects where the ground water enters and leaves the slope, ground water will not cross temperature isotherms, and therefore the heat transfer problem perpendicular to the ground surface is totally unaffected.

2.6 Time Dependent Surface Temperature.

It may often be necessary to investigate the velocity of a thaw front caused by surface temperature variations other than a step increase in temperature. In attempting to solve field problems within the framework of one-dimensional heat conduction, cases may arise in which the prescribed surface temperature bears little relation to a step increase in temperature.

The simplest method of introducing an arbitrary prescribed surface temperature into a method for calculating thaw depth in frozen soil is by the use of the Stefan solution. This solution assumes a linear temperature profile in the thawed zone, and ignores the temperature distribution in the frozen soil. The accuracy of the method has already been discussed in section 2.2 for the case of a step increase in temperature. If the surface temperature variation with time is denoted by the function $T_s(t)$, then the depth of thaw may be shown to be

$$X = \sqrt{\frac{2\, k_u \int_0^t T_s\, dt}{L}} \tag{2.51}$$

where $\int_0^t T_s\, dt$ is the area under the surface temperature-time curve, and is known as the Thaw Index.

This type of relationship is reviewed for example by Aldrich (1956).

The Thaw Index is usually given in units of degree days. Equation (2.51) might be applied to determine the thaw depth under arbitrary specification of the surface temperature, with the same order of accuracy as the simple Stefan solution for a step temperature described in section 2.2. As an example, the depth of thaw under a sinusoidal surface temperature application is expressed as follows. Let the surface temperature vary as a half sine wave between time 0 and time t_f, and denoting the maximum value by T_{max}, the expression for T_s is

$$T_s = T_{max} \sin \left(\frac{\pi t}{t_f}\right) \qquad (2.52)$$

and

$$\int_0^t T_s \, dt = \frac{T_{max} \, t_f}{\pi} \left(1 - \cos \frac{\pi t}{t_f}\right) \qquad (2.53)$$

Placing eq. (2.53) in eq. (2.51) the depth of thaw is expressed as

$$X = \sqrt{\frac{2 \, k_u \, T_{max} \, t_f}{\pi \, L} \left(1 - \cos \frac{\pi t}{t_f}\right)} \qquad (2.54)$$

As shown in Fig. 2.3, the Stefan solution for the step increase in surface temperature introduces significant over-estimations of the thaw rate α as the Stefan number increases. The Stefan number is defined as $c_u \, T_s/L$ and the solution given by eq. (2.51) assumes that the "sensible heat" $c_u \, T_s$ is small in comparison with L. Therefore a steady state or linear type of temperature distribution is valid. However, if $c_u \, T_s$ becomes larger, then some curvature of the thawed temperature profile results, and it is useful to consider the addition of an extra term to increase the order of accuracy.

An analysis which increases the order of accuracy in this way has been performed by Lock et al. (1969). Solutions are presented for the movement of the thaw interface due to the application of sinusoidal and power law expressions for the surface temperature. The analysis is subsequently extended by Lock (1971) to include arbitrary excursions of the surface temperature. The results for the sinusoidal and power law temperature functions are summarised here, and a sample problem solved.

If a sinusoidal surface temperature history is adopted, then the surface temperature for a thaw season of 180 days is written in a consistent notation as

$$\frac{T_s}{T_{max}} = \mathrm{Sin}\left(\frac{t}{t_c}\right) \tag{2.54}$$

where T_{max} is the peak surface temperature,

and t_c is a reference time of $180/\pi$ days.

The depth of thaw is given by

$$X = \sqrt{\frac{k\ T_{max}\ t_c}{L}} \left\{ 2\ \mathrm{Sin}\left(\frac{t}{2t_c}\right) - \frac{Ste}{3}\ \mathrm{Sin}\left(\frac{t}{2t_c}\right) \mathrm{Sin}\left(\frac{t}{t_c}\right) \right\} \tag{2.55}$$

An example of the use of this relationship is given later in section 5.2, and Fig. 5.5 presents the thaw interface history for a particular problem. If an equivalent step temperature is calculated as shown in Fig. 5.5, a thaw rate shown by the dotted line in Fig. 5.5 results. The equivalent step temperature is defined as that constant surface temperature which would give the same thaw index over the thaw season as the surface temperature sine wave. The equivalent step may be shown from eq. (2.53) to be

$$T_s = 2\ T_{max}/\pi \tag{2.56}$$

The thaw interface velocities for the sinusoidal and equivalent step temperature applications are also shown in Fig. 5.5, and are markedly different. The significance of this in geotechnical studies is indicated also in section 5.2.

The solution for depth of thaw in a soil whose surface temperature varies according to a power law between 0^oC and T_{max} over a time period of t_f is given by Lock et al. (1969) as

$$X = \sqrt{\frac{k_u\ T_{max}\ t_f}{L}}\left\{\left(\frac{2}{n+1}\right)^{1/2}\left(\frac{t}{t_f}\right)^{(n+1)/2} - \frac{Ste}{6}\left(\frac{2}{n+1}\right)^{1/2}\left(\frac{t}{t_f}\right)^{(3n+1)/2}\right\} \qquad (2.57)$$

where the surface temperature is described by

$$\frac{T_s}{T_{max}} = \left(\frac{t}{t_f}\right)^n \qquad (2.58)$$

and n is an arbitrary power.

When n = 0, the solution for the step temperature increase is recovered. As pointed out by Lock et al. (1969), that if the surface temperature recrosses the freezing point of the material, then the final depth of thaw is the same as that predicted by the simpler Stefan solution given by eq. (2.54). Therefore, if one were interested solely in the maximum thaw depth at the end of a thaw season, the correct result is already contained in the simpler Stefan solution.

2.7 Thawing in a Two Layer Profile.

In many field problems of practical interest, the assumption that a deposit of frozen soil is uniform with depth may be entirely unrealistic due to the presence of a surficial soil layer having different thermal properties. Many undisturbed locations in Arctic regions exhibit an organic layer of varying thickness, overlying a mineral soil with a considerably lower moisture content. Examples of a surficial layer which has no latent heat associated with it might also be cited, such as a gravel layer, styrofoam sheet or pavement surface. In general, a layer of different thermal properties is introduced between the temperature application and the plane where melting occurs.

No exact analytical solution exists for this problem, but bearing in mind the minor inaccuracies involved, the problem may be easily handled by the Stefan assumption of a linear temperature distribution in the thawed zone. Multi-layered soil profiles are handled in this manner by the U.S. Department of the Army (1966), but it is of interest to perform an analysis for a two-layer profile, as it represents the most common departure from homogeneity.

Consider in Fig. 2.14 the case of a surficial layer of height H, thermal conductivity k_1, and latent heat L_1, overlying an infinite depth of soil with properties k_2 and L_2. Ignoring the temperature distribution in the frozen soil, it is then evident that the time to thaw the overlying layer completely due to the application of a step increase in surface temperature is given by

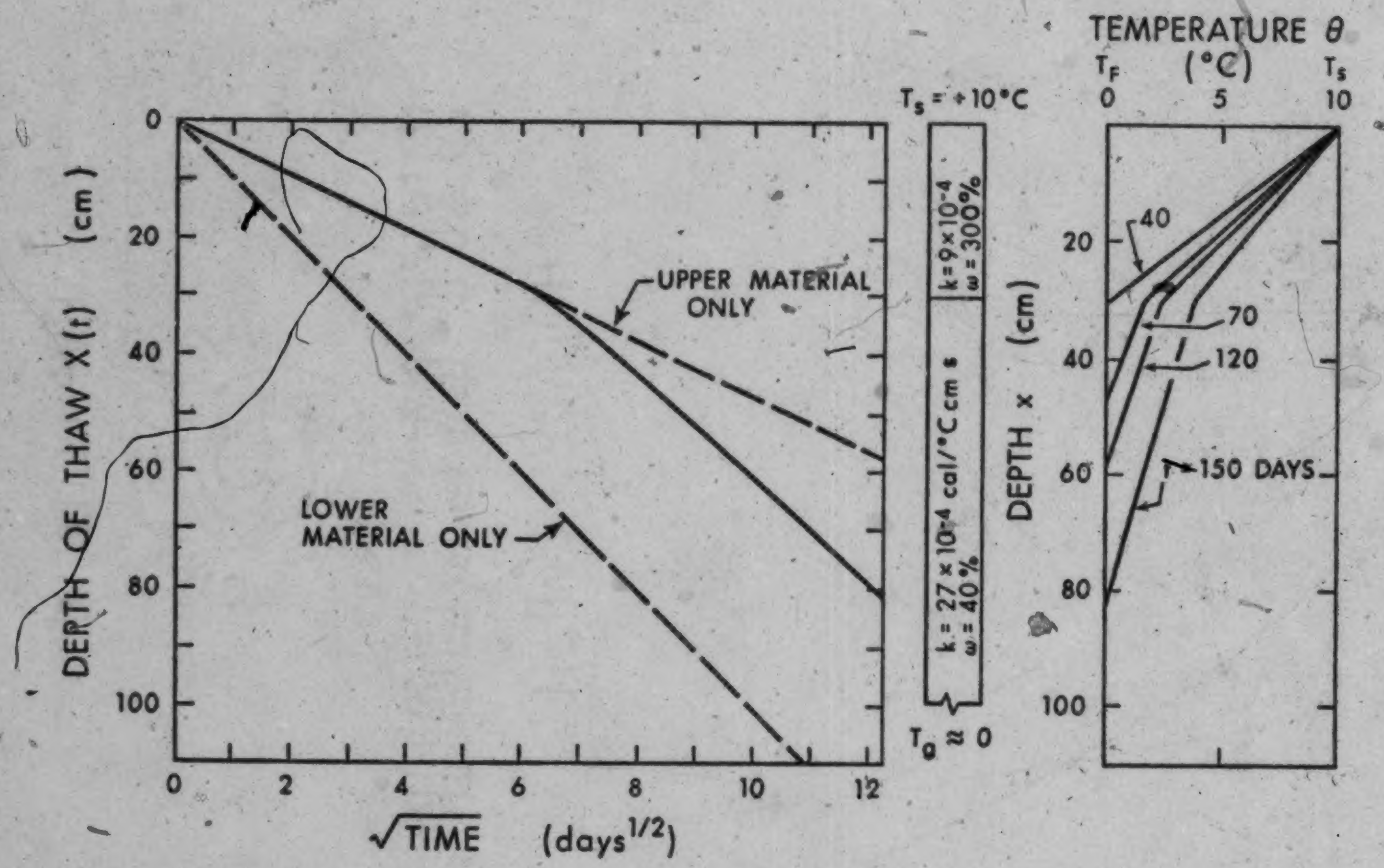

Fig. 2.14 Thawing in a two-layer system

$$t_o = \frac{H^2 L_1}{2k_1 T_s} \tag{2.59}$$

since

$$\alpha = \sqrt{\frac{2k_1 T_s}{L_1}}$$

from the Stefan solution for layer 1.

When the depth of thaw X becomes greater than H, two layers of different thermal properties co-exist in the thawed zone. Assuming, for consistency with the Stefan solution that the temperature distribution in each layer is linear, a simple solution for the rate of thaw in the underlying layer may be derived.

The heat balance relationships are:

at x = H,

$$k_1 \frac{\partial \theta_1}{\partial x} = k_2 \frac{\partial \theta_2}{\partial x} \tag{2.61}$$

and at x = X(t),

$$-k_2 \frac{\partial \theta_2}{\partial x} = L_2 \frac{dX}{dt} \tag{2.62}$$

where $\frac{\partial \theta_1}{\partial x}$ and $\frac{\partial \theta_2}{\partial x}$ are the temperature gradients in layers 1 and 2 respectively.

This leads eventually to the depth of thaw

$$X = \sqrt{\left(\frac{k_2}{k_1} H\right)^2 + \frac{2k_2 T_s (t-t_o)}{L_2}} - \left(\frac{k_2}{k_1} - 1\right) H \tag{2.63}$$

and the interface temperature between the two layers $T_1(t)$ is given by

$$T_1 = \frac{T_s}{1 - \left(\frac{H}{H - X}\right)\frac{k_2}{k_1}} \tag{2.64}$$

The melting temperature is always taken to be zero.

A sample solution is included in Fig. 2.14 for the case of a peat layer overlying a fine-grained soil of 40% moisture content. The thaw rate through the lower material only is shown as a dotted line, and at large times the thaw rate becomes parallel to the thaw rate for the two layer system. The results of the simplified solution were checked rigorously by a finite difference solution, and the results found to be in good agreement. Linear temperature profiles were maintained in each layer throughout the thawing process. Seider and Churchill (1965) also note the maintenance of linear temperature distributions in a two-layer system of insulation and soil.

The analysis may be applied also to calculating rates of thaw in the underlying soil when the surficial layer is dry, or without latent heat, as might be the case with materials such as gravel or styrofoam. In this case, as no latent heat "barrier" is present in the overlying layer, a linear profile of temperature is assumed to be established in the upper layer instantaneously. This assumption can be shown to be perfectly justified by considering the time factor $\kappa t/H^2$ for the upper layer. Experience with solutions to problems of the heat conduction type would indicate a time factor of 0.5 to be adequate to establish an almost linear profile of temperature in the upper layer. The time to achieve this time factor is

$$t = 0.5\ H^2/\kappa \tag{2.65}$$

For a one foot layer of dry sand, for example, the time to establish a linear temperature profile would be of the order

$$t = 0.5 \times 900/2 \times 10^{-3} = 2.2 \times 10^5 \text{ seconds}$$

which is approximately three days. This time span is likely insignificant when considering the depth of thaw over a complete thaw season, or the life-time of an engineering structure on thawing ground. If large depths of gravel are under consideration, however, a complete numerical solution to the problem might be advisable.

2.8 Thawing Around a Warm Pipe in Permafrost.

Considerable problems are associated with the production of hot oil from vertical wells completed through deep deposits of permafrost. A thaw annulus is expected to grow to 50 or 60 feet within the first two decades of operation of such a vertical well (Palmer, 1972), (Koch, 1971). Just as dramatic are the thermal effects of a heated surface transportation pipeline on the surrounding permafrost.

Lachenbruch (1970) has presented estimates of the growth of the thaw 'bulb' around a horizontal hot pipeline in the Arctic. The stability of a hot pipeline buried in sediments that are underconsolidated when thawed is a cause of much concern. This is not because of the melting in itself, but because of the effects of the rapid rate of melting on the stability of the thawed foundation.

Although a fairly complex two-dimensional problem in heat transfer must be solved to obtain the rate of melting around the pipe, the most critical rate of thawing occurs vertically below the pipe axis. The relationship between thaw depth and time under the pipe may then be used in a one-dimensional analysis to determine the rate of consolidation of the soil under the centre-line of the pipe.

The depth of thaw under the centre-line of a 48 inch hot pipe is plotted with time by Lachenbruch (1970) for two soil moisture contents and two ground temperatures. It is found that if the depth of thaw is plotted against $(\text{time})^{0.3}$, an almost perfect linear relationship is obtained in Fig. 2.15. It appears that the depth of thaw in this type of thawing configuration might be expressed as

$$X = Bt^{0.3} \tag{2.66}$$

where B is the thaw depth under the pipe centre-line after one year.

If the hot pipe configuration envisaged by Lachenbruch were considered to be a one-dimensional thawing situation, the Neumann solution might be used to solve the problem. This is equivalent to applying a step temperature over the complete surface of the half-space, instead of the limited surface directly affected by the pipeline. This approach would obviously be expected to over-estimate the thaw depth under the pipe axis. However, for a short time at the initiation of thawing, the thaw depth should be well approximated by a one-dimensional analysis. As the depth of thaw becomes significantly

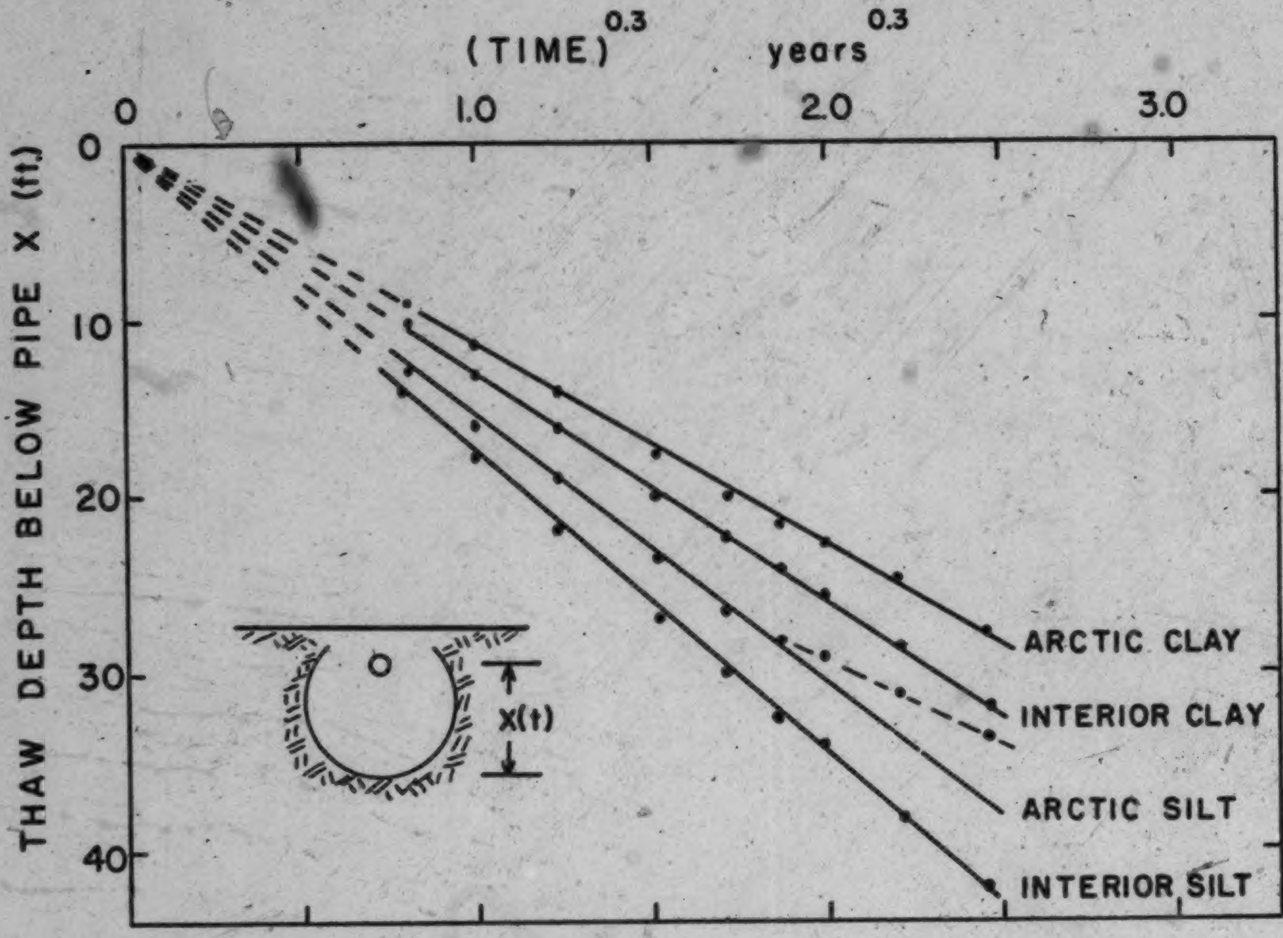

Fig. 2.15 Thaw depth below pipe axis fitted to $X = Bt^{0.3}$

larger than the pipe diameter, two-dimensional effects become more important. Using the thermal properties and temperatures given by Lachenbruch (1970), an α value may be calculated from the Neumann solution, and the depth of thaw compared with the rigorous two-dimensional numerical calculations performed by Lachenbruch. The calculations for the one and two dimensional cases were carried out using a moisture content of 65% for 'clay', and 17 1/2% for 'silt'. The 'Arctic' location is assumed to have a ground temperature of -8.9 C, and -0.8°C for the 'interior'. The temperature of the hot pipe is taken as 80°C. The one-dimensional α value represents the Neumann solution for these thermal properties (locations). The depth of thaw under a surface temperature which is applied over an infinite surface area is given as usual by

$$X = \alpha\sqrt{t}$$

The corresponding B values for these locations are taken from the two-dimensional analysis given by Lachenbruch, where the thaw depth is calculated (as demonstrated in Fig. 2.15) from

$$X = Bt^{0.3}$$

At a time of one year after commencing operation, $\sqrt{t}$ and $t^{0.3}$ are both unity, and therefore the α and B values for the different locations given in Table 2.2 represent the depth of thaw in feet after one year.

The depths of thaw using these one and two-dimensional representations are calculated also for a time of 0.5 years. For a pipe with a diameter of four feet, Table 2.2 indicates that no serious error is incurred by the one-dimensional analysis, providing the thaw depth does not exceed approximately 10 feet. When the thaw depth is at 14 feet, the one-dimensional analysis overestimates the correct thaw depth by 2 feet. At later times, the error in the one-dimensional solution becomes progressively larger as expected.

The fact that the depth of thaw under the centre-line of a hot pipe can be well approximated by a one-dimensional analysis for the first half-year of operation is used when analysing the data from a test pipeline loop at Inuvik, N.W.T. The field results show that one-dimensional heat flow conditions are preserved at early times, and this proves extremely useful in the analysis of the initial (and usually the most critical) excess pore pressure conditions in the thawing pipeline foundation. These predicted and observed thaw rates are described in detail in section 6.3.

TABLE 2.2 COMPARISON OF ONE AND TWO-DIMENSIONAL CALCULATIONS FOR THAW DEPTH UNDER A 48 INCH HOT PIPE

Location	1 - D α value ($ft/yr^{1/2}$)	2 - D B value ($ft/yr^{0.3}$)	1 - D Thaw Depth at t = 1/2 year	2 - D Thaw Depth at 1/2 year
Arctic Clay	13.06	11.5	9.23	9.0
Interior Clay	13.92	13.0	9.84	10.0
Arctic Silt	21.13	15.3	14.94	13.0
Interior Silt	22.67	17.4	16.03	14.0

CHAPTER III

THE ONE-DIMENSIONAL CONSOLIDATION OF THAWING SOILS

3.1 Introduction.

In the previous chapter it is described how a solution to the problem of melting in a permafrost soil might be established. The movement of the 0^oC isotherm with time may be determined from the heat transfer problem, and this isotherm is assumed to form the moving lower boundary to the region of interest in the associated problem of soil consolidation. The frozen soil does not enter into deliberations on soil consolidation, as it does not transmit large quantities of pore fluids, or participate in any significant deformations.

On thawing, the soil becomes a compressible porous medium, characterised by finite values of compressibility and permeability. The final effective stress in the soil may be calculated from a consideration of the total stress and the hydrostatic pore water pressure. The initial stresses in the thawed soil may be quantified by experiment, or as will be seen later, some rational assumptions may be made. Consequently the intermediate transient pore water stresses and effective stresses in the thawed soil might be described by a consolidation equation written in terms of excess pore water pressures.

It is proposed to work for the present within the framework of the linear Terzaghi consolidation theory. This theory of course involves several limiting and almost certainly inexact assumptions regarding the behaviour of the soil skeleton and the flow of water within the pore spaces of the soil. Frozen soil is a complex, non-homogeneous medium comprising at least three phases, and it is recognised that the subsequent consolidation of the thawed soil is probably a much more complicated process than the behavioural description that follows. However, the same might be said about the behaviour under load of natural unfrozen soil, yet it is encouraging to see the substantial power of simple theories such as the Terzaghi theory in accounting for a wide variety of phenomena in the field. Moreover, simplicity of a theory has the advantage that the results are often applicable to practice with greater ease. Subsequently, the limitations of the theoretical results are readily defined. Therefore, while cognizant of the limitations, in the following paragraphs the settlement of a thawing soil is explored using a well known theory of soil consolidation combined with a simple but important solution in heat transfer.

3.2 Formulation of the Linear Theory of Thaw-consolidation.

As illustrated in Fig. 3.1, a one-dimensional configuration is considered where a 'step' increase in temperature is imposed at the surface of a semi-infinite mass of frozen soil which is homogeneous and isotropic with respect to thermal and consolidation properties. The solution to the problem in heat conduction is presented in Chapter 2, and the movement of the thaw plane is given by

$$X(t) = \alpha\sqrt{t} \qquad (3.1)$$

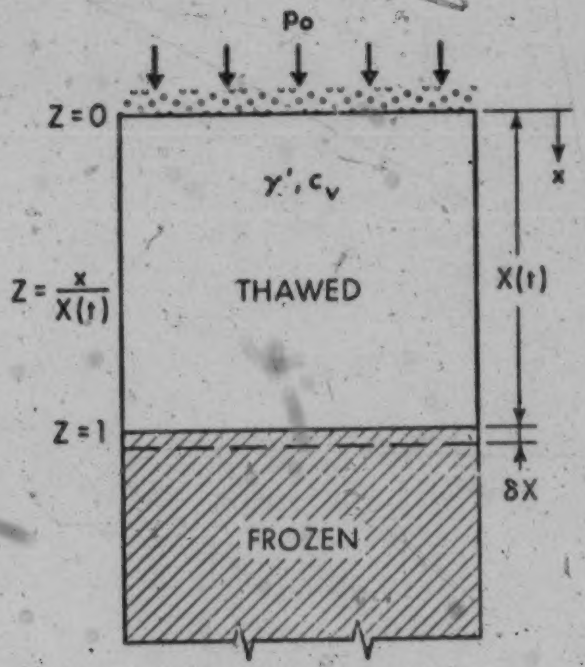

Fig. 3.1 One-dimensional thaw-consolidation

Other rates of thaw shall be considered in a later section.

The lower boundary of the consolidating soil is now defined. The governing equation of consolidation is

$$c_v \frac{\partial^2 u}{\partial x^2} = \frac{\partial u}{\partial t} - \frac{\partial \sigma}{\partial t} \tag{3.2}$$

where $u(x,t)$ denotes the excess pore pressure,

x denotes the depth measured from the ground surface,

σ denotes the total stress applied at the surface,

and c_v denotes the coefficient of consolidation.

If the applied stress does not vary with time, then eq. (3.2) becomes

$$0 < x < X(t) \; ; \qquad c_v \frac{\partial^2 u}{\partial x^2} = \frac{\partial u}{\partial t} \quad ; \quad t > 0 \tag{3.3}$$

The same limitations inherent in the derivation of this equation when applied to other problems in soil mechanics will also apply to thawing soils. The linear void ratio-effective stress relationship for instance may introduce considerable errors if the soil is exceedingly ice rich. In this case, large volume changes must occur before significant increases in effective stress take place.

The thawed soil is also assumed to be saturated, and therefore any solutions obtained will tend to overestimate the magnitude of the pore pressure if an air phase is present.

Boundary Conditions

We now consider the boundary conditions necessary to obtain a solution to the consolidation problem.

From eq. (3.1) it is obvious that initially, the thawed region does not exist, so the initial condition is

$$X = 0; \quad t = 0 \tag{3.4}$$

The upper surface of the soil is taken to be free-draining, and so

$$x = 0; \quad u = 0; \quad t > 0 \tag{3.5}$$

At the freeze-thaw interface, a balance between the rate of liberation of excess pore fluids and their discharge from the thaw line must be established.

If the soil is thawing very slowly and the discharge capability of the soil is large, then any pore fluids liberated will be expelled from the thaw line, and settlements will proceed concurrently with thawing. However, if a fast rate of thaw is maintained, and the discharge capacity of the thawed soil is not sufficient to expel all excess pore fluids, then excess pore pressures will be generated in the soil.

As the soil is compressible, the boundary condition states that any flow from the thaw line is accommodated by a change in volume of the soil. Consistent with Darcy's Law, the rate of expulsion of water from the thaw line is

$$\frac{dV}{dt} = -\frac{Ak}{\gamma_\omega} \frac{\partial u}{\partial x} (X,t) \tag{3.6}$$

where A is the cross-sectional area of an element,

k is the permeability of the soil,

$\frac{\partial u}{\partial x}(X, t)$ is the excess pore pressure gradient at the thaw interface,

and γ_ω is the unit weight of water.

In a small time increment Δt the thaw plane advances a distance ΔX. The volume of the soil element so thawed is

$$V = A \Delta X \tag{3.7}$$

The volume of water expelled from this soil element from eq. (3.6) is

$$\Delta V = -\frac{Ak}{\gamma_\omega} \frac{\partial u}{\partial x}(X,t)\, \Delta t \tag{3.8}$$

and is equal to the change in volume of the element.

Combining eq. (3.7) and (3.8) yields the volumetric strain in the soil element

$$\frac{\Delta V}{V} = -\frac{k \frac{\partial u}{\partial x}(X, t)}{\gamma_\omega \frac{dX}{dt}} \tag{3.9}$$

For a compressible soil, the volumetric strain is related to the effective stress by a relation such as

$$\frac{\Delta V}{V} = - m_v \Delta\sigma' \tag{3.10}$$

where m_v denotes the coefficient of volume compressibility, and $\Delta\sigma'$ is the change in effective stress corresponding to the volumetric strain.

Combining (3.9) and (3.10) gives

$$\Delta\sigma' = \frac{c_v \cdot \frac{\partial u(X,\ t)}{\partial x}}{\frac{dX}{dt}} \tag{3.11}$$

where the coefficient of consolidation is given by

$$c_v = \frac{k}{m_v\ \gamma_\omega} \tag{3.12}$$

The total stress at $x = X$ is

$$\sigma(X,\ t) = P_o + \gamma\ X \tag{3.13}$$

where P_o is the surface applied stress,

and γ is the bulk unit weight of the thawed soil.

At the thaw line the pore pressure is the sum of the excess and hydrostatic components

$$P_\omega(X,\ t) = u(X,\ t) + \gamma_\omega X \tag{3.14}$$

and so by definition the effective stress is

$$\sigma'(X,\ t) = \sigma(X,\ t) - P_\omega(X,\ t) = P_o + \gamma' X - u(X,\ t) \tag{3.15}$$

where γ' denotes the submerged unit weight of the soil.

The effective stress increment at the thaw line is the current effective stress less the initial effective stress, that is

$$\Delta\sigma' = \sigma'(X,\ t) - \sigma_o' \qquad (3.16)$$

where σ_o' denotes the effective stress in the soil if no consolidation were permitted on thawing, and is called the *residual stress.*

Combining eq. (3.15) and eq. (3.16) we find

$$\Delta\sigma' = P_o - \sigma_o' + \gamma' X - u(X,\ t) \qquad (3.17)$$

and placing this expression (3.17) in eq. (3.11) gives the relevant boundary condition at the thaw line

$$\text{at } x = X(t);\ \ P_o - \sigma_o' + \gamma' X - u = \frac{c_v \frac{\partial u}{\partial x}}{\frac{dX}{dt}}\ ;\ \ t > 0 \qquad (3.18)$$

There have been previous attempts to establish the boundary condition at the thaw line but they have been either incomplete (Tsytovitch et al. 1965) or incorrect (Zaretskii, 1968). The condition proposed by Zaretskii is similar to that developed here. However, in his derivation he takes a change in water content of the soil to be equal to the volumetric strain of an element and thereby introduces errors into his solution.

3.3 Solution of the Linear Equation of Thaw-consolidation.

The analytical solution to the linear Terzaghi consolidation equation (3.3) subject to the boundary conditions expressed by equations (3.1), (3.5) and (3.18) is required.

The essential feature to be contended with in problems of this type is the existence of a moving boundary. In the mathematical treatment it is necessary to satisfy a pore pressure condition at this moving boundary. For this reason, it might be anticipated that an exact solution for this type of problem could be difficult to obtain. For arbitrary rates of thaw, this is indeed the case, however the mathematical complexities are reduced considerably if thawing is considered to be proportional to the square root of time.

There are two methods of obtaining an exact analytical solution (if one exists) to a problem of this nature. The first employs direct methods such as the separation of variables technique or the Laplace transform, while the second employs indirect methods. An example of the latter is the semi-inverse method. A solution of a certain form is assumed and if, on evaluating the required constants from the boundary conditions, it is shown to satisfy all the necessary equations, it is the unique solution to the problem. An example of this method of attack is seen in the solution of the Neumann freezing problem in Carslaw and Jaeger (1947), p. 283-286.

However, a more satisfactory method of obtaining a solution is by the more direct separation of variables technique. The boundary condition (3.18) contains the quantities $(P_0 - \sigma_0')$, which is a constant, and the term $\gamma'X$, which is proportional to the square root of time. So it is necessary to derive a solution separately for each of these loading conditions, and then superimpose the results. Superposition of results is permissible here as both the equation of consolidation and the boundary conditions are linear.

Self-Weight Loading.

Setting $(P_o - \sigma_o')$ temporarily equal to zero, eq. (3.18) becomes

$$\gamma' X - u = \frac{c_v \frac{\partial u}{\partial x}}{\frac{dX}{dt}} \qquad (3.19)$$

Applying the transformation

$$z = \frac{x}{X(t)} \qquad (3.20)$$

to eq. (3.3), provides

$$\frac{\partial u}{\partial x} = \frac{1}{X} \frac{\partial u}{\partial z}$$

$$\frac{\partial^2 u}{\partial x^2} = \frac{1}{X^2} \frac{\partial^2 u}{\partial z^2}$$

The time derivative in the new (moving) co-ordinate system is transformed by

$$\left.\frac{\partial u}{\partial t}\right|_{\text{in } x} = \left.\frac{\partial u}{\partial t}\right|_{\text{in } z} + \frac{\partial u}{\partial z} \frac{dz}{dt}$$

$$= \left.\frac{\partial u}{\partial t}\right|_{\text{in } z} + \frac{\partial u}{\partial z} \frac{dz}{dX} \frac{dX}{dt}$$

From eq. (3.20) $\frac{dz}{dX} = - \frac{x}{X^2} = - \frac{z}{X}$

and so the time derivative becomes

$$\left.\frac{\partial u}{\partial t}\right|_{\text{in } x} = \left.\frac{\partial u}{\partial t}\right|_{\text{in } z} - \frac{z}{X}\,\frac{dX}{dt}\,\frac{\partial u}{\partial z} \qquad (3.21)$$

Substituting these derivitives in the consolidation equation yields

$$\frac{\partial u}{\partial t} = \frac{c_v}{X^2}\,\frac{\partial^2 u}{\partial z^2} + \frac{z}{X}\,\frac{dX}{dt}\,\frac{\partial u}{\partial z} \qquad (3.22)$$

The boundary conditions (3.5) and (3.19) become

$$z = 0\ ; \quad u = 0\ ; \quad t \geq 0 \qquad (3.23)$$

$$z = 1\ ; \quad \gamma' X - u = \frac{c_v \frac{\partial u}{\partial z}}{X \frac{dX}{dt}}\ ; \quad t > 0 \qquad (3.24)$$

Separating the variables z and t requires a solution of the form

$$u(z,\ t) = F(z).\ G(t) \qquad (3.25)$$

It may be shown that this is only possible if

$$G(t) = \sqrt{t}$$

or $$u = F(z).\sqrt{t} \qquad (3.26)$$

Substituting (3.1) in equations (3.22) and (3.24) gives

$$\frac{\partial u}{\partial t} = \frac{c_v}{\alpha^2 t}\,\frac{\partial^2 u}{\partial z^2} + \frac{z}{2t}\,\frac{\partial u}{\partial z} \qquad (3.27)$$

and $$\gamma' \alpha \sqrt{t} - u = \frac{2\,c_v}{\alpha^2}\,\frac{\partial u}{\partial z} \qquad (3.28)$$

By differentiating eq. (3.26), the following equalities are written as

$$\frac{\partial u}{\partial z} = \frac{dF}{dz}\sqrt{t}$$

$$\frac{\partial^2 u}{\partial z^2} = \frac{d^2F}{dz^2}\sqrt{t}$$

and $$\frac{\partial u}{\partial t} = \frac{F}{2\sqrt{t}}$$

Substituting these derivatives into eq. (3.23), (3.27) and (3.28), we obtain in terms of F(z)

$$\frac{d^2F}{dz^2} + \frac{\alpha^2}{2\,c_v}\left\{z\frac{dF}{dz} - F\right\} = 0 \qquad (3.29)$$

$$z = 0\ ; \qquad F = 0 \qquad (3.30)$$

$$z = 1\ ; \qquad \gamma'\alpha - F = \frac{2\,c_v}{\alpha^2}\frac{dF}{dz} \qquad (3.31)$$

Equations (3.29) and (3.31) are now reduced to ordinary differential equations, functions of the dependent variable z only.

The complete solution to (3.29) in Gibson (1958) is

$$F(z) = A\left[e^{-\frac{\alpha^2 z^2}{4\,c_v}} + \frac{\alpha\,z\sqrt{\pi}}{2\sqrt{c_v}}\ \mathrm{erf}\left(\frac{\alpha\,z}{2\sqrt{c_v}}\right)\right] + Bz \qquad (3.32)$$

(It is noted here that the square root sign in the error function term was erroneously omitted in Gibson (1958)).

The constants A and B are determined from eq. (3.30) and (3.31). From eq. (3.30), at $z = 0$, the terms inside the squared bracket are not zero, so to maintain F equal to zero requires the condition that

$$A = 0 \tag{3.33}$$

From eq. (3.32) and (3.33) $dF/dz = B$, and therefore from eq. (3.31)

$$\gamma'\alpha - Bz = \frac{2\, c_v}{\alpha^2}$$

or

$$B = \frac{\gamma'\alpha}{1 + \frac{2\, c_v}{\alpha^2}} \tag{3.34}$$

Making the simplification

$$R = \frac{\alpha}{2\sqrt{c_v}} \tag{3.35}$$

gives

$$F = \frac{\gamma'\alpha\, z}{1 + \frac{1}{2\, R^2}}$$

and so

$$u = F\sqrt{t} = \frac{\gamma'\alpha\sqrt{t}\, z}{1 + \frac{1}{2\, R^2}} \tag{3.36}$$

or in normalised form,

$$\frac{u}{\gamma' X} = \frac{z}{1 + \frac{1}{2\, R^2}} \tag{3.37}$$

Applied Loading.

For the case of the loading $(P_o - \sigma_o')$ which is constant with depth, and temporarily setting $\gamma' X = 0$, allows eq. (3.18) to be written as

$$x = X(t); \quad (P_o - \sigma_o') - u = \frac{c_v \frac{\partial u}{\partial x}}{\frac{dX}{dt}}; \quad t > 0$$

Transforming to z co-ordinates;

$$z = 1 \; ; \quad (P_o - \sigma_o') - u = \frac{c_v \frac{\partial u}{\partial z}}{X \frac{dX}{dt}}; \quad t > 0 \tag{3.38}$$

A solution to the governing eq. (3.22) is sought subject to eq. (3.38) and (3.23). It will be found that the only value of G(t) possible to transform eq. (3.22) and (3.38) to ordinary differential equations is

$$G(t) = 1 \tag{3.39}$$

or

$$\hat{u} = F(z) \tag{3.40}$$

thus

$$\frac{\partial u}{\partial z} = \frac{dF}{dz}$$

$$\frac{\partial^2 u}{\partial z^2} = \frac{d^2F}{dz^2}$$

and $\frac{\partial u}{\partial t} = 0$

Substitution of these derivatives in eq. (3.22) and (3.38) yields

$$\frac{d^2F}{dz^2} + \frac{\alpha^2}{2c_v} z \frac{dF}{dz} = 0 \qquad (3.41)$$

and

$$\text{at } z = 1 ; \ (P_o - \sigma_o') - F = \frac{2\,c_v}{\alpha^2} \frac{dF}{dz} \qquad (3.42)$$

The complete solution to (3.41) is

$$F(z) = A_1 \operatorname{erf}\left(\frac{\alpha z}{2\sqrt{c_v}}\right) + B_1 \qquad (3.43)$$

Substitution in (3.23) gives

$$B_1 = 0 \qquad (3.44)$$

and in eq. (3.42)

$$A_1 = \frac{P_o - \sigma_o'}{\operatorname{erf}\left(\frac{\alpha}{2\sqrt{c_v}}\right) + \frac{2\sqrt{c_v}}{\alpha\sqrt{\pi}}\, e^{-\frac{\alpha^2}{4\,c_v}}} \qquad (3.45)$$

Placing these values in eq. (3.43) and then in eq. (3.40) gives the solution

$$u = \frac{(P_o - \sigma_o') \operatorname{erf}\left(\frac{\alpha z}{2\sqrt{c_v}}\right)}{\operatorname{erf}\left(\frac{\alpha}{2\sqrt{c_v}}\right) + \frac{2\sqrt{c_v}}{\alpha\sqrt{\pi}}\, e^{-\frac{\alpha^2}{4\,c_v}}} \qquad (3.46)$$

Again, the most obvious simplification is to set

$$R = \frac{\alpha}{2\sqrt{c_v}} \qquad \text{in eq. (3.46)}$$

therefore

$$\frac{u}{P_o - \sigma_o'} = \frac{\text{erf}\,(Rz)}{\text{erf}(R) + \dfrac{e^{-R^2}}{\sqrt{\pi}\,R}} \tag{3.47}$$

Superimposing the results from eq. (3.36) and (3.47) finally gives

$$u\,(z,t) = \frac{(P_o - \sigma_o')\,\text{erf}(Rz)}{\text{erf}(R) + \dfrac{e^{-R^2}}{\sqrt{\pi}\,R}} + \frac{\gamma' X\, z}{1 + \dfrac{1}{2R^2}} \tag{3.48}$$

Dividing across by $(P_o - \sigma_o' + \gamma' X)$ yields the normalised excess pore pressure

$$\phi\,(z,\, R,\, W_r) = \frac{u\,(z,t)}{P_o - \sigma_o' + \gamma' X}$$

$$= \left(\frac{1}{1 + W_r}\right) \frac{\text{erf}\,(Rz)}{\text{erf}(R) + \dfrac{e^{-R^2}}{\sqrt{\pi}\,R}} + \frac{z}{\left(1 + \dfrac{1}{W_r}\right)\left(1 + \dfrac{1}{2R^2}\right)} \tag{3.49}$$

where $R = \dfrac{\alpha}{2\sqrt{c_v}}$, and is termed the *thaw-consolidation ratio,*

$W_r = \dfrac{\gamma' X}{P_o - \sigma_o'}$ is the *self-weight ratio,* and $z = \frac{x}{X(t)}$ is the normalised depth to the thaw plane.

Direct substitution of eq. (3.48) into the governing equation and boundary conditions shows that this solution does satisfy all requirements.

Settlements in a Thawing Soil.

It is also of considerable interest to determine the average degree of consolidation in the thawed soil. For this class of moving boundary problem we define this as the ratio of the consolidation settlement that has occurred up to time t, to the total consolidation settlement that would occur if thawing were suddenly stopped at t. The settlement associated with the ice-water density change will be treated separately.

The settlement ratio is

$$\frac{S_t}{S_{max}} = \frac{\int_0^X \left\{e_o - e(x,t)\right\} dx}{\int_0^X \left\{e_o - e_f\right\} dx} \tag{3.50}$$

where e_o, e_f and e are the initial, final and current void ratios respectively.

As a linear void ratio/effective stress assumption has been adopted thus far, eq. (3.50) is re-written in terms of excess pore water pressures as

$$\frac{S_t}{S_{max}} = \frac{\int_o^X \left(P_o + \gamma' x - u(x,t)\right) dx}{\int_o^X \left(P_o + \gamma' x\right) dx} \qquad (3.51)$$

Rewriting the pore pressure equation (3.48) in terms of x,

$$u(x,t) = \frac{(P_o - \sigma_o')\ \mathrm{erf}(R\frac{x}{X})}{\mathrm{erf}(R) + \frac{e^{-R^2}}{\sqrt{\pi}\ R}} + \frac{\gamma' x}{1 + \frac{1}{2R^2}} \qquad (3.52)$$

Integrating the quantities in (3.51) gives

$$\frac{S_t}{S_{max}} = \frac{P_o\ X + \frac{\gamma'\ X^2}{2} - \int_o^X u(x,t)\ dx}{P_o\ X + \frac{\gamma'\ X^2}{2}} \qquad (3.53)$$

Now from eq. (3.52)

$$\int_o^X u(x,t) dx = \frac{P_o - \sigma_o'}{\mathrm{erf}(R) + \frac{e^{-R^2}}{\sqrt{\pi}\ R}} \left\{ X\mathrm{erf}(R) + \frac{X}{\sqrt{\pi}\ R}\left(e^{-R^2} - 1\right)\right\}$$

$$+ \frac{\gamma'\ X^2}{2\ (1 + \frac{1}{2R^2})} \qquad (3.54)$$

Substituting the integral (3.54) in eq. (3.53) and again introducing W_r, the expression for the settlement ratio becomes

$$\frac{S_t}{S_{max}} = 1 - \frac{\text{erf}(R) + \dfrac{e^{-R^2} - 1}{\sqrt{\pi}\,R}}{\left(\text{erf}(R) + \dfrac{e^{-R^2}}{\sqrt{\pi}\,R}\right)\left(1 + \dfrac{W_r}{2}\right)}$$

$$- \frac{1}{\left(1 + \dfrac{1}{2R^2}\right)\left(1 + \dfrac{2}{W_r}\right)} \qquad (3.56)$$

The maximum consolidation settlement at time t is

$$S_{max} = m_v \left((P_o - \sigma_o{}')X + \frac{\gamma' X^2}{2}\right) \qquad (3.57)$$

So the settlement at any time t, S_t, is readily calculated if the ratio $\frac{S_t}{S_{max}}$ and S_{max} are known.

For the following two extreme cases of loading, the solution is summarised.

(a) Weightless soil, $\gamma' = 0$, and $W_r = 0$

$$\frac{u(z,t)}{P_o - \sigma_o{}'} = \frac{\text{erf}(Rz)}{\text{erf}(R) + \dfrac{e^{-R^2}}{\sqrt{\pi}\,R}}$$

and
$$\frac{S_t}{S_{max}} = 1 - \frac{\text{erf}(R) + \frac{e^{-R^2} - 1}{\sqrt{\pi}\, R}}{\text{erf}(R) + \frac{e^{-R^2}}{\sqrt{\pi}\, R}}$$

and
$$S_{max} = m_v(P_o - \sigma_o')X$$

(b) No applied loading, $(P_o - \sigma_o') = 0$; and $W_r = \infty$

$$\frac{u(z,t)}{\gamma' X} = \frac{z}{1 + \frac{1}{2R^2}}$$

and
$$\frac{S_t}{S_{max}} = 1 - \frac{1}{1 + \frac{1}{2R^2}}$$

and
$$S_{max} = m_v \frac{\gamma' X^2}{2}$$

3.4 Results of Solution.

The complete solution to the problem of consolidation in thawing soils, subject to the assumptions made, is shown to be a function of the three independent variables z, W_r and R. W_r is the ratio of the effective overburden pressure at the thaw line to the applied external loading. If an initial effective stress is present in the soil on thawing, it is subtracted from P_o. The thaw consolidation ratio R is a measure of the relative rates of generation and expulsion of excess pore fluids.

Normalized values of excess pore pressures have been computed from equations (3.47) and (3.37) for the two extreme values of W_r and are plotted in Figures 3.2 and 3.3. Excess pore pressures for intermediate values of W_r may be calculated from the more general eq. (3.49). It is of particular interest to note that for a soil consolidating only under its own weight the pore pressure distribution is linear for a given magnitude of the thaw-consolidation ratio R. The variation of the excess pore pressure gradient with R for this case is plotted in Fig. 3.4 in a form more convenient for use. The degree of consolidation has been plotted against R for different values of W_r in Fig. 3.5.

For the cases where the soil is consolidating solely under an applied load, or solely under the influence of self-weight, the relationships describing the excess pore pressure distribution and degree of consolidation are all independent of time. A similar feature was found by Gibson (1958) when considering the pore pressures generated by deposition of material at a rate proportional to the square root of time. The dimensionless thaw consolidation ratio is a fundamental parameter which, although independent of time, has a role similar to the time factor in more conventional consolidation problems.

As the excess pore pressure profile is time-independent, it is convenient to plot the excess pore pressure at the thaw line (z = 1) against R for the different W_r ratios in Fig. 3.6. As the most critical pore pressure always occurs at the thaw front, this plot represents the most interesting facet of the solution. The curve for W_r = 0 will prove particularly useful at a later stage when

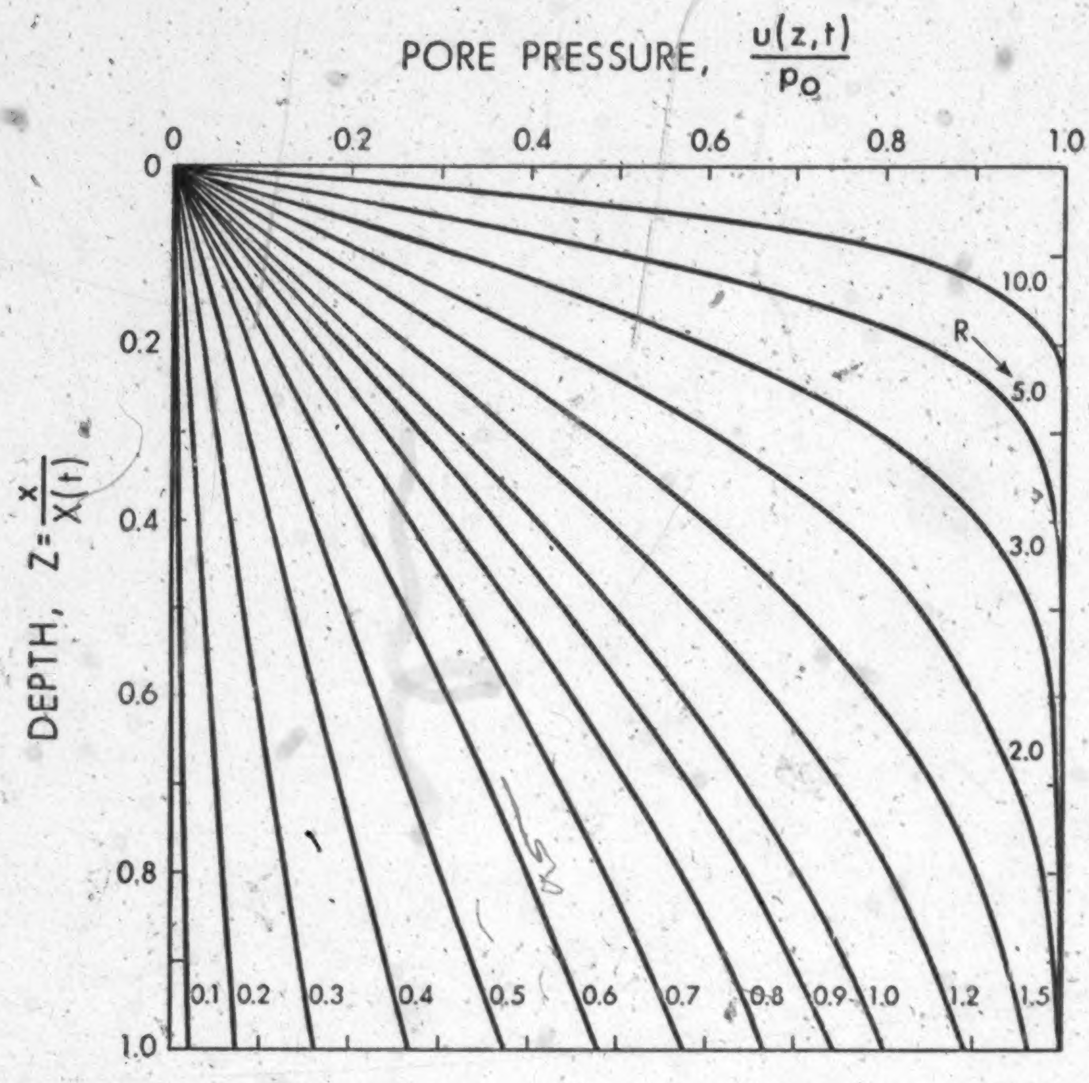

Fig. 3.2 Excess pore pressures for the applied loading condition, $W_c = 0$

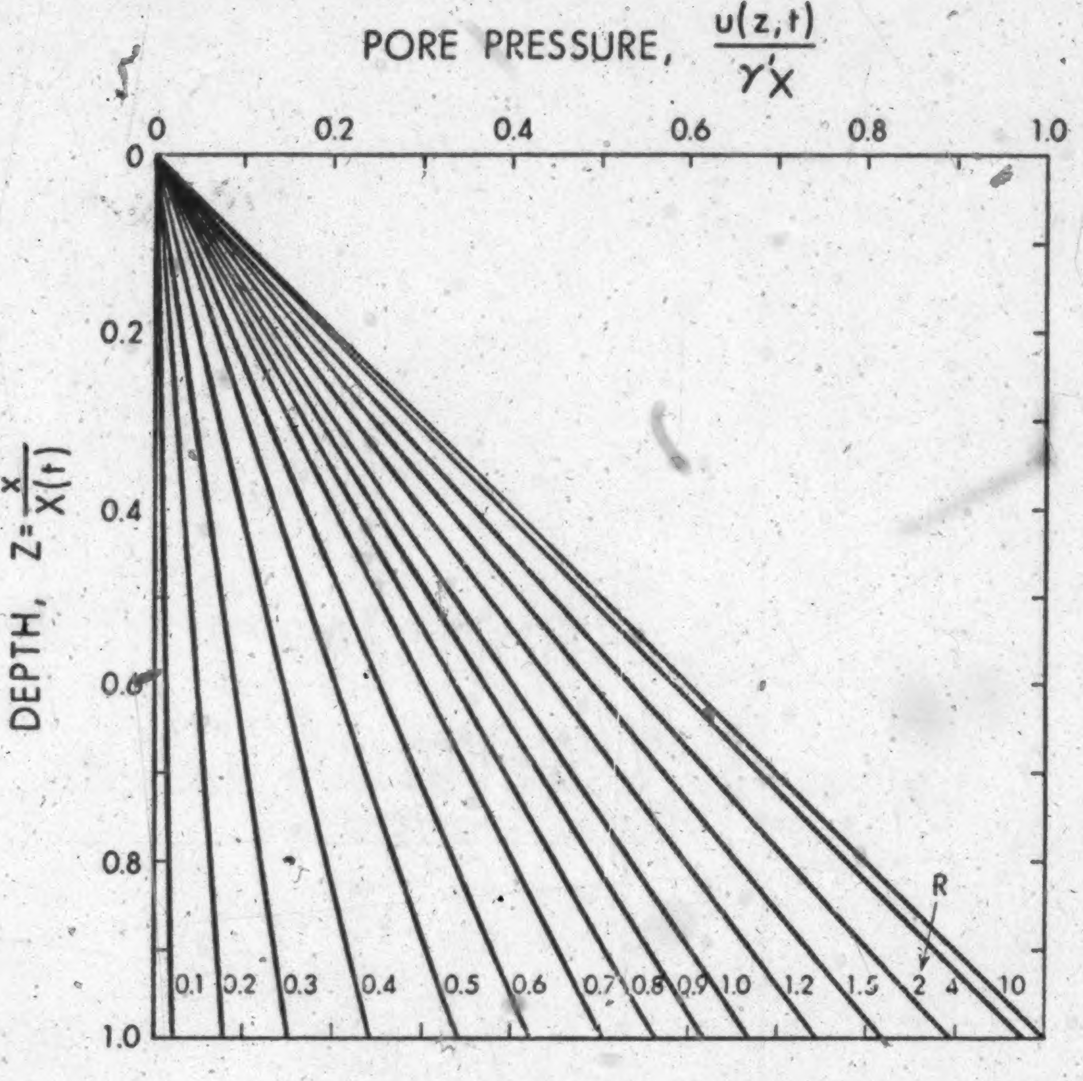

Fig. 3.3 Excess pore pressures for the self-weight loading condition, $W_r = \infty$

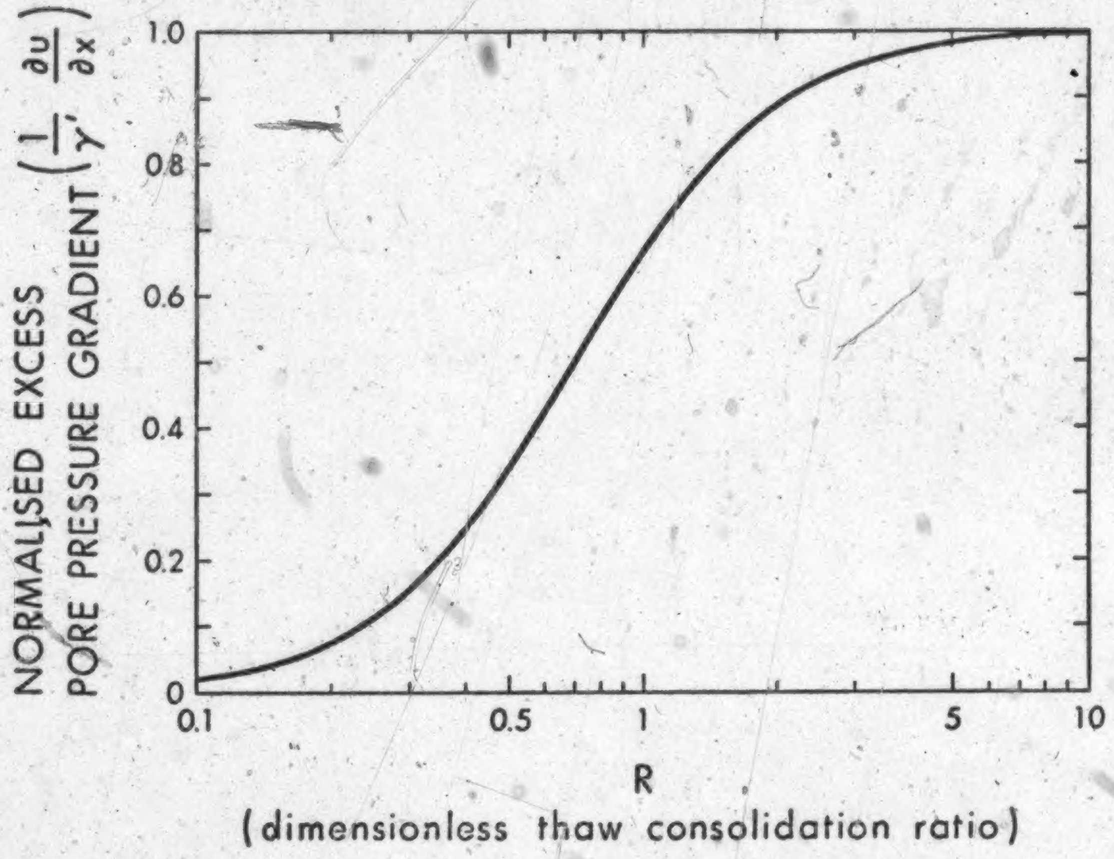

Fig. 3.4 Variation of hydraulic gradient with R, $W_r = \infty$

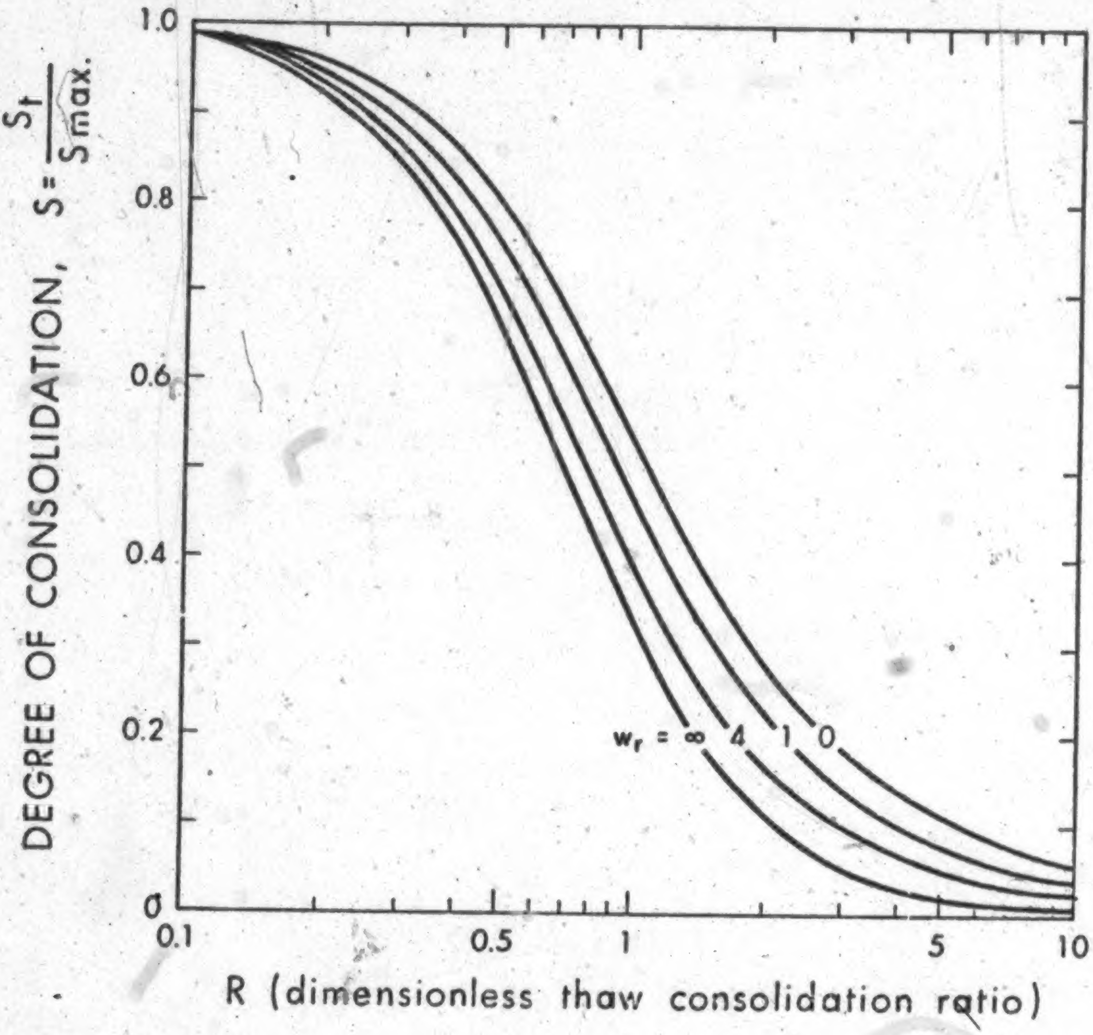

Fig. 3.5 Variation of S_t/S_{max} with R

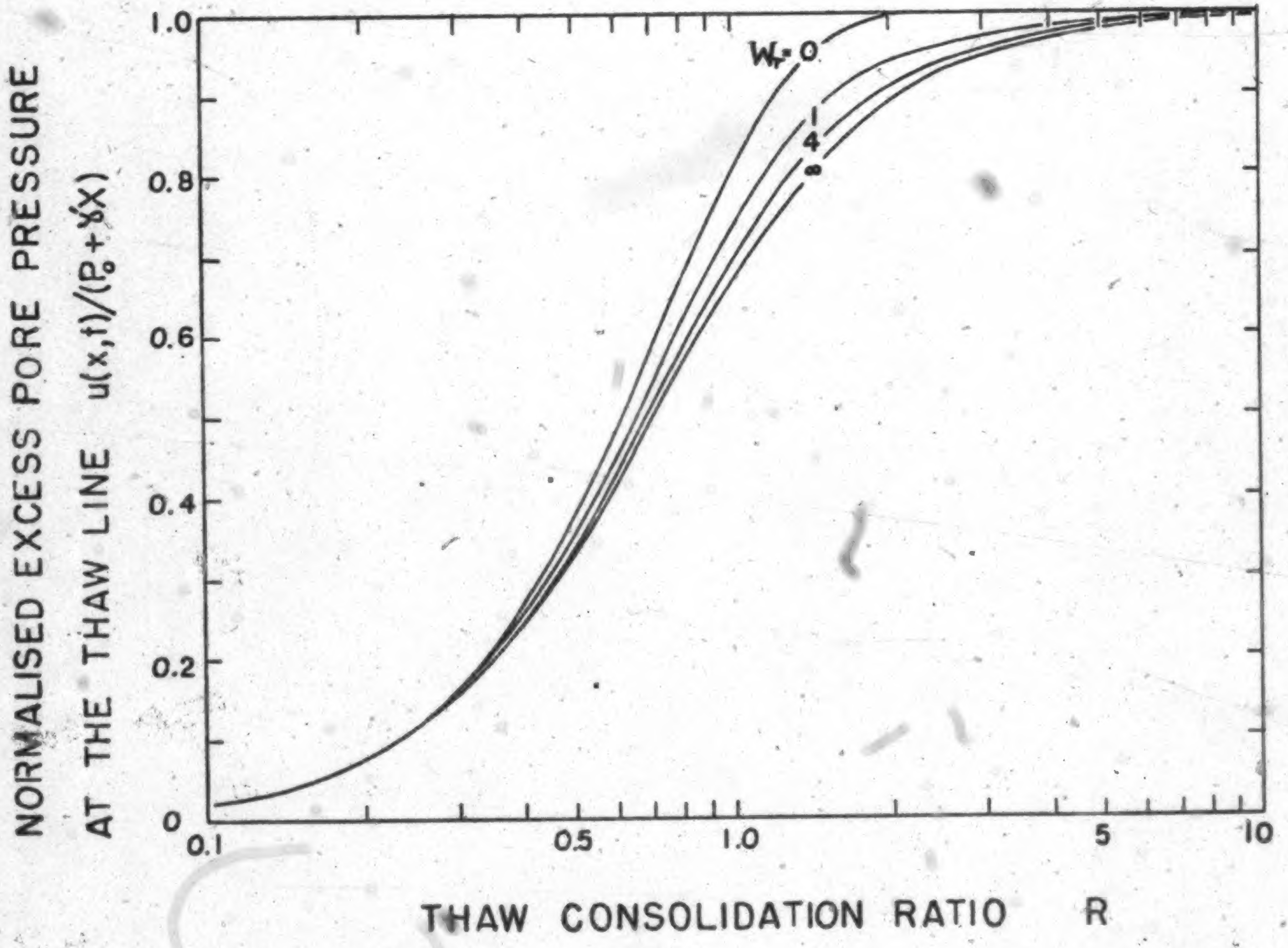

Fig. 3.6 Excess pore pressures at the thaw front plotted against R

assessing experimentally the validity of the theory.

3.5 Post-thawing conditions:

If the movement of the thaw front were to cease abruptly at, say, time $t = t_f$, then a more conventional fixed boundary problem arises. For the case where the depth of thaw is proportional to the square root of time, the position of the lower boundary X_f will be given by eq. (3.1). For this new problem, the governing differential equation (3.3) remains unchanged, however the initial values are given by the excess pore pressure distribution at the end of thawing.

The boundary condition at the base is rewritten from eq. (3.18) to give

$$\frac{\partial u}{\partial x} = \frac{P_o - \sigma_o' + \gamma' X_f - u}{c_v} \frac{dX}{dt} \tag{3.58}$$

The velocity of the thaw front $\frac{dX}{dt}$ is now zero, giving the impermeable condition.

$$\text{at} \quad x = X_f \quad ; \quad \frac{\partial u}{\partial x} = 0 \quad ; \quad t > t_f \tag{3.59}$$

The formulation of the problem may be summarised as follows. Setting $t_f = 0$ and $X_f = L$ for notational simplicity,

$$t > 0 \; ; \quad c_v \frac{\partial^2 u}{\partial x^2} = \frac{\partial u}{\partial t} \; ; \quad 0 < x < L \tag{3.60}$$

$$t > 0 \; ; \quad u = 0 \; ; \quad x = 0 \tag{3.61}$$

$$t > 0 \; ; \quad \frac{\partial u}{\partial x} = 0 \; ; \quad x = L \tag{3.62}$$

$$t = 0 \; ; \quad u = \frac{(P_o - \sigma_o')\,\mathrm{erf}(R\,\frac{x}{H})}{\mathrm{erf}(R) + \frac{e^{-R^2}}{\sqrt{\pi}\,R}} + \frac{\gamma' x}{1 + \frac{1}{2R^2}} \; ; \quad 0 \leq x \leq L \qquad (3.63)$$

The analytical solution to this problem may be expressed in the form of an infinite series, however because of the complexity of the initial values in eq. (3.63), an extremely difficult integral emerges. It is possible, however, to obtain a solution for the self-weight $(\gamma' x)$ loading condition, as the initial values are linear, and it may be found from Carslaw and Jaeger (1947) to be

$$u(x,t) = \frac{8\,u_f}{\pi^2} \sum_{n=0}^{\infty} \frac{1}{(2n+1)^2} \cos\frac{(2n+1)\pi x}{2L} \cdot e^{-c_v(2n+1)^2\pi^2 t} \qquad (3.64)$$

where $u_f = \frac{\gamma' L}{1 + \frac{1}{2R^2}}$

and is the excess pore pressure at the thaw line at completion of thawing.

In dimensionless form, eq. (3.64) becomes

$$\frac{u(z,T)}{u_f} = \sum_{n=0}^{\infty} \frac{2}{M^2} \cos(Mz)\, e^{-M^2 T} \qquad (3.65)$$

where $M = (2n + 1)\frac{\pi}{2}$

and $T = \frac{c_v t}{L^2}$

The excess pore pressure isochrones from eq. (3.65) are shown plotted in Fig. 3.7, and these isochrones are valid for all values of R during thaw.

The post thaw settlement is defined as the settlement occurring after t_f divided by the total post thaw settlement taking place between t_f and time ∞. The degree of post-thaw settlement for the post-thaw phase of consolidation may be obtained by integration of the infinite series (3.65) as follows:

$$\int_0^1 \frac{u(z,T)}{u_f}\,dz = \sum_{n=0}^{\infty} (-1)^n \frac{2}{M^3} e^{-M^2 T} \tag{3.66}$$

The degree of post-thaw settlement for this case will be defined as

$$S = 1 - \frac{\int_0^1 \frac{u(z,T)}{u_f}\,dz}{\int_0^1 \frac{u(z,0)}{u_f}\,dz} \tag{3.67}$$

The initial values (u(z,0) are given by the triangular distribution

$$u(z,0) = u_f z.$$

So,

$$\int_0^1 \frac{u(z,0)}{u_f}\,dz = 1/2$$

$$\therefore \quad S = 1 - 2\int_0^1 \frac{u(z,T)}{u_f}\,dz \tag{3.68}$$

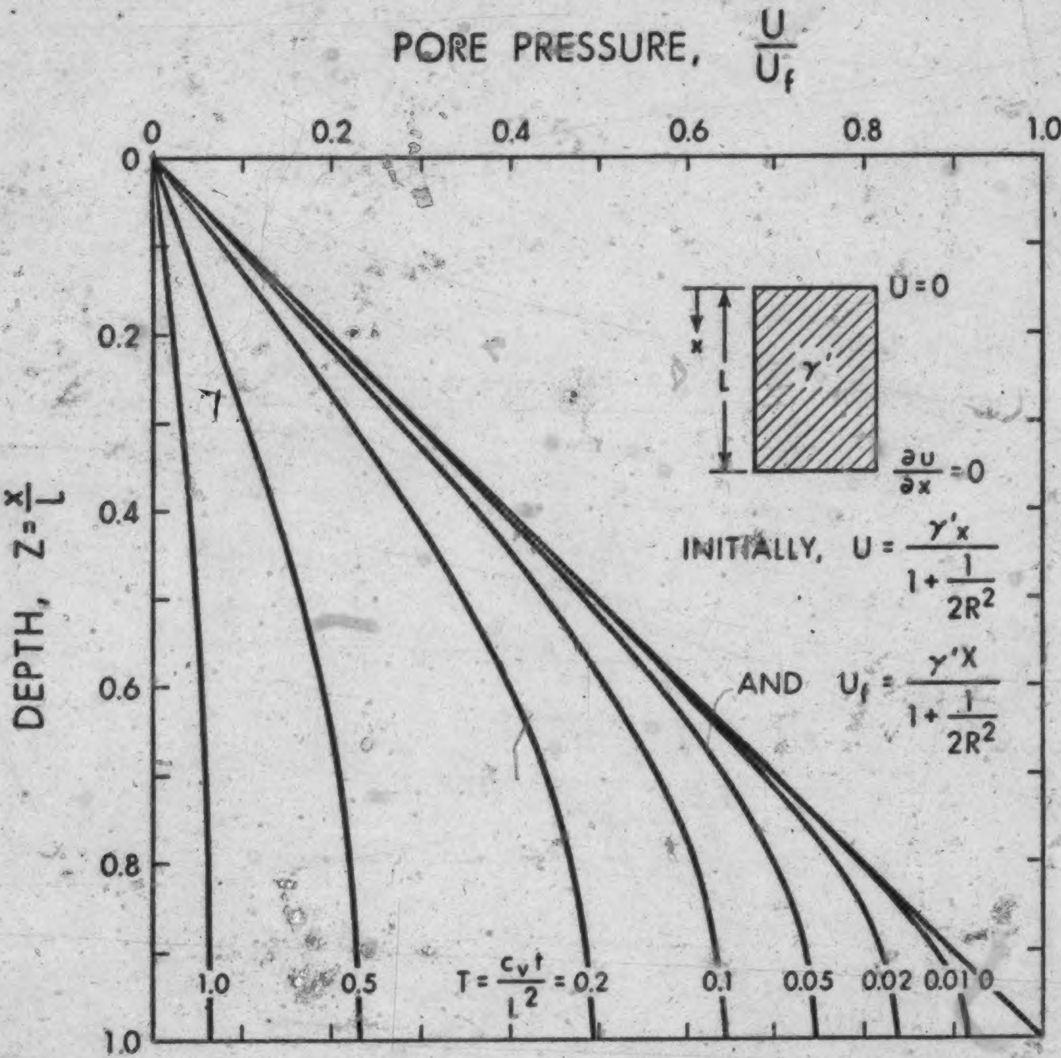

Fig. 3.7 Excess pore pressure isochrones after completion of thawing, $W_r = \infty$

Substituting the series expression (3.66) into (3.68) yields

$$S = 1 - 2 \sum_{n=0}^{\infty} (-1)^n \frac{2}{M^3} e^{-M^2 T} \tag{3.69}$$

The degree of post-thaw settlement expressed by eq. (3.69) is plotted in Fig. 3.9 against the time factor.

The post-thawing pore pressures and settlements for the applied loading ($P_0 - \sigma_0'$) condition must necessarily be evaluated by a finite difference numerical method. Because the initial pore pressure distribution is always linear for the γ' loading case, the degree of post-thaw settlement will always be independent of R. However, for the ($P_0 - \sigma_0'$) loading case, the shape of the initial pore pressure profile is governed by R, and therefore the degree of post-thaw settlement will in this case be weakly dependent on R. A simple finite difference program was written to solve the Terzaghi consolidation equation subject to the initial values for the ($P_0 - \sigma_0'$) loading case given by eq. (3.63). The excess pore pressure isochrones were then used to obtain the degree of post-thaw settlement for different R values during thaw. The excess pore pressures at the base of the thawed soil are shown plotted against time factor in Fig. 3.8. The degree of post-thaw settlement is plotted with the time factor in Fig. 3.9 for different R values. It is worth noting that little difference occurs in the settlement curves from R = 0.1 to R = 2. This is a broad range of values which bounds most R values likely to be encountered.

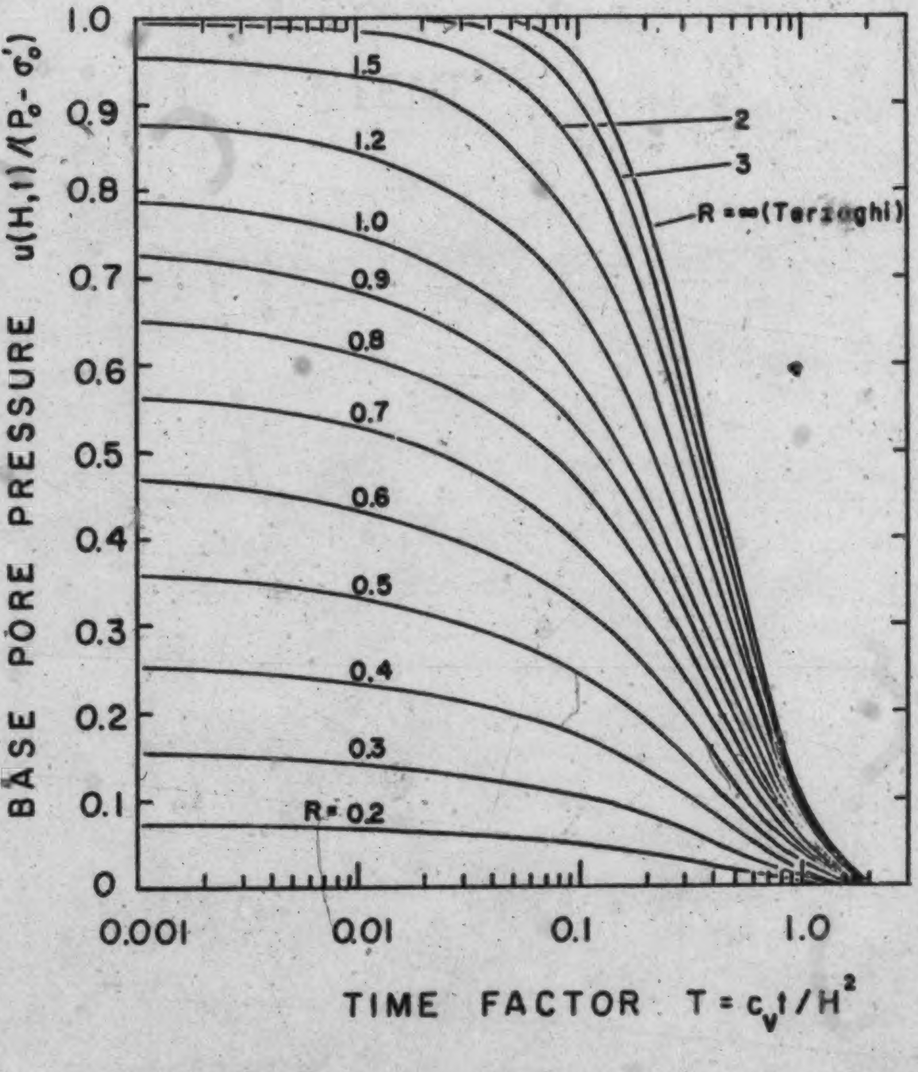

Fig. 3.8 Base pore pressures after completion of thawing, $W_r = 0$

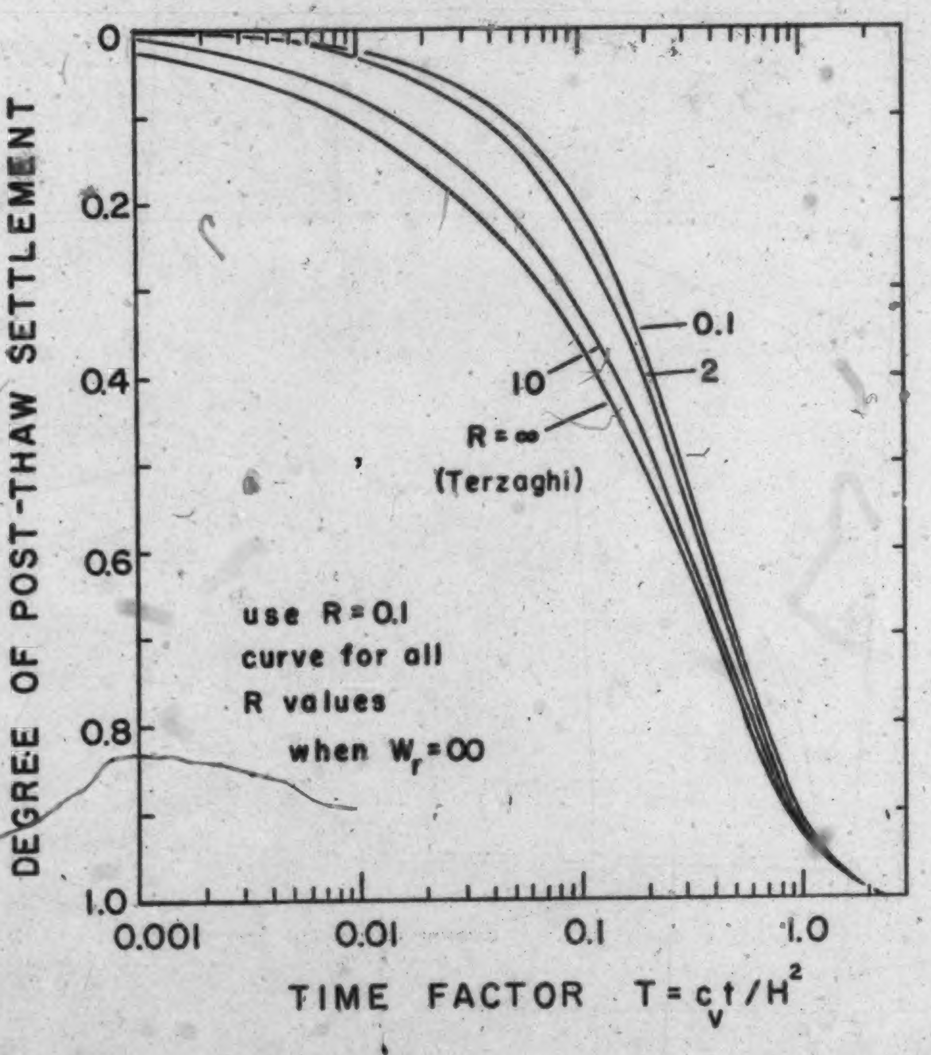

Fig. 3.9 Degree of settlement after completion of thawing

The settlement and excess pore pressure curves for $R = \infty$ indicate that an initially uniform excess pore pressure existed at the end of thaw, and therefore the subsequent development of settlements and the dissipation of excess pore pressures will correspond exactly to the classical Terzaghi solution to this problem in soil consolidation. The most important settlement curve is that for $R = 0.1$. This is the same settlement curve which is obtained from the classical Terzaghi solution for an initially linear profile of excess pore pressure, and is given by Terzaghi and Peck (1967) in their analysis for a hydraulic fill. This settlement curve is used extensively in the experimental verification of the theory as it is valid for all R less than unity (say), and for all loading conditions. It is interesting to note that the time factor for 50% post-thaw consolidation is 0.28, as distinct from 0.197 which is obtained from the classical Terzaghi solution for the oedometer boundary conditions.

3.6 Discussion and Application of Solution.

The degree of consolidation settlement and the excess pore pressures in a thawing soil have been shown to be primarily dependent on the R value. This dimensionless quantity relates α, which is an indication of the thaw rate, and therefore of the rate of liberation of excess pore fluids, to the coefficient of consolidation c_v, which describes the ability of the soil to dissipate the excess pore fluids. When R is zero, no excess pore pressures are maintained, and settlements proceed concurrently with thawing. When the R value is large (i.e. unity), severe pore pressure conditions are maintained at the thaw line, and the degree of consolidation settlement is considerably impeded. The R value may therefore be used as a convenient index as to the severity of pore pressure and settlement conditions in a thawing soil. When the excess pore pressure conditions are combined with a failure criterion of the Mohr-Coulomb type, the available shearing resistance of the thawing soil may also be calculated.

Dwelling briefly on the two parameters contained in the R value, it is certainly safe to conclude that the degree of uncertainty in obtaining a value for the thermal parameter α is much less than the uncertainty in estimating or measuring c_v. The complete range of α values which one might imagine for a wide range of Arctic problems probably lies between 3×10^{-2} and 9×10^{-2} cm/sec$^{1/2}$, a total variation by a factor of three. Even accounting for possible errors in conductivity data and moisture content, one would not expect the error in the estimation of α for a particular problem to be greater than 20%. The coefficient of consolidation c_v, on the other hand, could quite easily vary from 10^{-1} cm^2/sec for sandy soils to 10^{-5} cm^2/sec for very fine-grained clay soils. Even though the c_v value enters the R value under the square root sign, its potential variation and the factors affecting it, make the degree of uncertainty associated with obtaining the correct c_v value much higher. Accepting that the Terzaghi equation correctly describes the pore pressure dissipation in the thawed soil, it is therefore encouraging to see that the solution of practical thaw-consolidation problems is resolved into a correct determination of the coefficient of consolidation.

The excess pore pressure conditions under the applied loading condition are in general slightly more severe than those obtained under the self-weight loading condition, but the difference is small enough that no generalisations should be made regarding the control of loading conditions at this early stage. It will be seen later, for instance, that the provision of an applied loading P_o will in some cases reduce the normalised excess pore pressure in the thawing soil.

The residual stress σ_o' may be introduced as a constant or linearly increasing function into the preceeding analysis for linear thaw-consolidation without undue difficulty.

Assume that the residual stress σ_o' is represented as a linear function of depth by

$$\sigma_o'(x) = D_1 + D_2\, x \qquad (3.70)$$

The boundary condition at the thaw line eq. (3.18) may then be rewritten as

$$(P_o - D_1) + (\gamma' - D_2)\, x - u = \frac{c_v \frac{\partial u}{\partial x}}{\frac{dX}{dt}} \qquad (3.71)$$

where the constant coefficient D_1 has been combined with the constant external stress P_o, and the D_2 coefficient has been combined with γ'. In the final solution, P_o is now replaced with $(P_o - D_1)$ and γ' by $(\gamma' - D_2)$, and thus a residual stress function such as eq. (3.70) is immediately incorporated into the closed form solution for one-dimensional linear thaw-consolidation.

The theory formulated here provides a value of the settlement ratio S_t/S_{max} in the thawed soil. However, in order to calculate the actual transient settlements, a knowledge of the different components of total settlement and their relative rates is required. The total consolidation settlement S_{max} for an applied loading P_o is proportional to the depth of thaw X, and therefore to the square root of time. S_{max} for the self-weight loading case is proportional to X^2, and therefore proceeds linearly with time.

The other component of settlement arises from the volumetric contraction associated with the phase transformation from ice to water. This component of settlement occurs instanteously on thawing, and is obviously proportional to the depth of thaw and the square root of time, provided that the ice is uniformly distributed. Therefore in a situation involving both loading conditions, the total settlement is related to time and to the square root of time. For the oedometer conditions, however, where the self-weight component of the soil is ignored, the remaining components of total settlement are both related to the square root of time as follows. Writing the settlements for the oedometer loading conditions as the sum of the ice-water contraction and the consolidation settlements gives

$$S = J\,X + \left(\frac{S_t}{S_{max}}\right)S_{max}$$

where J is the strain associated with the ice-water change alone.

The total consolidation settlement S_{max} is written as

$$S_{max} = m_v(P_o - \sigma_o')X$$

Therefore the sum of the settlements at any time is

$$S = \left\{ J + m_v(P_o - \sigma_o') \frac{S_t}{S_{max}} \right\} X$$

For a uniform soil, the term inside the large bracket is a time-independent constant. Therefore the transient settlements taking place under oedometer stress conditions are related directly to the depth of thaw, and therefore to the square root of time. It will be seen in the following chapter whether these theoretical predictions are borne out for experiments carried out under oedometer loading conditions.

CHAPTER IV

LABORATORY TESTING OF THAWING SOILS

4.1 Thaw-Consolidation Tests on Remoulded Soils

In order to assess the validity of some of the most important theoretical relationships derived in previous chapters, it was necessary to develop a special oedometer for laboratory testing of thawing soils. This oedometer was designed and built to test the theory of thaw-consolidation, and the results of the study are presented by Smith (1972), and subsequently by Morgenstern and Smith (1973).

The oedometer was designed to satisfy the necessary stress and thermal boundary conditions during one-dimensional thaw-consolidation. The apparatus consisted basically of a rigid lucite thick-walled cylinder to maintain one-dimensional heat transfer, drainage and total stress conditions. Drainage is permitted at the top of the sample through a porous stone, and another porous stone at the base of the sample is connected to an electrical pore pressure transducer. A loading is applied vertically to the sample using a counterbalanced loading hanger, which bears on a plunger and load cap assembly. Temperatures at the top and bottom of the soil sample are controlled using thermo-electric elements and temperature control units built specially for the apparatus. Temperatures through the sample are measured using thermocouples and thermistors. The apparatus is described in detail by Smith (op cit), and a diagram of an improved apparatus appears in the next section.

Considerable care was taken in measuring the correct pore pressures at the base of the thawed soil sample. The pore pressures measured in tests performed on conventional unfrozen clay samples were found to be greatly affected by friction between the apparatus and soil sample, and by the 'hardness' of the pore pressure measuring system. The measuring system was made as incompressible as possible by keeping the volume of fluid in the measuring system as small as possible, and by carefully de-airing the fluid involved. Side friction on the sample was greatly reduced by lining the lucite barrel of the apparatus with a teflon sleeve, and a greased rubber membrane was placed between the soil and the teflon sleeve. In this way, almost ideal pore pressure responses were observed during standard oedometer tests on unfrozen clay soils.

The soils were prepared by remoulding a saturated slurry at a high moisture content, and then by consolidation in the device to a desired stress. The remoulded soils were frozen in the apparatus to a uniform temperature. Upon the application of a sudden increase in surface temperature, the soil commenced thawing. Settlements, pore pressures and temperatures were recorded as thawing proceeded, and subsequently when thawing was completed.

Using the curves for post-thaw settlement derived in Chapter 3, the value of the consolidation coefficient c_v was calculated. When combined with the observed thaw parameter α, the thaw-consolidation ratio R was determined for each test. The settlement ratio, S_t/S_{max}, and the observed pore pressure were plotted against R, and compared with the theoretical relationships derived from the thaw-consolidation theory. These results are reproduced in Fig. 4.1, and in this way a

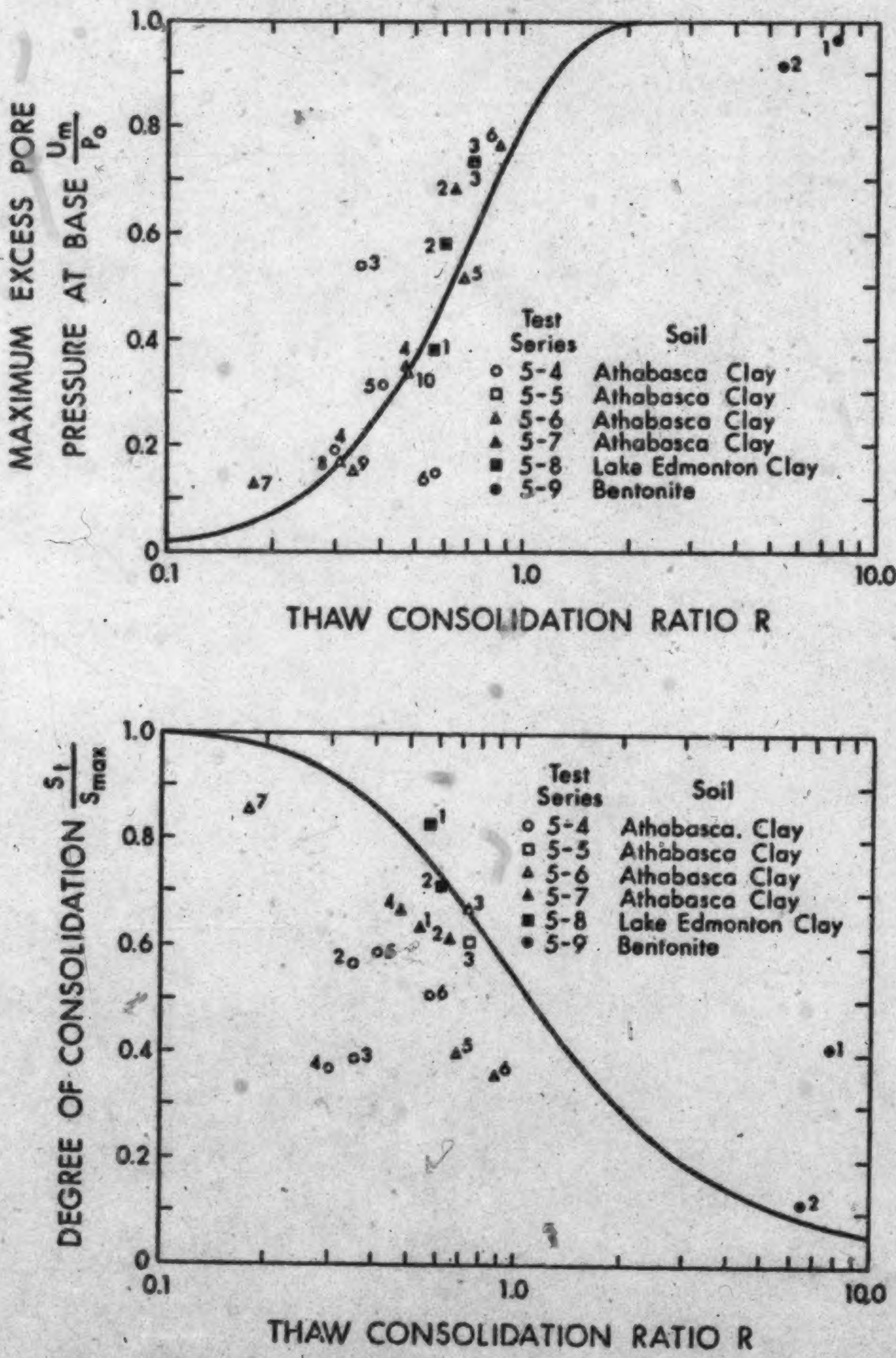

Fig. 4.1 Observed and Predicted Pore Pressures and Settlements for Remoulded Soils (after Smith, 1972)

preliminary investigation of the theory of thaw-consolidation was accomplished. The results of the tests on remoulded soils, the measurement of the thermal and consolidations coefficients, and the analysis of the data within the context of the thaw-consolidation theory are described in a complete manner by Smith (op cit) and will not be dwelt upon here. The principal conclusions of this interesting study might be summarised in the following sentences.

1) When a step increase in temperature is applied at the surface of a uniform soil sample, the depth of thaw penetration is observed to be proportional to the square root of time.

2) The rate of thaw α may be estimated with sufficient accuracy for most engineering applications using well established relationships and thermal properties.

3) Settlements during thawing under the application of a surface step temperature are proportional to the square root of time, for oedometer stress conditions.

4) The degree of settlement in the thawing soil follows the general trend predicted by the theory, but more precision in the data would be desirable.

5) The linear theory of thaw-consolidation was more than satisfactory in predicting the excess pore pressures maintained during thawing.

6) The versatility of the thaw-consolidation apparatus was demonstrated. From a single test, the parameters controlling the thaw and post-thaw settlements and pore pressures could be obtained, together with additional information on the rate of melting.

7) The importance of the in-situ permeability for predicting

c_v (and therefore R) was recognised when applying the theory to field problems.

Following the extremely encouraging results of this study on remoulded soils, it was clear that further testing of undisturbed permafrost soils would be of considerable interest before applying the theory to field problems involving thawing soils. Although all tests carried out to assess the validity of the theory were performed under the applied loading condition in the oedometer, it is clear that any statements regarding the applicability of the theory apply equally well to the self-weight loading condition as the formulation of the consolidation problem is the same for each loading situation.

4.2 The Design of an Improved Thaw-Consolidation Apparatus

It was necessary to design and fabricate an apparatus capable of satisfying the stress and thermal boundary conditions involved in a thaw-consolidation test. The apparatus developed by Smith (1972) was shown to meet these requirements in a satisfactory manner when testing remoulded soils. However based on experience obtained from a large number of tests, and anticipating the extra complexities in testing undisturbed samples, Smith (op cit) provided the following recommendations for improvements to the original apparatus design.

(a) The existing pore pressure measuring system was prone to plugging and leakage, and should be redesigned to allow flushing of the system.

(b) The outer steel jacket in the original apparatus was not required for the low pressures involved in testing.

(c) Provision should be made to measure deflection directly from the load cap.

(d) The sample should be mounted on a base plate, and a split oedometer barrel clamped around the sample. This innovation permits the placement of a frozen sample in the apparatus, which was previously impossible.

These recommendations were carried out, and the improved design is given in Fig. 4.2. Except for the improvements listed above, the same features were incorporated in the oedometer used by Smith (op cit).

Two thermo-electric modules powered by D.C. power supplies controlled the temperatures at the top and bottom surfaces of the soil sample. A lucite barrel lined with a teflon sleeve and a greased rubber membrane provided an almost frictionless boundary between the soil and the barrel of the oedometer. A lucite base plate was fitted with a porous stone and connected by a fine hole to the transducer and assembly of valves shown in Fig. 4.2. The system of valves allowed re-zeroing of the pore pressure transducer to atmospheric pressure without allowing the passage of any fluid in or out of the sample. An aluminium guide with a teflon bushing was provided for the plunger and load cap to prevent tilting of the load cap. A dial gauge accurate to 0.001 in. mounted on the barrel of the oedometer allowed measurement of settlement directly from the loading plunger. The whole apparatus was mounted in a cold room, whose temperature was set at the required initial temperature of the frozen sample. The pore pressure measuring system was de-aired using a 50% solution of ethylene glycol to prevent freezing in the tubes or transducer.

The method of measuring temperatures throughout the sample with

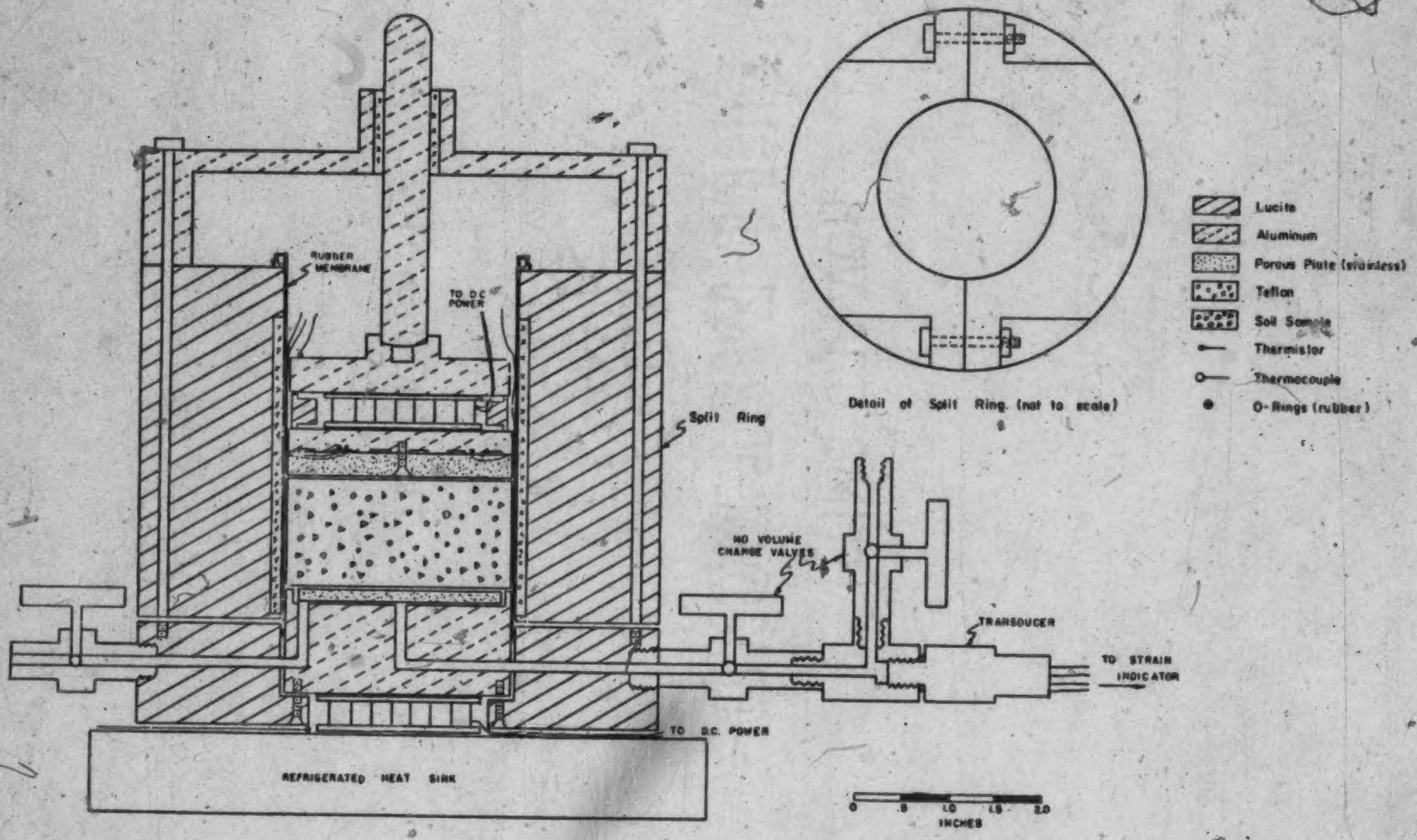

Fig. 4.2 Modified Design of Thaw-Consolidation Apparatus

thermocouples and thermistors, and the method of data acquisition, was identical to that reported by Smith (op cit), and the reader is referred to this work for any further information on the instrumentation used.

4.3 Thaw Consolidation Tests on Undisturbed Permafrost Samples

The extensive laboratory testing carried out by Smith (1972) demonstrated very good agreement between theoretical predictions and the observed behaviour for remoulded soils. However, it is obviously desireable to extend this work by testing undisturbed natural samples of permafrost. It is extremely important to investigate the effects of the natural structure of permafrost on the predictions provided by the thaw-consolidation theory, and therefore determine the applicability of the theory to field problems.

With the design improvements incorporated in the apparatus described in the previous section, it is now possible to place a frozen sample of the correct dimensions in the apparatus, and carry out a thaw-consolidation test.

Samples of frozen core approximately 3 1/2 inches in diameter were obtained from Norman Wells, N.W.T. and from Noell Lake, North-East of Inuvik, N.W.T. The core was inspected visually, and samples were selected for testing. The soil from Norman Wells was a sandy silt, with approximately 10% organic content. According to the NRC ice classification, the ice content varied from thirty percent visible ice (V_s - 30%) at a depth of four feet, to about five percent visible ice (V_s - 5%) from twelve to sixteen feet. Two small lengths of frozen core from the Noell Lake borehole were available from depths of five and fifteen feet. This hole was drilled close to the head scarp of a large thaw subsidence which was occurring at the edge of a lake. The upper sample was a brown silty clay with twenty percent ice (V_s - 20%), and the lower sample was a blue/grey silty clay with approximately twenty percent visible ice (V_s - 20%). The ice in the upper sample was evenly distributed, and was present in the lower sample in the form of disoriented bands of 1/4 to 1/2 inch in thickness. Two photographs of this lower material are given in Fig. 4.3. A summary of the properties of these soils is given in Table 4.1.

The samples were prepared in a large 'walk-in' cold room by first cutting a rough section of core to approximately 2 1/2 inches in length. The frozen soil was then clamped in a milling machine which was fitted with a specially constructed cutting tool. This cutting device was fabricated from a three inch long section of thin-walled steel tubing having an internal diameter of approximately 2.65 inches. The cutting edge of the cylinder was formed by bending the lip of the cylinder inwards and then machining the lip to a sharp edge. The internal diameter of the lip was machined to 2.5 inches exactly, and when mounted in the milling machine, the cylinder formed an effective device for cutting samples 2.5 inches in diameter for testing in the oedometer. With the cutting tool rotating at about 300 r.p.m., it was forced into the frozen core at a rate of 0.2 inches per minute. The cutting action produced a minute amount of melting at the cylindrical surface of the sample, but the effects were estimated to penetrate less than 1 m.m. into the sample. After the cutting tool had penetrated approximately two inches, it was withdrawn. The thawed "skin" around the sample was observed to refreeze almost instantly. The sample was removed from the milling machine, and the ends were trimmed square on a band saw.

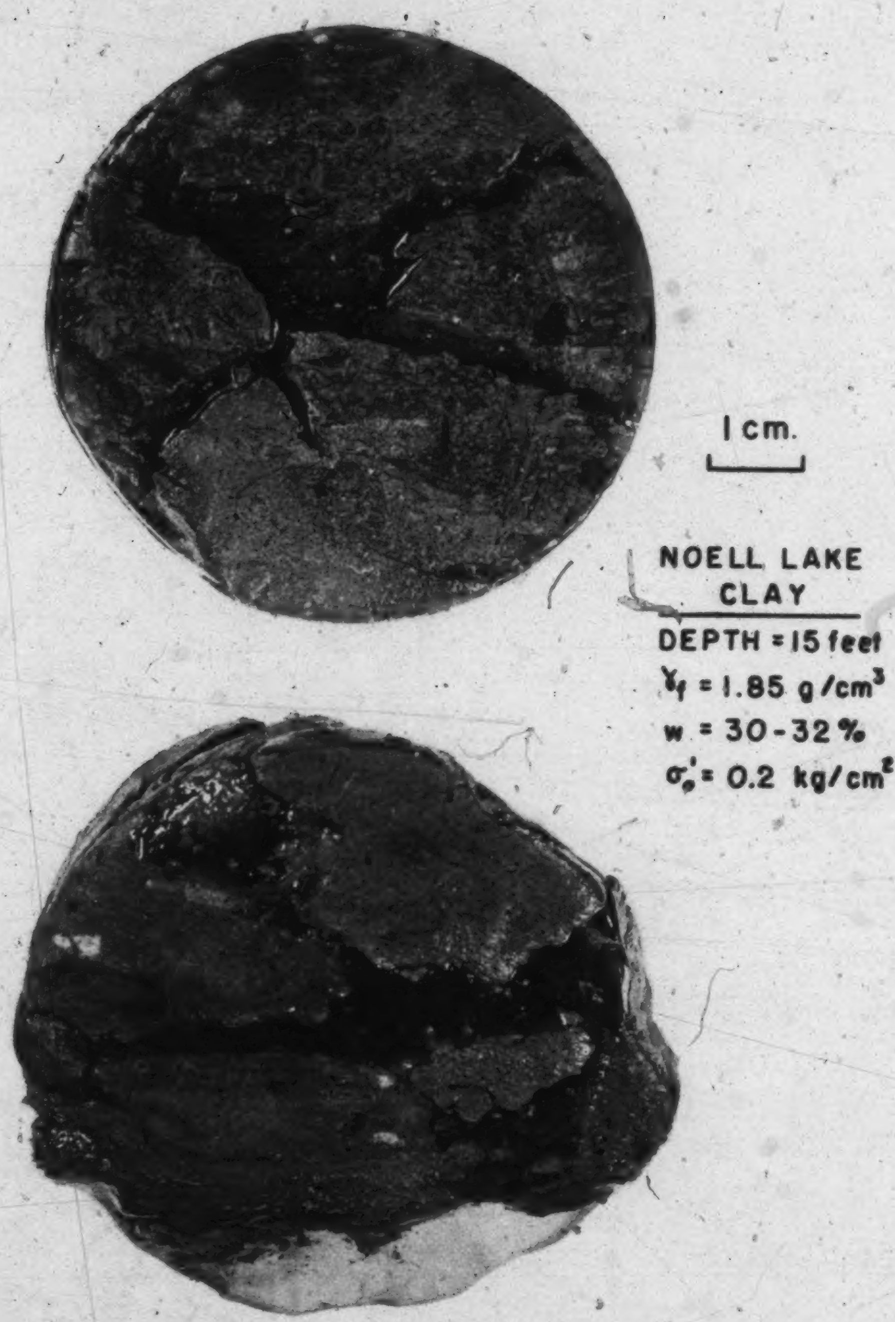

Fig. 4.3 Plan view of two samples of Noell Lake Clay

TABLE 4.1 SUMMARY OF SOIL PROPERTIES

Soil	% Clay M.I.T. scale	% Silt	Liquid Limit (%)	Plastic Limit (%)	G_s	Typical Coefficient of Consolidation cm^2/S	Typical Permeability cm/S
Undisturbed Norman Wells Silt	23	67	29	19	2.65	25×10^{-3}	$10^{-5} - 10^{-6}$
Reconstituted Athabasca Clay	45	54	40	20	2.65	4×10^{-3}	0.7×10^{-7}
Reconstituted Mountain River Clay	55	44	40	20	2.73	1×10^{-3}	0.5×10^{-7}
Undisturbed Noell Lake Clay	40	50	41	23	2.65	2×10^{-3}	1×10^{-7}
Reconstituted Devon Silt	23	55	30	22	2.65	5×10^{-3}	1×10^{-6}

The dimensions of the sample were carefully measured, and the sample weighed on a balance to 0.01 g. These data were used to calculate the frozen bulk density. The sample was quickly sealed in a plastic bag to prevent sublimation of the ice, and stored for later use. Trimmings and end cuttings from the sample preparation were used to obtain the initial moisture content of the frozen soil. Eight samples of permafrost were prepared in this manner, and the initial density and moisture content data are given in Table 4.2. Two reconstituted samples of Mountain River clay and Devon silt were also prepared to ascertain if the thaw-consolidation apparatus was functioning correctly. These samples were prepared by freezing de-aired slurries of the soil in lucite rings 2 1/2 inches in diameter. The samples were extruded from the lucite rings and trimmed for testing. The properties and initial data for these soils are also summarised in Tables 4.1 and 4.2.

The sample was set up in the apparatus by first allowing the component parts of the apparatus to come to the temperature of the room at which the test was being carried out. As stated previously, the pore pressure measuring system and porous stone were saturated with ethylene glycol. A meniscus of glycol was maintained on top of the porous stone, and a wet filter paper was carefully placed on the glycol, and the frozen sample lowered gently onto the filter paper. The weight of the sample on the porous stone and base plate squeezed out all excess glycol, and a rubber membrane was placed around the sample. The membrane was sealed to the base plate by a rubber O ring seal. The two sections of the split barrel were clamped around the sample, and then the barrel was bolted to the base plate. The membrane was then held at the top of the barrel, and the load cap

TABLE 4.2 SUMMARY OF OBSERVATIONS FROM THAW-CONSOLIDATION TESTS

Sample Number	Soil	Frozen Bulk Density γ_f (g/cm^3)	Water content ω (%)	Observed Thaw rate α cm/s^{½}	Coefficient of Consolidation c_v (cm^2/s)	Thaw-Consolidation ratio R	Total stress P_o (Kg/cm^2)	Residual Stress σ_o' (Kg/cm^2)	Base pore pressure $u/(P_o - \sigma_o')$	Settlement Ratio $\frac{S_t}{S_{max}}$	Thaw Strain (%)
NWU-2	Undisturbed	1.84	36	0.0582	0.0267	0.179	0.500	0.12	0.106	0.965	8.3
NWU-4	Norman Wells	1.72	40	0.0561	0.0166	0.218	0.304	0^*	0.238	0.981	16.1
NWU-9	silt	1.62	50	0.0447	0.00462	0.334	0.213	0^*	0.487	0.910	34.5
NWU-10		1.62	48	0.050	0.00338	0.430	0.200	0^*	0.320	0.820	29.2
I-2	Undisturbed	1.86	34	0.0673	0.00185	0.783	0.403	0.14	0.640	0.270	12.5
I-3	Noell Lake	1.81	33	0.0675	0.00337	0.582	0.403	0.06	0.493	0.504	14.3
I-4	Clay	1.42	79	0.0390	0.00676	0.238	0.200	0^*	0.323	0.907	38.5
I-5		1.50	75	0.0393	0.00764	0.225	0.200	0^*	0.531	0.913	36.6
MR-1	Mountain R. clay	1.51	80	0.0453	0.00061	0.920	0.200	0^*	0.720	0.657	35.8
DS-1	Devon silt	1.64	50	0.0608	0.00529	0.418	0.200	0^*	0.393	0.712	

* Data obtained by extrapolation of other test data to these high void ratios

assembly was pushed down the barrel to make contact with the soil sample. The overburden loading was then placed on the load hanger which was brought in contact with the load plunger. The vertical dial gauge was brought to bear on the load cap, and the initial reading was adjusted to equal the height of the sample. As the dial gauge had a 2 inch travel, this permitted the direct reading of sample height at any stage of the test. Any extraneous pore pressures in the measuring system were allowed to dissipate and the pore pressure measuring system was closed from the atmosphere. The assembled sample and apparatus were then left undisturbed for approximately four hours to allow the temperatures, height and pore pressure readings to become constant.

The test procedure during the thaw-consolidation testing from this point onwards was the same as that described by Smith (1972). After applying a step increase in surface temperature to the sample, pore pressures, settlements and temperatures were recorded at one-minute intervals until thawing and settlement were complete. The results of the ten tests performed were plotted against the square root of time, and the results are shown in Figures B1 to B10 in Appendix B. The pertinent data are included on the graphs, together with sample data points. In order to calculate the settlement ratio S_t/S_{max}, it was necessary to calculate the height of the sample in the thawed, undrained state (H_{th}). This was done for each sample by assuming 100% saturation, and using the relations

$$\gamma_f = \frac{G_s + e_{th}}{1 + 1.09\, e_{th}} \qquad (4.1)$$

and

$$\frac{H_f - H_{th}}{H_f} = \frac{1.09\, e_{th} - e_{th}}{1 + 1.09\, e_{th}} \tag{4.2}$$

where e_{th} is the thawed undrained void ratio calculated from eq. (4.1),

γ_f is the frozen bulk density,

and H_f and H_{th} are the frozen and thawed height of undrained soil.

The excess pore pressures were normalised as in the theoretical treatment by dividing by $(P_o - \sigma_o')$. P_o was the applied loading, and the residual stress σ_o' in most cases was inferred to be zero due to the ice rich nature of the soil. In three cases, however, where the void ratio was low, it was measured for separate samples of the same material by the method described later in this chapter. The observed results for normalised excess pore pressures, settlement ratio and α values are presented in Table 4.2. The coefficient of consolidation was calculated from the post-thaw settlement data in the same fashion as that described in Section 4.1. When combined with the α value, the thaw consolidation ratio R was calculated. Figure 4.4 shows the normalised pore pressures plotted against the observed R value. The theoretical relation from Chapter 3 is also included as a solid line. The observed settlement ratios S_t/S_{max} are plotted in Fig. 4.5 against the R value, together with the theoretical relationship. These results will be discussed in section 4.6, and are also given in Table 4.2. After complete consolidation had occurred, some additional loading

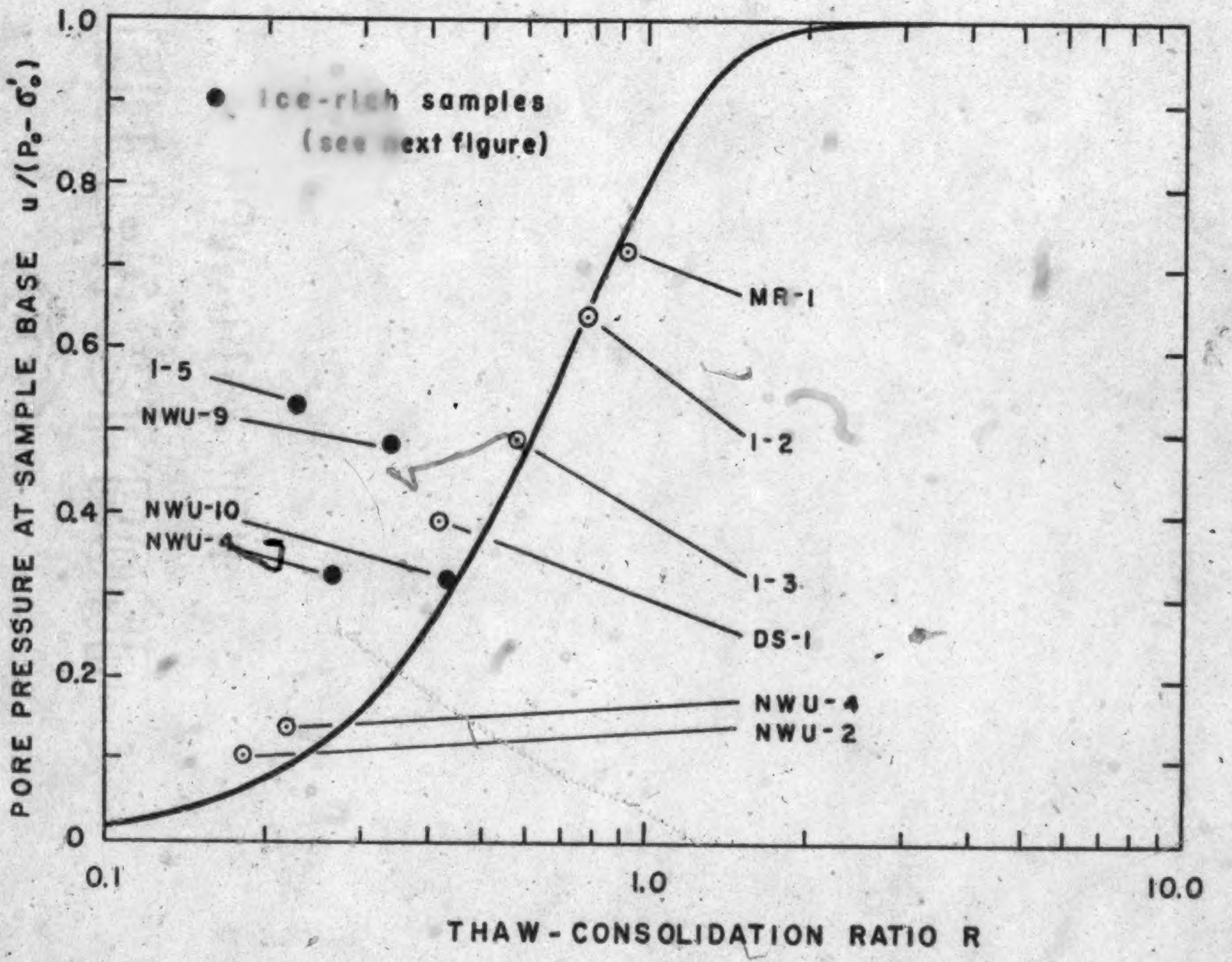

Fig. 4.4 Observed and Predicted Pore Pressures for Undisturbed Permafrost

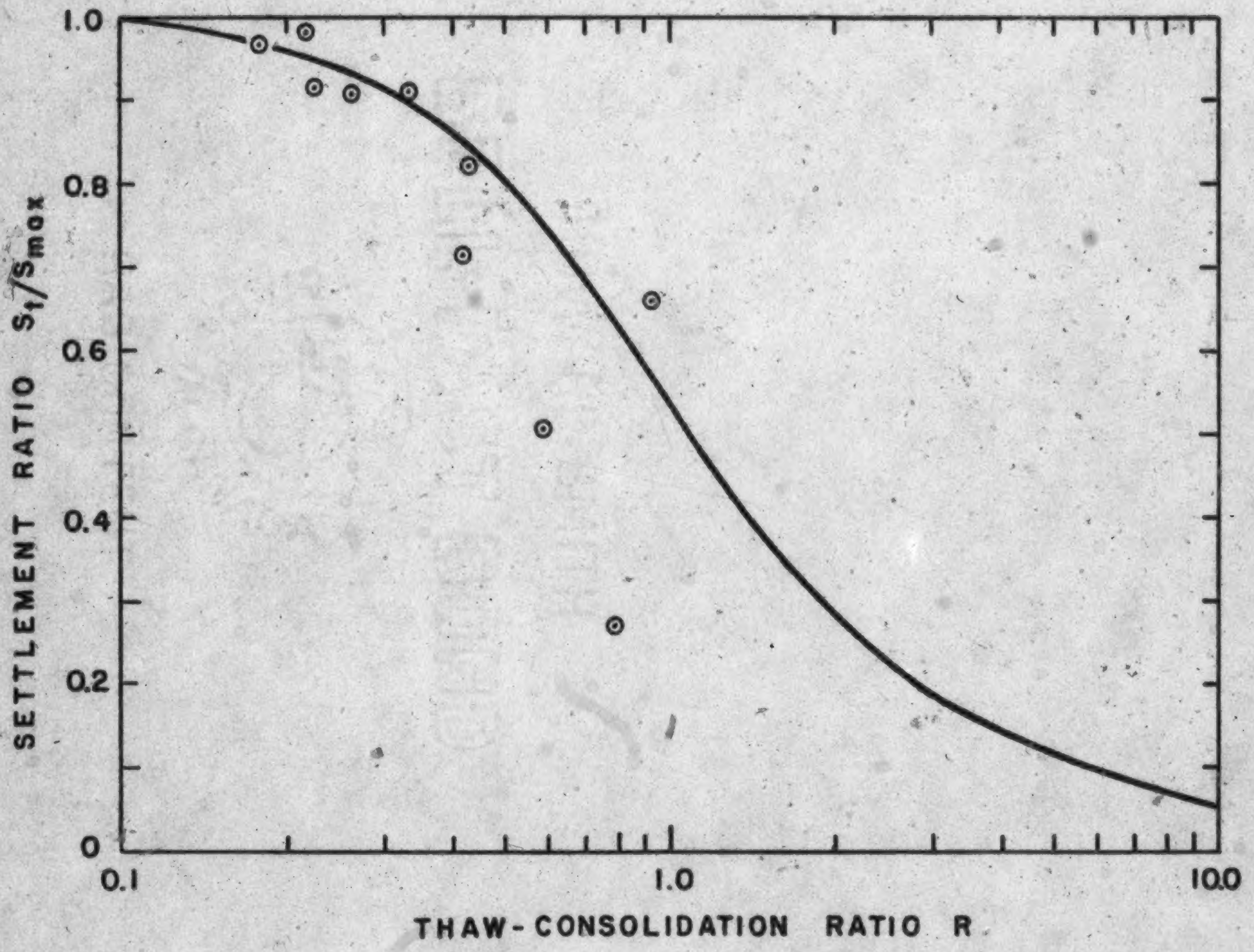

Fig. 4.5 Observed and Predicted Settlement Ratios for Undisturbed Permafrost

increments were applied in some cases to aid in defining the void ratio effective stress relationships, and obtain additional consolidation data.

If a thaw strain parameter is defined based on total settlement from the frozen to the thawed consolidated condition as the total change in specimen height divided by the original frozen height, then the results of the eight tests on undisturbed permafrost samples may be compared with results by other researchers. Speer et al. (1973) produced a correlation between thaw strain and the frozen bulk density based on the results of many tests on fine-grained soils from different Arctic locations. This correlation is reproduced in Fig. 4.6 together with the results of the eight tests described here. The data points are observed to fall close to the statistical correlation given by Speer et al.(op cit) in most cases.

The remaining study of importance is to determine the predictive power of simple analytical expressions for the thaw rate such as the Neumann solution, when combined with the simple expressions for the thermal properties described in Chapter 2. A value of α may be determined by calculating the heat capacities and conductivities from the data of Kersten (1949) and the known moisture content data. The latent heat term is calculated from eq. (2.15) based on the assumption that 10% moisture content (dry weight of soil) remains unfrozen at the initial temperature of $-5^{\circ}C$. This assumption is based on observations from the published literature that the ranges of silts and silty clays tested most likely have unfrozen moisture contents at $-5^{\circ}C$ of from 5% to 15% of the dry weight of soil. Using these thermal properties together with the initial and surface temperatures of $-5^{\circ}C$

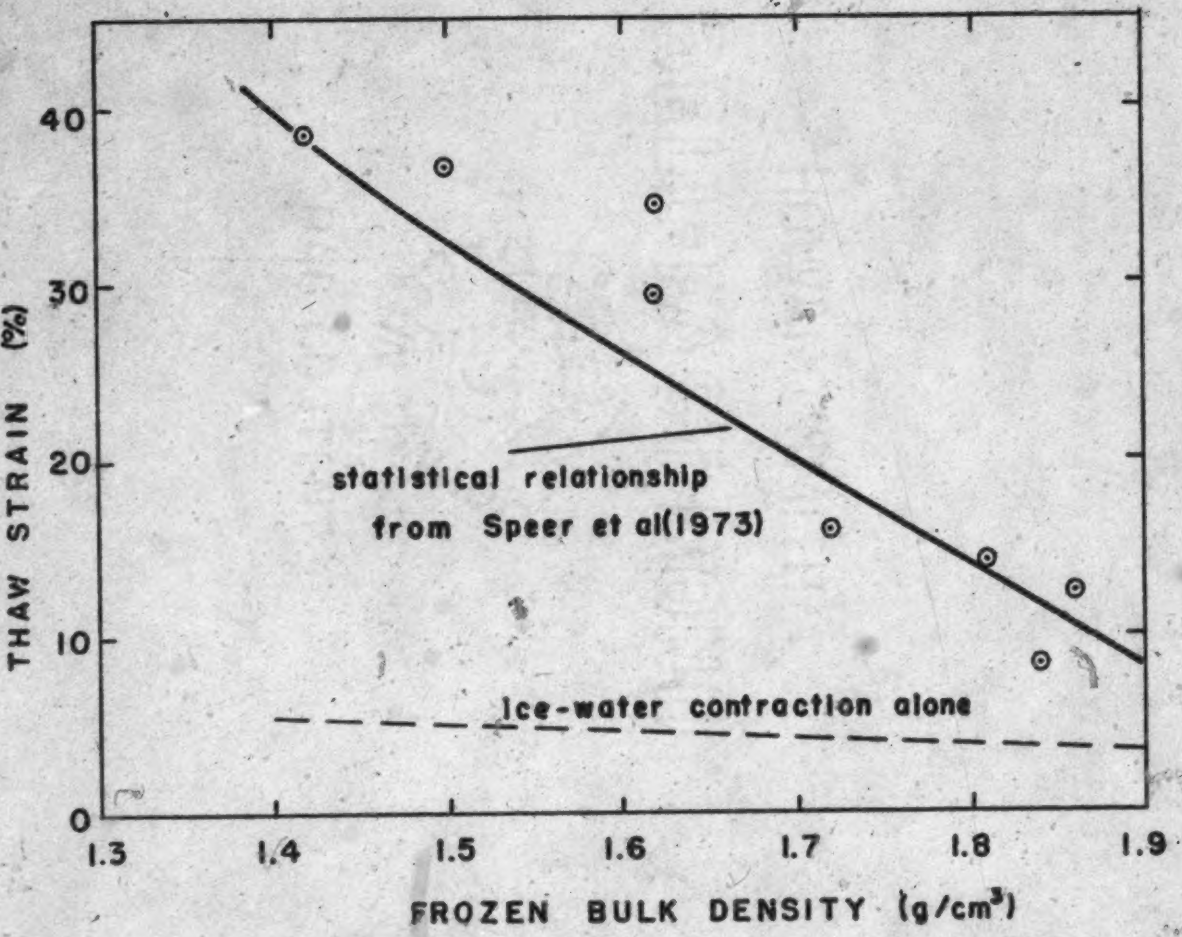

Fig. 4.6 Thaw Strains for Undisturbed Permafrost

and +21°C, the graphical solution of the Neumann solution in Fig. 2.2 is used to predict the α value. The observed value of α in the thaw consolidation test is then plotted against the corresponding predicted value of α in Fig. 4.7, for the eight tests on undisturbed samples. The dotted line at 45 degrees indicates the condition that the predicted α equals the observed α .

4.4 The Residual Stress in Thawed Soil

The boundary condition at the thaw line derived in Chapter 3 equates any flow from the thaw line with a change in volume of the soil. In the linear theory, the volumetric strain of the soil is proportional to the change in effective stress. The change in effective stress at the thaw line $\Delta\sigma'$ is given by eq. (3.16) as

$$\Delta\sigma' = \sigma'(X,t) - \sigma'_o \tag{3.16}$$

where $\sigma'(X,t)$ is the effective stress at the thaw line X; it is a function of time (t),

and σ'_o is the effective stress in the soil skeleton thawed under undrained conditions.

The initial effective stress in soil thawed under undrained conditions will be referred to as the residual stress. Only departures from the residual stress will result in volume changes.

The residual stress might conveniently be put equal to zero, and this is a reasonable assumption if the soil is rich in ice, or has a high void ratio in the thawed, undrained state. However, it should be noted that in cases where the stress and thermal histories associated with the formation of a specimen of permafrost are such as to reduce

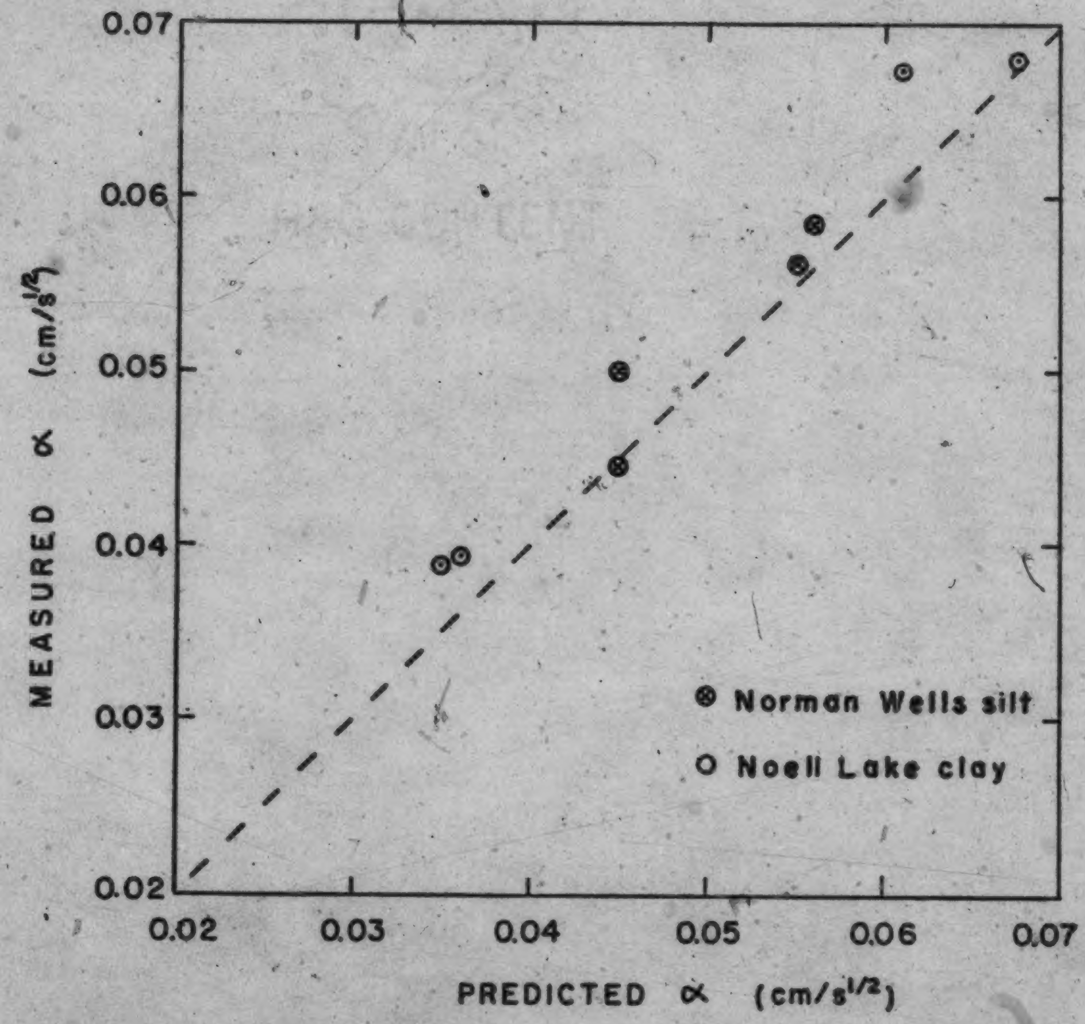

Fig. 4.7 Observed and Predicted Rates of Thawing for Undisturbed Permafrost

the void ratio of the soil, a significant residual stress may be present in the soil upon thawing. It has been shown in Chapter 3 how the residual stress is introduced into the theoretical analysis for thawing soils, and a discussion of the physical aspects of the parameter may now follow.

An appreciation of the physical meaning and importance of the residual stress within the context of the theory of thaw-consolidation is gained after consideration of the following experiment. A sample of unfrozen fine grained soil is prepared with a known stress history by consolidating a slurry to a known stress P_o. The sample has dissipated all excess pore pressures, and therefore P_o is an effective stress (see Fig. 4.8). The sample is now frozen in the absence of drainage, and the average void ratio changes a small amount from point A to B due to the volume expansion of water to ice in the soil pores. If the sample is now allowed to thaw again without drainage, the void ratio returns of course to point A. However, a striking increase is noticed in the pore water pressure, and if the sample has a high enough void ratio, the pore pressure may approach or even equal the total stress on the sample. This implies that the effective stress is greatly reduced, and indeed may be zero for all practical purposes. If the sample is now allowed to drain freely, consolidation will occur and the sample regains equilibrium at a much reduced void ratio, point C on Fig. 4.8.

Externally the soil in this sample has undergone a net decrease in volume represented by AC, under a constant external stress. During freezing, it is known that negative pore water pressures build up in fine grained soils. It may often be observed that small ice layers,

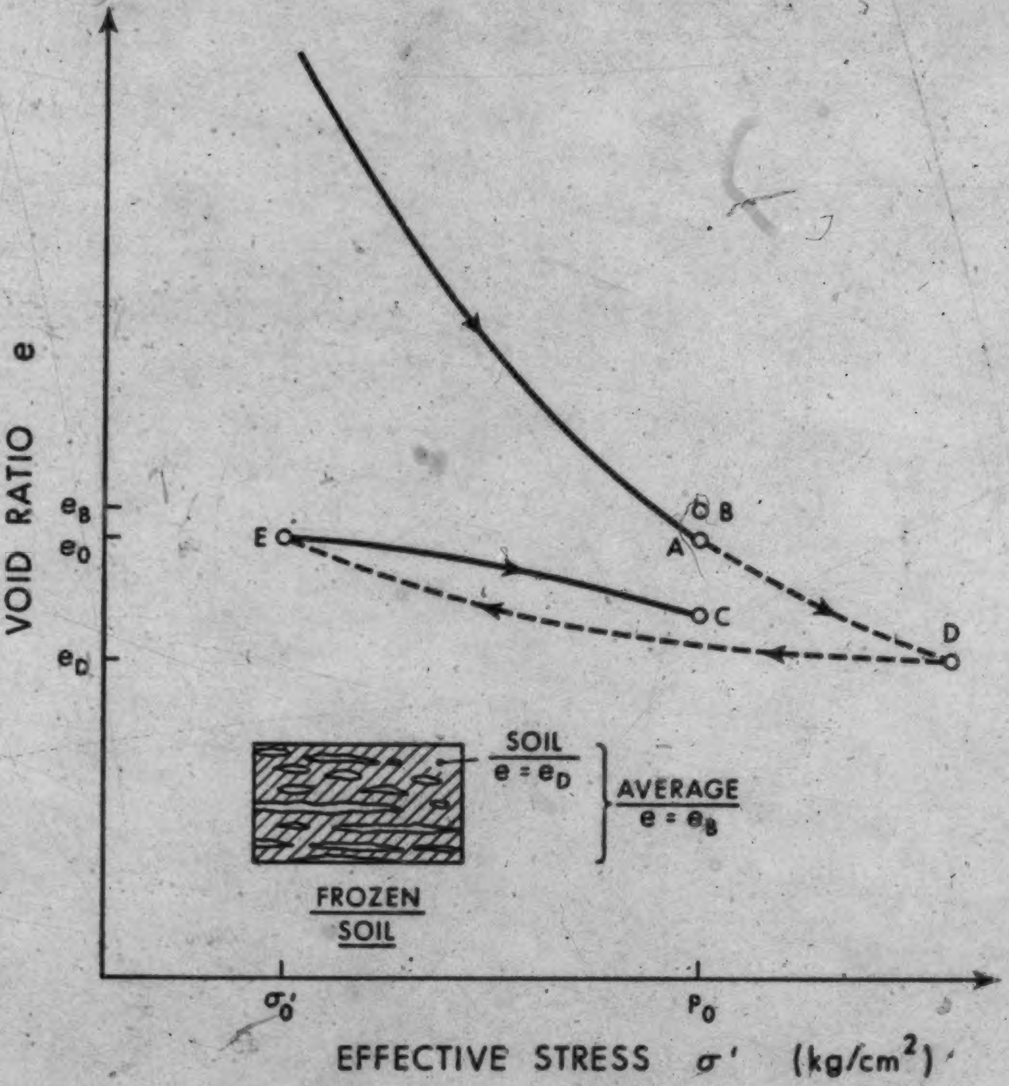

Fig. 4.8 Stress Path in a Closed System Freeze-Thaw Cycle (Schematic)

lenses, and other discrete segments of ice form upon freezing, even when freezing has taken place in the absence of free access to water. It must be concluded then that as the total quantity of water in the sample has remained unchanged, the remaining elements of soil are now overconsolidated with respect to the external total stress. That is, the areas of soil between discrete ice segments have experienced an effective stress greater than P_o. There is an abundance of evidence for the existence of negative pore pressures during freezing (e.g., Williams (1966), Wissa and Martin (1968)). In cases where a significant clay fraction is present, it is well known that the negative pressures can be exceedingly high.

On thawing, the overconsolidated elements of the soil possess an effective stress greater than P_o. However, a quantity of free water is available on a local scale from the thawed ice segments, and the soil swells almost instantaneously to absorb the excess water in the macro pores that result from the thawing of the segregated ice. The stress path taken by the soil elements is shown by the dotted line ADE in Fig. 4.8. If the soil is capable of absorbing all the free water, then the remaining effective stress is the residual stress. Alternatively if the soil swells to a zero effective stress condition, and free water is still available, then the residual stress is zero, and excess pore fluids remain in the soil. If free drainage is now permitted at the soil boundaries, the soil reconsolidates to the effective stress P_o, and the reloading behaviour is typical of that of an overconsolidated unfrozen soil. The reloading path is represented by the line EC in Fig. 4.8.

The net strain from the frozen to the fully thawed consolidated state (BC) is sometimes known as the thaw strain. In this simple experiment, the stress history of the soil is well defined, and it has been demonstrated how the thermal history is an extremely important factor in determining the residual stress in the thawed soil (σ'_o), and the subsequent stress-strain behaviour of the soil.

The behaviour of permafrost is influenced by the stress and thermal histories, and the drainage conditions when the soil existed in a thawed state. When a sample of frozen soil is removed from the ground, the first measurement in the thawed state that may be made is the determination of the residual stress. This constitutes the starting point for estimations of the excess pore pressure and settlements in a thawed soil.

If the soil is to remain essentially undrained for any significant period of time for reasons of fast thaw rates, low coefficient of consolidation, or the lack of a free draining boundary, then the residual stress σ'_o will control the initial undrained shear strength of the soil mass. The relationship controlling the undrained strength of a purely frictional thawed soil is

$$\frac{c_u}{\sigma'_o} = \frac{K_o + A(1 - K_o)\sin\phi'}{1 + (2A-1)\sin\phi'}$$

where c_u is the undrained shear strength of the thawed soil,

K_o is the ratio between the lateral and vertical effective stresses under conditions of no lateral yield,

A is the pore pressure parameter,

and ϕ' is the effective angle of shearing resistance of the soil mass.

In a soil which is simultaneously thawing and consolidating in a one-dimensional configuration, the excess pore pressures are controlled by the stress increment $(P_o + \gamma'X - \sigma_o')$. If the combination of stress and thermal histories were such as to generate high values of σ_o', it is conceivable that σ_o' could be greater than $(P_o + \gamma'X)$, and negative pore pressures would result on thawing, accompanied by settlements in this instance smaller than those due to the ice-water transformation alone.

4.5 The Measurement of Residual Stress

In the following, an apparatus is described that will permit the measurement of the residual stress in a thawed soil. The restrictions that must be placed on the test configuration are that no water be allowed to enter or leave the sample during thawing, and that no lateral yielding be permitted so that one-dimensional conditions are ensured.

The test might be carried out in either of two ways with a saturated soil. The first method is to set the total load σ on a sample equal to some constant value (e.g., the effective overburden load that the sample might be subjected to in the field), and then after complete thawing the residual stress is calculated by measuring the pore water stress, and subtracting it from the total stress. A second procedure, which might be described as a 'null' method, can be undertaken by thawing the frozen soil and continuously adjusting the total stress σ so that the pore water stress is always zero. In this way, the residual stress on completion of thaw is equal to the total stress on the sample.

The second of these methods is probably to be preferred, as it eliminates all pore pressure response effects in the soil and in the pore pressure measuring system.

An apparatus of the oedometer type was designed and constructed to accept a 2.5 inch diameter sample of frozen soil. The principle feature is a split lucite barrel which was bolted to a lucite base (as shown in Fig. 4.9). A greased rubber membrane was placed around the sample with porous stones and filter papers at both ends. The membrane was then sealed to the base plate and the aluminum load cap with rubber 'O' rings. The porous stones at each end of the sample were connected to a pore pressure transducer by means of the system of valves and tubing also shown in Fig. 4.9. This enabled the measurement of pore water pressures at the top and bottom of the sample at completion of thawing, and permitted the observation of subsequent consolidation behaviour of the thawed sample under additional load increments. The complete pore pressure measuring system was saturated with 50% ethylene glycol prior to testing to prevent damage to the valves and transducer in a cold environment. Temperature sensing equipment and temperature control devices are also present on the prototype, but these are not necessary for the measurement of the residual stress and the subsequent consolidation properties.

The test was carried out by carefully machining the frozen sample to the required diameter, and trimming to a height of 1 to 1.5 inches. The sample was mounted in the apparatus as described above, and allowed to come to thermal equilibrium in a cold room at

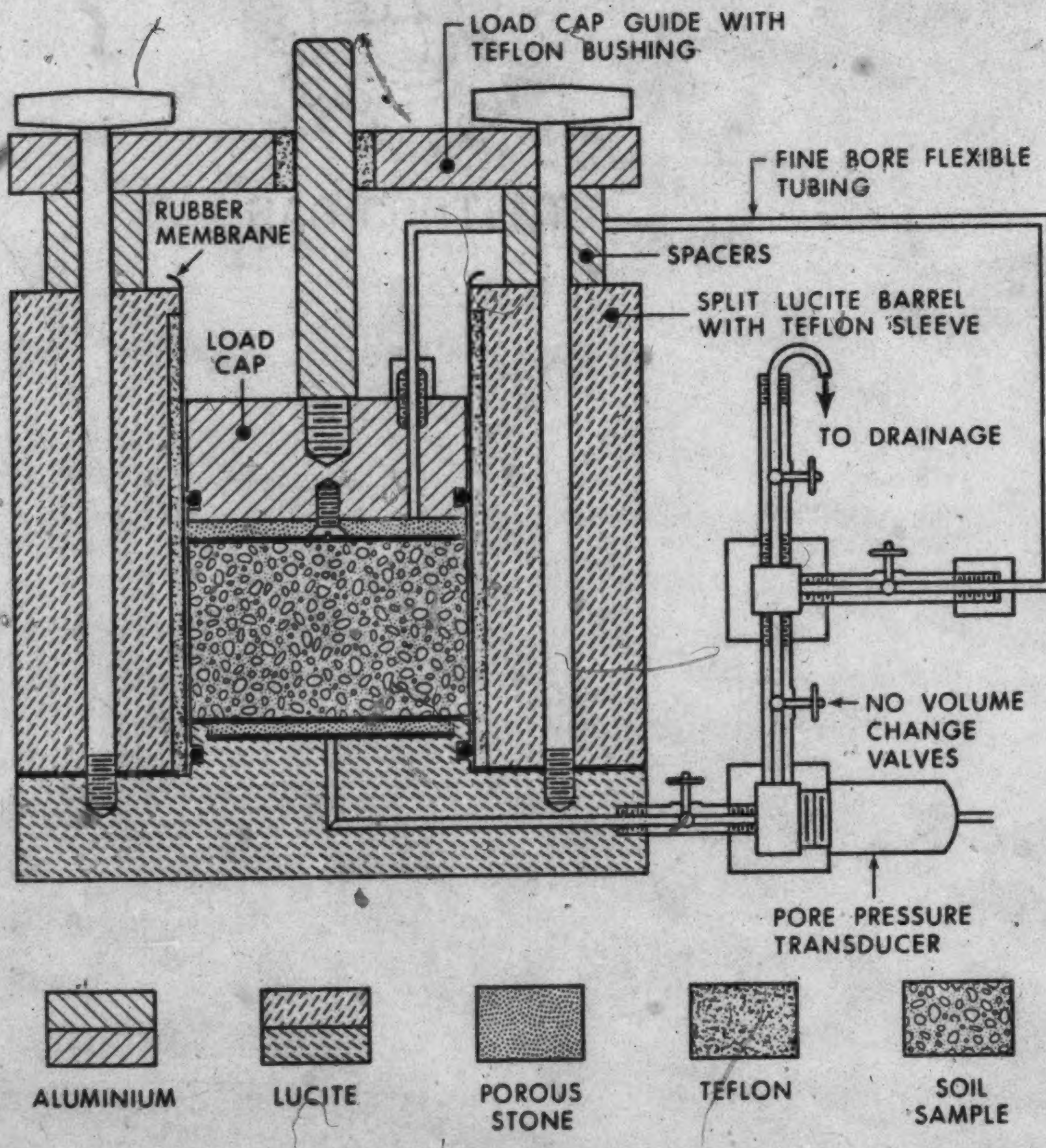

Fig. 4.9 Apparatus for Measurement of Residual Stress

at about -5°C. Great care was taken to ensure that the valves, tubes and porous stones were completely deaired with ethylene glycol. When the sample, membrane, and base plate were assembled, the two halves of the split barrel were clamped together around the sample, and were in turn bolted to the base.

A large load of the order of 1 kg/cm^2 was placed on the frozen sample for a short period of time in order to ensure that the sample and load cap were seated. Any extraneous pore pressures in the measuring system were allowed to dissipate, and the valves were closed in preparation for the measurement of the pore pressure. An initial vertical dial gauge reading was taken, and thawing was commenced in an uncontrolled fashion, usually from the top downwards. It was usually adequate to thaw the sample by circulating warm water around the load cap, finally allowing the sample to come into thermal equilibrium with a room temperature of about +10°C. While the test was in progress, the pore pressure at the top of the sample was continuously monitored and the total load varied to keep the pore pressure zero. When thermal equilibrium was regained at the positive temperature, the total stress on the sample was then equal to the residual stress in the thawed soil.

Additional load increments were then placed on the sample to determine the permeability, compressibility, and consolidation coefficients in the usual manner.

On completion of testing, the sample was removed, its water content determined, and the void ratio at the thawed undrained condition e_{th} was calculated.

Measurements of the residual stress were made on reconstituted samples of Athabasca silty clay from Northern Alberta, and on samples of a blue silty clay from the Mountain River, N.W.T. A summary of the properties of these materials is given in Table 4.1. The soils were prepared as slurries, and deaired. In some cases the slurries were consolidated to a convenient void ratio and then frozen in the apparatus. In other cases, frozen samples were prepared from the slurry, and after machining to the correct dimensions, were placed in the apparatus.

In either case, the sample was thawed, and the residual stress measured as described above. At completion of thawing, the void ratio of the sample was compared with the void ratio prior to freezing. For a successful test, these void ratios should be the same, demonstrating that no drainage occurred through the freeze-thaw cycle. Additional load increments were placed on the thawed soil and the consolidation properties defined. The sample could then be refrozen without drainage, and the residual stress measured for the lower void ratio. This procedure could be carried out several times until the relationship between the thawed void ratio e and σ_0' was defined. A typical set of test results for Athabasca clay, series A4, is shown in Fig. 4.10. It is worth noting that any relationship between e and σ_0' does not represent a stress path taken by the soil, but rather the locus of a series of points taken from a set of stress paths such as those indicated in Fig. 4.10.

In the test series A4, the soil was remoulded and consolidated to 0.2 kg/cm^2. The sample was then frozen for the first time, and the residual stress was found to be immeasurably small. The soil was

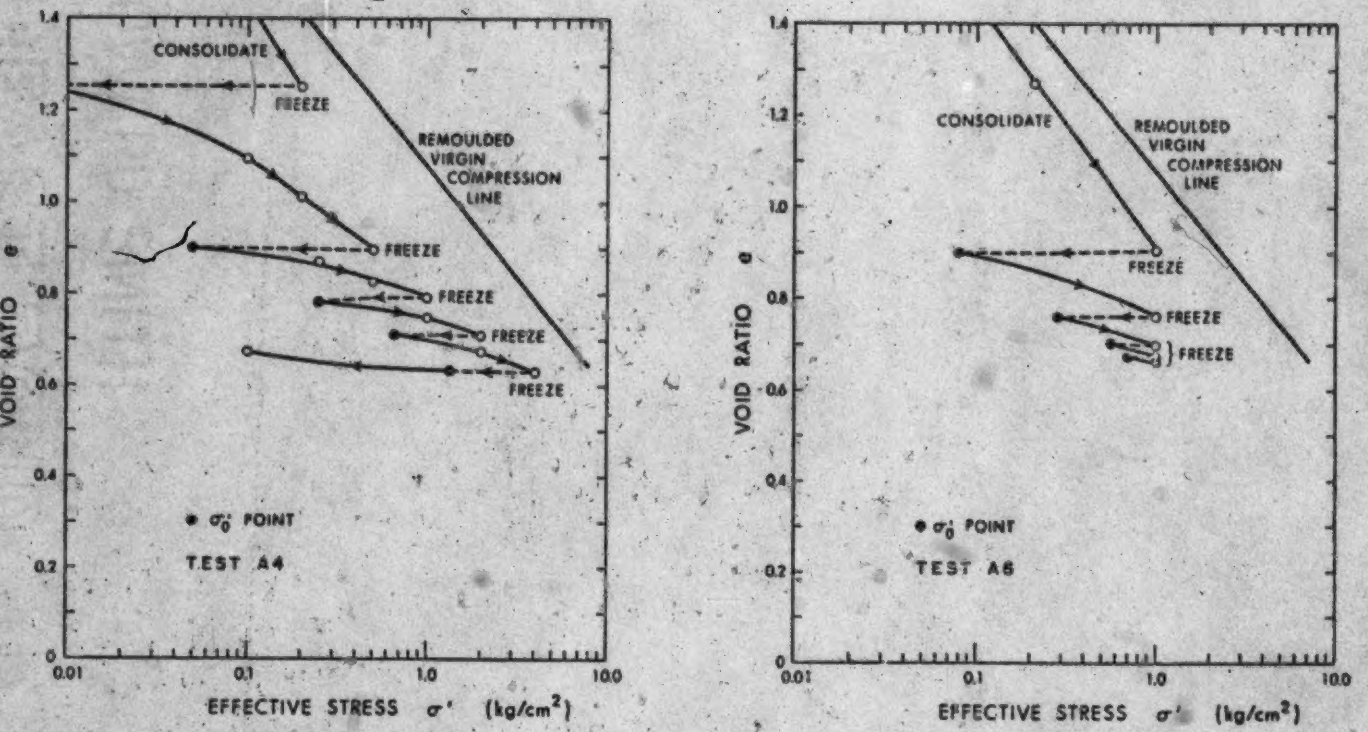

Fig. 4.10 The Measurement of Residual Stress for Reconstituted Athabasca Clay

consolidated to a higher stress and frozen. Upon thawing the residual stress was measured, and the process was repeated several times after consolidating to a higher load each time. To determine the effect of a different stress history on the residual stress, another remoulded sample was consolidated to 1.0 kg/cm^2 in test series A6, shown in Fig. 4.10 also. It was then frozen for the first time, and the residual stress measured in the thawed soil. Subsequent measurements of σ_0' were undertaken by reconsolidating the sample to the same stress of 1.0 kg/cm^2.

As freeze-thaw cycling continued in the absence of drainage during freezing, the residual stress increased steadily until it approached the overburden stress. The consolidation which occurred on reloading steadily reduced as the cycling proceeded. This behaviour is to be expected, as it is inconceivable that continued cycling would continue to cause steady decreases in the void ratio *ad infinitum*. Furthermore, this test series demonstrates that if the effective overburden stress is close to the residual stress in the thawed soil, then subsequent settlements due to consolidation after thaw will be small. The combined results for tests A4 and A6 are plotted in Fig. 4.11 as thawed void ratio against the logarithm of the residual stress σ_0'. Although entirely different stress paths were taken by the two soil samples, approximately the same relationship is found between e and σ_0'.

A strong linear correlation exists between the void ratio of the thawed soil and the logarithm of the residual stress. This relationship appears to be sensibly independent of the previous stress and thermal history effects, at least for the limited studies undertaken so far.

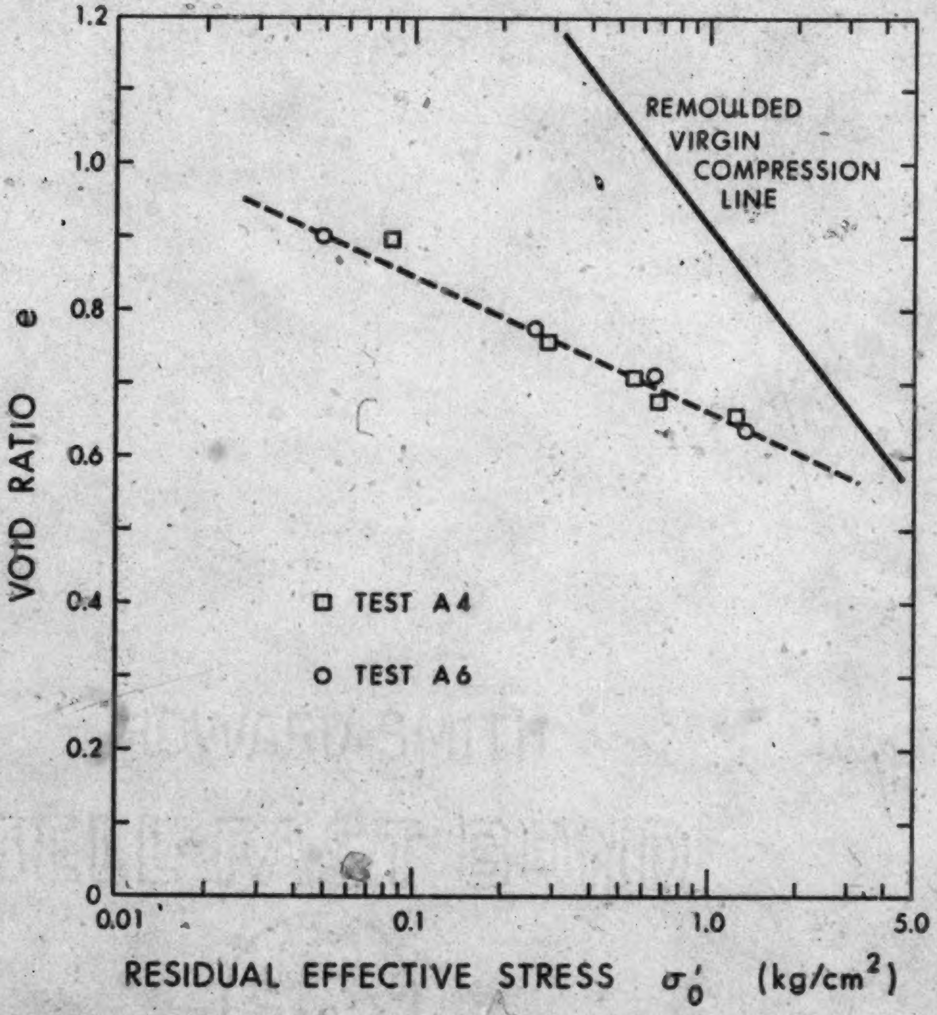

Fig. 4.11 e versus σ_0' for Reconstituted Athabasca Clay

Two remoulded samples of Mountain River clay were subjected to different sequences of consolidation and freezing. The stress paths taken by the two test samples MR1 and MR2 are shown in Fig. 4.12. A summary of the residual stress data is shown in Fig. 4.13. Again the uniqueness of the void ratio-log residual stress line is demonstrated. A summary of other typical consolidation properties obtained during these tests is given in Table 4.1.

Undisturbed samples of Norman Wells silt were from different depths, cut to the required dimensions and a profile of void ratio with depth was obtained from moisture content determinations. The frozen bulk density of each sample was measured before testing.

A sample was placed in the apparatus and allowed to come to a uniform temperature of -5°C. The sample was then thawed as described previously, and the residual stress was measured. The results of tests on several samples are given in Fig. 4.14. To obtain some additional data, further consolidation to a lower void ratio was allowed under additional loading, and the sample refrozen prior to measuring the residual stress. Although the samples were no longer undisturbed, the data are included in Fig. 4.14. The depth, void ratio, frozen bulk density, residual stress, and coefficient of consolidation are summarised in Table 4.3.

Again a linear relationship between void ratio and the logarithm of σ_0' is found. Fig. 4.14 also shows the virgin compression curve for a remoulded sample of the material not subjected to any freezing. Generally, the increased scatter in the residual stress data for the samples at higher stresses simply reflects the increased difficulties in measuring pore pressures as the soil becomes less compressible.

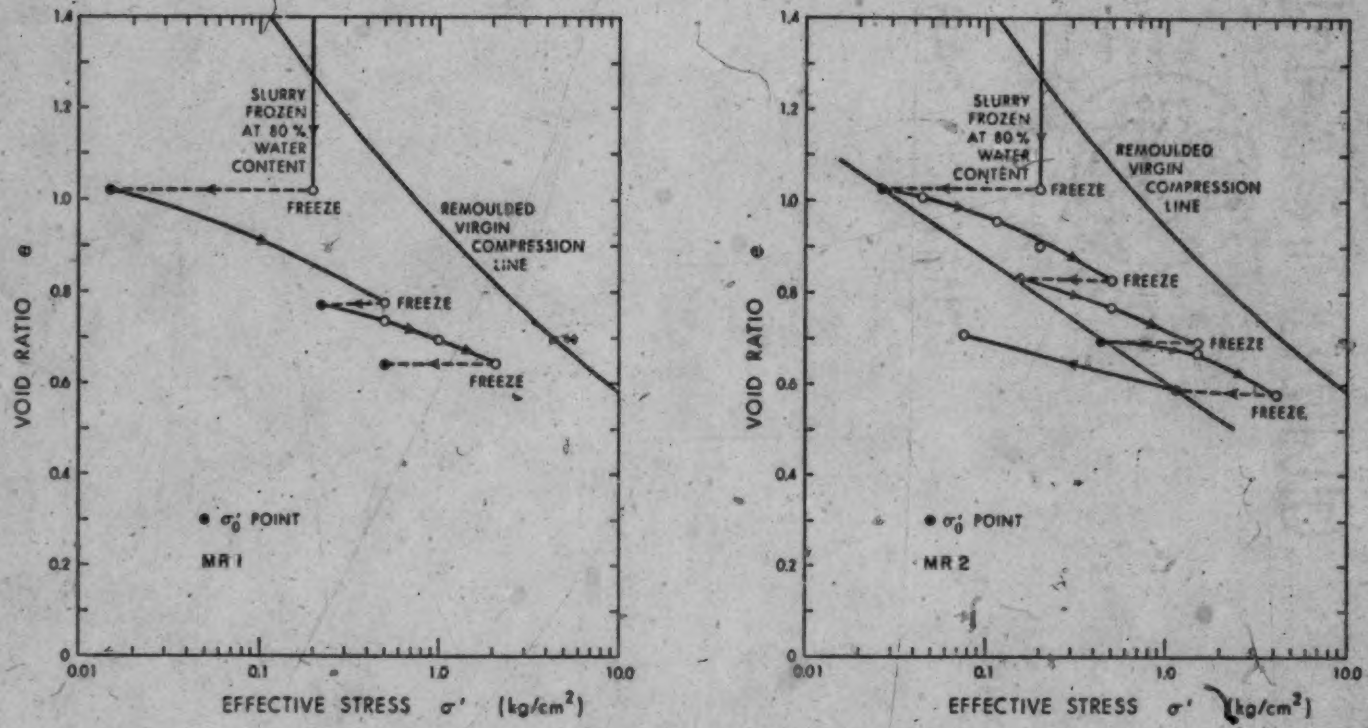

Fig. 4.12 The Measurement of Residual Stress for Reconstituted Mountain River Clay

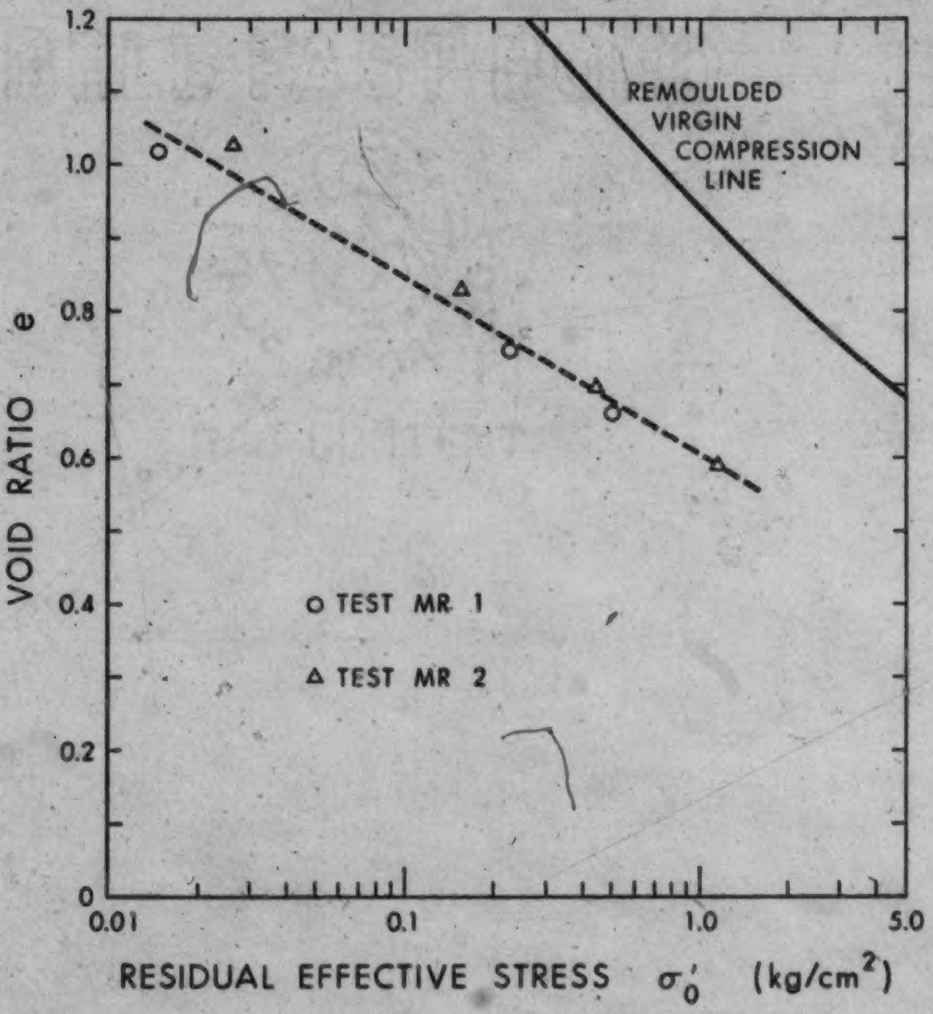

Fig. 4.13 e versus σ_0' for Reconstituted Mountain River Clay

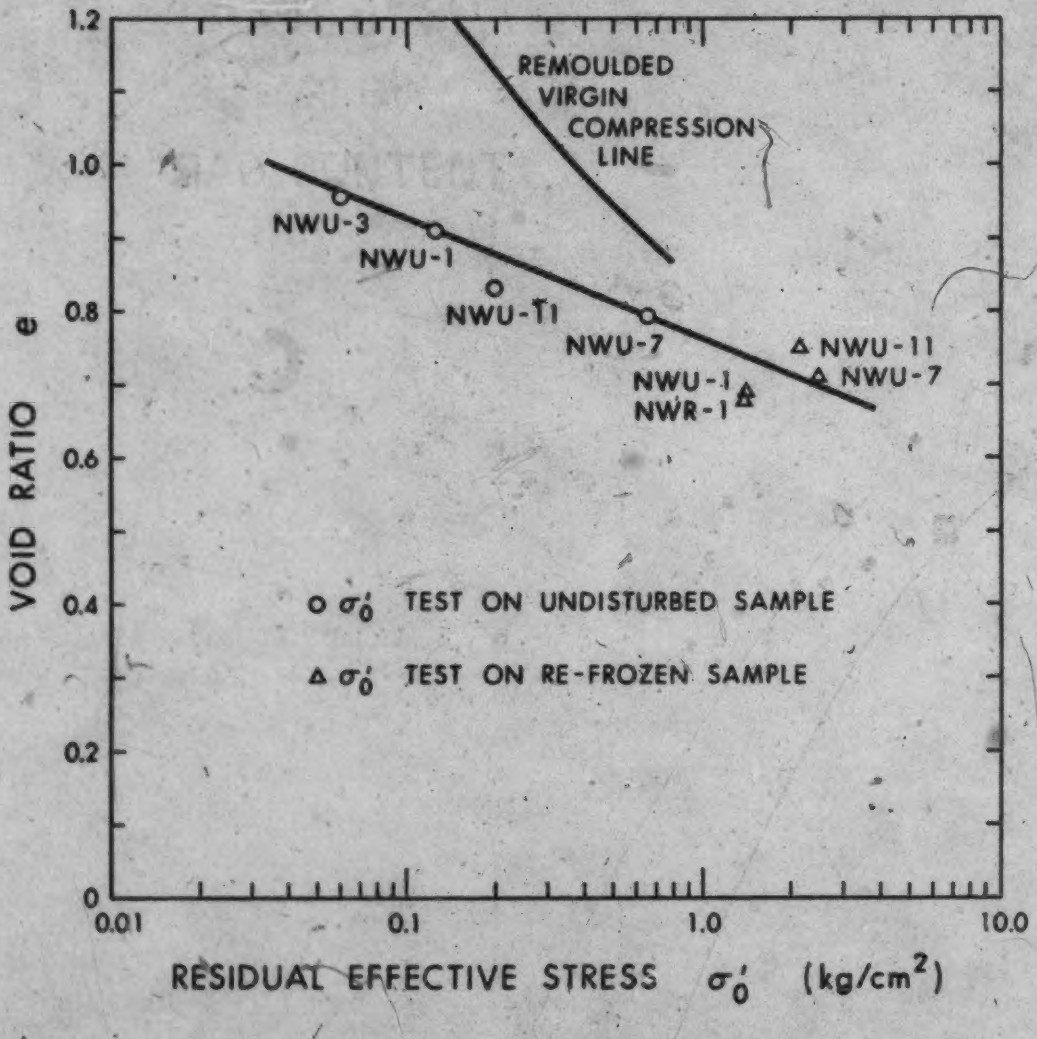

Fig. 4.14 Residual Stresses for Undisturbed Norman Wells Silt

TABLE 4.3 LABORATORY RESULTS FOR RESIDUAL STRESSES IN UNDISTURBED SAMPLES

Test	Depth (ft.) x	Ice Description (NRC)	Frozen Bulk Density $\gamma_f (g/cm^3)$	Thawed Void Ratio e	Residual Stress σ'_o kg/cm^2	Consolidation Coefficient c_v cm^2/S
NWU- 9	4-5	V_s 25%	1.62	1.320	0	0.46×10^{-2}
NWU- 3	5.5-6.5	V_s 5%	1.79	0.955	0.060	2×10^{-2}
NWU- 1	9-10	V_s 5-10%	1.85	0.910	0.125	3×10^{-2}
NWU- 7	14-15	V_s 5%	1.90	0.795	0.650	3×10^{-2}
NWU-11	15.5-16.5	V_s 10%	1.88	0.835	0.195	3×10^{-2}

It appears that for the site in question the residual stress increases approximately linearly with depth. The residual stress is shown plotted with depth in Fig. 4.15. The variability of the test data between 14 and 16 feet reflects the local changes in void ratio at that depth.

It is clear that considerably more testing would be required to establish the relationship accurately for a relatively incompressible material such as this. However, it is encouraging to observe that a material which possesses five to ten per cent visible segregated ice (see Table 4.3) exhibits a significantly large residual stress on thawing.

In addition to the measurement of the residual stress, the coefficient of consolidation was determined for the thawed samples of undisturbed permafrost. This was done by placing a load equal to the effective overburden weight on the sample, and allowing consolidation to occur from the initial effective stress (σ_0') to the final effective stress ($P_0 + \gamma' x$). In this way, the coefficients c_v, m_v and k were determined accurately over the correct stress range. The results for the undisturbed samples of Norman Wells silt are shown as a graph of the coefficient of consolidation with depth in Fig. 4.16. It is seen that below the permafrost table the coefficient of consolidation is relatively constant at $2.5 \times 10^{-2} cm^2/s$. This value is in all likelihood large enough to ensure a stable foundation at this site if thawing were to occur at any reasonable rate.

4.6 Interpretation of Laboratory Test Results

The laboratory testing carried out by Smith (1972) demonstrated

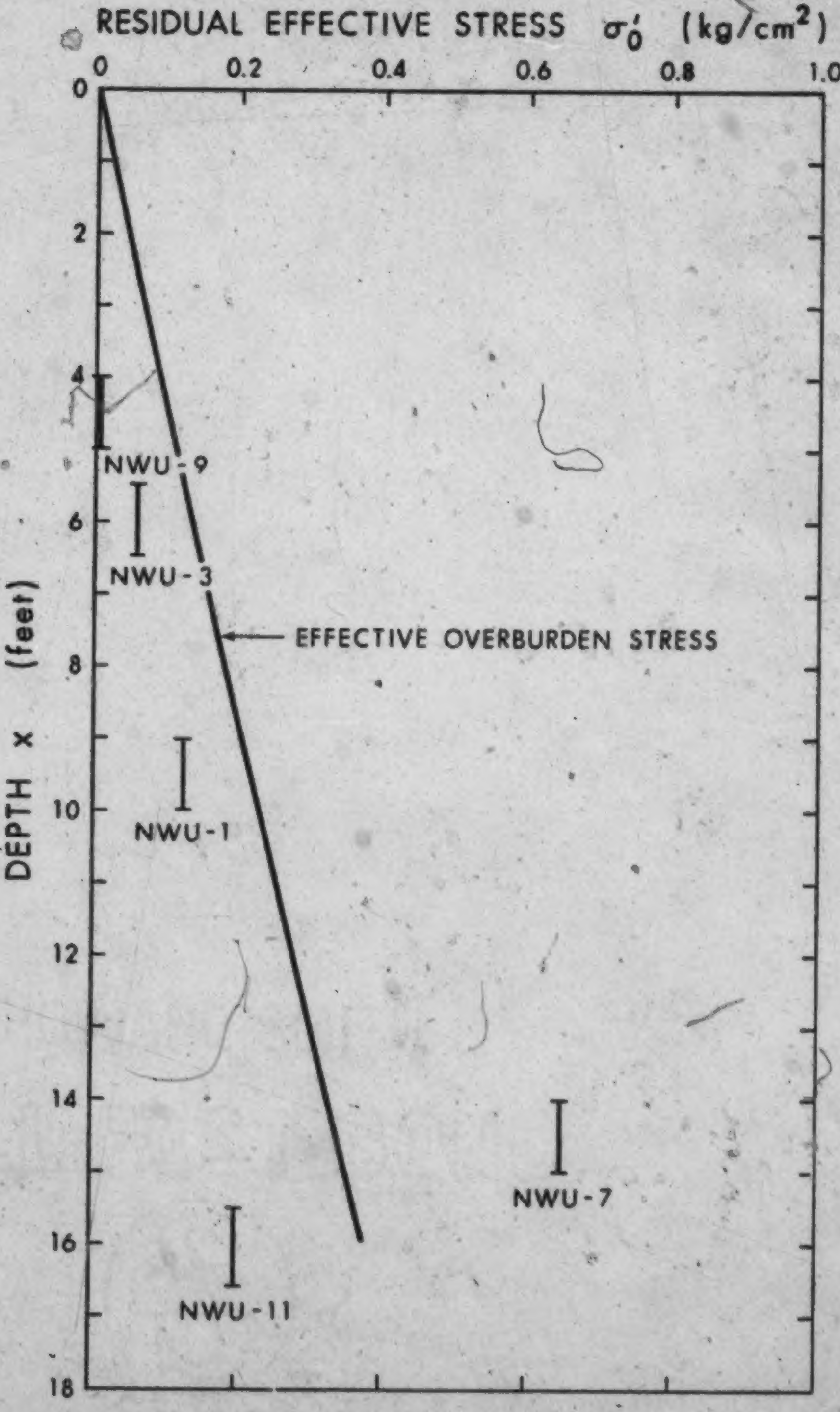

Fig. 4.15 Variation of Residual Stresses with Depth

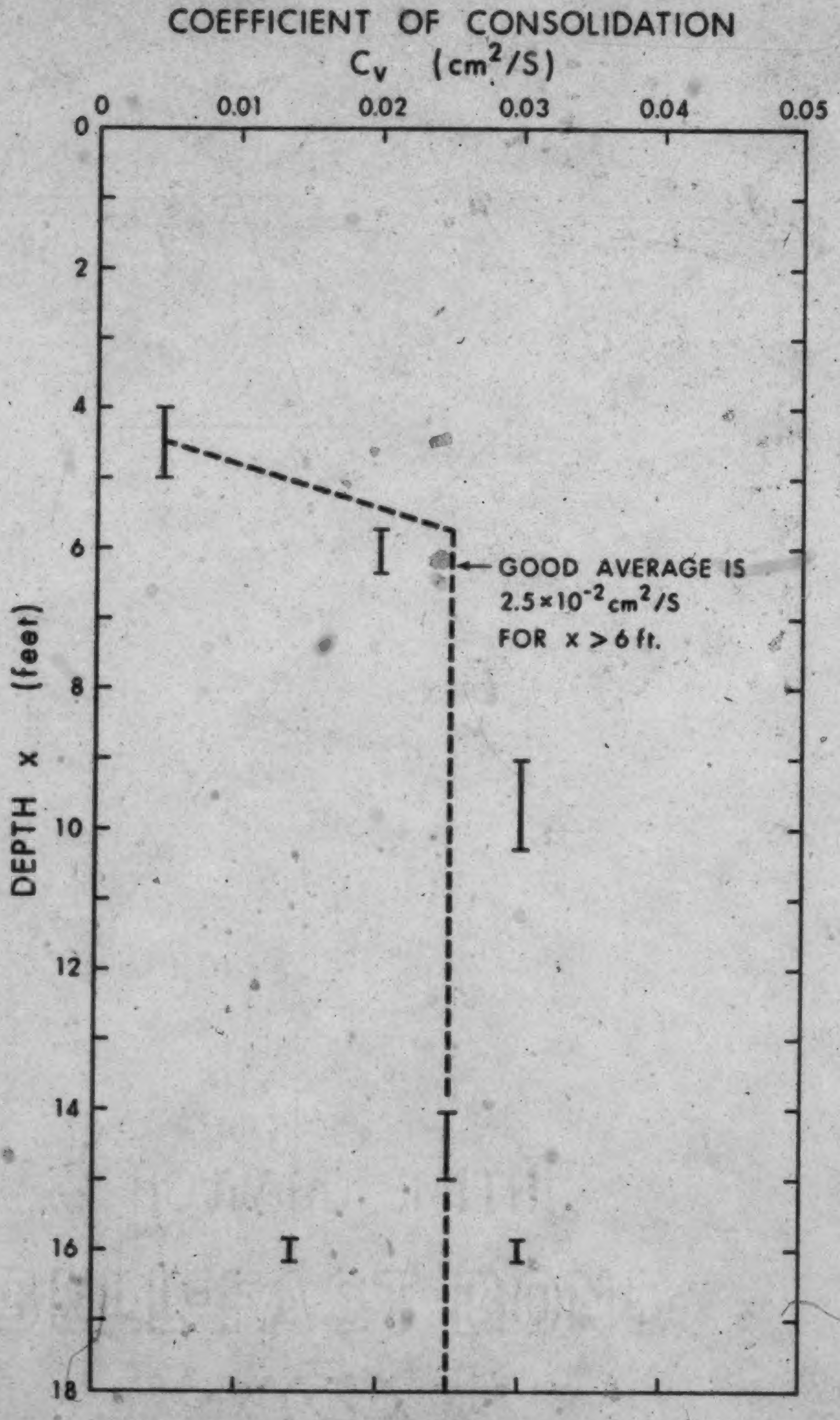

Fig. 4.16 Coefficient of Consolidation with Depth

that the rate of thawing through remoulded samples of frozen soil can be predicted with reasonable accuracy. It was also shown that the excess pore pressures and settlements in a thawing soil are dependent on the R value, and agree well with the predictions made by the linear theory of thaw-consolidation.

Using the modified design of the thaw-consolidation apparatus, thaw-consolidation tests were successfully carried out on several undisturbed samples of two Arctic soils, and two other reconstituted soils. The agreement between the observed rate of melting and the α value determined from the Neumann solution is remarkable, with deviations usually less than 5-10%. Bearing in mind that no special consideration was given to the unfrozen moisture content relationships for the soils, and that the conductivity data of Kersten (1949) were used to predict the α value, the predictive power of this simple procedure is excellent and extremely encouraging. The two parameters α and c_v enter into the R value, which is known to control the transient behaviour of pore pressures and settlements in thawing soils, and if α can be determined in advance to the degree of accuracy shown in Fig. 4.7, then attention may be diverted from heat transfer problem and directed towards resolving the consolidation problem and obtaining the correct value of the consolidation coefficient c_v to use in analysis.

Using the c_v value determined in the post-thaw phase of consolidation and the measured α value, an R value is determined for each test. In Fig. 4.5 the theoretical and observed settlement ratios are plotted with R, and the results are generally in good agreement. The two test results showing very low settlement ratios are most likely due to non-homogeneity of the ice features in the sample. The scale of the ice features in these samples (I2 and I3) were large when compared with the sample size, and in all probability, large ice layers were encountered by the thaw plane near the base of the samples. In Figs. B5 and B6, the settlement against root time curves are non-linear, demonstrating the probable non-homogeneity of the samples. In general, however, the ability of the theory in predicting the settlement ratio is reasonable.

The normalised excess pore pressures when interpreted in the context of the linear theory demonstrate excellent agreement between prediction and observation. Considering the extremely transient nature of the heat and moisture flow in the soil, and the general difficulty with pore pressure measurement in any configuration, these results are felt to constitute a successful verification of not only the theory of thaw-consolidation, but also of the functioning of the laboratory equipment. In four of the eight tests on undisturbed material, the thaw strain in the soil was less than twenty per cent. In the remaining four tests, very much larger strains occurred. This large strain behaviour is best predicted in advance by using the frozen bulk density of the sample as in Fig. 4.6, and by essentially disregarding the ice features in the sample. This observation is based on the results from samples I-2 and I-3, where the visible ice amounted to 20% by volume. However, the thaw strain under an approximate overburden load was only of the order of 12%. This strain could have been predicted by use of the frozen bulk density correlation given in Fig. 4.6, whereas an estimation of strain based on visible ice would have overestimated the strains for these samples.

It appears from the results given in Fig. 4.4 that the excess pore pressures in the samples exhibiting large strains were considerably higher than those predicted by the linear theory of thaw-consolidation. A better correspondence between theory and observation is obtained by incorperating a non-linear void ratio-effective stress function to describe the high degree of non-linearity of the constitutive relation for the soil when large strains occur. This analysis has been carried out, and is described fully in section 5.3. The method of plotting the void ratio against effective stress, and the use of this data to determine σ_0' is described also in section 5.3, and was used here in the interpretation of the four tests exhibiting large strains. The value of σ_0' was combined with the applied stress P_0 to obtain the stress increment, and then the normalised pore pressure curves in Fig. 5.7 were used to predict the excess pore pressures in the thawing soil. The effect of applying this non-linear $e - \sigma'$ function in interpretation of the excess pore pressures is shown in Fig. 4.17. The pore pressure when interpreted in the context of the linear theory is plotted, and then the resulting change in predicted pore pressure is shown when the non-linear theory is used to interpret the results. This extension to the linear theory is shown to improve the predictive power of the linear thaw-consolidation model considerably, and the predicted and observed pore pressures no longer differ greatly.

Finally, the frozen bulk density appears to correlate reasonably with the thaw strain, and the relationship proposed by Speer et al. seems to fit the observed soil strains in a satisfactory

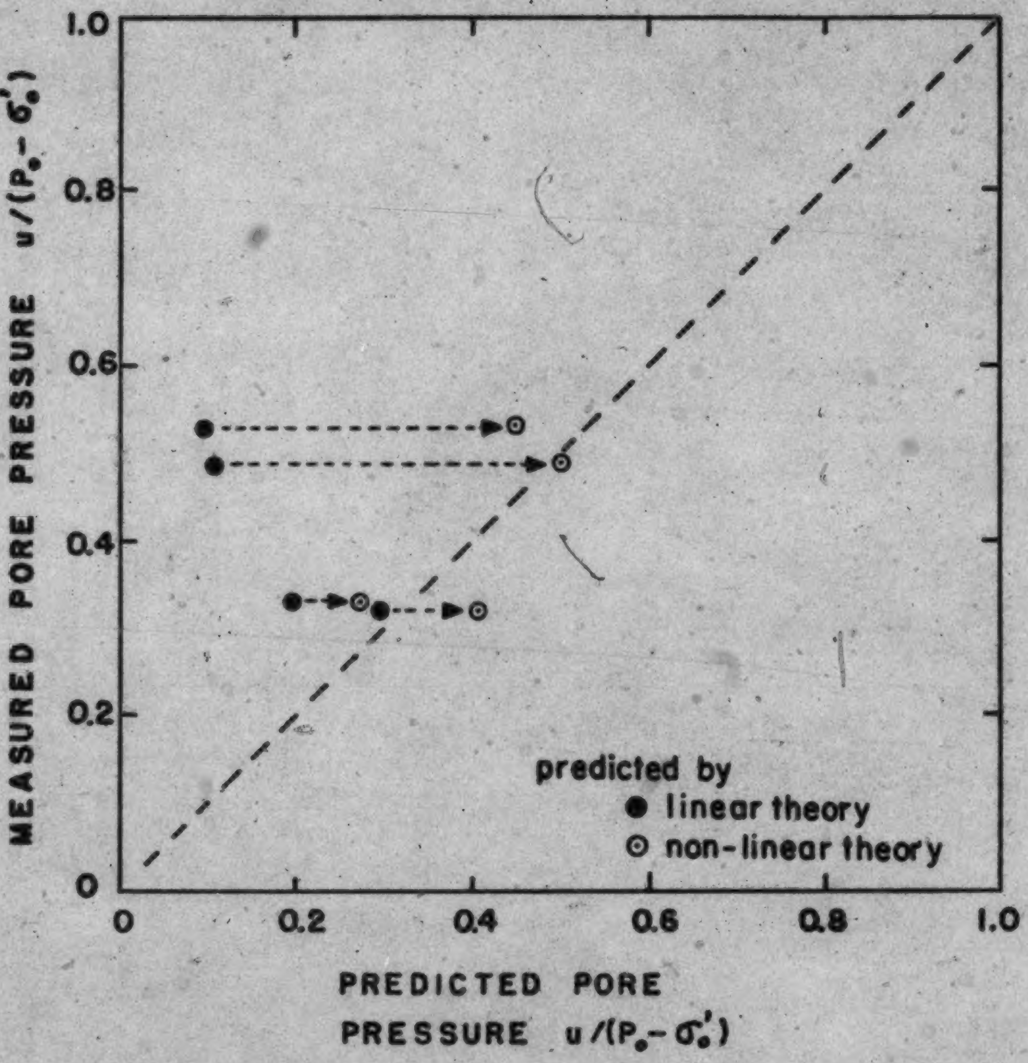

Fig. 4.17 Pore Pressures in Ice-Rich Samples Interpreted Using Non-Linear Theory

manner. Although the correlation is entirely empirical in origin, it appears to be capable of estimating the total settlement approximately, and is therefore useful in a preliminary analysis.

The existence of a residual stress in permafrost thawed under undrained conditions has far-reaching implications. The higher the residual stress in the thawed soil, the smaller will be the subsequent consolidation settlement, the lower will be the pore pressures generated during thaw and the higher will be the undrained shear strength. If the depositional sequence and the thermal history associated with the formation of a body of permafrost are such that the void ratio decreases significantly with depth, substantial values of the residual stress would be anticipated. Hence, the thawed soil would have a finite shear strength and problems such as the stability of the thaw bulb around a buried warm oil pipeline become less acute. The residual stress will generate a finite frictional resistance and the thawed soil will not behave like a viscous fluid as suggested in the prognostications of Lachenbruch (1970).

The influence of the residual stress is also of concern in the consideration of the effects of thawing permafrost on the behaviour of an oil well. The arching of the soil about the well will affect the stresses transferred to the casing which tend to make it buckle. It is of interest to note that Palmer (1972) has drawn attention to the control of arching by the effective stresses existing in the thawing soil during thaw and subsequent consolidation. He refers to the "extent of initial consolidation" which is related algebraically to the residual stress and observes that it is a property of the site rather than of the soil type. He notes further that it can only be determined by thaw consolidation tests on undisturbed cores.

In many cases of foundation design it may be prudent to remove the top few feet of highly compressible ice-rich material in order to limit thaw-induced deformations of the foundation. However, unless the residual stress can be shown to have a significant value compared with the effective overburden stress, serious deformations may still occur as the thaw plane penetrates deeper into the underlying ground. On the other hand, if a stratum with a high residual stress is accessible without excessive excavation, it may be possible to found flexible structures directly on it without concern for subsequent thaw. For example, oil tanks might be buried in the permafrost rather than placed on the extremely thick pads of gravel currently used.

The existence of the residual stress enables one to develop support conditions in thawing ground with greater confidence in their performance. This study of the residual stress has not only improved the ability to predict excess pore pressures and deformations in a thawing soil but it has also provided further insight into some of the processes involved in the formation of permafrost. Much more experimental work on natural permafrost samples is necessary to gain further knowledge concerning the distribution of residual stresses in the field and their effect on the behaviour of thawing soils.

CHAPTER V

EXTENSIONS TO THE THEORY OF CONSOLIDATION FOR THAWING SOILS

5.1 Introduction

In Chapter 3 a theory of consolidation for thawing soils is developed. Although the simplicity of the treatment allows the expression of the solution in an analytical form, and consequently permits examination of the variables controlling the excess pore pressures and settlements, it is recognised that important deviations from the assumptions made for the theory given in Chapter 3 may occur. In the following section several of the more important and obvious limitations of the simplified theory are discussed, and extensions are provided to increase the versatility of the theory. The more comprehensive the extension of course, the more complex will be the resulting solution. At the present stage of knowledge, it is considered more important to formulate the simple physical statements associated with each extension in turn, and observe the effects of the most important parameters, rather than attempting to establish some general, all-purpose numerical procedure that would account for many extensions simultaneously. When it has been decided which effects are important, and which are likely to be encountered in practice, then the implementation of such a general procedure might be suggested.

Each of the theoretical cases considered in this chapter is designed to extend the range of practical problems that may be embraced by the theory set out in Chapter 3.

5.2 Arbitrary Movement of the Thaw Interface

One of the most serious limitations of the linear theory described above is the assumption that the thaw interface moves proportional to $\sqrt{t}$. This is a valid relationship for the important case where a step increase in temperature is applied at the surface of a homogeneous frozen mass of soil. But for reasons of non-homogeneity, varying surface temperatures or two dimensional effects, a more general relationship between thaw depth and time may emerge from the associated problem in heat transfer. In section 6.2 such a relationship is extracted from a solution for heat conduction around a hot pipeline in permafrost.

An analytical solution in closed form is available for the case of thaw depth proportional to $\sqrt{t}$, but it appears unlikely that such exact solutions might be obtained for arbitrary movements of the thaw front. However, numerical methods may be employed to obtain a solution for the consolidation problem to almost any required degree of accuracy.

Let the movement of the thaw front be given by

$$X(t) = Bt^n \tag{5.1}$$

and its velocity by

$$\frac{dX}{dt} = n\,Bt^{n-1} \tag{5.2}$$

This power law permits expression of a variety of realistic relationships between X and t, with B and n specified as constants.

Rewriting the boundary equation (3.18) at the thaw interface using equations (5.1) and (5.2) provides the set of equations

$$t > 0; \quad u = 0; \quad x = 0 \tag{5.3}$$

$$t > 0; \quad \frac{\partial u}{\partial t} = c_v \frac{\partial^2 u}{\partial x^2}; \quad 0 < x < X(t) \tag{5.4}$$

$$t > 0; \quad (P_o - \sigma'_o) + \gamma' B t^n - u = \frac{c_v \frac{\partial u}{\partial x}}{n\,Bt^{n-1}}; \quad x = X(t) \tag{5.5}$$

$$t \geq 0; \quad X = Bt^n$$

These equations may be written in finite difference form, using a scheme proposed by Crank and Nicholson (1947), and the moving boundary is accounted for by either of the methods described by Murray and Landis (1959). The advantage of the Crank-Nicholson scheme is that it remains unconditionally stable for all values of the time step Δt, and the accuracy is much improved over other somewhat simpler methods.

The simultaneous equations so produced are tridiagonal when written in matrix form, and a simple algorithm derived from the Gaussian Elimination technique for simultaneous equations provides a fast efficient solution. The details of the finite difference scheme and the Gaussian Elimination algorithm are summarised in Appendix A.3.

Excess pore pressures $u(x,t)$, were evaluated at selected times by a program written for a digital computer. The degree of consolidation in the thawed soil was evaluated as in the linear theory from the expression

$$\frac{S_t}{S_{max}} = 1 - \frac{\int_0^X u\,dx}{(P_o - \sigma_o')X + \frac{\gamma' X^2}{2}} \qquad (5.6)$$

The integral term in equation (5.6) may be evaluated using a simple numerical integration technique such as the trapezoidal rule. A listing of the computer program is presented in Appendix A.4.

Values of the normalized excess pore pressure at the thaw interface, and the degree of consolidation are plotted against a time factor for the two extreme loading conditions $\gamma' = 0$, and $(P_o - \sigma_o') = 0$ in Figs. 5.1, 5.2, 5.3 and 5.4. It was found that for a given value of the power n, a unique relationship emerged between excess pore pressure, or settlement, and the time factor. The time factor T is defined as

$$T = \frac{c_v t}{X(t)^2} \qquad (5.7)$$

Values of n from zero to unity were chosen to cover the full range of physically realistic problems. A value of n equal to zero corresponds to a conventional fixed boundary consolidation problem, with the depth of consolidating soil set permanently equal to B, and an initial excess pore pressure equal to $(P_o - \sigma_o') + \gamma' X$. These results for n = 0 are plotted for comparison purposes, to form a lower bound to the family of curves.

The constant velocity thaw front (n = 1) is thought to be the upper bound for this set of curves, as this thaw rate is only achieved

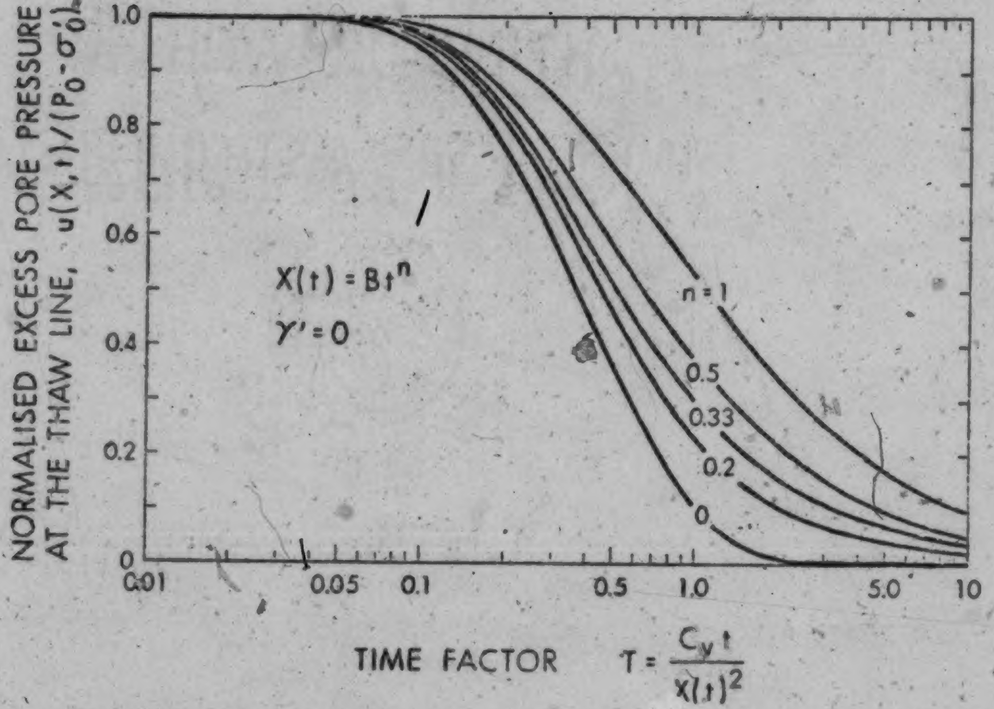

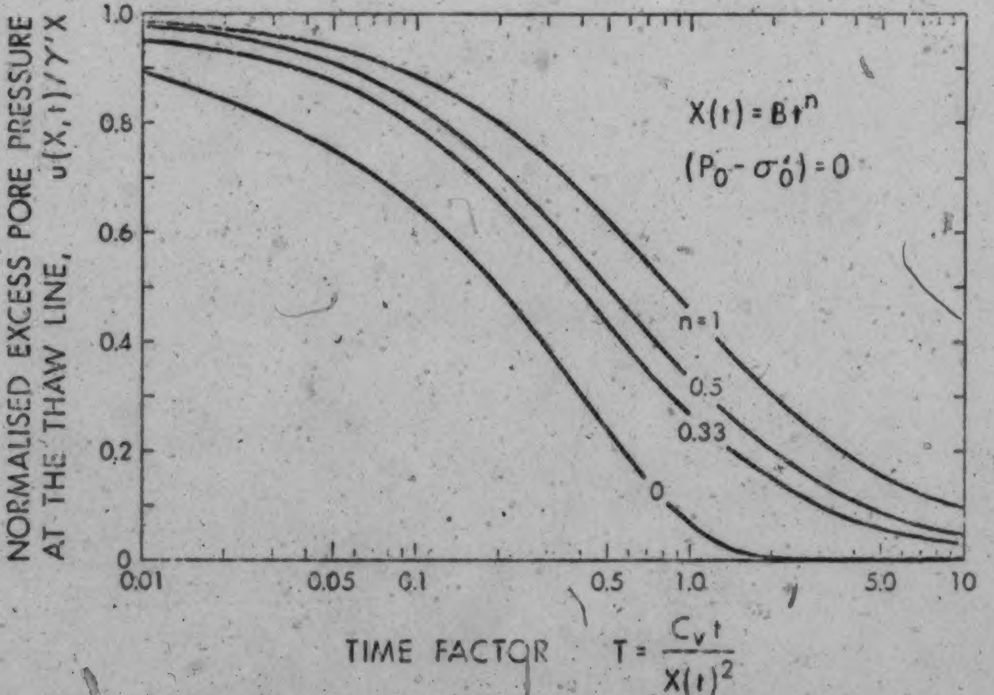

Fig. 5.1 and 5.2 Excess Pore Pressures at the Thaw Line

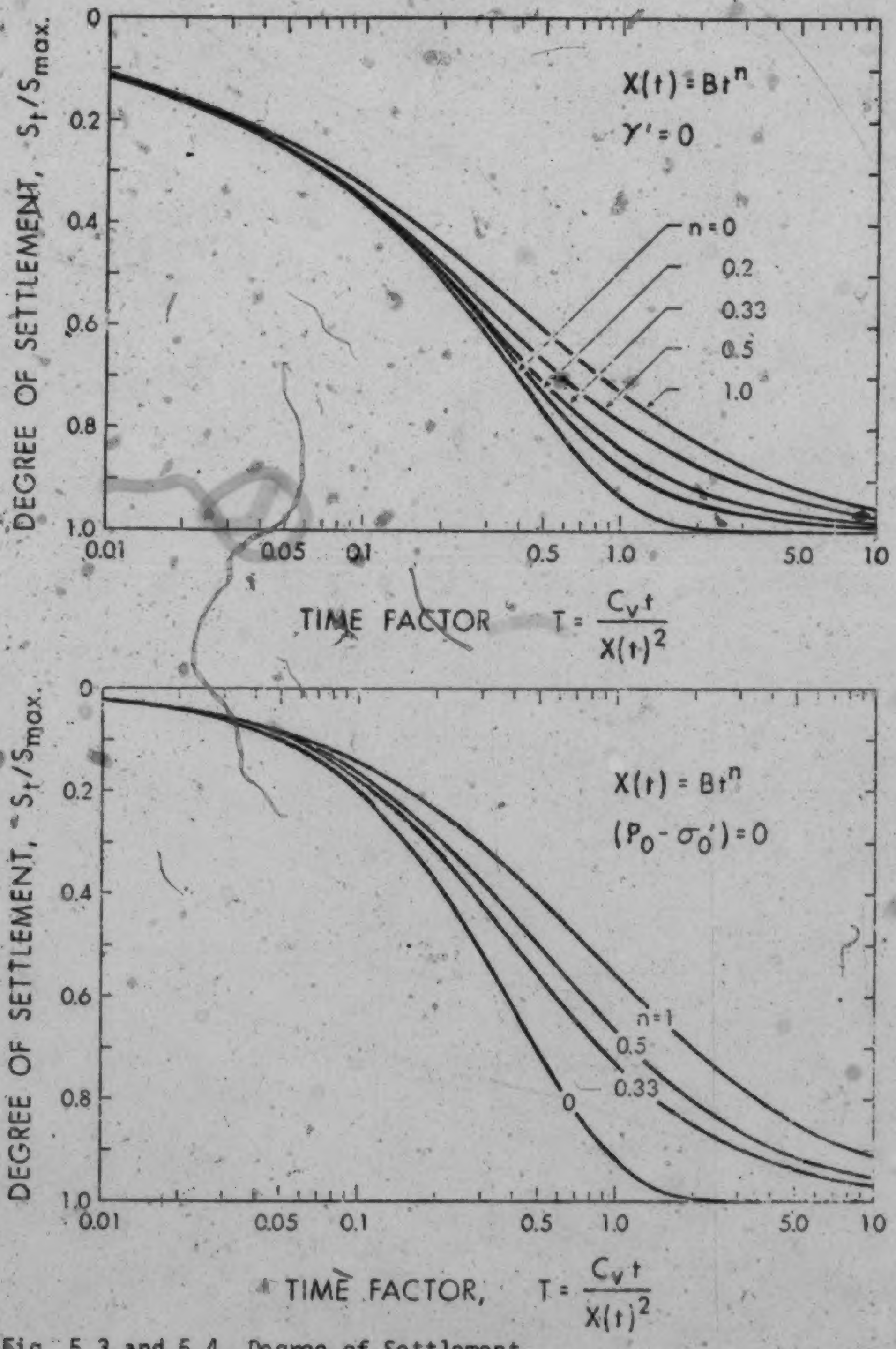

Fig. 5.3 and 5.4 Degree of Settlement

when, for example, the surface temperature of a homogeneous soil mass increases exponentially with time. The curious fact emerges that for the constant velocity thaw front, the time factor T decreases with increasing time.

For thawing proportional to the square root of time ($n = 1/2$), the time factor T is constant for all time, and it may be shown to be

$$T = \frac{1}{4R^2} \qquad \text{for } n = 1/2 \tag{5.8}$$

where R is the thaw-consolidation ratio defined by equation (3.35) for the linear theory described earlier. For $n < 1/2$, the time factor will increase with increasing time.

For the loading case $\gamma' = 0$, the settlement curves are very similar for S_t/S_{max} less than 0.5. Using the method proposed by Fox (1948), it may be shown that these curves are well approximated by

$$\frac{S_t}{S_{max}} = \frac{2}{\sqrt{\pi}} \sqrt{T} \tag{5.9}$$

$$\left(\frac{S_t}{S_{max}} < 0.5; \quad \gamma' = 0\right)$$

For the "self-weight" loading condition $(P_0 - \sigma_0') = 0$, no such simple relationship is valid.

The excess pore pressures at the thaw line in Figs. 5.1 and 5.2 are strongly dependent on the value of n. It is clear that in the class of problems where n is less than 0.5, excess pore pressure development at earlier times will be more critical, but stability will tend to improve as time progresses.

The solutions for any combination of the two extreme loading conditions may be obtained by simple superposition of the excess pore pressures.

So far, the power law relationship between thaw depth and time has been discussed in reasonable detail. Although a relationship of this type may be "fitted" to many realistic problems, the function itself has no theoretical background in the theory of heat conduction in melting soils. A further practical example of the use of the computer program in handling an arbitrary movement of the thaw plane is now considered. When the surface temperature of a homogeneous semi-infinite mass of frozen soil varies sinusoidally, the movement of the thaw plane is given by eq. (2.55). It has been shown in Chapter 2 how the approximation of the surface temperature sine wave by an average step increase in temperature is a reasonable procedure, if the maximum depth of thaw at the end of a thaw season is the primary concern. However, when one is considering the build-up of pore pressures under such thawing conditions, it is the velocity of the thaw front, dX/dt, which controls the excess pore pressures to a greater extent. Therefore it is of concern to calculate the excess pore pressures in a thawing soil which is subject to a sinusoidal application of surface temperature, and compare them with the pore pressures maintained in a soil thawing under an average step increase in surface temperature. It should also be pointed out that in some cases where the thawing of an active layer is taking place under natural conditions, it may be more correct to consider the surface temperature as varying in a sinusoidal manner.

Assuming a thaw season of 180 days, and the surface temperature varying sinusoidally between zero and 10°C, we have

$$\frac{T_s(t)}{10} = \mathrm{Sin}\left(\frac{\pi\ t}{180}\right) \tag{5.10}$$

where t is the time in days.

Taking the values for thawed conductivity and soil latent heat as

$k_u = 0.0025$ cal/°C.cm.S

$L = 32$ cal/cm^3

and using eq. (2.55) as derived by Lock et al. (1970), the relationship between thaw depth and time is given by

$$X = 62.2 \left\{ 2\ \mathrm{Sin}\left(\frac{t}{360}\right) - 0.0754\ \mathrm{Sin}\left(\frac{t}{360}\right) . \mathrm{Sin}\left(\frac{t}{180}\right) \right\} \tag{5.11}$$

where t is in days,

and X is in cm.

This particular example is the same as that used in Section (2.6) to determine the depth of thaw under a surface temperature sine wave. Equation (5.11), together with its derivative, dX/dt, are used in the subroutine "THAW" in the computer program listed in Appendix A.4. The functions X and dX/dt, the velocity of the thaw interface, are plotted in Fig. 5.5. The computer program prints the excess pore pressures and the degree of consolidation settlement as before. The excess pore pressures at the thaw line are plotted for two different loading conditions in Fig. 5.6, and two different c_v values for each. The excess pore pressures rise steadily and reach a peak approximately where the slope of the depth of thaw against the square root of time is a maximum in Fig. 5.6.

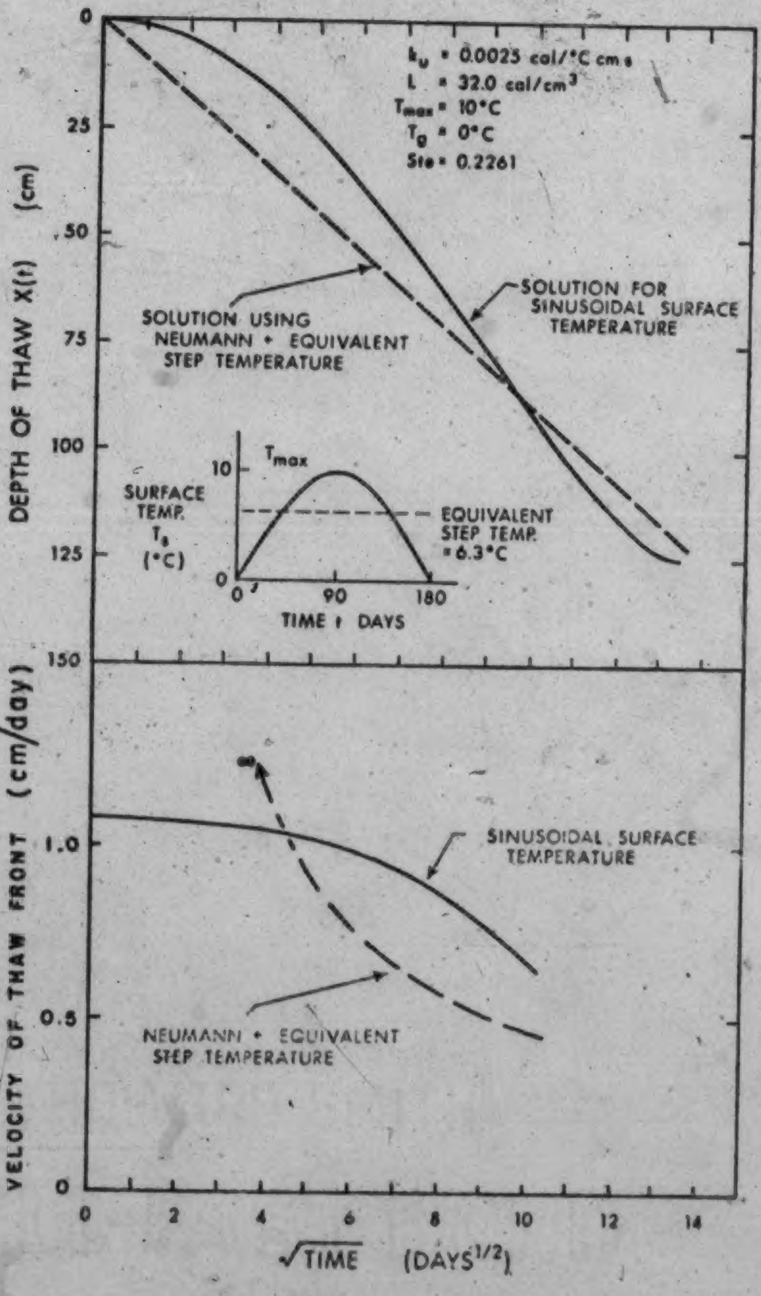

Fig. 5.5 Rate of Thawing for Sinusoidal Surface Temperature

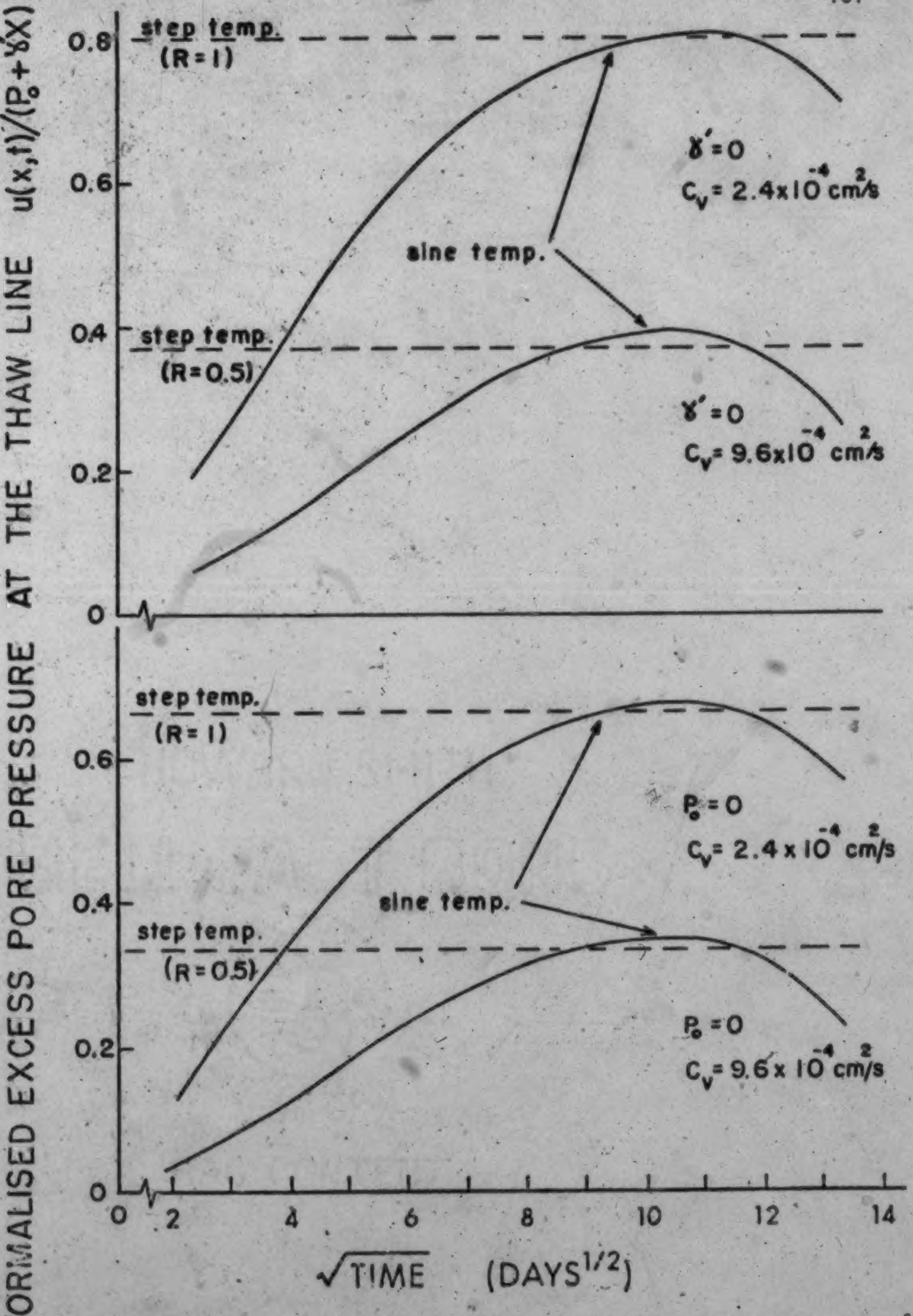

Fig. 5.6 Excess Pore Pressures for a Sinsoidal Surface Temperature

For comparison purposes, the excess pore pressures obtained by thawing under an average step temperature change equivalent to the sinusoidal surface temperature application are also plotted in Fig. 5.6. The normalised excess pore pressures at the thaw line for a particular step temperature application and coefficient of consolidation are constant with time, and are shown by the dotted lines in Fig. 5.6. It is seen from Fig. 5.5 that the velocity of the thaw front is initially greater for the step application of T_s, however at later times as the sinusoidal surface temperature rises to its peak, the thaw front velocity resulting from the surface sine wave is greater by a considerable amount. Consequently, Fig. 5.6 shows that the corresponding excess pore pressures at the thaw line rise just slightly above the excess pore pressures calculated for the equivalent step increase in surface temperature.

It might be argued that an equivalent step increase in temperature will produce a rate of thawing that will always provide an upper bound to geotechnical problems such as the build-up and maintenance of excess pore water pressures. It could be supposed even further that the equivalent step surface temperature would produce effects that were much too severe, and would overestimate the adverse conditions associated with a fast rate of thawing. It is demonstrated here that these arguments are not valid, and that indeed over a certain part of the thawing season, the excess pore pressures under the sine wave surface temperature exceed slightly those obtained under the equivalent step temperature. It is concluded that an average step temperature may be used with some confidence when predicting the maximum excess pore pressure in a thawing season, in a soil whose surface temperature varies sinusoidally. Nevertheless, if appropriate surface temperature data are available, a more accurate prediction of the variation of pore pressure with time is obtained readily using the computer program given in Appendix A.4.

5.3 The Non-Linearity of the Stress-Strain Relationship for the Soil Skeleton

Natural deposits of permafrost exhibit a wide range of void ratios in the field. Because the ice matrix in the pore spaces of a frozen soil is capable of supporting stress for an indefinite time period, a much wider range of void ratios may be expected in the Arctic than those encountered in more temperature latitudes. Void ratios in fine-grained permafrost soils may range from almost pure ice to a void ratio corresponding to the Plastic Limit or less. In many cases, extremely ice-rich materials are limited to a fairly small depth below the surface.

However, significant depths of soil may be encountered where the soil might still be termed ice-rich. After thawing of these deposits, large quantities of water must be expelled from the soil pore spaces before appreciable gains in effective stress are to be realised. Stated in another way, the constitutive relationship for the skeleton of such soils may be quite highly non-linear.

It is of considerable interest therefore, to examine the limitations of applying a linear stress-strain law (such as that used in Chapter 3) to soils exhibiting varying degress of non-linearity in the soil skeleton. Several methods of incorporating a non-linear relation for the soil skeleton might be proposed in an analysis for excess pore pressures and settlements in a thawing soil. Let the initial void ratio in the thawed condition before drainage is permitted be denoted by e_o, and the final void ratio under the effective overburden loading be denoted by e_f. A schematic diagram of a typical relationship between void ratio and effective stress is given in Fig. 5.7. Also shown are different analytical functions which might be used to describe the soil behaviour. Of the four models shown, the first two are dealt with immediately, and the remaining models are discussed in the next two sections.

The first relationship between e and σ' shown in Fig. 5.7 is the linear Terzaghi assumption for the skeleton of a compressible soil, and this relationship and its incorporation into the one-dimensional theory of thaw-consolidation have been dealt with fully in Chapter 3.

The second model attempts to simulate the behaviour of the soil skeleton to a higher order of accuracy by assuming that the soil may expel a quantity of water to obtain a void ratio e_1, with no gain in effective stress. The skeleton may now consolidate from e_1 to e_f until the effective stress is equal to the final overburden stress, along a path which is linear but has a slope less than the linear model described above. The coefficient of compressibility must now be redefined as

$$m_v' = \frac{e_1 - e_f}{(1 + e_1)\,(P_o + \gamma' X)} + \frac{e_1 - e_f}{e_o - e_f}\, m_v \tag{5.12}$$

where m_v is the coefficient used in the linear analysis.

Rederiving the boundary equation (3.18), for the bi-linear analysis:

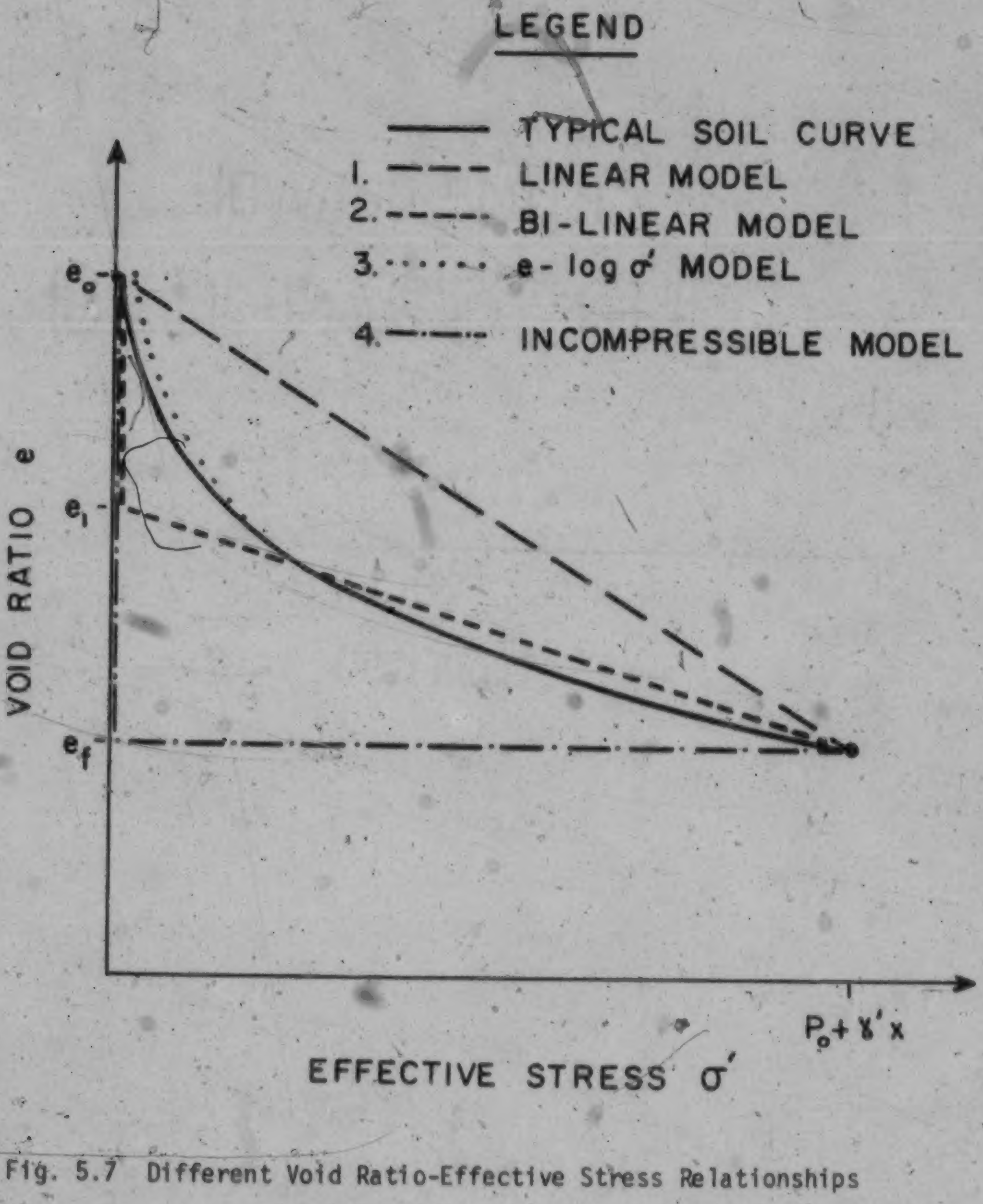

Fig. 5.7 Different Void Ratio-Effective Stress Relationships

$$P_o + \frac{e_o - e_1}{(1 + e_o)\, m_v'} + \gamma' X = \frac{c_v \frac{\partial u}{\partial x}}{dX/dt} \tag{5.13}$$

where $c_v = \frac{k}{m_v' \gamma_\omega}$

However, the quantity

$$\frac{e_o - e_1}{(1 + e_o)\, m_v'}$$

is a constant, and therefore may be added to the constant P_o loading term, and the solution may be expressed as a trivial extension to that obtained in Chapter 3. For the P_o loading condition only (oedometer conditions) the solution for the excess pore pressures is

$$u = \frac{\left\{P_o + \frac{e_o - e_1}{(1 + e_o)\, m_v'}\right\} \mathrm{erf}(Rz)}{\mathrm{erf}(R) + \frac{e^{-R^2}}{\sqrt{\pi}\, R}} \tag{5.14}$$

Although the m_v value is now reduced by the ratio given in eq. (5.12), and the R value is also reduced, an extra term appears in the numerator of eq. (5.14), tending to increase the excess pore pressures. This is certainly the simplest method of introducing some degree of non-linearity into the solution of the thaw-consolidation equation.

5.4 Influence of a Non-Linear Effective Stress-Strain Relation

Because high initial void ratios are expected in thawed soils, the subsequent stress-strain behaviour of the soil skeleton may be markedly non-linear as shown schematically in Fig. 5.7. Initially, the skeleton of such ice-rich, fine-grained soils must expel considerable quantities of water with only small corresponding increases in effective stress. As consolidation proceeds under successive increments in stress, however, the skeleton becomes progressively less compressible, requiring less volumetric strains to gain increased effective stress. As this behaviour is thought to be quite common in ice-rich permafrost soils, it is of considerable interest to investigate the influence of this non-linearity on the consolidation of thawing soils.

If the soil is thawed and no drainage is permitted, then the effective stress in the soil is denoted by σ_0'. If drainage is now permitted under the influence of subsequent loading increments, then the void ratio-effective stress curve may be found experimentally. Laboratory tests described in Chapter 4 suggest that for some thawed soils tested in this manner, a straight line is obtained by plotting e against the logarithm of effective stress. The same empirical relationship was incorporated by Davis and Raymond (1965) when formulating a theory of consolidation for normally consolidated unfrozen soils.

Although the permeability k, and the slope of the stress-strain curve m_v both change over a range of loadings, it may be assumed on experimental grounds that they change in such a way as to maintain the consolidation coefficient c_v approximately constant. Following Davis and Raymond (1965), a constant c_v value is adopted together with the stress-strain relationship

$$e = e_0 - I_c \log_{10}\left(\frac{\sigma'}{\sigma_0'}\right) \tag{5.15}$$

where I_c is the slope of the e/log σ' line (compression index)

and σ' is the current effective stress.

The general one-dimensional equation of consolidation for a saturated soil is then written as

$$-c_v\left[\frac{1}{\sigma'}\frac{\partial^2 u}{\partial x^2} - \left(\frac{1}{\sigma'}\right)^2 \frac{\partial u}{\partial x}\frac{\partial \sigma'}{\partial x}\right] = \frac{1}{\sigma'}\frac{\partial \sigma'}{\partial t} \qquad (5.16)$$

This equation is valid in the thawed soil regardless of loading type or drainage conditions at the boundaries.

For the same loading conditions considered previously, the total and pore water stresses respectively are

$$\sigma = P_o + \gamma' x + \gamma_w x \qquad (5.17)$$

$$P_w = u + \gamma_w x \qquad (5.18)$$

and with the water table at the surface x = 0, the effective stress is then the difference between these stress components.

$$\sigma' = \sigma - P_w = P_o + \gamma' x - u \qquad (5.19)$$

These equations are valid for any initial effective stress σ'_o developed on thaw, so

$$\frac{\partial \sigma'}{\partial x} = \gamma' - \frac{\partial u}{\partial x} \qquad (5.20)$$

$$\frac{\partial \sigma'}{\partial x} = -\frac{\partial u}{\partial t} \qquad (5.21)$$

and substitution of these expressions into eq. (5.16) yields

$$\frac{\partial u}{\partial t} = c_v \left[\frac{\partial^2 u}{\partial x^2} - \left(\frac{\gamma' - \frac{\partial u}{\partial x}}{P_o + \gamma' x - u} \right) \frac{\partial u}{\partial x} \right] \tag{5.22}$$

A linearizing transformation for this non-linear equation such as that used by David and Raymond is only available for the case $\gamma' = 0$. This condition where applied loads dominate will be studied here. Numerical means must be employed to solve a loading combination involving self-weight stresses.

Setting $\gamma' = 0$ in equations (5.19) and (5.22), and applying a linearising transformation to the governing eq. (5.22) gives

$$\frac{\partial w}{\partial t} = c_v \frac{\partial^2 w}{\partial x^2} \tag{5.23}$$

where $w = \log_{10}\left(\frac{P_o - u}{P_o}\right)$ (5.24)

The boundary condition at the surface is now

$$x = 0; \quad u = 0; \quad w = 0 \tag{5.25}$$

At the thaw line, the boundary condition used previously must be now rederived for consistency. Previously, a continuity requirement generated equation (3.9), that is

$$\frac{\Delta V}{V} = -\frac{e_o - e}{1 + e} = -\frac{k \frac{\partial u}{\partial x}}{\gamma_\omega \, dX/dt} \quad \text{at } x = X(t). \tag{3.9}$$

Defining the volumetric compressibility m_v as

$$m_v = - \frac{1}{1 + e} \frac{de}{d\sigma'} \qquad (5.26)$$

where e is the void ratio; and using the empirical equation (5.15) we obtain on differentiation

$$m_v = \frac{0.434 \; I_c}{(1 + e) \; \sigma'} \qquad (5.27)$$

So, using equations (5.15) and (5.27) it may be shown that

$$\frac{e_o - e}{1 + e} = \frac{m_v}{0.434} \sigma' \; \log_{10} \; \frac{\sigma'}{\sigma_o'} \qquad (5.28)$$

The boundary condition (3.9) after substitution of (5.19) and (5.28) becomes

at $x = X(t)$;

$$\frac{P_o + \gamma' X - u}{0.434} \log_{10} \left(\frac{P_o + \gamma' X - u}{\sigma_o'} \right) = \frac{c_v \frac{\partial u}{\partial x}}{\frac{dX}{dt}} \; ; \qquad t > 0 \qquad (5.29)$$

Setting $\gamma' = 0$, provides the boundary condition required to study the applied loading condition. Rewriting in terms of $w(x,t)$, the transformed variable:

$$x = X(t); \qquad \log_{10} \left(\frac{\sigma_o'}{P_o} \right) - w = \frac{c_v \frac{\partial w}{\partial x}}{\frac{dX}{dt}} \; ; \qquad t > 0 \qquad (5.30)$$

The term $\log_{10} \left(\frac{\sigma_o'}{P_o} \right)$ is a constant, and so the equations

(5.23), (5.25), and (5.30) in terms of the transformed variable w are entirely analogous to the corresponding equations derived for the linear theory in terms of $u(x,t)$. Consequently the solution for the linear thaw-consolidation equation may be applied directly to obtain $w(x,t)$. For $\sqrt{t}$ thawing

$$W = \frac{w\,(z,t)}{\log_{10}\left(\frac{\sigma_o'}{P_o}\right)} = \frac{\mathrm{erf}\,(R\,z)}{\mathrm{erf}(R) + \frac{e^{-R^2}}{\sqrt{\pi}\,R}} \tag{5.31}$$

where $z = \frac{x}{X(t)}$ (5.32)

and the excess pore pressure is obtained from the modification

$$\frac{u(z,t)}{(P_o - \sigma_o')} = 1 - \left(\frac{\sigma_o'}{P_o}\right)^W \tag{5.33}$$

Equations (5.31) and (5.33) form the exact solution for a thawing soil with consolidation occurring solely due to an applied load P_o. The soil has an initial void ratio in the thawed state corresponding to an initial effect stress of σ_o'.

The effects of self-weight stresses may be determined relatively simply by numerical methods, and it is considered sufficient for the scope of this study to examine the effects of an applied load P_o upon the excess pore pressures.

The ratio P_o/σ_o' is a measure of the effective stress change in the thawing soil, and therefore of the non-linearity of the effective stress-strain curve. This ratio now enters as an additional dimensionless quantity, and its effect on the excess pore pressure distribution in the thawed soil may be investigated. As in the linear theory, the normalised excess pore presure distribution is unchanged throughout the thaw-consolidation process, although it is now dependent on the stress ratio P_o/σ_o'. The degree of settlement in the thawed soil however is independent of time and the ratio P_o/σ_o'. This fact was also recognized by Davis and Raymond (1965), for this type of stress-strain relationship. Consequently, the linear theory may be used equally well for calculating the degree of consolidation settlement.

Figure (5.8) shows the excess pore pressure at the thaw front, as a function of the stress ratio and the thaw-consolidation ratio R. It is seen that as the stress increment ratio increases, the excess pore pressure condition at the thaw line increases to a more critical level.

In cases where high initial void ratios are present in the soil on thawing, the excess pore pressures may be underestimated considerably, if only a linear relation between void ratio and effective stress is considered. The logarithmic function given by eq. (5.15) provides a method of accounting for any required degree of non-linearity. The function however always requires some value of σ_o', the residual stress. In very ice rich soils where this extension is obviously most useful, σ_o' is immeasureably small or zero, and so apparently cannot be used in the analysis, as the stress ratio is now infinite. However, it must be remembered that the reason for the introduction of such a function shown by the dotted line in Fig. 5.7 is to model in some way the high degree of curvature between e_o and some void ratio e_1. If a sample of frozen soil is thawed under a small nominal loading (often the weight of the load cap in an oedometer), it consolidates to a void ratio e_1 shown in Fig. 5.9. Now the stress path taken by the soil to

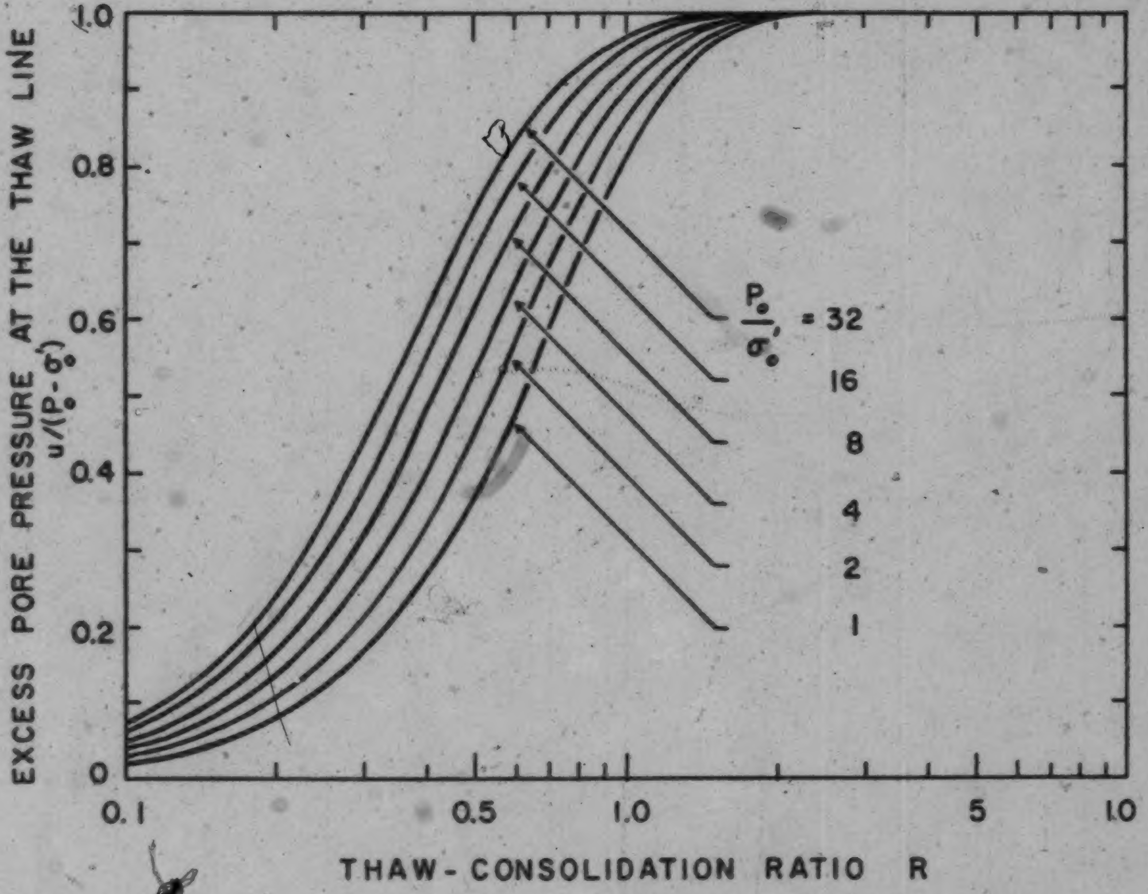

Fig. 5.8 Pore Pressures at Thaw Line for Non-linear Theory

arrive at this void ratio is unknown, but it does not appear important to know it in any case. Additional load increments are now placed on the sample, and the void ratio at the end of consolidation of each increment is determined in the usual manner. A typical set of data is shown plotted both on natural scales and logarithmic scales in Fig. 5.9. If the points plotted on the e vs. log σ' diagram are now extrapolated back to meet a horizontal line drawn through e_o, the initial void ratio, a complete functional relationship between e and σ' is obtained. This construction is shown by a dotted line in the e vs. log σ' plot in Fig. 5.9. A very small value of σ_o' is now obtained, and whether or not this value is the actual value for the residual stress in the undrained thawed soil is probably immaterial, as we are solely interested in obtaining a value of the stress ratio P_o/σ_o' that will express the high degree of non-linearity associated with the soil compressibility behaviour. The "fictional" portion of the e vs. log σ' curve between e_o and e_1 is also plotted on the graph of e vs. σ' on a natural scale. It is seen that for practical situations the fictional value of σ_o' is so small that the first part of the e vs. σ' curve is approximated to a high degree of accuracy. The excess pore pressures in a thawing soil exhibiting this e vs. σ' relationship would be determined by using a stress ratio equal to the final effective stress P_o divided by the value of σ_o', which in the case shown here is 0.02 kg/cm^2.

It is concluded then that the use of a logarithmic variation of effective stress with void ratio may be used with considerable advantage in the theory of consolidation for thawing soils. When the soil is initially at a high void ratio, and subsequent consolidation

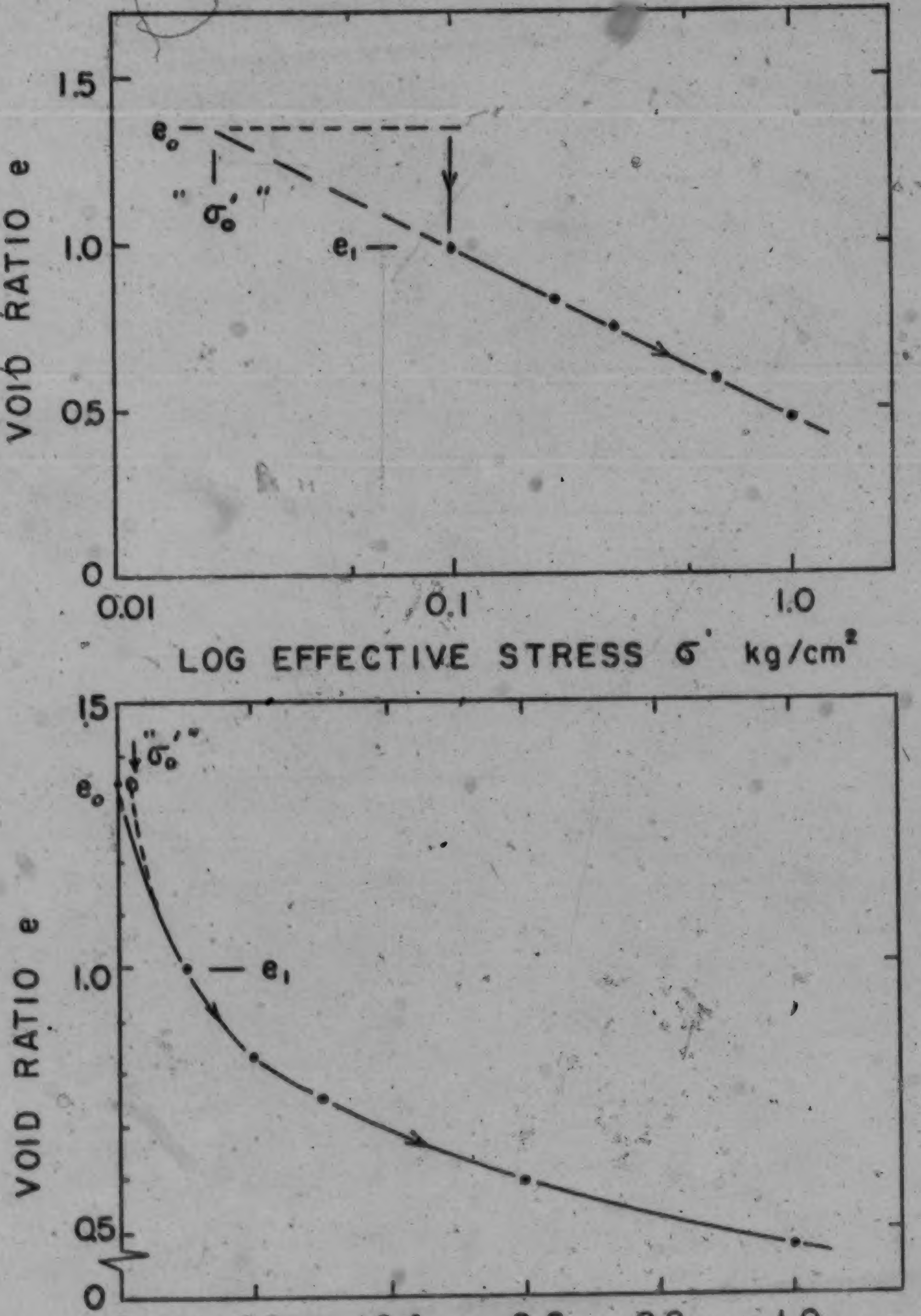

Fig. 5.9 e - σ' Curves on Natural and Logarithmic Scales

causes large strains in the soil skeleton, a residual stress that may have little physical basis may be determined. This enables the soil stress-strain behaviour in the initial highly compressible condition to be modelled mathematically.

5.5 The Thawing of Ice-Rich Incompressible Soils

The fourth model in Fig. 5.7 relating void ratio to effective stress is visualised as a bi-linear relationship which is vertical initially, and on reaching a final void ratio e_f, proceeds horizontally to the final effective stress. In many cases of practical interest, the solid constituents of the frozen soil are of coarser grained material. Thawing of such soils permits the liberation of any moisture which is in excess of the final void ratio e_f. Further loading of a coarser-grained soil produces little additional compression, and so consideration of a model such as this provides a useful insight into the thawing behaviour of ice-rich incompressible soils, and also gives a convenient lower bound to the series of void ratio-effective stress relationships which it is possible to consider for any soil. One might envisage a further application of this stress-strain relation involving a finer-grained soil.

In a clayey silt, for example, it is common to find rythmic ice banding in the frozen material. If the interbedded soil layers are highly overconsolidated with respect to the present overburden stress, and would themselves demonstrate little compression on thawing, then perhaps an approximate analysis could be carried out by assuming a rigid incompressible soil skeleton accompanied by uniformly distributed excess ice. However, it is clear that upon adoption of this model, the settlement ratio S_t/S_{max} is always 100%, provided that the discharge capacity of the soil is not exceeded (i.e. the effective stress at the thaw line does not become zero.)

The excess ice content of an ice-rich incompressible soil is defined on the basis of thawed void ratios as follows,

$$E_i = \frac{e_o - e_f}{1 + e_o} \tag{5.34}$$

As the soil skeleton in the thawed zone is considered incompressible, the equation governing dissipation of the excess pore pressures in that zone is the Laplace equation in one-dimension.

$$\frac{d^2u}{dx^2} = 0 \tag{5.35}$$

The solution to (5.35) is written simply in the form

$$u = Ax + B \tag{5.36}$$

At the surface, a free drainage boundary exists, and so

$$B = 0 \tag{5.37}$$

At the thaw line, the continuity equation (3.9) derived previously is written down

$$\text{at } x = X(t); \qquad \frac{\Delta V}{V} = - \frac{k \frac{\partial u}{\partial x}}{\gamma_\omega \frac{dX}{dt}} \tag{3.9}$$

As the soil is incompressible and therefore possesses no capability for transient storage of excess pore fluids, all excess water must be expelled from the thaw front, and so

$$\frac{\Delta v}{v} = -E_i \tag{5.38}$$

and substituting eq. (5.38) into (3.9) the boundary condition at the thaw line is obtained:

$$\text{at } x = X(t); \quad \frac{\partial u}{\partial x} = \frac{\gamma_\omega E_i}{k} \frac{dX}{dt} \tag{5.39}$$

Combining eq. (5.36), (5.37) and (5.39) the solution is

$$u = \frac{\gamma_\omega E_i}{k} \frac{dX}{dt} x \tag{5.40}$$

Normalising the excess pore pressure and the depth x, the solution is rewritten as

$$\frac{u}{P_o + \gamma' X} = \frac{\gamma_\omega E_i z}{k (P_o + \gamma' X)} X \frac{dX}{dt} \tag{5.41}$$

It is desirable to compare the results obtained from this incompressible analysis with those obtained using the linear theory described in Chapter 3. This is only possible if we define an equivalent coefficient of volume compressibility for the incompressible analysis to be

$$m_v^* = \frac{\Delta V/V}{\Delta\sigma'} = \frac{E_i}{P_o + \gamma' X} \tag{5.42}$$

The corresponding coefficient of consolidation is

$$c_v^* = \frac{k}{m_v^* \gamma_\omega} = \frac{k (P_o + \gamma' X)}{E_i \gamma_\omega} \tag{5.43}$$

The inverse of this term appears in eq. (5.41), and therefore a method of comparison with the linear theory of thaw-consolidation suggests itself.

For thawing proportional to the square root of time,

$$X \frac{dX}{dt} = \frac{\alpha^2}{2} \tag{5.44}$$

and at the thaw line

$$z = 1 \tag{5.45}$$

and so, placing the equations (5.43), (5.44) and (5.45) in eq. (5.41) provides

$$\frac{u}{P_o + \gamma' X} = \frac{\alpha^2}{2c_v^*} \tag{5.46}$$

To facilitate the comparison, the analagous thaw-consolidation ratio is defined as

$$R^* = \frac{\alpha}{2\sqrt{c_v^*}}$$

and from eq. (5.46) the much simplified expression is:

$$\frac{u}{P_o' + \gamma' X} = 2(R^*)^2 \tag{5.47}$$

Equation (5.47) allows the expression of the normalised excess pore pressures at the thaw line in terms of an equivalent R value, which applies to an incompressible soil with excess ice. The relationship is shown plotted in Fig. (5.10) together with the corresponding relationship for the linear theory of thaw-consolidation. The relationship expressed by eq. (5.47) is independent of the self-weight ratio W_r. At the lower R values, the excess pore pressures predicted by the two theories are very similar. However, in the middle range of R values, the incompressible model predicts a marked increase, and at R = 0.7 the excess pore pressures become equal to the effective overburden load. It must be remarked that although the incompressible model appears to predict pore pressures that are independent of the self-weight ratio, the m_v^* value and hence the R^* value contain the quantity $(P_o + \gamma' X)$. This term varies with time if γ' is not zero, and so therefore does the R^* value.

Under conditions of no external loading ($P_o = 0$), the discharge capacity is exceeded in all cases to a certain finite depth. As the discharge capacity is proportional to the quantity $\gamma' X$, at small depths of thaw the rate of liberation of excess water exceeds the small discharge capacity. The depth to which the thawing soil will remain totally unconsolidated may be found by establishing an inequality from eq. (5.47). That is

$$\frac{u}{P_o + \gamma' X} = 2(R^*)^2 > 1 \tag{5.48}$$

or

$$\frac{\alpha^2}{2c_v} = \frac{\alpha^2 \gamma_\omega m_v^*}{2k} > 1 \tag{5.49}$$

and setting $P_o = 0$ in eq. (5.42) for m_v^* gives the condition

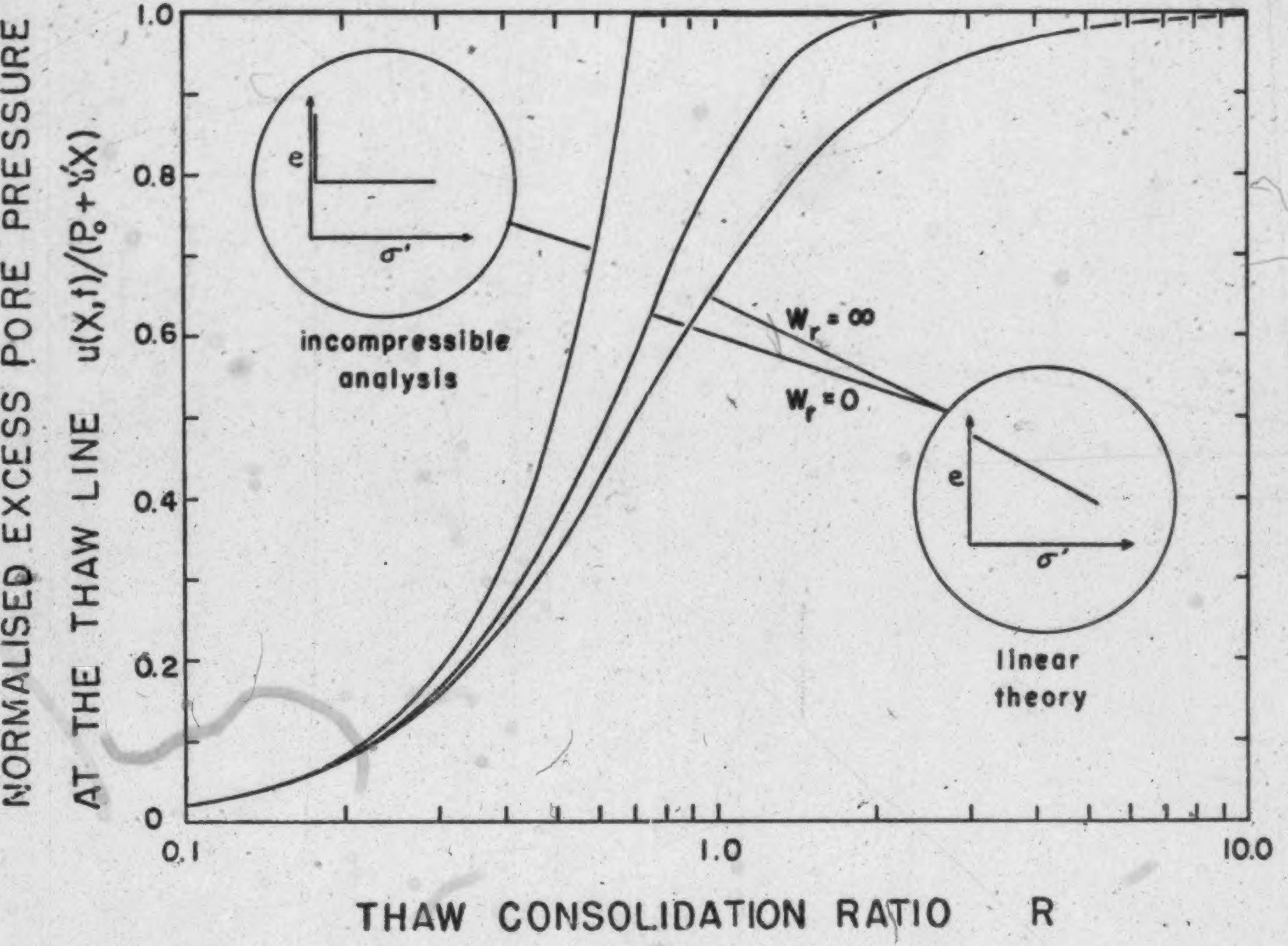

Fig. 5.10 Pore Pressures from Incompressible Analysis.

$$\frac{\alpha^2 \gamma_\omega E_i}{2k \gamma' X} > 1 \qquad (5.50)$$

or

$$X < \frac{\alpha^2 \gamma_\omega E_i}{2k \gamma'} \qquad (5.51)$$

If the depth of thaw is less than this critical depth of X, then the thawing soil is totally underconsolidated for the self-weight (γ') loading conditions. This is the most striking difference between the incompressible model and the results predicted by the linearly compressible relationship, which always predicts a constant degree of consolidation at the thaw line, with no critical depth of thaw such as that given by eq. (5.51). This preliminary study would suggest that for soils exhibiting a high degree of curvature of the stress-strain curve, and which are thawing under self-weight conditions, excess pore pressure conditions would be most critical at early times, and would improve with depth.

The excess pore pressure conditions can be greatly improved in the analysis described above by the simple provision of a surcharge, P_o. By the same argument developed above, the placement of a surcharge of magnitude

$$P_o = \frac{\alpha^2 \gamma_\omega E_i}{2k} \qquad (5.52)$$

will increase the discharge capacity to the extent where some degree of consolidation is obtained from the initiation of thawing onwards.

In summary, the stability of thawing ice-rich soils which have an incompressible soil matrix may be considerably improved by the provision of a surcharge loading. This has the effect of increasing the discharge capability of the soil to an acceptable level. If, however, the surcharge loading were not distributed uniformly on the surface, as in the case of a berm, then additional shear stresses would be induced in the subgrade. Such shear stresses might reduce the stability of the subgrade, and thus negate some of the beneficial effects of the surcharge loading.

5.6 The Consolidation of a Thawing Soil With a Layered Profile

So far the solutions to problems in the one-dimensional thawing of permafrost soils have confined themselves to the treatment of a single compressible layer exibiting a homogeneous set of geotechnical and thermal properties. In many cases of practical importance, the depositional and thermal history associated with a natural deposit of permafrost may be such that extreme changes in consolidation and thermal properties occur with increasing depth. These changes in properties may occur gradually, but are more likely to be quite discrete. A sudden change in depositional history for example may bring about a distinct change in soil type. In such instances, two or more discrete layers of soil may be assumed present, each possessing a different water content, latent heat, permeability and coefficient of consolidation.

It has already been shown in section 2.7 how the movement of the thaw plane through a soil profile displaying two different sets of thermal properties is analysed approximately. Once the history of the thaw interface is established, attention may be focused on the associated problem in soil consolidation. Figure 5.11 shows

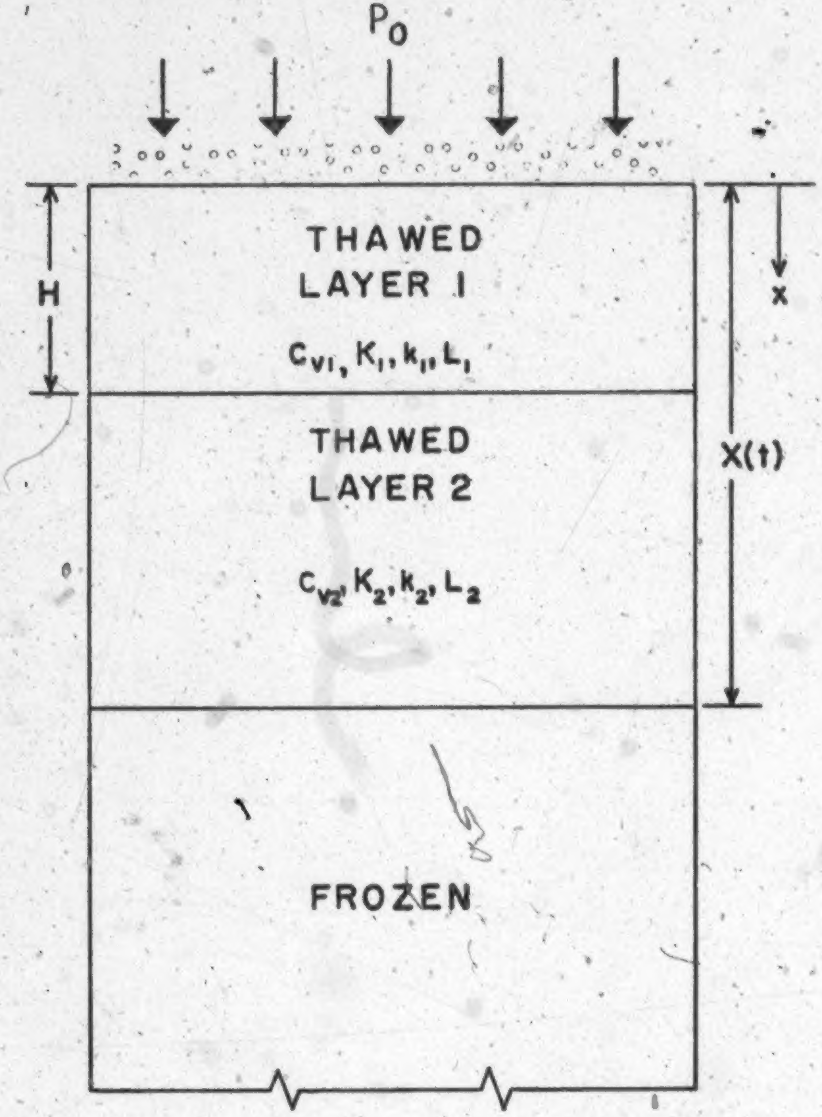

Fig. 5.11 Thaw-consolidation in a Two-layer Profile

schematically the consolidation of a two-layer profile, each layer having the properties c_v, K, k and L, the coefficient of consolidation, permeability, thermal conductivity and the volumetric latent heat respectively.

The movement of the thaw interface X(t) through the two-layer profile is derived in terms of the Stefan formulation in section 2.7 and is rewritten here as

$$X = \alpha\sqrt{t} = \sqrt{\frac{2k_1\ T_s}{L_1}}\ \sqrt{t} \quad ; \qquad X \leq H \tag{2.60}$$

where T_s is the suddenly applied increase in surface temperature.

On penetrating the second layer, the motion of the thaw plane is described by

$$X = \sqrt{\left(\frac{k_2}{k_1}\ H\right)^2 + \frac{2k_2\ T_s}{L_2}\ (t - t_o)}\ - \left(\frac{k_2}{k_1} - 1\right) H \quad ; \qquad X > H \tag{2.63}$$

where t_o is the time to thaw the first layer of thickness H, and is given by

$$t_o = H^2/\alpha^2$$

The consolidation problem is summarised formally as follows for $t > t_o$, when the thaw interface has entered the lower layer.

In layer 1,

$$t > 0; \qquad \frac{\partial u_1}{\partial t} = c_{v_1}\ \frac{\partial^2 u_1}{\partial x^2} \ ; \qquad 0 < x < H \tag{5.53}$$

$$t \geq 0; \qquad u_1 = 0 \ ; \qquad x = 0 \tag{5.54}$$

In layer 2,

$$t > t_o; \quad \frac{\partial u_2}{\partial t} = c_{v_2} \frac{\partial^2 u_2}{\partial x^2} \quad ; \quad H < x < X(t) \qquad (5.55)$$

$$t > t_o; \quad P_o - \sigma_o' + \gamma' X - u_2 = \frac{c_{v_2} \frac{\partial u_2}{\partial x}}{\frac{dX}{dt}} \quad ; \quad x = X(t) \qquad (5.56)$$

At the interface between the two layers, the excess pore pressures are equal and so

$$t > t_o; \quad u_1 = u_2; \quad x = H \qquad (5.57)$$

The equation of continuity for excess pore fluids must also be satisfied giving

$$t > t_o; \quad K_1 \frac{\partial u_1}{\partial x} = K_2 \frac{\partial u_2}{\partial x} \quad ; \quad x = H \qquad (5.58)$$

The system of equations (5.53) to (5.58) describe the dissipation of excess pore pressures in the two layer soil mass for $X > H$. The solution to the consolidation problem for $X < H$ is known analytically from the results presented in Chapter 3. The equations presented above can be generalised to treat the problem of thawing in a multi-layered system. If the thaw plane is passing through layer n of a multi-layered profile, there will be (n-1) equations of the type expressed by equations (5.57) and (5.58) at the (n-1) internal interfaces. The same equations for the free drainage surface at $x = 0$, and for the thaw plane at $x = X(t)$ will apply as before. It is only necessary, however, for the scope of the present study to examine some of the effects of the passage of a thaw plane through a two-layer system.

The equations (5.53) and (5.58) are written in finite difference form in preparation for solution. The details of the numerical method are given in Appendix A.5. A computer program was written to solve the resulting finite difference equations for the excess pore pressures $u_1(x,t)$ and $u_2(x,t)$. The settlements are computed as usual by numerical integration of the excess pore pressures using the trapezoidal rule. A listing of the computer program and the method of data entry are given in Appendix A.6.

The program is used to investigate the effects of a surface layer having different consolidation properties on the maintenace of excess pore pressures in the underlying thawing layer. Two simple cases are solved for an applied surface loading where the upper layer has a lower coefficient of consolidation and permeability, and also where the coefficients of the upper layer are considerably higher. The same thermal properties are assumed to exist in each layer, in order to examine the effect of a change in geotechnical properties alone. The excess pore pressures while the thaw plane is in the upper layer are calculated from the linear theory in Chapter 3. The excess pore pressure profiles are shown in Fig. 5.12 and Fig. 5.13. for typical properties exhibited by "silt over clay", and "clay over silt" situations. As the thaw plane enters the underlying layer, a sudden change in the excess pore pressure at the thaw line occurs. Each figure also denotes by an arrow the excess pore pressure which would be obtained if only the lower layer were present.

The excess pore pressure in the two-layer profiles apparently

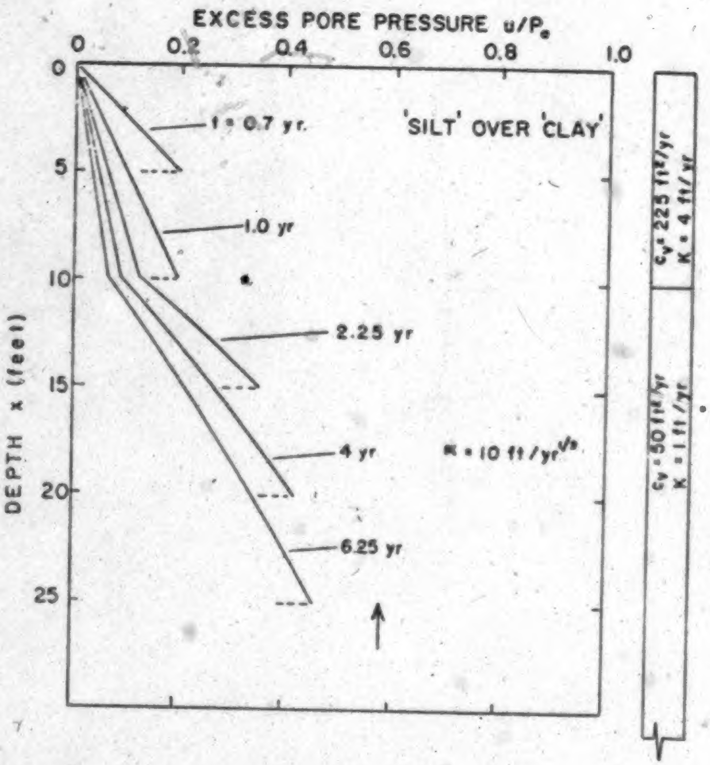

Fig. 5.12 Excess Pore Pressures for 'Silt Over Clay'

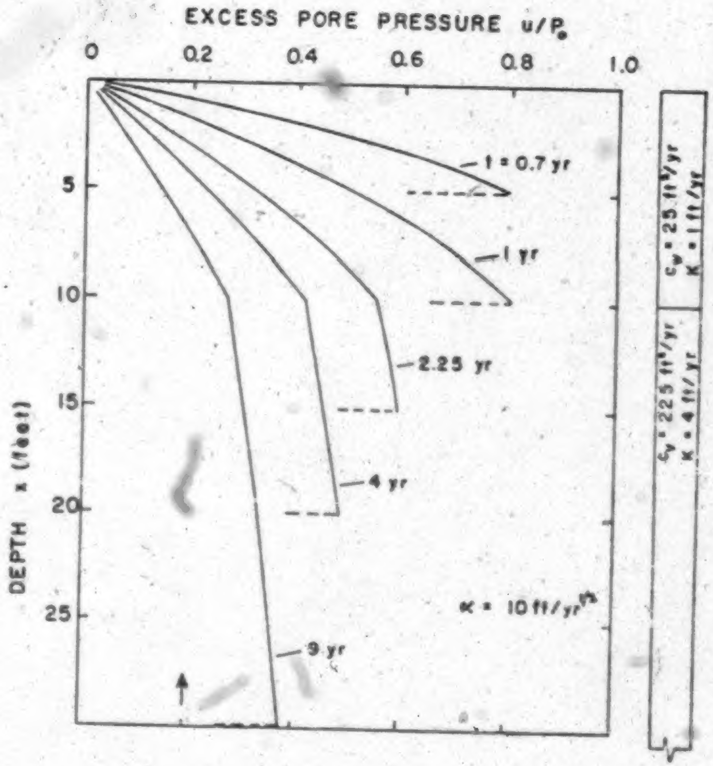

Fig. 5.13 Excess Pore Pressures for 'Clay over Silt'

approach this value in an asymptotic fashion, but in fact after some years of thawing, the effects of the surface layer on the thaw line pore pressures are still pronounced. The conclusion might be drawn from the results of these two simple problems that the prescence of a surface layer which participates in thawing and the subsequent consolidation, although possibly minor in extent, may have long term effects of the thawing of the underlying layer.

A more realistic field situation is considered in order to demonstrate the applicability of the computer procedure in Appendix A.6 to the solution of practical problems. The excess pore pressures are obtained for the thawing of an ice-rich silty clay soil which is overlain by a five foot layer of peat. A surface temperature of +10°C is applied to the surface of the peat, which has widely differing thermal and consolidation properties from the underlying clay stratum. The rate of thaw and the thaw line pore pressures are computed also for the case where the peat layer is removed, and the same surface temperature is applied. In this simple manner, some of the effects of the removal of a surface organic layer on the stability of a thawing soil may be demonstrated theoretically. The thermal and consolidation properties for the two layers are assumed to be as follows.

Peat

Water content $\omega = 550\%$

Submerged density $\gamma' = 3.5\ \mathrm{lb/ft^3}$

Depth $H = 5$ feet

Latent heat $L_1 = 71.1\ \mathrm{cal/cm^3}$

Thawed conductivity $k_u = 9 \times 10^{-4}\ \mathrm{cal/^{o}C.cm.S.}$

Surface temperature $T_s = 10^{o}C$

Thaw rate in peat alone $\alpha = 2.92$ ft/year$^{1/2}$

Consolidation coefficient $c_v = 2200$ ft^2/year

Permeability $K = 130$ ft/year

Silty clay

Water content $\omega = 50\%$

Submerged density $\gamma' = 45$ lb/ft^3

Latent heat $L_2 = 46$ cal/cm^3

Thawed conductivity $k_u = 27 \times 10^{-4}$ cal/^{o}C.cm.S.

Thaw rate in clay alone (if peat removed) $\alpha = 6.32$ ft/yr$^{1/2}$

Consolidation coefficient $c_v = 36$ ft^2/yr

Permeability $K = 1.0$ ft/yr.

The excess pore pressure profiles at different times for thawing in the two layer profile are shown in Fig. 5.14. Also shown are the thaw depth with time and the normalised excess pore pressure at the thaw line. The same relationships are shown for the case where the peat layer is removed, given by a dotted line in Fig. 5.14. After ten years of thawing, it is seen that the thaw penetration into the silty clay layer has been reduced by some fifty percent. More significantly, the build-up of excess pore pressures at the thaw line is such that only about fifty percent of the pressure is attained of that value which would be calculated if no peat layer were present. The prescence of the peat layer is, in general, responsible for three effects, all of which serve to make less critical the stability of

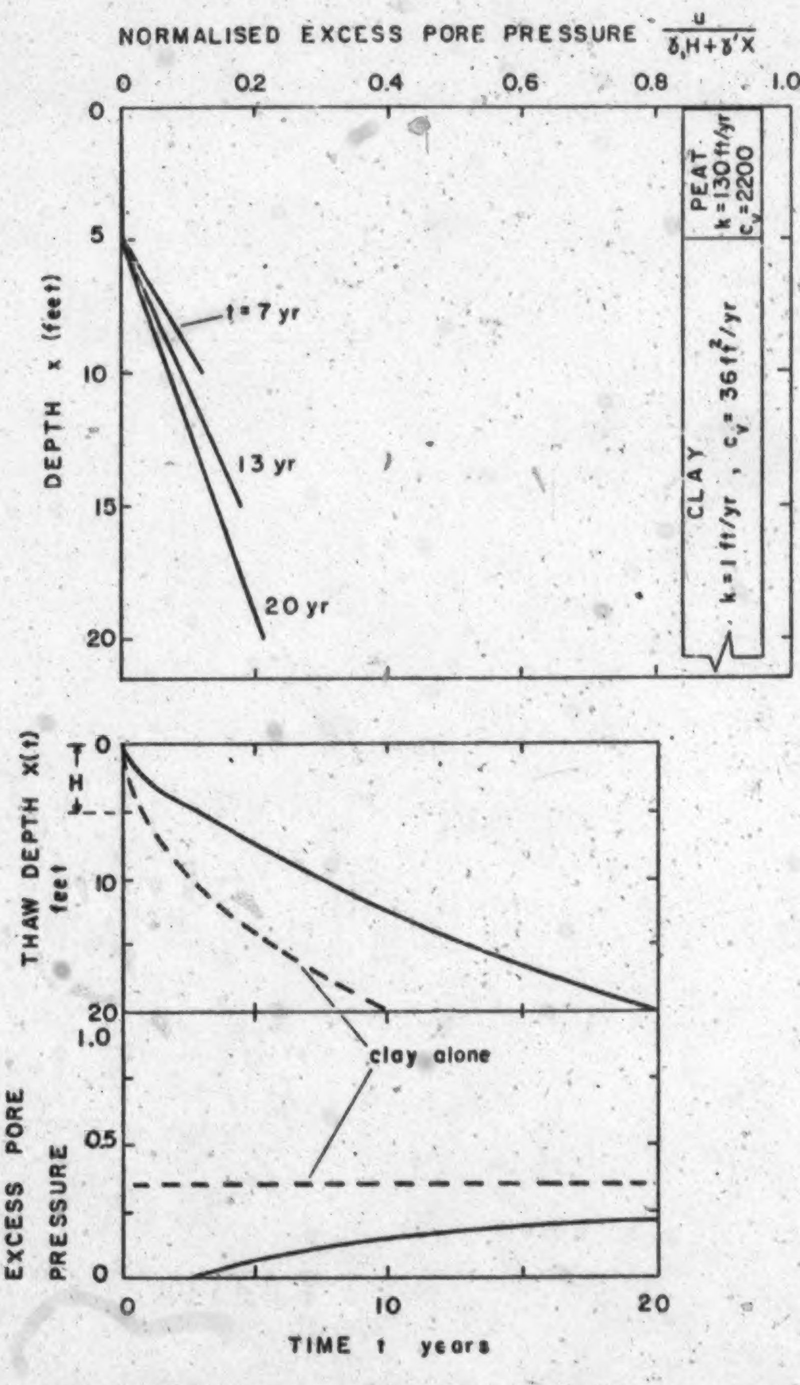

Fig. 5.14 Excess Pore Pressures for 'Peat Over Clay'

the underlying thawing layer,

(i) A high latent heat barrier is available to impede thawing of the upper layer.

(ii) After thawing of the peat, its lower thermal conductivity reduces the rate of thaw in the underlying stratum, so reducing the overall thaw penetration, and the excess pore pressure maintained in the underlying layer.

(iii) A relatively free draining boundary is provided, and negligible excess pore pressures are maintained at the base of the peat layer.

If the peat were removed and replaced for example by a layer of gravel, conditions (ii) and (iii) would still be available to improve foundation conditions, however the latent heat barrier described by (i) would in all probability not be available.

5.7 The Analysis of a Compressible Soil with Discrete Ice Lenses

When a fine-grained soil freezes, a combination of the ambient conditions may prove extremely favourable for the formation of segregated ice. Some of the conditions favourable for the creation of ice features in frozen soil have been discussed in Chapter 1, and they include the slow rate of heat removal from the freezing plane, the availability of water to the freezing plane, and a low overburden pressure at the level of freezing. The conditions for the formation of segregated ice near the surface of a deposit of a freezing soil are very often realised. In soils with silt-sized particles, segregated ice in the form of discrete layers or bands often occurs. In the finer grained plastic soils, ice banding is also found, with the bands oriented perpendicularly to the maximum principal stress. However, vertical ice veins and other ice forms are also found regularly in the soils with more clay sized particles.

So far a complete analysis of the position and magnitude of ice layers or even the amount of distributed ice which may be found in a freezing soil has not been carried out. It would therefore seem that the analogous problem in thawing soils would defy analysis as well. The interaction between the heat and mass balances at the frost interface, the transfer of heat in the frozen and thawed zones combined with the thermodynamic relationships for ice/water/soil interfaces seem to preclude the use of a simple mechanical description of the problem of freezing in fine-grained soils. Hardly content with the problems involved with these considerations, some authors proceed even further to attempt to describe the moisture transfer in unsaturated soils.

The solution of problems involving the thawing of soils containing horizontal ice bands is rendered considerably simpler by knowledge of the position and extent of the segregated ice forms initially. A situation involving a layer of saturated compressible soil overlying a single layer of ice will be analysed. It is obviously impractical to suggest that the analysis developed here be used generally to predict the excess pore pressures and thus the stability in a thawing soil containing ice lenses, but hopefully all the important variables might be contained in a dimensionless statement which would indicate the potential stability above a thawing ice layer. Such a dimensionless statement would not only provide a stability index such as the 'R' value derived in Chapter 3, but should also suggest remedial measures which might be applied to improve stability.

At the outset, a solution is considered for excess pore pressures in a thawing soil over a layer of ice which extends downwards indefinitely. This assumption is made for simplicity at this point, and it will be seen later how the procedure is modified to include any ice layer of finite thickness. It is assumed that a step increase in temperature has been applied at the surface and that the thaw ~~plane~~ is moving through the frozen soil at a rate given by the simple Stefan formula

$$X = \alpha\sqrt{t} = \sqrt{\frac{2k_u T_s}{L_s}}\,\sqrt{t} \tag{5.59}$$

where L_s is the volumetric latent heat of the soil.

The excess pore pressures obtained while the thaw plane is still in the soil are given by the linear theory of thaw-consolidation in Chapter 3. For the case of self-weight loading only, the excess pore pressures exhibit a linear profile with depth, and can therefore be written as

$$u = B\,\gamma' x \tag{5.60}$$

where $B = \dfrac{1}{1 + \frac{1}{2R^2}}$ and is a constant with time.

When the thaw plane encounters the ice layer, the height of soil solids above the thaw line remains constant with time. If we now assume that the strains in the soil skeleton associated with any increase in excess pore water pressure (caused by the extra influx of water into the soil) are small, then the distance between the soil surface and the thaw plane becomes constant. This assumption is expressed schematically in Fig. 5.15, and essentially implies that

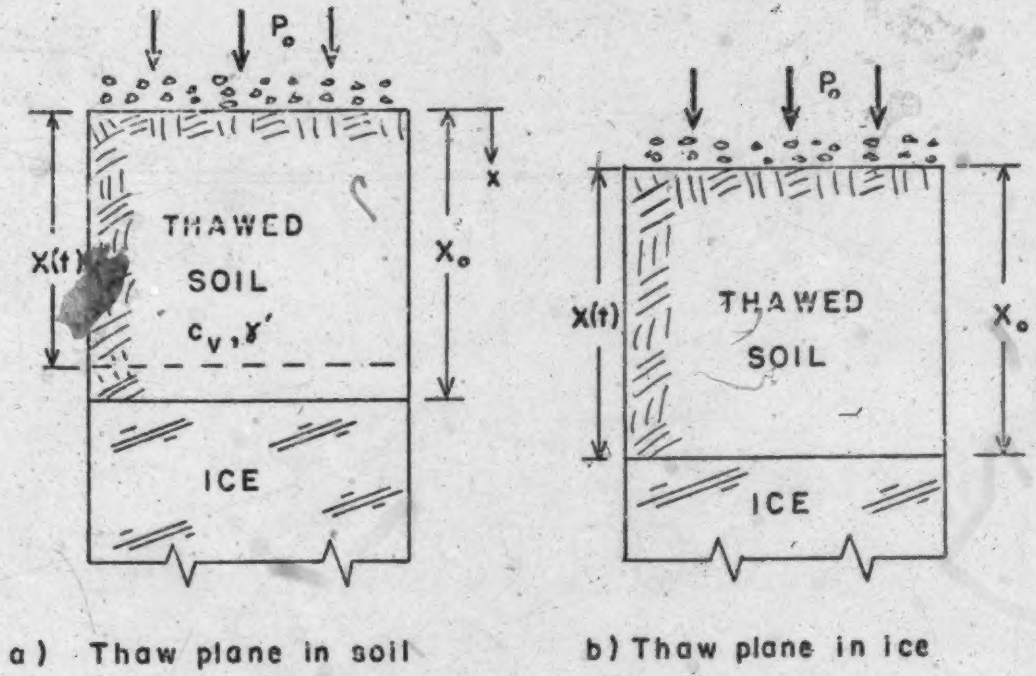

a) Thaw plane in soil b) Thaw plane in ice

Fig. 5.15 Thawing in a Soil-Ice Profile

the soil is not absorbing an excessive percentage of the water discharge from the thaw plane to the surface. It will be seen later from the solution to the problem that this is a reasonable assumption. If the distance X_o from the surface to the thaw plane is now a constant, then certainly a steady state temperature distribution exists in the thawed zone, where the temperature is T_s at the soil surface and T_f at the thaw line. Applying the usual heat balance equation at the thaw line:

$$-k_u \frac{\partial \theta}{\partial x} = L_w \frac{dX}{dt} \qquad (5.61)$$

where $\frac{dX}{dt}$ is the rate of advance of the thaw plane into the ice layer,

L_w is the volumetric latent heat of water,

and

$$\frac{\partial \theta}{\partial x} = \frac{-(T_s - T_f)}{X_o} \qquad (5.62)$$

From this, the rate of degradation of the ice layer is

$$\frac{dX}{dt} = \frac{k_u(T_s - T_f)}{L_w X_o} \qquad (5.63)$$

This is a constant velocity with time, as distinct from the solution to the heat transfer problem through soil, where the velocity dX/dt is proportional to time$^{-1/2}$. It is clear that the thaw front velocity will be reduced when an ice layer is encountered, as L_w is greater than L_s, the latent heat of the frozen soil. At first sight this might be thought to improve the excess pore pressure conditions in the soil above the ice lens, however it must be remembered that all the melt water from an ice lens enters the soil as excess pore fluid, whereas when thawing through a mixture of soil and ice, only a portion of the melt water may be thought of as excess pore fluid.

As no new thawed soil is entering the thawed zone, the usual boundary condition expressing the continuity of water at the thaw line is no longer valid, and the problem in soil consolidation concerns a fixed height of soil X_o. At the thaw boundary at the surface of the ice lens, the continuity of the mass of water is satisfied as follows:

$$\text{at } x = X_o; \qquad \gamma_i \frac{dX}{dt} = K\frac{\partial u}{\partial x}\,; \qquad t > t_o \tag{5.64}$$

where $t_o = X_o^2/\alpha^2$, and is the time to thaw the soil above the ice,

K is the permeability of the thawed soil,

and γ_i is the unit weight of ice.

Substituting the rate of melting of the ice given by eq. (5.63), we obtain

$$\text{at } x = X_o; \qquad \frac{\partial u}{\partial x} = \frac{\gamma_i}{K}\,\frac{k_u(T_s - T_f)}{L_w\,X_o} \tag{5.65}$$

$$\text{Letting } z = \frac{x}{X_o} \tag{5.66}$$

and dividing eq. (5.65) by $(P_o + \gamma' X_o)$ to normalise the excess pore pressures

$$\frac{\partial\, u/(P_o + \gamma' X_o)}{\partial\, z} = \frac{\gamma_i\, k_u(T_s - T_f)}{K(P_o + \gamma' X_o)\, L_w} \tag{5.67}$$

The right hand side of eq. (5.67) is a dimensionless quantity which shall be denoted by

$$A = \frac{\gamma_i \, k_u (T_s - T_f)}{K(P_o + \gamma' X_o) \, L_w} \tag{5.68}$$

The dimensionless excess pore pressure gradient applied at the base of the soil after encountering the ice lens is given by

$$\frac{1}{P_o + \gamma' X_o} \frac{\partial u}{\partial z} = A \tag{5.69}$$

The solution for the excess pore pressure u(z,t) above a thawing ice layer may now be found. The linear Terzaghi consolidation equation is assumed to govern the dissipation of excess pore pressures, therefore:

$$0 < z < 1; \qquad \frac{\partial u}{\partial T} = \frac{\partial^2 u}{\partial z^2}; \qquad T > 0 \tag{5.70}$$

where $T = \dfrac{c_v t}{X_o^2}$

and the time t_o is set equal to zero for simplicity.

Within the assumptions of the Terzaghi theory, the coefficient of consolidation is an independent constant, and so the value of c_v used here is the same as that value used when the thaw plane is in the soil. The surface is free-draining, and

$$z = 0; \qquad u = 0; \qquad T > 0 \tag{5.71}$$

At the base of the fixed height of soil, a constant influx of water provides the boundary condition (5.69)

$$z = 1; \quad \frac{1}{(P_o + \gamma' X_o)} \frac{\partial u}{\partial z} = A; \quad T > 0 \tag{5.72}$$

The case of self-weight loading will be considered from now onwards, due to the simplicity of the initial values. The applied loading condition must necessarily be analysed numerically. From eq. (5.60) the initial values are written as

$$0 \leq z \leq 1; \quad \frac{u}{\gamma' X_o} = B\,z; \quad T = 0 \tag{5.73}$$

As the equation of consolidation is linear, and the initial values form a linear distribution, the solution is simplified by taking the initial values from eq. (5.73) as a new reference line for the pore pressures, and then consider the further disturbance to the pore pressure distribution by the normalised gradient A applied at the base. This is performed mathematically by making the substitution

$$\omega = \frac{u}{\gamma' X_o} - B\,z \tag{5.74}$$

and $$\frac{\partial \omega}{\partial z} = \frac{1}{\gamma' X_o} \frac{\partial u}{\partial z} - B \tag{5.75}$$

The surface condition (5.71) and the governing equation (5.70) remain unchanged in terms of the transformed dependent variable $\omega(z,t)$. The boundary condition at X_o becomes

$$z = 1; \quad \frac{\partial\omega}{\partial x} = (A - B); \quad T > 0 \tag{5.76}$$

The initial values become

$$0 \leq z \leq 1; \quad \omega = 0; \quad T = 0 \tag{5.77}$$

The solution to eq. (5.70) subject to equations (5.71), (5.76) and (5.77) is obtained from Carslaw and Jaeger, 1947, page 113, and is

$$\omega(z,t) = (A - B)\left\{ z - \sum_{n=0}^{\infty} \frac{2(-1)^n}{M^2} \mathrm{Sin}(M\,z)e^{-M^2T} \right\} \tag{5.78}$$

where $M = (2n + 1)\pi/2$

Replacing ω by $u(z,t)$, the excess pore pressures are

$$\frac{u(z,t)}{\gamma' X_o} = A\,z - (A - B)\sum_{n=0}^{\infty} (-1)^n \frac{2}{M^2}\ \mathrm{Sin}(M\,z)e^{-M^2T} \tag{5.79}$$

where A and B are the dimensionless physical constants defined by equations (5.60) and (5.68), and which express the initial and final excess pore pressure gradients in the thawed soil. This solution converges slowly for small values of the time factor T. The solution (5.79) was evaluated by summing the terms in the infinite series on the computer. Figure 5.16 shows the normalised excess pore pressure at the thaw line plotted with the time factor for different A values. The value of the initial pore

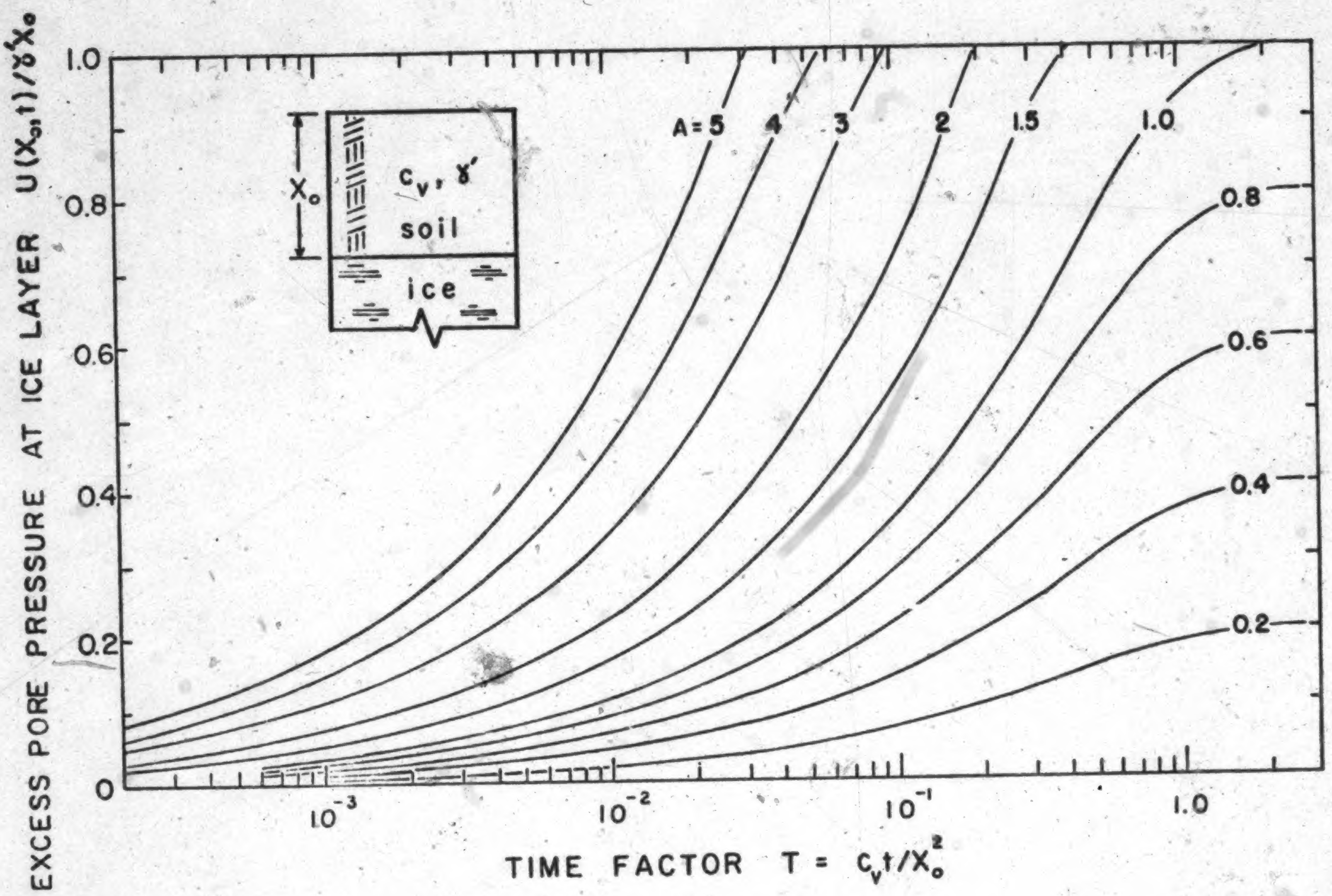

Fig. 5.16 Pore Pressures at a Soil-Ice Interface

pressure gradient B is taken to be zero, as it is desirable to isolate the effects of the thawing of the ice layer alone. The corresponding curves for any other positive value of B are easily evaluated from eq. (5.79), or they may also be obtained from curves for B = 0 given in Fig. 5.16 by the use of the relation

$$u\Big|_{B \neq 0} = A - \left(\frac{A - B}{A}\right)\left\{A - u\Big|_{B = 0}\right\} \qquad (5.80)$$

where $u\Big|_{B = 0}$ represents the normalised pore pressure for B = 0 given in Fig. 5.16,

and $u\Big|_{B \neq 0}$ represents the required pore pressure for any non-zero value of B.

The preceding solution is valid where the ice layer continues indefinitely below the soil.

When the ice layer is of finite thickness, as is usually the case, the time to thaw the layer completely is calculated from eq. (5.63) as

$$t_f = \frac{h_i \, X_o \, L_\omega}{k_u(T_s - T_f)} \qquad (5.81)$$

where h_i is the original thickness of the ice layer,

and t_f is the time required to thaw the ice layer completely.

This time may be converted into a time factor by

$$T_f = \frac{c_v t_f}{X_o^2} = \frac{c_v \, h_i \, L_\omega}{k_u(T_s - T_F) \, X_o} \qquad (5.82)$$

Knowing the time factor at the conclusion of thawing of the ice lens, Fig. 5.16 may be used to determine the final (and usually the worst) pore pressure conditions over the ice layer.

It is seen from Fig. 5.16 that if the value of A is less than unity, then the normalised excess pore pressure will rise to this value, and maintain in the limit a pore pressure numerically equal to A. If, on the other hand, the A value is greater than unity, then stability is only assured for a finite period of time, and eventually the excess pore pressures become equal to the effective overburden weight, and complete instability results.

It appears then that stability of a compressible soil mass may be gained in two ways. If the A value is less than unity, then some effective stress is assured indefinitely at the thaw line. When A is greater than unity, instability results unless by calculating T_f from eq. (5.82) it may be shown using Fig. 5.16 that the normalised pore pressures never attain their maximum value. It is seen that T_f is proportional directly to h_i, and inversely to X_o. This indicates that only small ice layers may be tolerated close to the surface, and that larger layers might be thawed quite safely at larger depths. The presence of the term $(P_o + \gamma' X_o)$ on the denominator also reinforces this statement concerning the increase of stability with depth. This also suggests a method of increasing stability. If a surcharge loading P_o were placed over the thawing ground containing ice lenses, the A value is reduced. If large ice layers are present near the surface, and instability is predicted at low values of $\gamma' X_o$, the placement of gravel fill might well be used to reduce the A value below unity, and thus render a foundation considerably more stable on thawing.

In order to enhance the explanation of the relative effects of various parameters on the stability of the ice layer, a sample problem is solved in real dimensions. To lend some realism to the sample solution, a set of soil properties shall be adopted which are the same as those found at the Inuvik test pipeline site (see Chapter 6). This soil is a clayey silt, and the following set of representative soil properties are used

permeability	$K = 2.5 \times 10^{-5}$ cm/s
coefficient of consolidation	$c_v = 1.1 \times 10^{-2}$ cm^2/s
water content	$\omega = 40\%$
submerged unit weight	$\gamma' = 0.82$ g/cm^3
soil latent heat	$L_s = 41.4$ cal/cm^3
thawed conductivity	$k_u = 2.5 \times 10^{-3}$ cal/^{o}C.cm.s

Two rates of thawing shall be examined; one corresponding to the fast rate of thawing under a hot pipeline, say;

surface temperature $T_s = 71^oC$,

and the other corresponding to a natural rate of thaw which might take place in the active layer;

surface temperature $T_s = 12^oC$.

Using the Stefan solution, the α values for thawing in the soil are calculated to be

$\alpha_1 = 0.093$ cm/s$^{1/2}$ for the high T_s

and $\alpha_2 = 0.038$ cm/s$^{1/2}$ for the low T_s.

Combining these with the c_v value provides the two R values:

$R_1 = 0.443$

$R_2 = 0.181$

The pore pressure maintained in the soil, and therefore the initial values for the ice layer problem are

$B_1 = 0.283$

$B_2 = 0.061$

The effects of an ice layer in this thawing soil are now considered. For each rate of thawing cited above, the top of the ice layer is assumed to be at 1m. or at 3m. For $X_0 = 1$m, the A values for the two rates of thawing are 1.0 and 0.169 respectively. The relationship between time factor and time may be calculated from eq. (5.70) for each depth of ice layer, X_0. Figure 5.16 and eq. (5.80) are now used to plot the excess pore pressures at the ice/soil interface with time. Figure 5.17 shows the normalised pore pressure plotted with time in days for the two thaw rates and depth of ice layers. The history of the thaw interface is also plotted for each case.

For the fast rate of thawing, the pore pressure above an ice layer at a depth of 1m. rises to 94% of the maximum effective stress within 10 days. This represents a thickness of 20 cm. of ice thawed in this time. An ice layer at 3m. depth under these thawing conditions produces pore pressures that are not significantly more critical than those produced by thawing in the soil.

For the slow rate of thawing, the prescence of an ice layer at 1m. depth does not produce pore pressures in the soil that deteriorate significantly with time. In fact, if ice were present at depth 3m. under these thawing conditions, Fig. 5.17 shows that

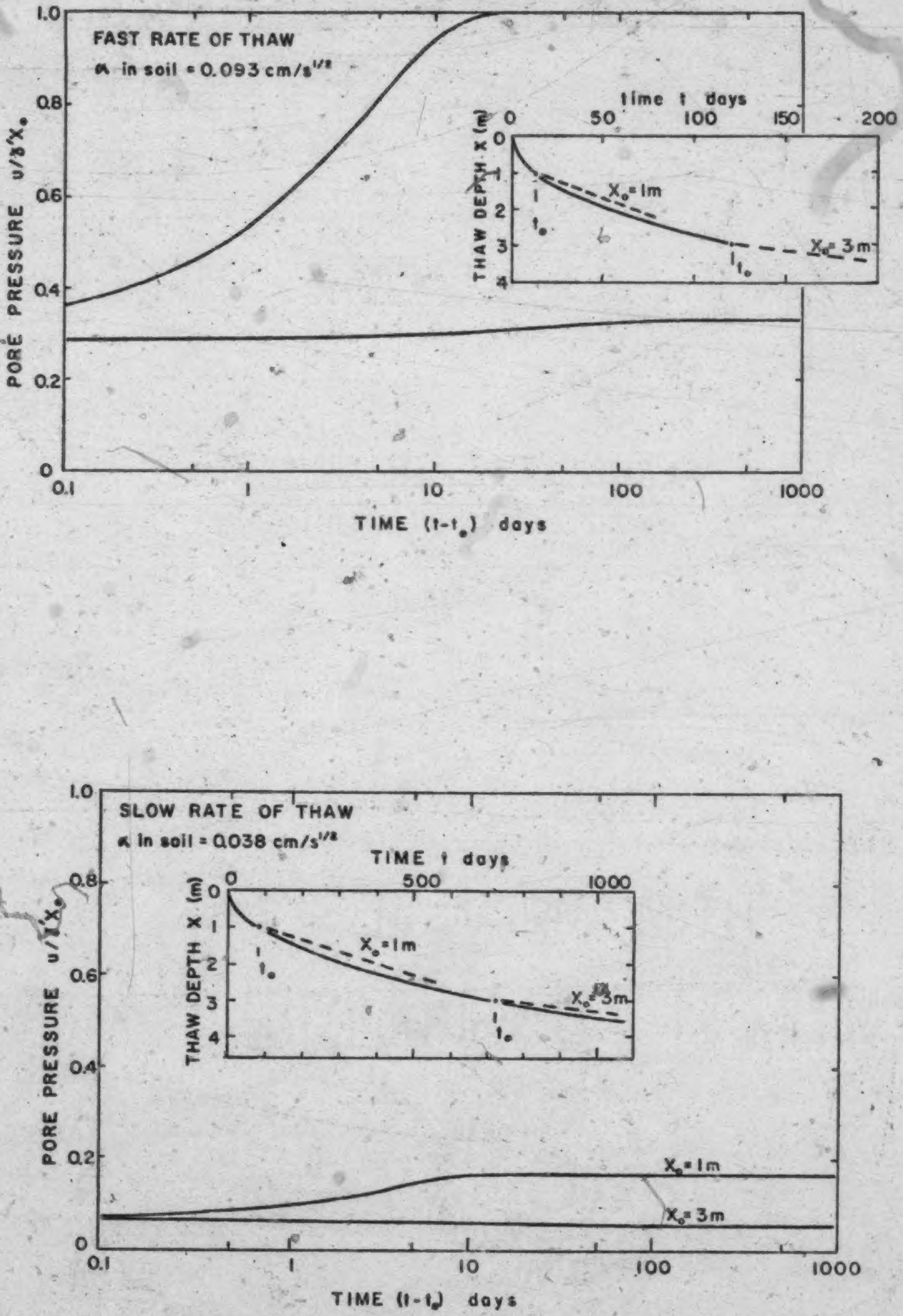

Fig. 5.17 Sample Solution for Pore Pressures at a Soil-Ice Interface

the pore pressure actually reduces slightly with time as the thaw plane progresses through the ice.

The results from this sample problem suggest that although the settlements are obviously considerable, the pore pressure conditions in the soil above a thawing ice layer may not be as critical as hitherto supposed.

CHAPTER VI

ANALYSIS OF FIELD PROBLEMS

6.1 Introduction

In this section attention is directed towards the application of some of the methods and the theoretical relationships established previously to some practical problems that might be encountered in the field.

One of the most dramatic and indeed topical aspects of industrial development in the Arctic is the effect of the operation of a hot oil pipeline on the underlying frozen ground. Some important effects of a pipeline on its foundation are analysed over the expected period of operation for an Arctic location. In the following paragraphs, improvements to a thawing foundation using vertical sand drains are also considered.

It would obviously be extremely desirable to obtain many field case histories, and anlyse them within the context of the theory of thaw-consolidation. It is only possible, however, to present analysis of one case study at this time, as there is only one well-documented set of data available to the Author at the present. This concerns the behaviour of the 48-inch warm pipeline at Inuvik which will be dealt with in some detail.

6.2 Thawing Under a Hot Pipeline

A practical study of thawing under a hot oil pipeline is included to illustrate the application of the extension to the theory described in section 5.2, where the power law relation between thaw depth and time is used. The settlements and excess pore pressures under the centerline of a pipeline are analysed, subject to the thaw rate given by Lachenbruch (1970). A clay substratum of 65% moisture content was considered by Lachenbruch in order to assess some thermal effects of a heated pipeline in permafrost. The thaw 'bulb' and the rate of thaw under the centre-line are shown in Fig. 6.1.

Various coefficients of consolidation c_v have been used to estimate the performance of the pipe for the first 20 years. The material overlying the pipe is assumed to act as a surcharge loading, and for simplicity to be comprised of a material of much higher permeability than the underlying frozen soil. It therefore does not play any active role in the drainage conditions.

From properties chosen by Lachenbruch, one finds that 2.42 m of surcharge material at a dry density of 1.75 t/m^3 causes a surcharge loading of 4.25 t/m^2. The thawing soil at 65% moisture content has a submerged unit weight of 0.62 t/m^3. The rate of thaw for the Arctic (clay) case is well approximated by

$$X = 3.56\, t^{0.3} \tag{6.1}$$

$$\text{or } B = 3.56$$

$$\text{and } n = 0.3.$$

The coefficients of consolidation taken to assess the performance of the pipe are

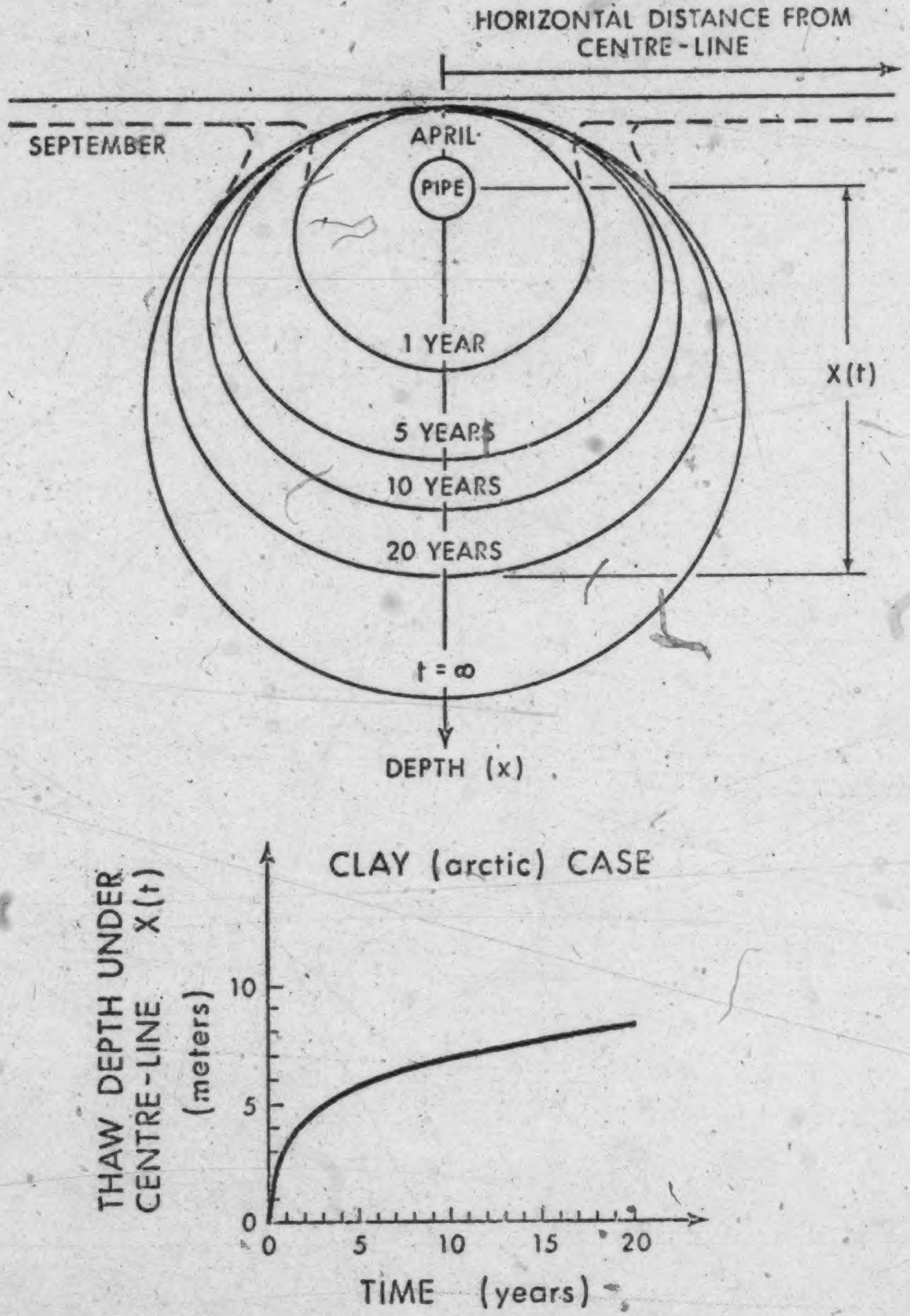

Fig. 6.1 Thawing under the Centre-line of a Hot Pipeline
(After Lachenbruch, 1970)

$$c_v = 3 \times 10^{-4},\ 15 \times 10^{-4},\ \text{and } 30 \times 10^{-4}\ \text{cm}^2/\text{sec}$$
$$= 10,\ 50,\ \text{and } 100\ \ \text{ft}^2/\text{year}$$

Finally, the closure of the thaw bulb as calculated by Lachenbruch is assumed not to affect the one-dimensional drainage under the centreline of the pipeline.

The results for the normalised excess pore pressures are shown plotted with time for different c_v values in Fig. 6.2, for the centreline of the pipeline.

If the thaw depth against time curve is approximated by a square root of time relationship, and an α value approximately calculated for the first two years of thawing, the dotted line in Fig. 6.2 shows the excess pore pressures calculated using the linear theory reviewed earlier.

As expected, under these thawing conditions the excess pore water pressures are the most severe in the initial few years of thawing. For a silty clay with a c_v of 15×10^{-4} cm^2/sec, excess pore pressures equal to 50% of the effective overburden loading may be expected even after two years of operation. However, it also appears that if no severe stability problems occur in the initial years of operation, then increased stability may usually be expected as time proceeds, provided that soil conditions do not deteriorate significantly with depth.

The settlement of the pipeline is comprised of the sum of the consolidation settlement, and the settlement resulting from the density change in the water phase on thawing. The consolidation settlement at any time may however be shown to be proportional to the product of

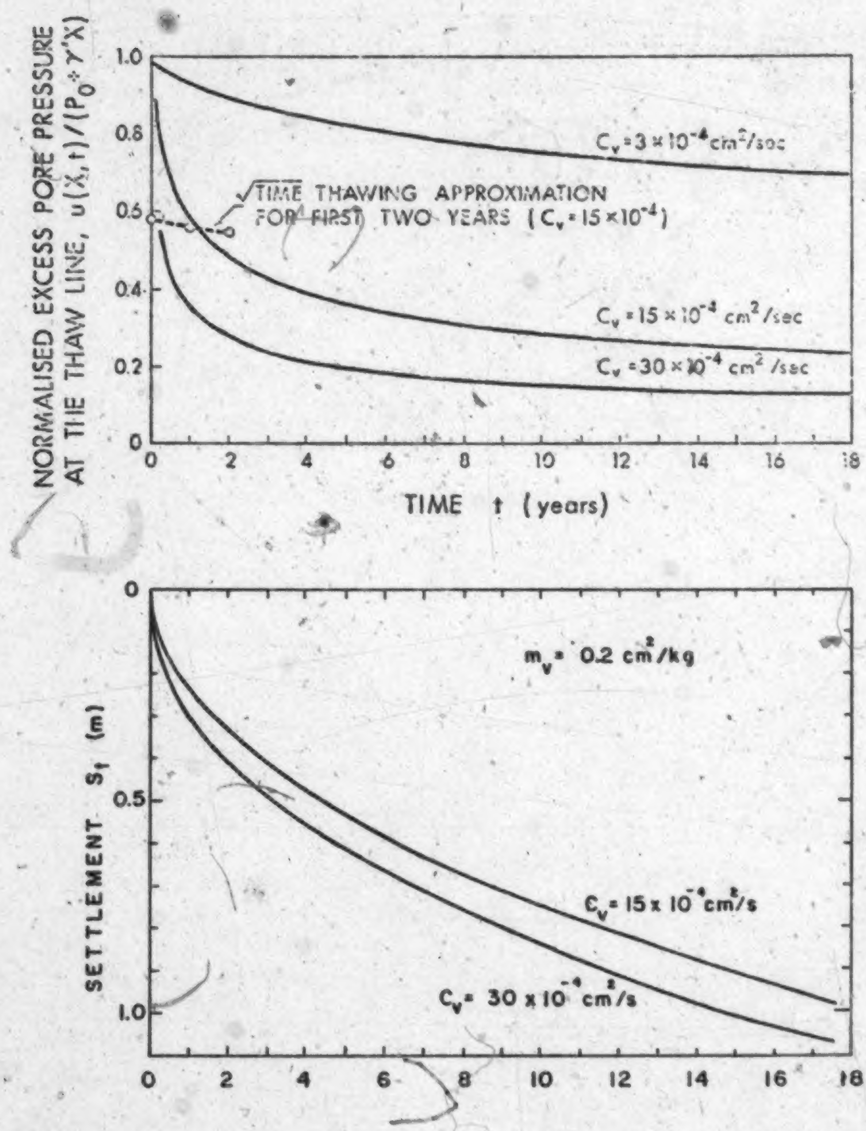

Fig. 6.2 Pore Pressures and Settlements under the Centre-Line of a Hot Pipeline

S_t/S_{max} and the depth of thaw X. At early times, the degree of consolidation S_t/S_{max} is low. At longer times, the velocity of the thaw front decreases, and S_t/S_{max} increases. Hence a more linear settlement-time curve is to be expected than that suggested by the thaw depth-time relationship.

Figure 6.2 also shows the transient settlements, S_t, under the centre-line of the pipe if the coefficient of volume compressibility is 0.2 cm^2/kg. It is seen that the curvature of these settlement-time relationships is considerably less than the curvature of the thaw depth vs time function given in Fig. 6.1.

6.3 Thaw-Consolidation with Vertical Sand Drains

In cases where the soil properties in a thawing soil foundation are such as to cause the build-up of excess pore pressures and the possibility of an unstable foundation, it may be desirable to consider certain remedial measures which would improve foundation conditions in an economical manner. One of the best-known methods of improvement for deep deposits of unfrozen soils is by the use of vertical sand drains, (Casagrande and Poulos, 1969; Barron, 1948). In general, the presence of a sand drain boundary with zero excess pore pressure serves to shorten the drainage path for excess pore fluids, and accelerate the rate of consolidation.

The sand drain problem is usually a two dimensional problem in the radial direction r, and the depth x. For unfrozen soils the two-dimensional equation may be solved by a method due to Carrillo (1942) who showed that the solution to the two-dimensional problem is the product of a pair of one-dimensional solutions.

Attention is now turned to the problem of accelerating the consolidation of a thawing permafrost foundation. Vertical sand drains have been installed to improve foundation performance of a thawing foundation under dykes constructed on permafrost in Northern Manitoba. However, when referring to the design of foundations at the Kettle Generating Station in Northern Manitoba, MacPherson et al. (1970) stated that the use of sand drains had limitations because "the extent of the drainage required to carry away the liberated water as the permafrost thaws is not known". Clearly, it is of considerable interest to explore the possibility of solving the required equations, and make available a program which might provide a firmer basis for rational design.

It is doubtful whether the solution to this problem is available in analytical form, and the method of Carrillo cannot be utilised due to the differing nature of the boundary conditions.

Figure 6.3 shows schematically a typical situation involving sand drains, and also shows how the "effective radius" of the drains is calculated from the spacing. It shall be assumed that the thaw plane remains planar at depth $X(t)$, and that a one-dimensional thawing situation is present, i.e.,

$$X(t) = \alpha \sqrt{t} \tag{6.2}$$

As cylindrical symmetry is preserved at all times, the consolidation problem is two-dimensional, with vertical and radial flow components, but without tangential flow. Accepting that the Terzaghi-Rendulic consolidation theory is adequate to describe the flow of water in the

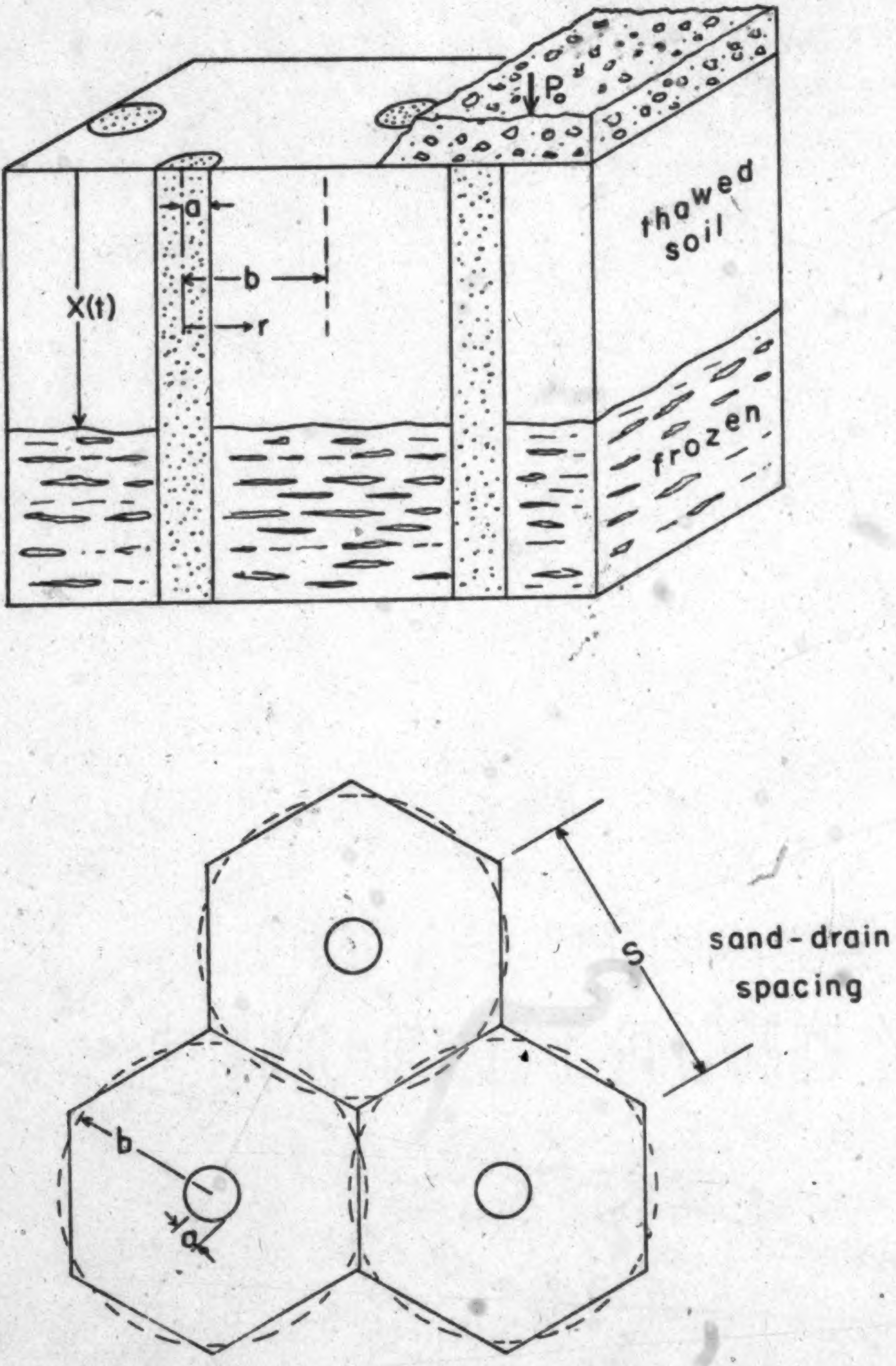

Fig. 6.3 Thaw-Consolidation with Vertical Sand Drains

thawed soil, the governing consolidation equation is

$$a < r < b; \quad 0 < x < X(t); \quad t > 0;$$

$$\frac{\partial u}{\partial t} = c_v \left\{ \frac{\partial^2 u}{\partial x^2} + \frac{\partial^2 u}{\partial r^2} + \frac{1}{r}\,\frac{\partial u}{\partial r} \right\} \tag{6.3}$$

Implicit in this equation are the statements that the consolidation coefficient is isotropic, the material properties are homogeneous, and that the total stress of any soil element is constant with time.

In designing the numerical procedure for solving this problem, a stationary co-ordinate system might be adopted, whereby the finite difference equation for the thaw line must be written at a moving boundary. In this case, considerable simplifications are introduced if a transformation is employed which places the co-ordinate system in motion, thus rendering the thaw boundary stationary.

Setting $z = \frac{x}{X(t)}$ the governing equation (6.3) is rewritten as

$$\frac{\partial u}{\partial t} = \frac{c_v}{X^2}\,\frac{\partial^2 u}{\partial z^2} + \frac{z}{X}\,\frac{dX}{dt}\,\frac{\partial u}{\partial z} + c_v \left\{ \frac{\partial^2 u}{\partial r^2} + \frac{1}{r}\,\frac{\partial u}{\partial r} \right\} \tag{6.4}$$

As the r co-ordinate is orthogonal to the z-direction, the last term in the equation is unaffected by this transformation.

Since $\frac{dX}{dt} = {}^{\alpha}/2\sqrt{t}$ eq. (6.4) becomes

$$\frac{\partial u}{\partial t} = \frac{c_v}{\alpha^2 t}\,\frac{\partial^2 u}{\partial z^2} + \frac{z}{2t}\,\frac{\partial u}{\partial z} + c_v \left\{ \frac{\partial^2 u}{\partial r^2} + \frac{1}{r}\,\frac{\partial u}{\partial r} \right\} \tag{6.5}$$

The derivatives $\frac{\partial u}{\partial z}$ and $\frac{\partial u}{\partial r}$ pose no special problems in the implicit finite difference method adopted, and a set of linear tridiagonal equations are still obtained when the finite difference equations are written in matrix form.

The boundary conditions in terms of r and the new depth co-ordinate z are summarised as follows. At the interface with the sand drain, the soil is free-draining, so

$$r = a; \quad 0 \leq z \leq 1; \quad u = 0; \quad t > 0$$

At the effective radius, from symmetry, no drainage occurs, and

$$r = b; \quad 0 < z < 1; \quad \frac{\partial u}{\partial z} = 0; \quad t > 0$$

At the surface, a free draining surface is provided, and

$$a \leq r \leq b; \quad z = 0; \quad u = 0; \quad t > 0$$

At the thaw interface, vertical continuity of the pore water provides as before

$$a < r < b; \quad z = 1; \quad P_o - \sigma_o' + \gamma' X - u = \frac{c_v \frac{\partial u}{\partial z}}{X \frac{dX}{dt}}; \quad t > 0 \quad (6.5a)$$

or as $X\frac{dX}{dt} = \frac{\alpha^2}{2}$

$$P_o - \sigma_o' + \gamma' X - u = \frac{2c_v}{\alpha^2} \frac{\partial u}{\partial z}$$

Hence the excess pore pressure conditions at the boundaries are completely specified.

As it is not feasible to obtain an analytical solution to this problem, a finite difference numerical method is adopted.

There are many approaches available for solution to this type of two-dimensional problem. Few, however, have been used in solving problems with a moving boundary. The Alternating Direction Implicit method (ADI) is adopted to solve the differential equation. The method is discussed by Peaceman and Rachford (1955) and basically the scheme provides a method of numerical integration which does not need excessive computation time. For a linear 2-D equation of the heat conduction type, it has been shown to be stable and convergent for all values of the time interval Δt. If the subscript i refers to the number of discrete intervals in the z direction, and j to the number of intervals in the r direction, and k in the time direction, then the method is summarised as follows:

$$\frac{V_{i,j} - u_{i,j,k}}{\Delta t/2} = c_v\, \delta_r^2(V_{i,j}) + \frac{c_v}{r}\, \delta_r(V_{ij}) + \frac{c_v}{\alpha^2 t}\, \delta_z^2(u_{i,j,k}) + \frac{z}{2t}\, \delta_z(u_{i,j,k}) \qquad (6.6)$$

where δ_r^2, δ_r, δ_z^2 and δ_z refer to the second and first order central difference operators in the r and z directions respectively.

The resulting set of tridiagonal equations is solved for the matrix $V_{i,j}$, which is an intermediate set of values at $\Delta t/2$. In this first step, the integration is carried out in the r-direction, and using the values $V_{i,j}$ the direction of integration is changed, and the following set of equations leads to the solution at the (k + 1) time step.

$$\frac{u_{i,j,k+1} - V_{i,j}}{\Delta t/2} = c_v\, \delta_z^2(u_{i,j,k+1}) + \frac{z}{2t}\, \delta_z(u_{i,j,k+1})$$

$$+ c_v\, \delta_r^2(V_{i,j}) + \frac{c_v}{r}\, \delta_r(V_{i,j}) \qquad (6.7)$$

The equations (6.6) and (6.7) are written in finite difference form according to the Crank-Nicholson scheme. It is still possible to obtain a set of linear tridiagonal equations even though the presence of the first order derivatives δ_z and δ_r complicate the resulting equations slightly. This is only possible if these derivatives are raised to the first power, as is the case here. The details of the finite difference equations and the program are given in Appendix A.7. The tridiagonal equations are solved by the Gaussian Elimination technique used previously in section 5.2.

The computer program calculates the normalised excess pore pressures, and then a vertical integration is carried out on each vertical column of nodal points to calculate the vertical settlement at each point on the surface. A settlement profile may then be plotted as thawing proceeds.

The program is used to calculate excess pore pressures and settlement profiles at the surface for a typical set of conditions. The results are shown in Figs. 6.4 and 6.5.

The excess pore pressure distribution at the effective radius

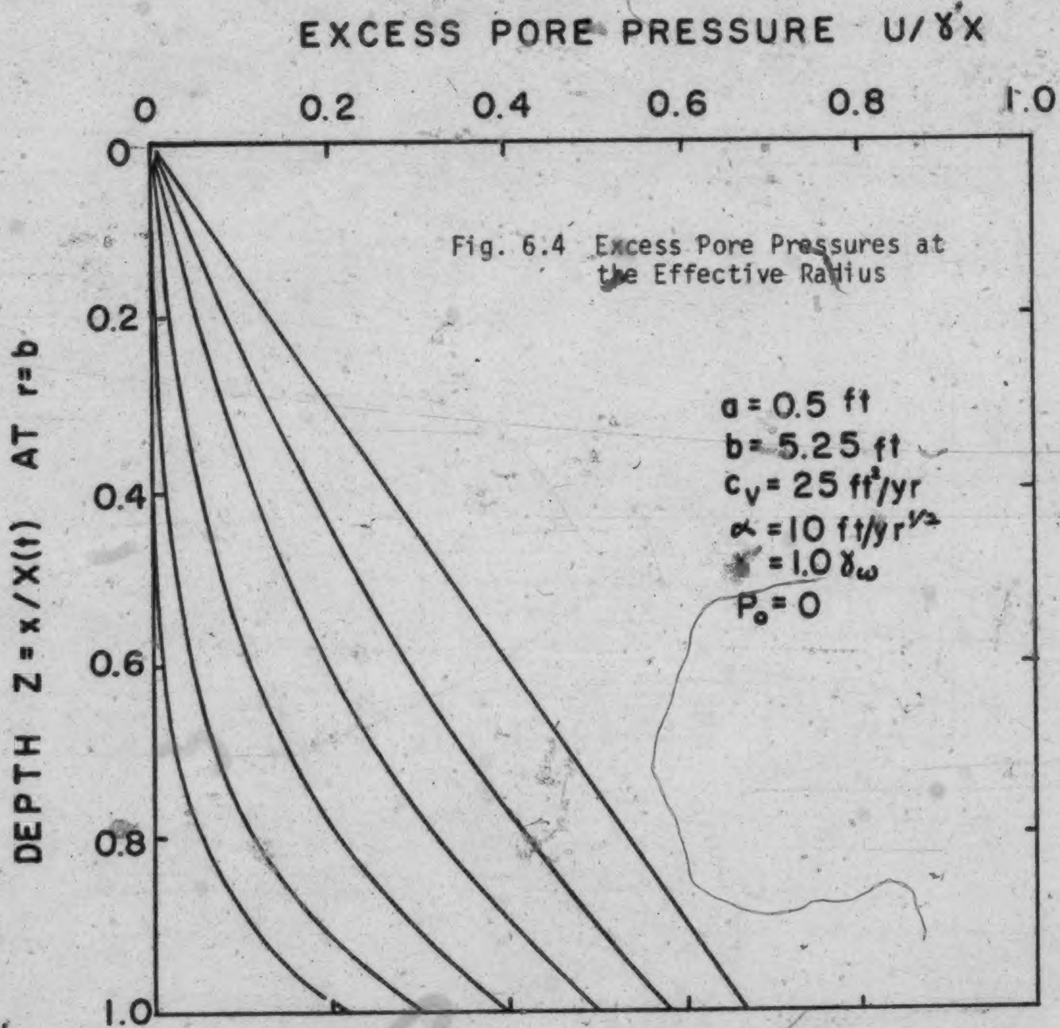

Fig. 6.4 Excess Pore Pressures at the Effective Radius

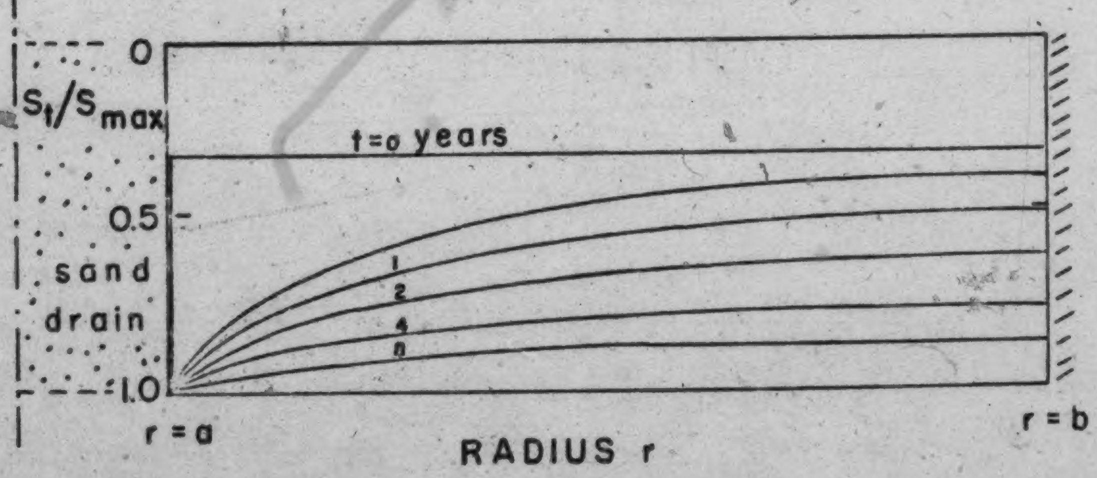

Fig. 6.5 Surface Settlement Profiles Around a Sand Drain

shows that the excess pore pressure at the thaw line reduces with time, and the pore pressure gradient increases. The results suggest that the depth of thaw must become significantly larger than the effective radius b, before any satisfactory reduction in pore pressure is obtained. In the example shown, the drain spacing is 10 feet giving an effective radius of 5.25 feet. The excess pore pressure at r = b is reduced from 66% to 40% after four years, when the depth of thaw X = 20 feet. In the same time however, Fig. 6.5 shows that the degree of settlement is accelerated from 33% to 77%. So it might be suggested that no significant improvement in foundation conditions need be expected until the thaw depth is considerably greater than the sand drain spacing.

This observation suggests another design alternative. If the sand drain spacing is varied with depth in such a way that when the thaw depth is small, the drain spacing is reduced, and at greater depths the spacing may be greatly increased. This would simply be achieved by incorporating two or three different sets of sand drains, each set penetrating to a different depth, as shown in Fig. 6.6. The analysis of such a foundation might be accomplished in an approximate way by changing the effective radius b at certain specified depths in the accompanying computer program.

Certain other practical problems accompany the use of sand drains as a remedial measure. If the surface of the sand drain is not in contact with continuously thawed soil or water, then freeze-back of the surface of the drain might cause drainage impedance and build-up of excess pore pressures. However, the sand drain will at least be functional for approximately one-half of the year. Also, if large

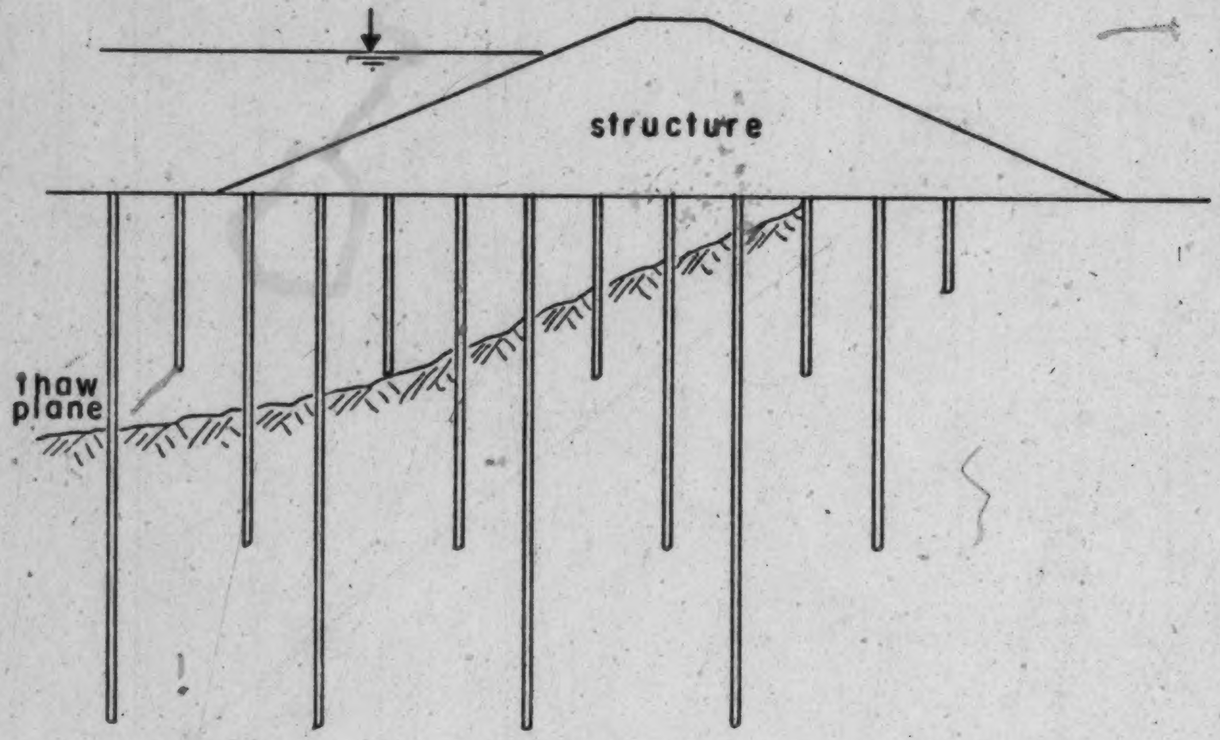

Fig. 6.6 Optimised Use of Sand Drains in a Thawing Foundation

settlements occur in the thawing soil, it is unclear how the drain itself would deform, and if it would carry a significant portion of the structural load on the soil.

Further investigations are needed, but these preliminary considerations suggest that the use of sand drains in a thawing foundation might be less effective than hitherto believed, unless the design is optimised in a manner such as that shown in Fig. 6.6.

6.4 Analysis of the Performance of a Hot Oil Test Pipeline at Inuvik N.W.T.

In order to study the behaviour of permafrost as a foundation material for a warm-oil pipeline, Mackenzie Valley Pipe Line Research Ltd. installed a 27 m. test section of 61 cm diameter pipe near Inuvik, N.W.T. The objectives of the field test were to measure pore water pressures, temperatures and settlements in the foundation as thawing proceeded. Frozen bulk densities of the foundation materials were measured in order to predict the thaw strains underneath the pipe, and comparisons could then be made between the predicted and observed values for pipe settlement.

It is proposed to examine the data from the test site in some detail, as this constitutes the only completely documented case of thawing of a fine grained permafrost soil that is available at the present time.

The data and references used in this study are taken from publications by Rowley et al. (1972) and Watson et al. (1973).

The stratigraphy of the test site is shown in Fig. 6.7. Hot oil at 71^{o}C was circulated through the pipe from July 21, 1971, and

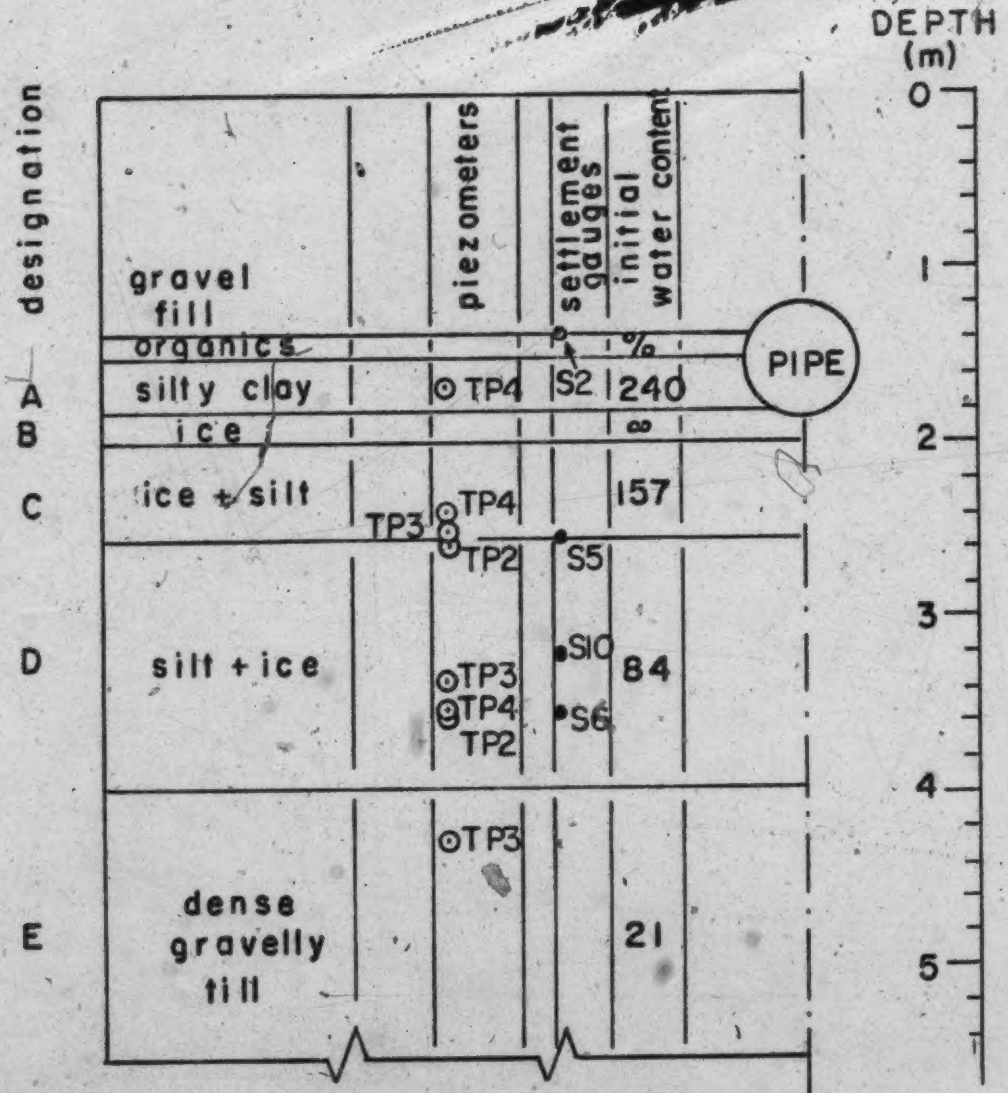

Fig. 6.7 Configuration of the Inuvik Test Facility

the results are analysed for the three months following this date. About 36 days after thawing had commenced the thaw bulb entered a layer of dense gravelly till, and no further significant settlements occurred. In the intervening period the thaw bulb moved through a layer of ice rich silt, grading from almost pure ice just below the pipe to about 30% excess ice at the upper boundary of the dense till.

Settlement gauges and piezometers were installed at the depths shown in Fig. 6.7 and the data from this instrumentation is analysed here in the context of the thaw-consolidation theory. Figure 6.7 does not show the horizontal position of piezometers and settlement gauges, which were positioned for the most part 0.3 m from the centre-line of the pipe. The approximate moisture content of each layer is included.

The properties of the ice-rich clayey silt layer are given by Rowley et al. (1972). The grain sizes are comprised of 53% silt and 40% clay, the remainder being sand. Undrained strength values obtained from unconfined compression tests and penetrometer readings varied from 925 to 1000 p.s.f. at the thaw front, and 1300 to 2000 p.s.f. at the top of the silt layer. In situ permeability tests conducted on the thawed silt layer gave values from 0.53×10^{-4} to 2.29×10^{-4} cm/s, averaging 1×10^{-4} cm/s. However, data from laboratory tests (Watson, 1973) on the same material gave a permeability of 0.17×10^{-4} to 0.26×10^{-4} cm/s.

Thermal Calculations

The rate of thaw underneath the centre-line of the pipe was observed in the test facility, and this thaw rate is compared here with a simple theoretical prediction based on a one-dimensional solution of the Stefan type.

Figure 6.8 shows the latent heat of the soil plotted with depth, and the dotted line indicates the relationship assumed for the theoretical prediction, based on moisture content data.

The expected thaw strains based on frozen bulk density for each layer indicate that on thawing, the soil will consolidate in the thawed zone to approximately 45% moisture content. From the data of Kersten (1949) presented in Fig. 2.5, it is estimated that the thermal conductivity of the thawed soil will be given by

$$k_u = 2.52 \times 10^{-3} \text{ cal/cm}^\circ\text{C sec.} \tag{6.8}$$

The surface temperature at the pipe base is given as

$$T_s = 71^\circ\text{C} \tag{6.9}$$

From Fig. 6.8 the latent heat may be expressed as

$$L = 70 - 9.75\ X \tag{6.10}$$

where X is in m.

From the predicted thaw strains, it is expected that the ice-rich clayey silt layer will settle approximately 0.9 m over a depth of 2.21m, therefore

$$\frac{S}{X} = \frac{0.9}{2.21}$$

or

$$S = 0.403\ X \tag{6.11}$$

It is not desireable, however, to calculate a depth of thaw from the initial position of the pipe, as in this case it would be

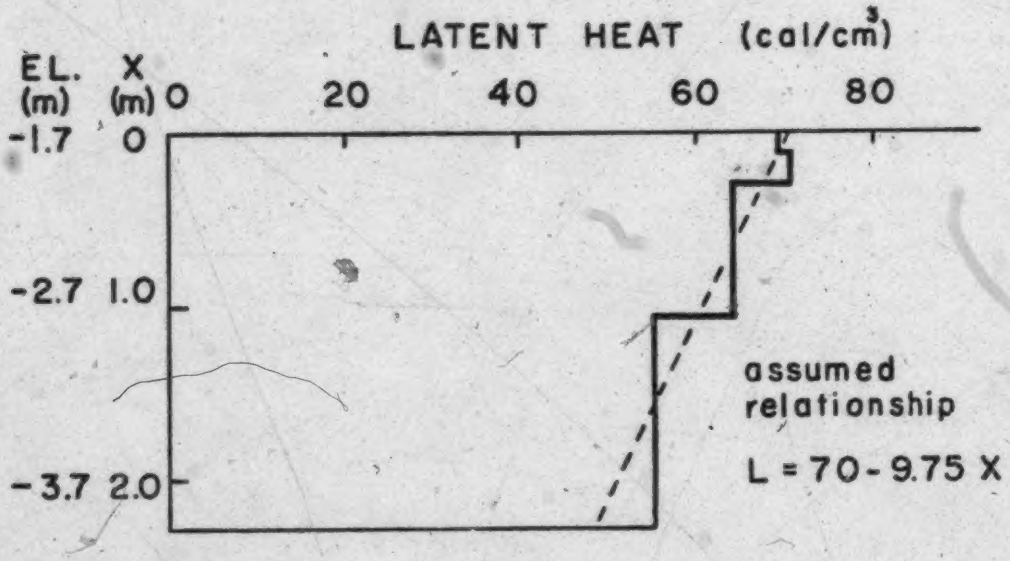

Fig. 6.8 Estimated Latent Heat with Depth

meaningless considering the large movement of the heat source. A depth of thaw is defined from the heat source (pipe base) as

$$\bar{X} = X - S \tag{6.12}$$

and from eq. (6.11), the settlement is re-written as

$$S = \frac{0.403}{1 - 0.403}\,\bar{X} = 0.674\,\bar{X} \tag{6.13}$$

Substituting eq. (6.13) and (6.12) in eq. (6.10) a value for latent heat in terms of the new variable $\bar{X}$ is obtained as

$$X = \bar{X} + S = 1.674\,\bar{X}$$

and therefore

$$L = 70 - 16.32\,\bar{X} \tag{6.14}$$

Using the simple Stefan formulation, and combining equations (6.14), (6.8) and (6.9), a relationship is obtained between the thaw depth from the pipe base, $\bar{X}$, and time.

$$\bar{X} = \sqrt{\frac{2k_u\,T_s\,t}{L(\bar{X})}}$$

or

$$\bar{X} = \sqrt{\frac{3.091\,t}{70 - 16.32\,\bar{X}}} \tag{6.15}$$

This equation is a cubic in $\bar{X}$, but may most easily be solved by rearranging in the form

$$t = \left(22.646 - 5.28\,\bar{X}\right)\bar{X}^2 \tag{6.16}$$

where $\bar{X}$ is in metres,

and t in days.

Equation (6.16) is plotted in Fig. 6.9, together with the observed values taken from Watson et al. (1973). These values are included in Table 6.1.

TABLE 6.1 PREDICTED AND OBSERVED THAW PENETRATION

El. pipe base (m)	El. thaw depth (m)	Date	Time t (days)	time days$^{1/2}$	Observed thaw depth $\overline{X}$ (m)	Predicted thaw depth $\overline{X}$ (m)
1.80	1.75	July 22	0	0	0	0
2.03	2.80	July 28	6	2.45	0.77	0.55
2.39	3.25	Aug 5	14	3.74	0.86	0.87
2.60	3.73	Aug 15	24	4.90	1.13	1.20
2.82	4.30	Sept 1	41	6.40	1.48	1.75
2.98	4.90	Oct 1	71	8.43	1.92	-

The comparison between a simple theoretical calculation of this form and the observed data in the early stages is excellent, and the deviation at later times is possibly due to the two-dimensional thawing effects around the pipe. The data could not be continued past October 1st as the hot oil supply failed at this time.

Final Effective Stresses

The final effective pressures are readily calculated on the basis of original moisture content data, assuming 100% saturation. The thawed soil above the level of the pipe base is assumed to act as a surcharge loading. Although principally comprised of gravel, a

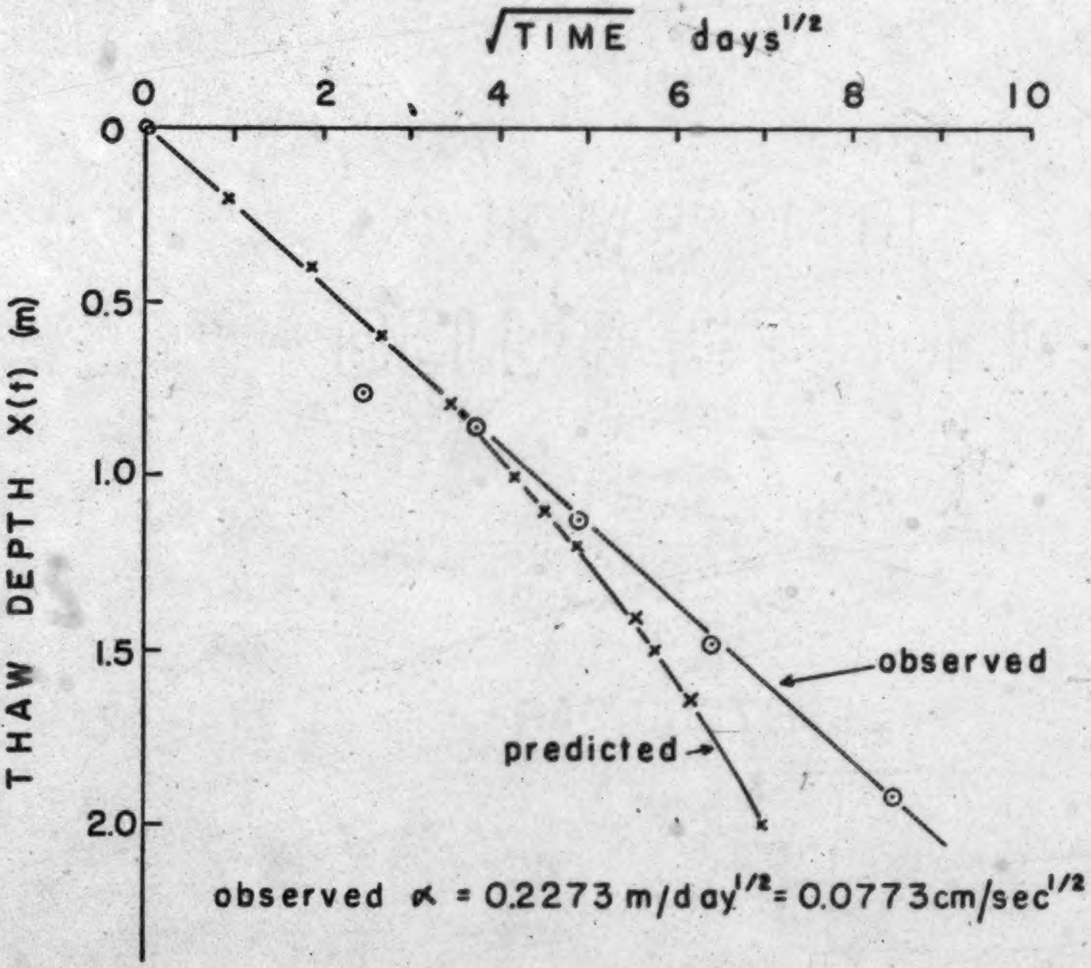

Fig. 6.9 Predicted and Observed Thawing at Inuvik

small depth of silt and compressed organics which are initially thawed also augment the surcharge. The anticipated large strains in the ice-rich clayey silt appear to complicate the calculation of overburden stresses. However, it may be argued that even though excessive strains are taking place above a given point in the thawing foundation, the same height of soil solids, and therefore the same final effective stress, remains above this point until the thaw plane passes. Thus, the final effective stress may be calculated accurately for any point on the thaw plane from the initial moisture content data for the frozen material. The ultimate effective stresses are calculated in this manner from the moisture content data given in Fig. 6.7, and the calculations are provided in Table 6.2. The first three layers may be assumed to comprise the applied loading P_o. The remaining layers of interest are shown to exhibit an average submerged unit weight of $\gamma' = 0.434$ t/m^3. The variation of the final effective stress is shown plotted against the original depth from the ground surface in Fig. 6.10.

TABLE 6.2 FINAL EFFECTIVE STRESSES

Layer	Designation	Original depth (m)	Original height H_0(m)	Unit weight γ' (t/m^3)	Stress $\gamma' H_o$ t/m^2	
Gravel	-	0 - 1.37	1.37	1.22	1.67	P_o = 1.77
Organics	-	1.37 - 1.52	0.15	0.22	0.03	
Silt clay	A	1.52 - 1.82	0.30	0.22	0.07	
Ice	B	1.82 - 1.98	0.16	0	0	av.γ' = 0.434
Ice + silt	C	1.98 - 2.74	0.76	0.32	0.243	
Silt + ice	D	2.74 - 3.96	1.22	0.51	0.622	
Till	E	3.96 and below	-	1.22	-	

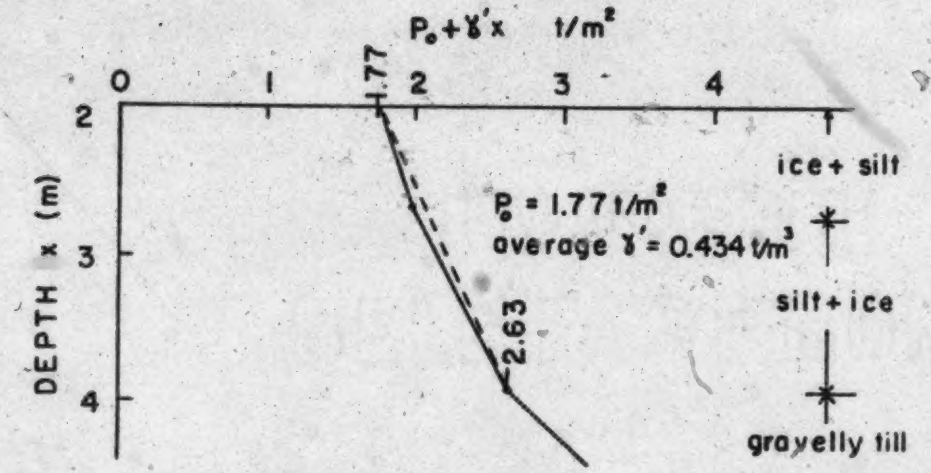

Fig. 6.10 Final Effective Stresses

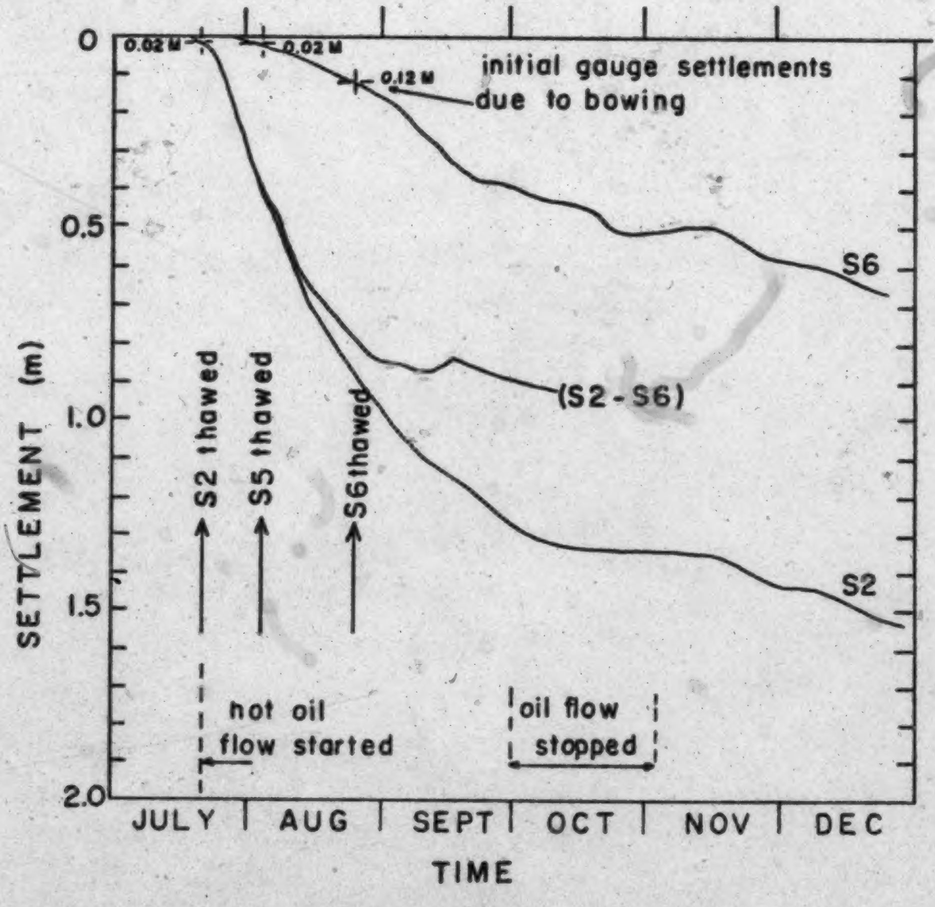

Fig. 6.11 Settlement Records in the Thawing Foundation

Excess Pore Water Pressures

Attention is now turned to calculating from the recorded data the excess pore water pressure at a point when the thaw plane passes that point. Watson et al. (1973) present data from eight piezometer locations, at depths shown in Fig. 6.7. When the thaw plane passes a piezometer tip, the actual head of water is read from the data. The position to the water table is monitored continuously from open standpipes near the surface. The excess head of water may be calculated. The excess pore pressure is then normalised by dividing it by the final effective stress at that point (See Fig. 6.10). A summary of the data is presented in Table 6.3.

TABLE 6.3 ANALYSIS OF PIEZOMETER DATA

Piezometer	Depth (m)	$U_{max}(t/m^2)$	$(P_o + \gamma'X)$ (t/m^2)	$u/(P_o + \gamma'X)$	W_r
TP2	2.65	0.3	2.00	15 %	0.13
TP2	3.56	0.51	2.42	21 %	0.37
TP3	2.59	0.76	1.95	39 %	0.1
TP3	3.35	0.42	2.32	18.1%	0.31
TP3	4.27	0.49	3.00	16.3%	0.7
TP4	1.65	0.25	1.65	15.2%	0
TP4	2.59	0.34	1.98	17.2%	0.1
TP4	3.50	1.08	2.40	35.0%	0.35

The normalised excess pore pressures vary between 15% and 21%, excepting two readings which are appreciably higher.

Settlement Data

Two sets of settlement data permit analysis (S2 - S6) and (S3 - S10). The gauge S3 was installed at the same level as S2. Other sets of gauges were present, but were too far removed from the axis of the pipeline to be of concern here.

The data are best analysed by considering the relative movements of a pair of gauges located at different depths in the compressible silt layer. Long after the thaw plane has passed the lower gauge and entered the dense till, the settlement curve levels out, and this value is used for the maximum settlement at that point. This value of maximum settlement may then be used to calculate m_v for the compressible silt layer.

In order to obtain values for consolidation settlement, the observed readings must be corrected for the following factors.

(i) "Bowing" or bending of the settlement rods.

(ii) Thawing of the pure ice layer at the pipe base.

(iii) The ice/water volume contraction on thaw.

For (i), the correction is clearly seen from Fig. 6.11. The gauge S_2 had moved 0.02 m when the thaw plane passes it, however the gauge S6 had moved 0.12 m when the thaw plane passed that gauge. This introduces a correction of (0.12 - 0.02) = +0.10 m to all readings (S2 - S6) due to bending of the settlement rods caused by horizontal movement of thawed material.

For (ii), the pure ice layer 0.16 m thick and a very small depth of soil above the ice layer provide a correction of -0.19 m, when making settlement calculations for the silt layer alone.

For (iii), the ice water contraction results in a volume contraction of

$$\left(\frac{\Delta V}{V}\right)_{i/\omega} = \frac{e_{frozen} - e_{thawed}}{1 + e_{frozen}}$$

Now $e_{frozen} = \frac{\gamma_\omega}{\gamma_{ice}} \; e_{thawed}$

$$\left(\frac{\Delta V}{V}\right)_{i/\omega} = \frac{\frac{\gamma_\omega}{\gamma_{ice}} \omega G_s - \omega G_s}{1 + \frac{\gamma_\omega}{\gamma_{ice}} \omega G_s}$$

$$\left(\frac{\Delta V}{V}\right)_{i/\omega} = \frac{\frac{\gamma_\omega}{\gamma_{ice}} - 1}{\frac{1}{\omega G_s} + \frac{\gamma_\omega}{\gamma_{ice}}} \qquad (6.17)$$

S2 - S6

The bending correction (i) is 0.1 m in this case. The correction for the pure ice layer (ii) is -0.19 m, and the correction for the ice-water transformation (iii) is $-0.0625\ H_0$. The initial elevations of the settlements gauges are

S2; EL = 1.34

S6; EL = 3.55

therefore the original height of frozen soil is

S2 - S6 = 2.21 m

and $\left(\frac{\Delta V}{V}\right)_{i/\omega} = 0.0625 \times 2.21 = 0.138$ m

The initial height of compressible thawed soil therefore is

$$H = 2.21 - 0.138 - 0.19$$

$$H = 1.882 \text{ m.}$$

The coefficient of volume compressibility m_v is defined as

$$m_v = \frac{S_{max}}{H(P_o + 0.5\gamma' H)} \qquad (6.18)$$

Applying the preceding corrections to the maximum settlement value in the data, provides

$$S_{max} = 0.86 + 0.1 - 0.19 - 0.138$$
$$= 0.632 \text{ m.}$$

Therefore from eq. (6.18)

$$m_v = \frac{0.6319}{1.882\ (1.77 + 0.217 \times 1.882)} = 0.152\ m^2/t$$

Again consulting the settlement data in Fig. 6.11, the settlement, S_t, when the thaw plane passed S_t, is given by

$$S_t = 0.79 + 0.1 - 0.19 - 0.138$$

$$S_t = 0.562 \text{ m.}$$

$$\therefore \frac{S_t}{S_{max}} = \frac{0.562}{0.632} = 0.889$$

W_r at the depth S6 is $\frac{0.434 \times 1.882}{1.77}$

or $W_r = 0.461.$

Using the theoretical curves in Fig. 3.5 for S_t/S_{max} vs. R, the required R value is 0.32. Combining this value of R with the observed

α value, the consolidation coefficient is found to be

$$c_v = 1.46 \times 10^{-2}\ \text{cm}^2/\text{s}. \quad [500\ \text{ft}^2/\text{yr.}]$$

S3 - S10

Using a similar approach for the relative settlements of gauges S3 and S10, the following is obtained

$$\left.\begin{array}{ll} \text{S3;} & \text{EL} = 1.36 \\ \text{S10;} & \text{EL} = 3.19 \end{array}\right\} \therefore H_o = 1.83$$

$S_t = 0.56$, $S_{max} = 0.72$, and hence the settlement ratio S_t/S_{max} is 0.777.

m_v for the south side of the pipe from this data using the corrected height of thawed soil initially as 1.526 m. is

$$m_v = 0.224\ \text{m}^2/\text{ton}.$$

Calculation of Intermediate Transient Settlement Values

Using the m_v value obtained for S2 - S6 at maximum settlement, it is of interest to predict the transient shape of the settlement curve with time. Again, settlement due to the ice/water volume change, thawing of the pure ice layer, as well as consolidation settlement must be considered.

Bearing in mind that $\overline{X}$ is the depth from the heat source to the thaw plane,

$$\overline{X} = \alpha\sqrt{t} \tag{6.19}$$

It is also known that S_{max} was defined in terms of the initial, unconsolidated height of soil, thus

$$S_{max} = m_v X(P_o + 1/2\ \gamma' X) \tag{6.20}$$

and

$$\frac{S_t}{S_{max}} = \text{constant} \tag{6.21}$$

Now $$S_t = X - \overline{X} = X - \alpha\sqrt{t} \tag{6.22}$$

Combining equations (6.20), (6.21) and (6.22) provides the relationship

$$\frac{S_t}{S_{max}} = \frac{X - \alpha\sqrt{t}}{m_v\ X(P_o + 0.5\gamma' X)}$$

or

$$m_v\ P_o \frac{S_t}{S_{max}}\ X + m_v \frac{S_t}{S_{max}} 0.5\gamma' X^2 = X - \alpha\sqrt{t}$$

which gives

$$0.5\gamma' m_v \frac{S_t}{S_{max}}\ X^2 + \left\{m_v\ P_o \frac{S_t}{S_{max}} - 1\right\} X + \alpha\sqrt{t} = 0 \tag{6.23}$$

For a given time t, this is a quadratic in X, i.e. the depth of thaw if no settlement were occurring.

When the constants for the case in question are introduced into eq. (6.23) the following quadratic evolves:

$$X = 12.75 - \sqrt{162.7 - 7.41\sqrt{t}} \tag{6.24}$$

where X is in metres,

and t is in days.

Equation (6.20) is used to obtain S_{max}, and then S_t is easily obtained.

A table of observed and calculated settlements including the necessary corrections for ice layers and the ice/water phase change is given in Table 6.4.

TABLE 6.4 OBSERVED AND PREDICTED SETTLEMENTS

	OBSERVED				PREDICTED		
Date	t days	S m.	$\sqrt{t}$ days$^{1/2}$	X m.	S_{max} m.	S_t m.	$S = S_t +$ i/w+ice m.
21/7/71	0	0	0	0	0	0	0
23	2	0.13	1.42	0.42[illegible]	0.122	0.109	0.330
25	4	0.17	2.00	0.605	0.177	0.157	0.392
27	6	0.23	2.45	0.744	0.221	0.197	0.442
29	8	0.32	2.83	0.863	0.260	0.231	0.485
31	10	0.39	3.16	0.966	0.295	0.262	0.523
2/8/71	12	0.44	3.46	1.060	0.326	0.290	0.563
4	14	0.51	3.74	1.149	0.357	0.318	0.593
6	16	0.56	4.00	1.231	0.386	0.343	0.624
8	18	0.60	4.24	1.308	0.414	0.368	0.654
10	20	0.65	4.47	1.381	0.440	0.391	0.682
12	22	0.70	4.69	1.452	0.466	0.414	0.711
14	24	0.74	4.90	1.519	0.491	0.437	0.739
16	26	0.775	5.10	1.584	0.516	0.458	0.764
18	28	0.80	5.29	1.645	0.539	0.479	0.790
20	30	0.83	5.48	1.707	0.563	0.500	0.816
22	32	0.855	5.66	1.765	0.585	0.520	0.840

Table 6.4 Continued/...

	OBSERVED			PREDICTED			
Date	t days	S m.	$\sqrt{t}$ days$^{1/2}$	X m.	S_{max} m.	S_t m.	$S = S_t$ + i/w + ice m.
24	34	0.87	5.83	1.821	0.607	0.540	0.864
26	36	0.89	6.00	1.876	0.629	0.559	0.887
24/9/71	64	0.96	8.00	-	-	-	-

Fig. 6.12 presents the predicted and observed data for (S2 - S6). The curves must agree at the "end thaw" time; as m_v was calculated from the observed data in any case. The real value of the plot is the comparison between transient settlement behaviour prior to complete thawing. The predicted values agree well with the observed settlement curve at later times. In the earlier stages, however, the theory considerably overestimates the settlement rate. This may be because in the theoretical treatment, the 0.16 m ice layer was presumed to thaw almost instantaneously, as indeed probably happened. However, the field settlement plot does not reflect this sudden settlement to the same extent, and consequently lags behind the predicted values.

The reasons for this are not clear, but it may possibly be due to non-uniform thickness of the ice layer, giving an arching effect in the overlying soil. Horizontal movements of material slipping in towards the pipeline may also have delayed the vertical settlements.

Summary of Results

The S_t/S_{max} values obtained from the two sets of settlement

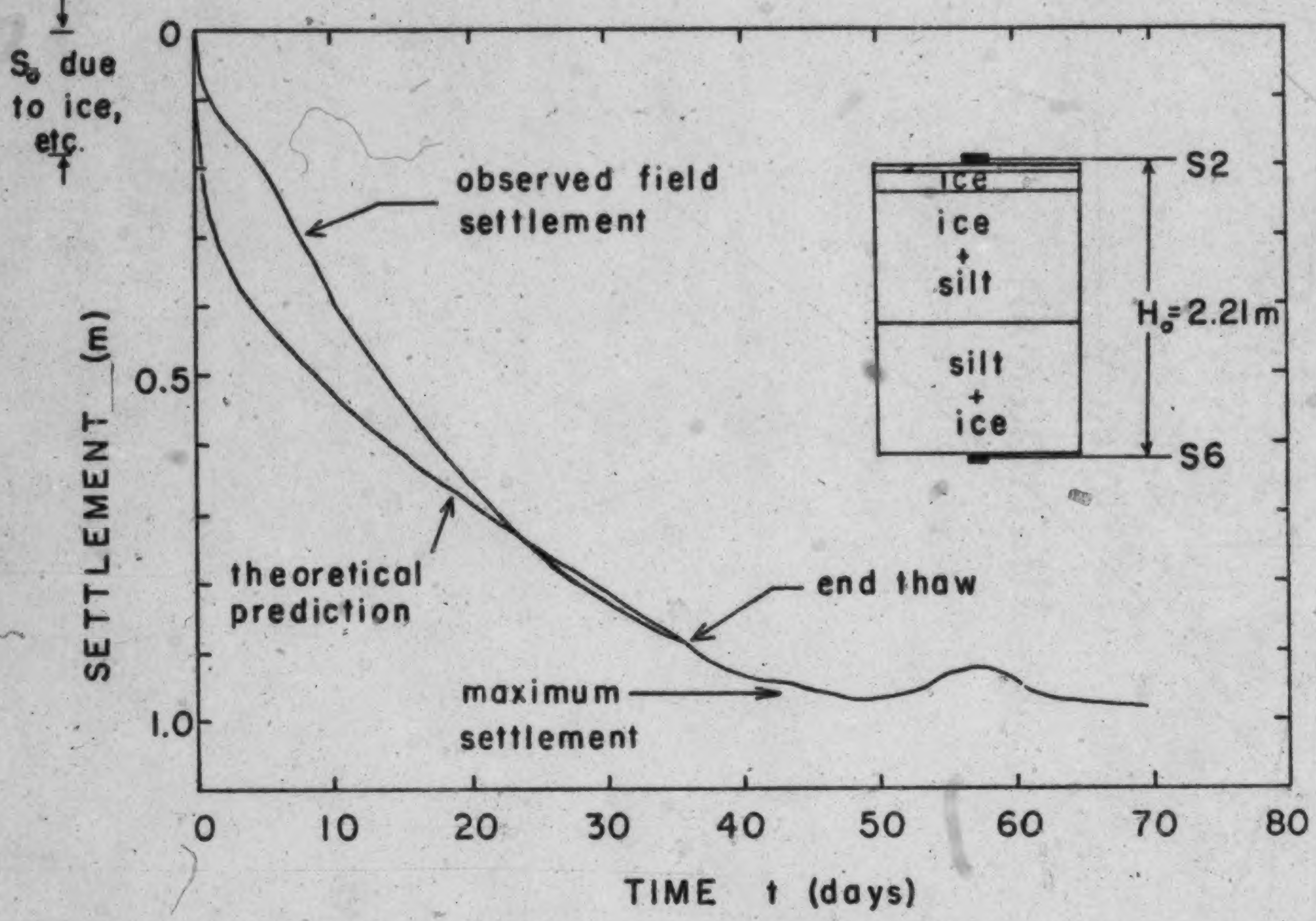

Fig. 6.12 Observed and Calculated Transient Settlements

data enabled two calculations of the required R value in the field to be made. The required coefficient on consolidation was then calculated. As the m_v value for each location was known exactly from the total settlement data, the permeability k required to give the degree of consolidation could be calculated. These two values of the required k are included in Table 6.5, together with the data and similar calculations for the eight piezometer locations considered.

In general, the theory of thaw-consolidation indicates that the excess pore pressure data and the settlement data are entirely consistent with each other. This is so because the required permeability values to obtain the observed settlement ratios and the observed excess pore pressures lie within the same range of values. The theory would indicate that the following narrow range of soil properties were exhibited in the clayey silt layer on thawing:

c_v 1.2 - 1.8 x 10^{-2} cm^2/s (400 - 600 ft^2/yr)

m_v 1.7 - 2.2 cm^2/Kg

k 0.2 - 0.4 x 10^{-4} cm/s

It now remains to compare the required permeability in the field with those that were actually measured for this material in field and laboratory tests.

Rowley et al. (1972) have given values for permeability obtained in a field test of 0.53 x 10^{-4} to 2.29 x 10^{-4} cm/s. These values seem high for a soil of this type, and it was suggested that the macro structure of the thawed permafrost was responsible for the large values.

An open stand pipe with a 9 inch by 1 1/2 inch cylindrical tip was used in the test. The head of water used in the stand pipe

TABLE 6.5 SUMMARY OF DATA FROM PORE PRESSURE AND SETTLEMENT READINGS

Source	Gauge and Depth	%	R. req.	c_v req. (cm^2/s)	c_v req. $ft^2/yr.$	m_v calc m^2/ton	m_v calc $cm^2/gm.$	k req. cm/s
Piezometer	TP2 (2.65)	15%	0.29	1.77×10^{-2}	600	0.154	1.54×10^{-3}	0.272×10^{-4}
"	TP2 (3.56)	21%	0.355	1.19×10^{-2}	404	0.154	1.54×10^{-3}	0.183×10^{-4}
"	TP3 (2.59)	39%	0.52	0.55×10^{-2}	187	0.224	2.24×10^{-3}	0.123×10^{-4}
"	TP3 (3.35)	18.1%	0.325	1.42×10^{-2}	482	0.224	2.24×10^{-3}	0.318×10^{-4}
"	TP3 (4.27)	16.3%	0.305	1.61×10^{-2}	546	0.224	2.24×10^{-3}	0.36×10^{-4}
"	TP4 (1.65)	15.2%	0.290	1.77×10^{-2}	600	0.224	2.24×10^{-3}	0.396×10^{-4}
"	TP4 (2.59)	17.2%	0.310	1.55×10^{-2}	525	0.224	2.24×10^{-3}	0.347×10^{-4}
"	TP4 (3.50)	45.0%	0.580	0.443×10^{-2}	150	0.224	2.24×10^{-3}	0.1×10^{-4}
Settlement	S2 - S6 (2.0-3.55)	88.9%	0.33	1.38×10^{-2}	467	0.154	1.54×10^{-3}	0.225×10^{-4}
Settlement	S3 - S10 (2.0-3.19)	77.7%	0.49	0.62×10^{-2}	210	0.224	2.2×10^{-3}	0.139×10^{-4}
							Average k required =	0.246×10^{-4}

was approximately 3.0 m (10 feet) above the ground water table. The tip was brought close to the thaw plane at different times, and the test carried out under a constant head. This head of water represents a water pressure of 0.3 Kg/cm^2 in excess of the hydrostatic ground water condition. Referring again to the diagram of final effective stresses with depth in Fig. 6.10, it is seen that at no point in the clayey-silt substratum does the effective overburden pressure approach a pressure of 0.3 Kg/cm^2. This means in effect that the water pressure exceeded the maximum effective overburden stress, causing hydraulic 'jacking' of the substratum, and the permeability results so obtained must be considered suspect. Field permeability testing in such situations must be carried out with great care, giving due consideration to the range of effective stresses involved.

Laboratory data on the permeability of the clayey-silt layer have been provided by Watson (1973). The soil samples were thawed under a small stress, and the permeability calculated from constant head tests. The void ratio and permeability were determined for successive increments of loading. The data from two such tests have been provided, and the results are summarised in Table 6.6

TABLE 6.6 LABORATORY DATA FOR INUVIK CLAYEY SILT

Load σ' (Kg/cm^2)	Void Ratio e	Permeability k (cm/s)
0	3.1	-
0.186	1.2	0.247×10^{-4}
0.293	1.16	0.161×10^{-4}
0.880	1.02	0.043×10^{-4}

TABLE 6.6 continued...

Load σ' (Kg/cm^2)	Void Ratio 3	Permeability k (cm/s)
0	3.01	-
0.293	1.22	0.108×10^{-4}
0.585	1.09	0.052×10^{-4}
0.880	1.02	0.027×10^{-4}

Figure 6.13 shows the void ratio plotted against effective stress, and the permeability, k. Both relationships are linear on a semi-logarithmic plot. Using these relationships, the permeability may be plotted directly with effective stress, to obtain the graph shown in Fig. 6.14.

The graph also shows the narrow range of effective stress experienced by the clayey silt layer shown in Fig. 6.10. Taking the widest range of permeabilities possible, the permeability of the laboratory samples in the stress range of interest lies between 0.17×10^{-4} and 0.26×10^{-4} cm/s. Although this range of values is determined from specimens of the foundation soil tested in the laboratory, and it is true that the macro-structure in the field may not be adequately represented, the laboratory values are considered a great deal more representative of the soil behaviour than the results of the field tests, which must be regarded as too high, for the reasons cited above.

Table 6.5 indicates the use of the observed pore pressures and settlements to obtain the R value in the field that is required.

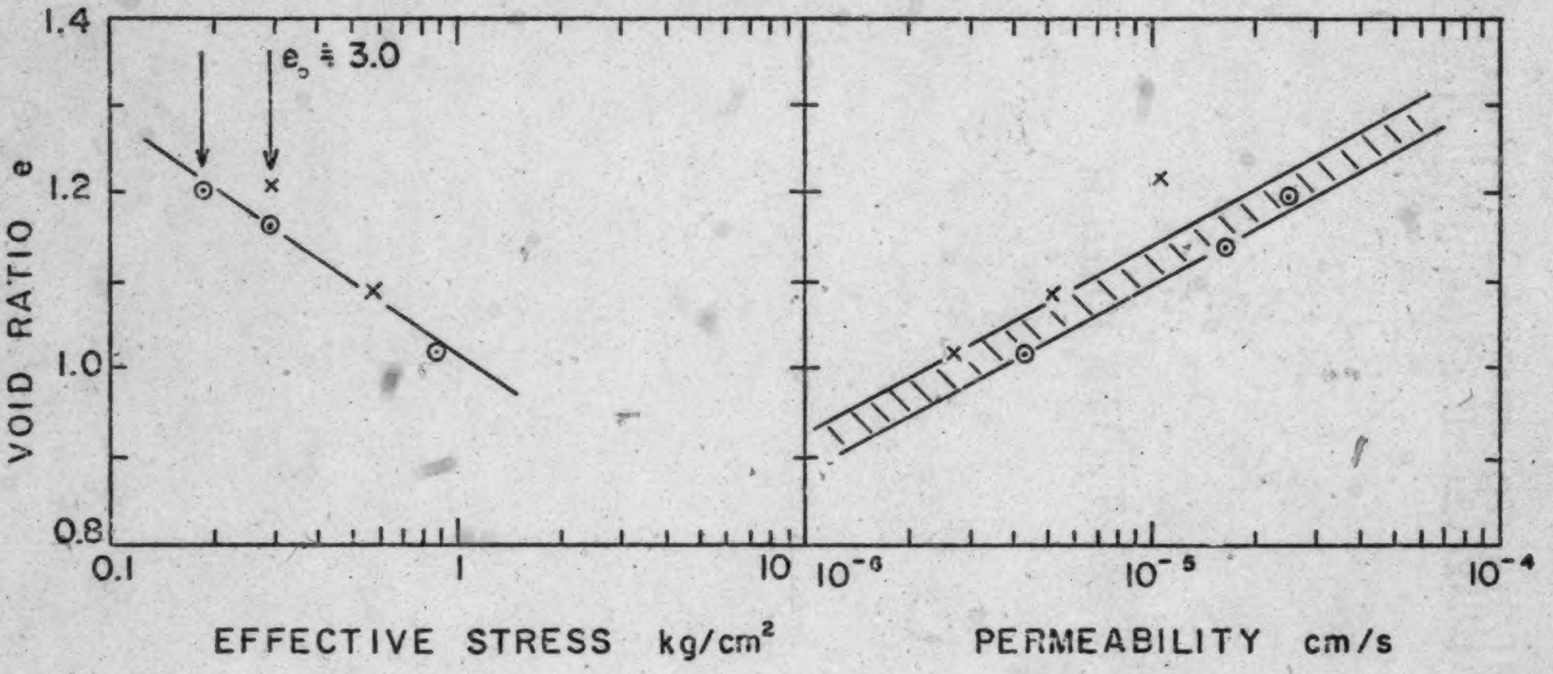

Fig. 6.13 Laboratory Results for Inuvik Clayey Silt

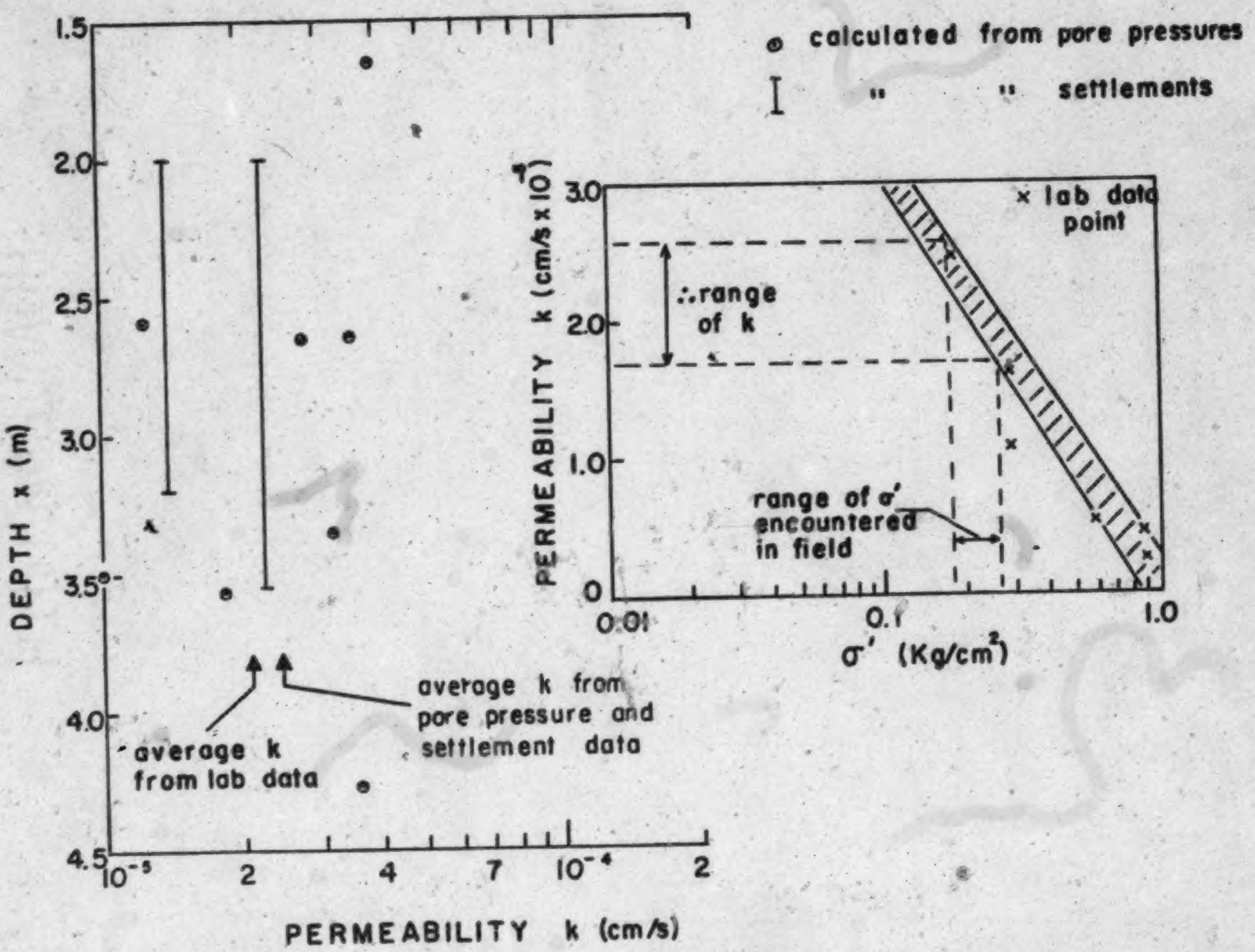

Fig. 6.14 Permeability Calculated from Observed Pore Pressures and Settlements

for consistency with the theory. As the α and m_v values may be accurately calculated from the observed performance of the foundation, the remaining unknown quantity in the R value is the permeability, k. Table 6.5 also shows the calculation of the permeability value required in the field to verify the predictions of the thaw consolidation theory. There are ten such "required" permeability values at different depths, and these are plotted against depth in Fig. 6.14. Table 6.5 also shows the average required permeability is calculated to be 0.25×10^{-4} cm/s.

The narrow range of permeability values obtained from laboratory testing is also indicated in Fig. 6.14. These values have an average of 0.22×10^{-4} cm/s.

The range of permeability values required to validate the one-dimensional theory of thaw-consolidation presented in this thesis is 0.1 to 0.4×10^{-4} cm/s, with an average of 0.25×10^{-4} cm/s. Laboratory testing on thawed samples at the effective stress range experienced in the field gave a range of permeability values of 0.17 to 0.26×10^{-4} cm/s, with an average of 0.22×10^{-4} cm/s. It is therefore concluded that the agreement between the theoretical predictions presented here and the observed behaviour of the foundation is excellent, particularly when the extreme variability of a parameter such as the permeability is recognised.

It is suggested that if the quantities involved in the calculation of the R value had been estimated in advance of the operation of the test pipe line, and the one-dimensional thaw-consolidation theory used to predict the pore pressures and settlements under the structure, remarkable agreement between theory and observation would have been obtained. Both theory and observation demonstrate that although the total amount of settlement might be considered excessive in some cases, the soil properties were such as to ensure a reasonably stable foundation while thawing was taking place. Approximately eighty percent of the maximum available effective stress was attained by the soil immediately on thawing, and between eighty and ninety percent of the settlement took place at the same time.

The analysis of the field data presented here assumes the existence of a homogeneous soil profile, and the maintenance of one-dimensional thawing conditions. Clearly, neither of these assumptions are completely realised within the thaw bulb. The soil profile exhibits a decreasing ice content with depth, and therefore is non-homogeneous in this respect. However, calculations of m_v, and therefore of c_v are based on an average total settlement throughout the layers of interest. In this way the differing soil properties are averaged, so that the theory for homogeneous soils may be used for analysis. The assumption of one-dimensional compression and drainage conditions is assured under the centre-line of the pipe. Examination of the shape of the thaw line and the surface settlement profiles given by Watson et al (1973) assures that at

Although this test pipe line loop constitutes the only complete case history available at the present, it is extremely well documented and reported. The comparisons between theoretical and

0.3 m from the pipe axis (where the instrumentation was installed) the assumption of one-dimensionality is still reasonable.

Although this test pipe line loop constitutes the only complete case history available at the present, it is extremely well documented and reported. The comparisons between theoretical and observed behaviour considerably increases the confidence in the predictive power of the thaw-consolidation theory.

CHAPTER VII

CONCLUDING REMARKS

In this thesis, the equations governing the consolidation of thawing soils have been presented in a form sufficiently general for many applications. In situations where a uniform frozen soil is thawing due to the application of a constant surface temperature, a useful solution in closed form becomes available. In such instances, the thaw-consolidation ratio, R, enjoys a privileged position, as it controls to a large extent the maintenance of pore water pressures and the degree of settlement. With careful determination of the coefficient of consolidation, it should be possible to provide a fairly reliable forecast of the foundation conditions.

It has been demonstrated how numerical solutions may be used to account for features which would have to be excluded or oversimplified using an analytical solution.

The concept of the residual stress was introduced to describe the conditions in the thawed soil if no drainage were permitted. This parameter has been successfully measured for reconstituted and natural samples of thawed soil. Its influence on the build-up of pore pressures and the subsequent deformations in the thawing soil is clearly important, and some implications are cited for cases where the residual stress is large compared with the overburden loading.

The predictive power of the theory has been shown to be-substantial by carrying out carefully controlled laboratory tests, and by analysing in detail the performance of a thawing foundation under a hot oil pipeline.

While the theory in its present form lends itself admirably to many applications, the present work indicates that further research in certain areas is of high priority. It has been demonstrated quite conclusively that at the present state of understanding, further research into the thermal properties of soils must be considered subordinate to the requirement for a more exact knowledge of geotechnical properties. The coefficient of consolidation is the most important single parameter in this respect, and it in turn contains the permeability of thawed soil. When applying the theory to field problems, the correct in-situ permeability becomes a most important quantity indeed. In large scale projects, the in-situ measurement of permeability may be warranted, and it is of paramount importance that the permeability be determined at the correct effective stress level, as the strong dependence of permeability on effective stress or void ratio is well known.

The preliminary measurements of residual stress described in this work have suggested that a significant increase in this quantity with depth may be expected, where the void ratio decreases with depth. Further testing of samples from natural permafrost profiles appears to be of the highest priority, as it may provide great insight into the natural structure of permafrost, and assist in the more economic design of warm structures in contact with frozen ground.

The analyses performed here have been limited to establishing the physics of thawing soils in a one-dimensional geometrical configuration. However, many field problems are obviously multi-dimensional in nature. Although no serious conceptual difficulty should arise in their treatment, multi-dimensional problems might very usefully be formulated and solved to augment the analytical power of the design engineer.

Finally, the extreme shortage of well-documented field case records is obvious, and any research carried out in this area will certainly be well-received, and will greatly enhance the present state of knowledge concerning the realistic behaviour of thawing soils.

REFERENCES

Aldrich, H.P. 1956. Frost penetration below highway and airfield pavements. Highway Research Board Bull. 135.

Aldrich, H.P. and Paynter, H.M. 1953. Analytical studies of freezing and thawing in soils. ACFEL Tech. Report 42. U.S. Army Corps of Engg.

Anderson, D. and Morgenstern, N.R. 1973. Physics, Physical Chemistry and Mechanics of frozen ground. Proc. 2nd Int. Conf. on Permafrost, Yakutsk, USSR.

Anderson, D.M., Tice, A.R. and McKim, H.L. 1973. The unfrozen water in frozen soils. Paper in preparation for the Second Int. Conf. on Permafrost, Yakutsk, USSR.

Barron, R. 1948. Consolidation of fine grained soils by Drain Wells. Trans. Am. Soc. Civ. Engrs. 113, p.718.

Berggren, W.P. 1943. Predictions of temperature distribution unfrozen soils. Trans. Am. Geophys. Union. Pt.3.

Brown, R.J.E. 1970. Permafrost in Canada: its influence on northern development. University of Toronto Press, Toronto.

Brown, W.G. and Johnston, G.H. 1970. Dikes on Permafrost: predicting thaw and settlement. Can. Geot. Journal. 7, p.365-371.

Carrillo, N. 1942. Simple two and three-dimensional cases in the theory of consolidation of soils. J. Math. and Phys. 21, no. 1, p.1.

Carslaw, H.S. and Jaeger, J.C. 1947. Conduction of heat in solids. Clarendon Press, Oxford.

Casagrande, L. and Poulos, S. 1969. On the effectiveness of sand drains. Can. Geotech. J. 6, p.287-326.

Crank, J. and Nicholson, P. 1947. A practical method for the numerical evaluation of solutions of partial differential equations of the heat conduction type. Proc. Cambridge Phil.Soc. 43, p. 50-67.

Davis, E.H. and Raymond, G.P. 1965. A non linear theory of consolidation. Geotechnique, 15, p.161-173.

Dept. of the U.S. Army. 1966. Calculation methods for determination of depths of freeze and thaw in soils. Report TM5-852-6.

Dillon, H.B. and Andersland, O.B. 1966. Predicting unfrozen water contents in frozen soils. Can. Geotech. J. 3, no.2, p.53-59.

Feldman, G.M. 1965. Solution of the one dimensional problem of consolidation of thawing soils with consideration of variable permeability and compressibility. Reports of 8th all-union Interdepartmental Conf. on Geocryology. [In Russian], no.5. Yakutsk.

Fox, E.N. 1948. The mathematical solution for the early stages of consolidation. Proc. 2nd. Int. Conf. Soil Mechs. and Found. Eng. 1, p.41-42.

Gibson, R.E. 1958. The progress of consolidation in a clay layer increasing in thickness with time. Geotechnique, 8, p.171-182.

Ho, D.M., Harr, M.E. and Leonards, G.A. 1970. Transient temperature distribution in insulated pavements. Predictions and observations. Can. Geotech. J. 7, p.275-284.

Kersten, M.S. 1949. Laboratory research for the determination of the thermal properties of soils. Final Report, Eng. Experiment Station, Minnesota University, Minneapolis, Minn.

Kiselev, M.F., Kostinenko, G.I. and Nyzovkin, G.A. 1965. Calculation of foundation settlements on thawing soils. Proc. 6th Int. Conf. Soil. Mech. and Found. Eng. 3, p.98-102.

Koch, R.D. 1971. The design of Alaskan North Slope production wells. Proc. Inst. Mech. Eng., 185, p.989-1001.

Lachenbruch, A.H. 1970. Some estimates of the thermal effects of a heated pipeline in permafrost. U.S. Geol. Surv., Circular 632.

Ladanyi, B. 1972. An engineering theory of creep in frozen soils. Can. Geotech. J. 9, p.63-80.

Lock, G.S.H. 1971. On the perturbation solution of the ice-water layer problem. Int. J. of Heat and Mass Transfer 14, p.642-644.

Lock, G.S.H., Gunderson, J.R., Quon, D. and Donnelly, J.K. 1969. A study on one-dimensional ice formation with particular reference to periodic growth and decay. Int. J. of Heat and Mass Transfer 12 (1), p.1343-1352.

Mackay, J.R. 1971. The origin of massive icy beds in permafrost, Western Arctic Coast, Canada. Can. J. Earth Sci. 8, p.397-422.

Macpherson, J.G., Watson, G.H. and Koropatnick, A. 1970. Dikes on permafrost foundations in northern Manitoba. Can. Geotech. J. 7, p.356-364.

Makowski, M.W. and Mochlinski, K. 1956. An evaluation of two rapid methods of assessing the thermal resistivity of soil. Proc. Inst. Elec. Engineers, 103, A. no. 11, p.453-464.

Malyshev, M.V. 1966. Calculation of the settlement of foundations on thawing soil. Soil Mechs. and Found. Eng. No. 4, (July-Aug.), p.260-265.

McRoberts, E.C. 1972. Personal Communication.

Morgenstern, N.R. and Smith, L.B. 1972. Thaw-consolidation tests on remoulded clays. Can. Geotech. J. 10, p.25-40.

Moulton, L.K. 1969. Prediction of the depth of frost penetration: a review of literature. Engineering Experiment Station, Report 5, West Virginia University.

Murray, W.D. and Landis, F. 1959. Numerical and Machine solutions of transient heat-conduction problems involving melting or freezing. Trans. Am. Soc. Mech. Eng., 81, p.106-112.

Palmer, A.C. 1973. Thawing and differential settlements close to oil wells through permafrost. Proc. Second Int. Conf. on Permafrost, Yakutsk, July, 1973.

Peaceman, D.W. and Rachford, H.H. 1955. The numerical solution of parabolic and elliptic differential equations. J. SIAM, 3, p.28-41.

Penner, E. 1967. Heaving pressure in soils during unidirectional freezing. Can. Geotech. J. 4, p.398-408.

Penner, E. 1970. Thermal conductivity of frozen soils. Can. J. Earth Sci. 7, p.982-987.

Rowley, R.K., Watson, G.H., Wilson, T.M. and Auld, R.G. 1972. Performance of a 48-inch warm-oil pipeline supported on permafrost. Proc. 25th Canadian Geotechnical Conf., Ottawa.

Scott, R.F. 1969. The freezing process and mechanics of frozen ground. U.S. Army CRREL Monograph II-D1.

Seider, W.D. and Churchill, S.W. 1965. The effect of insulation on freezing front motion. Heat Transfer-Cleveland. Chem. Eng. Progress Symposium Series 59, Vol. 61, Am. Inst. Chem. Eng., p.179-184.

Skaven-Haug, S. 1972. The design of frost foundations, frostheat and soilheat. Norwegian Geotechnical Institute, Publication no. 90.

Smith, L.B. 1972. Thaw consolidation tests on remoulded clays. Unpublished M.Sc. thesis. University of Alberta, Edmonton, Alberta.

Speer, T.L., Watson, G.H. and Rowley, R.K. 1973. Effects of ground-ice variability and resulting thaw settlements in buried warm-oil pipelines. Proc. 2nd Int. Conf. on Permafrost, Yakutsk.

Terzaghi, K. and Peck, R.B. 1967. Soil mechanics in engineering practice. John Wiley & Sons, New York.

Tsytovich, N.A. 1957. The fundamentals of frozen ground mechanics and new investigations. Proc. 4th Int. Conf. Soil Mechs. and Found. Eng. p.116-119.

Tsytovich, N.A. 1965. Permafrost in the U.S.S.R. as foundations for structures. Proc. 6th Int. Conf. Soil Mechs. and Found. Eng. p.155-167.

Tsytovich, N.A., Zaretskii, Y.K., Grigoreva, V.G. and Termartirosyan, Z.G. 1965. Consolidation of thawing soils. Proc. 6th Int. Conf. Soil Mechs. Found. Eng. 1, p.390-394.

Vialov, S.C. 1963. Rheology of frozen soils. Proc. NAS-NRC, Int. Permafrost Conf., Purdue Univ., Lafayette, Indiana, p.332-339.

Watson, G.H. 1973. Personal communication.

Watson, G.H., Rowley, R.K. and Slusarchuk, W.A. 1973. Performance of a warm oil pipeline buried in permafrost. Proc. 2nd Int. Conf. on Permafrost, Yakutsk, July 1973.

Williams, P.J. 1966. Pore pressures at a penetrating frost line and their prediction. Geotechnique 16, no.3, p.187-208.

Wissa, A.E.Z. and Martin, P.T. 1968. Behaviour of soils under flexible pavements: development of rapid frost susceptibility tests. Dept. Civil Engg. M.I.T. Research Report R68-77.

Yao, L.Y. and Broms, B.B. 1965. Excess pore pressures which develope during thawing of frozen fine-grained subgrade soils. Highway Research Record 101, p.39-57.

Zaretskii, Y.K. 1968. Calculation of the settlement of thawing soils. Soil Mechs. and Found. Eng. (May-June), no.3, p.151-155.

APPENDIX A

DETAILS OF FINITE DIFFERENCES PROCEDURES AND PROGRAM LISTINGS

A.1 Finite Difference Procedure for the One Dimensional Thawing of Soils

This procedure is very similar to that described by Ho, Harr and Leonards (1970). The finite difference scheme described here is designed to investigate some of the effects of temperature and phase properties on the rate of thaw and the temperature distribution in a melting soil, and is not intended as a user-oriented computer program.

The governing differential equation of one-dimensional conductive heat transfer is from Section 2.3

$$\frac{\partial\theta}{\partial t} = \frac{1}{c_o(\theta)} \cdot \frac{\partial}{\partial x}\left\{k(\theta)\,\frac{\partial\theta}{\partial x}\right\} - \frac{L\,\omega\,\gamma_d}{c_o(\theta)}\,\frac{d\,W_u}{dt} \qquad (A.1)$$

Assuming a constant discrete interval in the x-direction, and writing the governing equation in finite difference form according to the simple explicit method, we obtain

$$\theta_{i,j+1} = A\,\theta_{i+1,j} - (A + B - 1)\,\theta_{i,j} + B\,\theta_{i-1,j} - L\,\omega\,\gamma_d\,\Delta W_u / c_o(\theta_{i,j}) \qquad (A.2)$$

where i and j are the finite difference subscripts in the x and t directions respectively,

$$A = \frac{2\,\Delta t}{c_o(\theta_{i,j})(\Delta x)^2\left\{\frac{1}{k(\theta_{i+1,j})} + \frac{1}{k(\theta_{i,j})}\right\}} \tag{A.3}$$

and
$$B = \frac{2\,\Delta t}{c_o(\theta_{i,j})(\Delta x)^2\left\{\frac{1}{k(\theta_{i,j})} + \frac{1}{k(\theta_{i-1,j})}\right\}} \tag{A.4}$$

and where $c_o(\theta_{i,j})$ and $k(\theta_{i,j})$ represent the values of those functions at the temperature $\theta = \theta_{i,j}$

For a stable solution the inequality

$$A + B \leq 1 \tag{A.5}$$

must be satisfied, and this limitation on the time step Δt is the chief drawback to this numerical method. However in this instance, this restriction is easily counterbalanced by the ease of programming this simple method.

The quantity ΔW_u is the fraction of the total moisture content that changes phase in the time interval Δt.

Thus

$$\Delta W_u = W_u(\theta_{i,j+1}) - W_u(\theta_{i,j}) \tag{A.6}$$

The quantity $W_u(\theta_{i,\,j+1})$ is unknown at the time level j, hence the finite difference equation is essentially implicit in form. For arbitrary functions of $W_u(\theta)$, we must solve each finite difference equation by the Newton-Raphson Iteration method. This method is extremely efficient, and converges rapidly to give the solution $\theta_{i,j+1}$.

The arbitrary functions $c_o(\theta)$, $k(\theta)$ and $W_u(\theta)$ are included in the program as function subprograms, and they may be varied by changing the required cards in each function subprogram.

A.2 Program Listing for One Dimensional Heat Conduction

Purpose:- To calculate the temperature distributions and depth of thaw in a saturated soil.

Description:- The program uses a simple explicit finite difference procedure to calculate the conductive heat transfer in a melting soil. The latent heat of the soil is accounted for in the manner described by Ho, Harr and Leonards (1970).

Usage:- The data is input on a single data card FORTRAN format (9F8.0) in the order

k_u, k_f, P, Q, R, H, T_s, T_g, ω

where k_u and k_f are the conductivities of the fully thawed and fully frozen soil respectively,

P, Q and R define the unfrozen moisture content/temperature relationship by the equation $W_u = \left(P + \exp(Q\theta+R)\right)/100$ and θ is the temperature,

H is the height of soil considered,

T_s and T_g are the surface and ground temperatures,

and ω is the water content expressed as a fraction.

Units:- The units used are centimeters, grams, seconds and degrees Centigrade.

Output:- The program will print out the time in seconds, hours and hours$^{1/2}$ and the temperature profile at every time step.

Example of Data Input:-

k_u = 0.00245 cal/cm.s.^{o}C

k_f = 0.005 cal/cm.s.^{o}C

P = 0

Q = 0.4

R = 4.6

H = 500 cm.

T_s = 10^{o}C

T_g = -3^{o}C

ω = 0.4 (See overleaf for program listing.)

A.3 Finite Difference Procedure for Thaw Consolidation with Arbitrary Movement of the Thaw Plane

The finite difference grid is fixed in space in the x-direction, and the moving boundary is denoted by node 'n'. The previous (n-1) nodes are equally spaced at Δx. For any arbitrary specification of the thaw plane

$$X = X(t) \tag{A.7}$$

the integer number 'n' is calculated by

$$n = \frac{X}{\Delta X} + 1 \tag{A.8}$$

and this indicates the position of the thaw plane in the finite difference grid. This value is stored in the computer program in an integer location, and so any fraction of a grid spacing is truncated. We denote the fraction of the grid spacing between nodes (n-1) and n by V,

```
      REAL U(200).UNEXT(200)
      COMMON P.Q.R.TCT.TCF.W.GAMD
  1   READ(5.2)TCT.TCF.P.Q.R.H,TS,TI,W
      WRITE(6.83)TCT.TCF.H
 83   FORMAT(' './/' THERMAL CONDUCTIVITY IN THAWED SOIL IS'.F10.5/
     1' THERMAL CONDUCTIVITY IN THE FROZEN SOIL IS'.F10.5/
     2' THE HEIGHT OF SOIL CONSIDERED IS'.F10.3)
  2   FORMAT(9F8.0)
      WRITE(6.73)P.Q.R
 73   FORMAT('0'.'P='.F8.2.'  Q='.F8.2.'  R='.F8.2)
      N=40
      N=30
      DX=H/N
      GAMD=2.7/(1.+W*2.7)
      CCF=TCF
      IF(TCT.GT.TCF)   CCF=TCT
      DT=GAMD*DX*DX*(0.2+0.5*W)/(2.2*CCF)
      DT0=0.2*DT
      DTF=DT
      WRITE(6.42)DT.DX
 42   FORMAT('0'.'THE TIME STEP IS'.F10.3.'   DX='.F10.3)
      DO 3 I=1.N
  3   U(I)=TI
      OUT=0.4
      TOUT=0.4
      TIME=0.
      TOL=0.00005
  4   U(N+1)=U(N-1)
      IF(U(1))61.61.62
 61   DT=DT0
      GO TO 63
 62   DT=DTF
 63   BET=DT/(DX*DX)
      DO 5 I=1.N
      T=U(I)
      TP=U(I+1)
      IF(I.EQ.1)   GO TO 6
      TM=U(I-1)
      GO TO 7
  6   TM=TS
  7   A=2.*BET/(CO(T)*(1./TC(TP) + 1./TC(T)))
      IF(I.GT.1)   GO TO 44
      B=2.*BET*TC(TM)/CO(T)
      GO TO 45
 44   B=2.*BET/(CO(T)*(1./TC(T) + 1./TC(TM)))
 45   AB=A+B
      IF(AB.LT.1.)   GO TO 46
      WRITE(6.47)I
 47   FORMAT('0'.'  THE'.I3.'TH NODE IS UNSTABLE. AND THE TIME STEP WILL
     1 BE HALVED...')
      DT=DT/1.5
      BET=BET/1.5
      GO TO 4
 46   E=79.6*W*GAMD/CO(T)
      D=A*TP+(1.-A-B)*T+B*TM+E*WU(T)
C-----COMMENCE THE ITERATION TO FIND U(I.J+1)...
C-----LET THE INITIAL APPROXIMATION BE U(I.J)...
      KOUNT=0
      SOL=T
  8   STONE=SOL
      F=SOL-D+E*WU(SOL)
      IF(SOL.LT.0.)   GO TO 15
      IF(T.LT.0.)   GO TO 50
      FDASH=1.
      GO TO 16
 50   FDASH=1. + E*(WU(SOL)-WU(T))/(SOL-T)
      GO TO 16
 15   FDASH=1.+E*Q*EXP(Q*SOL+R)/100.
 16   SOL=SOL-F/FDASH
      DIFF=ABS(SOL-STONE)
      KOUNT=KOUNT+1
      IF(KOUNT.LT.20)   GO TO 9
      IF(T.GT.-0.2) GO TO 105
      SOL=0.5*(SOL+STONE)
      WRITE(6,106)I
  106 FORMAT(' ',' THE SOLUTION FAILED TO CONVERGE AT NODE',I5)
      GO TO 11
  105 SOL=0.0001
      WRITE(6,10)I
  10  FORMAT(' ',' THE ',I4,'TH NODE HAS COMPLETELY CHANGED PHASE')
      GO TO 11
   9  IF(DIFF.GT.TOL)   GO TO 8
  11  UNEXT(I)=SOL
   5  CONTINUE
      TIME=TIME+DT
      HOURS=TIME/3600.
      SQHR=SQRT(HOURS)
      DO 12 I=1,N
  12  U(I)=UNEXT(I)
      WRITE(6,13)TIME,HOURS,SQHR,(U(I),I=1,N)
  13  FORMAT(' ','TIME=',F12.1,'  HOURS=',F10.2,'  ROOT TIME=',F10.3/
     1(10F10.4))
  18  IF(U(N).LT.-0.1)   GO TO 4
      GO TO 1
      END


      REAL FUNCTION TC(T)
      COMMON P,Q,R,TCT,TCF,W,GAMD
C-----THIS FUNCTION EVALUATES THE CONDUCTIVITY AS A FUNCTION OF
C-----TEMPERATURE....
C-----*******************************************
      IF(T.LT.0.)   GO TO 1
      WU=1.
      GO TO 2
   1  WU=(P+EXP(Q*T+R))/100.
   2  TC=TCF+WU*(TCT-TCF)
      RETURN
      END


      REAL FUNCTION CO(T)
      COMMON P,Q,R,TCT,TCF,W,GAMD
C-----THIS FUNCTION EVALUATES THE APPARENT VOLUMETRIC SPECIFIC HEAT
C-----OF THE SOIL...
C-----**********************************************
      IF(T.LT.0.)   GO TO 1
      WU=1.
      GO TO 2
   1  WU=(P+EXP(Q*T+R))/100.
   2  CO=GAMD*(0.2+0.5*W*(1.+WU))
      RETURN
      END


      REAL FUNCTION WU(T)
C-----THIS FUNCTION EVALUATES THE UNFROZEN MOISTURE CONTENT OF THE SOIL
C-----AT THE TEMPERATURE **T** ......
C-----****************************************************
      COMMON P,Q,R,TCT,TCF,W,GAMD
      IF(T.LT.0.)   GO TO 1
      WU=1.
      GO TO 2
   1  WU=(P+EXP(Q*T+R))/100.
   2  RETURN
      END
```

and it is calculated from the relation

$$V = \frac{X}{\Delta X} - (n-1) \qquad (A.9)$$

Thus there are (n-1) nodes spaced equally at Δx and one node with a spacing of V(Δx).

The finite difference equations for the first (n-2) nodes were written as usual according to the Crank-Nicholson (1947) scheme for the unknown values of the pore pressure at the (j + 1) time interval:

$$-\beta\, u_{i-1,\,j+1} + 2(1+\beta)\, u_{i,j+1} - \beta\, u_{i+1,j+1}$$

$$= \beta\, u_{i-1,j} + 2(1-\beta)\, u_{i,j} + \beta\, u_{i+1,j}\ ; \quad i = 1, \text{--}\ (n-2) \qquad (A.10)$$

where $\beta = \dfrac{c_v\, \Delta t}{(\Delta x)^2}$

Δt is the time increment,

i is the nodal subscript in the x-direction,

and j is the subscript in the time direction.

The pore pressure at the surface is always taken to be zero, and so

$$u_{o,j} = u_{o,j+1} = 0 \qquad (A.11)$$

For the (n-1) node, the unequal spacing of the nodes requires a different equation.

Let

V_{j+1} = fractional node spacing at the j+1 time level,

and V_i = node spacing at the i level.

These values of V are calculated from eq. (A.9) using

$X(t_{j+1})$ and $X(t_j)$ respectively.

Using the Crank Nicholson scheme

$$\frac{\partial u}{\partial t} = 1/2\, c_v \left\{ \left.\frac{\partial^2 u}{\partial x^2}\right|_j + \left.\frac{\partial^2 u}{\partial x^2}\right|_{j+1} \right\}$$

we obtain after application of the usual central difference operators

$$\frac{-\beta V_{j+1}}{1 + V_{j+1}} u_{n-2,j+1} + (1+\beta) u_{n-1,j+1} - \frac{\beta}{1 + V_{j+1}} u_{n,j+1}$$

$$= \frac{\beta V_j}{1 + V_j} u_{n-2,j} + (1-\beta) u_{n-1,j} + \frac{\beta}{1 + V_j} u_{n,j} \qquad \text{(A.12)}$$

For the derivation of the equation at the n th node we must assume for consistency with the previous equations the existence of a fictional node (n+1) at a distance $V(\Delta x)$ below the boundary node n.

At the moving boundary on node n the following equations must be satisfied at the two time levels j and (j+1).

At $t = t_j,\ t_{j+1}$ $\quad \frac{\partial u}{\partial t} = c_v \frac{\partial^2 u}{\partial x^2}$ (A.13)

and $\quad P_o + \gamma' X - u = \dfrac{c_v \frac{\partial u}{\partial x}}{\frac{dX}{dt}}$ (A.14)

Writing eq. (A.13) in finite difference form

$$-\beta_{j+1} u_{n+1,j+1} + 2(1+\beta_{j+1}) u_{n,j+1} - \beta_{j+1} u_{n-1,j+1}$$

$$= \beta_j u_{n+1,j} + 2(1-\beta_j) u_{n,j} + \beta_j u_{n-1,j} \qquad \text{(A.15)}$$

where $\beta_{j+1} = \dfrac{c_v \, \Delta t}{V_{j+1}^2 \, (\Delta x)^2}$

and $\beta_j = \dfrac{c_v \, \Delta t}{V_j^2 \, (\Delta x)^2}$.

Writing (A.14) in finite difference form

$$u_{n+1,j} = 2(P_j - u_{n,j}) \frac{V_j \, (\Delta x)}{c_v} \left.\frac{dX}{dt}\right|_j + u_{n-1,j} \tag{A.16}$$

and $u_{n+1,j+1}$

$$= 2 \, (P_{j+1} - u_{n+1,j}) \frac{V_{j+1} \, (\Delta x)}{c_v} \left.\frac{dX}{dt}\right|_{j+1} + u_{n-1,j+1} \tag{A.17}$$

where P_j and P_{j+1} are the values of $(P_o + \gamma' X)$ at the j and (j+1) time levels,

and $\left.\frac{dX}{dt}\right|_j$ and $\left.\frac{dX}{dt}\right|_{j+1}$ are the known velocities of the thaw front at t_j and t_{j+1}.

These values may be obtained by differentiation of the function X(t).

Equations (A.16) and (A.17) may now be substituted in eq. (A.15) to eliminate the unknown values at the fictional node (n+1), and finally the equation for the node n is written as

$$(1 + \beta_{j+1} + \beta_{j+1} C_{j+1}) \, u_{n,j+1} - \beta_{j+1} \, u_{n-1,j+1}$$

$$= (1 - \beta_j - \beta_j C_j) \, u_{n,j} + \beta_j \, u_{n-1,j} + \beta_{j+1} C_{j+1} P_{j+1} + \beta_j C_j P_j \tag{A.18}$$

where $$C_{j+1} = \frac{V_{j+1}\ (\Delta x)}{c_v}\ \frac{dX}{dt}\bigg|_{j+1} \tag{A.19}$$

and $$C_j = \frac{V_j\ (\Delta x)}{c_v}\ \frac{dX}{dt}\bigg|_j$$

The values for P, C, β and dX/dt are calculated for each new time step, and used in eq. (A.19).

The equations may now be written in tridiagonal matrix form, and solved by a very efficient algarithm derived from the Gaussian Elimination technique for solving simultaneous linear equations.

$$\begin{bmatrix} a_1 & b_1 & & & & & \\ c_2 & a_2 & b_2 & & & & \\ & - & - & - & & & \\ & & - & - & - & & \\ & & & c_i & a_i & b_i & \\ & & & & - & - & - \\ & & & & & a_n & b_n \end{bmatrix} \begin{Bmatrix} x_1 \\ x_2 \\ - \\ - \\ x_i \\ - \\ x_n \end{Bmatrix} = \begin{Bmatrix} d_1 \\ d_2 \\ - \\ - \\ d_i \\ - \\ d_n \end{Bmatrix} \tag{A.20}$$

Briefly, if the coefficients of the diagonal, super-diagonal, the sub-diagonal, the right hand sides and the solution vector are denoted by a_i, b_i, c_i, d_i and x_i respectively, then the algorithm for solution proceeds as follows.

1. Change into upper triangular form using

$$a_i = a_i - b_{i-1}\ c_i/a_{i-1}$$

and $d_i = d_i - d_{i-1}\, c_i/a_{i-1}$; $i = 2, ----, n$

$c_i = 0$

2. Back Substitute using

$x_{n+1} = 0$

$x_i = (d_i - b_i\, x_{i+1})/a_i$; $i = n, (n-1), ----, 1$

The solution vector is now available in x_i, and this will generally form the solution at the (j+1) time step, $u_{i,j+1}$.

A.4 Program Listing for Thaw-Consolidation With Arbitrary Movement of the Thaw Plane

Purpose:- To determine the excess pore pressures and degree of consolidation in a thawing soil, when the movement of the thaw plane is specified by an arbitrary function.

Description:- The program uses a Crank-Nicholson finite difference procedure to solve the equation of consolidation subject to the boundary condition at the thaw line. It uses a fixed grid, and the boundary moves across the grid with time. The listing shows a thaw boundary movement described by

$$X = B\, t^n$$

where B and n are entered as data. If one wishes to specify an alternative function, then the two cards specifying X(t) and $\frac{dX(t)}{dt}$ may be changed in subroutine THAW. The card specifying T0 on line 24 of the main program must also be changed to be consistent with the initial thaw depth X0.

Usage:- The program requires data on two cards as follows. The first cards in FORTRAN format (7F10.0) accepts the following data in order,

B, n, t_f, c_v, Δx, P_o, γ'

where B and n are parameters describing the movement of the thaw plane,

t_f is the termination time for the program,

Δx is the grid spacing in the x direction,

P_o is the surface applied loading,

and γ' is the submerged unit weight of the soil.

The second card accepts one parameter in FORTRAN format (I2) denoted by NG. This parameter changes the size of the time increment used, and usually lies between 20 and 200. It may be varied to determine the effect of the size of the time step. If it is specified too small, the time increments become very large and instability of the numerical procedure may result.

Units:- The units used are lbs, feet and years;or tons, metres and years.

Output:- The program prints out the thaw depth, time, time$^{1/2}$, time factor, degree of settlement and the normalised excess pore pressure distribution, and this information is printed out two hundred times between $t = 0$ and $t = t_f$.

Example of Data Input:-

B = 11.7 feet/year$^{0.3}$

n = 0.3

t_f = 20 years

c_v = 100 ft^2/year

$\Delta x = 0.5$ feet

$P_o = 870$ lbs/ft^2

$\gamma' = 38$ lb/ft^3

NG = 50 (See overleaf for program listing.)

A.5 Numerical Solution for Thaw-Consolidation in a Two-Layer Profile

We assume the solution for thawing and consolidation in the upper layer to be defined accurately by the analytical solution given in Chapter 3. We require a solution for the excess pore pressures and settlements when the thaw plane enters the underlying layer at depth H. Letting the finite difference interval in the x-direction be Δx_1, then there will be 'm' finite difference nodes in the upper layer defined by

$$m = H/\Delta x_1 \tag{A.21}$$

The movement of the thaw plane in the lower layer is given by the relationship defined in Section 2.9. In the same manner as in Appendix A.3, the position of the thaw plane in the finite difference grid is given by

$$X = H + (n - m - 1)\,\Delta x_2 + V(\Delta x_2) \tag{A.22}$$

Writing the equations for the top layer we have

$$-\beta_1\, u_{i-1,\,j+1} + 2(1+\beta_1)\, u_{i,j+1} - \beta_1\, u_{i+1,j+1}$$

$$= \beta_1\, u_{i-1,j} + 2(1-\beta_1)\, u_{i,j} + \beta_1\, u_{i+1,j} \qquad i = 1,2,\text{-}(m-1) \tag{A.23}$$

where $\beta_1 = \dfrac{c_{v_1}\,\Delta t}{(\Delta x_1)^2}$

```
C-----PROGRAM TO CALCULATE THE PCRE PRESSURES IN A THAWING SOIL.
C-----THE PROGRAM USES THE CRANK-NICHOLSON FINITE DIFFERENCE METHOD..
C-----IT IS A FIXED GRID. MCVING BOUNDARY SITUATION. AND THE SOIL IS
C-----ASSUMED HOMOGENEOUS...  ONE DIMENSIONAL FLOW IS PERMITTED. AND
C-----THE PROGRAM'CAN INCORPERATE ANY SPECIFIED RATE OF THAW....
C-----************************************************************
      REAL U(500).A(500).B(500).C(500).D(500)
      CCMMON DX.PO
C------ENTER THE PARAMETERS NECESSARY FOR SOLUTION
   99 READ(5,101)CB.CN.TF.CV.DX.PO.GAMD
  101 FORMAT(7F10.0)
      WRITE(6.102)CB.CN.TF.CV.DX.PO.GAMD
  102 FORMAT('1'.'         DATA  INPUT:-'/'   THE RATE OF THAW IS GIVEN BY
     1:'/20X.'X(T) ='.F6.2.'.TIME**'.F5.3/'THE SOLUTION WILL BE TERMINAT
     2ED AT TIME='.F10.3/'THE COEFFICIENT OF CONSOLIDATICN IS'.F10.5/
     3'THE GRID SPACING IN THE X-DIRECTION IS'.F7.3/'THE APPLIED LOAD AT
     4 THE SURFACE IS'.F10.4/'THE SUBMERGED UNIT WEIGHT OF THE SOIL IS'.
     5F8.3)
      READ(5.31)NG
   31 FORMAT(I2)
      TOUT=TF/200.
      TOUTP=TOUT
      X0=2.1*DX
      T0=(X0/CB)**(1./CN)
      TIME=T0
      U(1)=0.2*P(PO.GAMD.X0)
      U(2)=U(1)
      DT=T0/20.
      X=X0
      DERIV=X/TIME
      CALL POSIT(X.DX.N.V.NP)
      N1=NP
      V1=V
      N=N1+1
      U(N)=U(1)
      CALL OUTPUT(U.X.N1.V1.GAMD.TIME)
   25 TIME=TIME+DT
      IF(TIME.GT.TF)   GO TO 99
      BT=CV*DT/(DX*DX)
C-----  STORE  X AND DX/DT AT THE JTH TIME STEP.....
      XJ=X
      DERJ=DERIV
C-----CALCULATE X AND DX/DT AT THE (J+1)TH TIME STEP.....
      CALL THAW(X.DERIV.TIME.CB.CN)
      XJ1=X
      DERJ1=DERIV
      CALL POSIT(X.DX.N2.V2.NP)
      N2=NP
      IREM=0
      IF(N2.EQ.N1)   GO TO 1
      IREM=N2-N1
      V2=V2+IREM
      MARK=1
    1 D(1)=2.*(1.-BT)*U(1)+BT*U(2)
      N=N1+1
      NL2=N-2
      IF(NL2.LE.1)   GO TO 4
      DO 2 I=2.NL2
    2 D(I)=BT*(U(I+1)+U(I-1))  +2.*(1.-BT)*U(I)
    4 D(N-1)=BT*V1*U(N-2)/(1.+V1) +(1.-BT)*U(N-1) + BT*U(N)/(1.+V1)
      DO 3 I=1.NL2
      A(I)=2.*(1.+BT)
      B(I)=-BT
    3 C(I)=-BT
      C(1)=0.
      A(N-1)=1.+BT
      C(N-1)=-BT*V2/(1.+V2)
      B(N-1)=-BT/(1.+V2)
C-----CALCULATE THE COEFFICIENTS FOR THE FINITE DIFFERENCE EQUATION
C-----AT THE BOUNDARY(NTH) NODE ......
      BJ=CV*DT/(V1*V1*DX*DX)
      BJ1=CV*DT/(V2*V2*DX*DX)
      PJ=P(P0.GAMD.XJ)
      PJ1=P(P0.GAMD.XJ1)
      CJ=V1*DX*DERJ/CV
      CJ1=V2*DX*DERJ1/CV
      A(N)=1.+BJ1*(1.+CJ1)
      C(N)=-BJ1
      B(N)=0.
      D(N)=(1.-BJ-BJ*CJ)*U(N)+BJ*U(N-1) +BJ1*CJ1*PJ1 +BJ*CJ*PJ
      CALL GAUSEL(A.B.C.D.N)
      DO 8 I=1.N
    8 U(I)=C(I)
      IF(MARK.EQ.0)   GO TO 10
      DIST=V2*DX
      GRAD=(U(N)-U(N1))/DIST
      UX=U(N)
      DO 5 I=N.N2
    5 U(I)=U(N1)+GRAD*(I-N1)*DX
      U(N2+1)=UX
   10 N1=N2
      V1=V2-IREM
      MARK=0
      DT=DX/(NG*DERIV)
      TIME2=TIME/2.
      IF(DT.LT.TIME2)     GO TO 30
      DT=TIME2
   30 IF(TIME.LT.TOUTP)   GO TO 25
      TOUTP=TOUTP+TOUT
      CALL OUTPUT(U.X.N1.V1.GAMD.TIME.CV)
      GO TO 25
      END



      SUBROUTINE GAUSEL(A.B.C.D.N)
C-----************************************************************
C-----THIS SUBROUTINE SOLVES 'N' LINEAR SIMULTANEOUS TRIDIAGONAL
C-----EQUATIONS. AND STORES THE RESULT IN THE ARRAY C(I).......
C-----************************************************************
      REAL A(1).B(1).C(1).D(1)
      IF(N.GT.1)GO TO 8
      C(N)=D(N)/A(N)
      GO TO 6
C----- TO CHANGE TO UPPER TRIANGULAR FORM.
    8 DO 5 I=2.N
      A(I)=A(I)-B(I-1)*C(I)/A(I-1)
      D(I)=D(I)-D(I-1)*C(I)/A(I-1)
    5 C(I)=0.
C----- BACK SUBSTITUTION..
      C(N+1)=0.
      I=N
    4 C(I)=(D(I)-B(I)*C(I+1))/A(I)
      IF(I.LE.1)GO TO 6
    7 I=I-1
      GO TO 4
    6 RETURN
      END
      SUBROUTINE OUTPUT(U.X.NI.VI.GAMD.TIME.CV)
      REAL U(1).UOUT(500)
      COMMON DX.PO
      NL1=NI-1
      SUM=0.
      DO 1 I=1.NL1
    1 SUM=SUM+2.*U(I)
      SUM=SUM+U(NI)
      SUM=SUM*0.5*DX
      SUM=SUM+0.5*VI*DX*(U(NI)+U(NI+1))
      SETEND=PO*X+GAMD*0.5*X*X
      SET=SUM/SETEND
      SET=1.-SET
      TIMDAY=TIME
      RTDAY=SQRT(TIMDAY)
      WRITE(6.8)X.TIMDAY.RTDAY
    8 FORMAT('0'.'   THE DEPTH OF THAW IS'.F12.4.'AND T='.F10.4.' YEAR
     1S AND ROOT YEARS='.F10.4)
      TIMFAC=CV*TIME/(X*X)
      WRITE(6.2)TIMFAC.SET.NI.VI
    2 FORMAT('0'.'TIME FACTOR CV.T/X**2 ='.F14.6.'   DEGREE OF SETTLEMEN
     1T ='.F10.5/'NI='.I5.'     AND THE FRACTION IS'.F10.4)
      N=NI+1
      P=PO+GAMD*X
      DO 4 I=1.N
    4 UOUT(I)=U(I)/P
      WRITE(6.3)(UOUT(I).I=1.N)
    3 FORMAT(' '.10F10.3)
      RETURN
      END


      SUBROUTINE THAW(X.DERIV.TIME.CB.CN)
C-----THIS SUBROUTINE CALCULATES THE DEPTH OF THAW FROM THE FORMULA
C-----                     X(T) = B.T**N
C-----THE ROUTINE ALSO CALCULATES THE DERIVATIVE DX/DT....
C------*************************************************************
      X=CB*(TIME**CN)
      DERIV=CN*CB*(TIME**(CN-1.))
      RETURN
      END


      SUBROUTINE POSIT(X.DX.N.V.NP)
C-----THIS ROUTINE GIVES THE POSITION OF THE FREEZE-THAW INTERFACE
C-----FROM THE RESULTS FROM SUBROUTINE'THAW' AND OUTPUTS A NODE AND
C-----THE FRACTION OF A NODE SPACING WHERE THE INTERFACE IS......
      NP=X/DX
      V=X/DX-NP
      N=NP+1
C-----  'N' IS THE NUMBER OF FINITE DIFFERENCE EQUATIONS FOR THE NEXT
C-----TIME STEP..........
      RETURN
      END


      REAL FUNCTION P(PO.GAMD.X)
C-----THIS FUNCTION CALCULATES THE EFFECTIVE OVERBURDEN STRESS
C-----AT THE FREEZE-THAW INTERFACE....
      P=PO+GAMD*X
      RETURN
      END
```

The equations for the lower layer are identical except to replace β_1 by β_2, where

$$\beta_2 = \frac{c_{v_2}\,\Delta t}{(\Delta x_2)^2}$$

These equations apply to the nodes

$$i = (m + 1), ---- (n - 2)$$

and the equations for the nodes $(n - 1)$ and n are identical with those for the same nodes described in Appendix A.3.

The only remaining node is the interfacial node 'm', between the two layers in question. At this node, the continuity of water flow and the equality of excess pore pressures must be satisfied simultaneously with the governing consolidation equation for each layer.

The node m forms the last node in layer 1 and the first node in layer 2. As the excess pore pressure in each layer must be the same in both layers at this point, the sets of finite difference equations for each layer may be linked by considering these two nodes as the same node, and so obtaining only one finite difference equation for the node.

The equations of consolidation for each layer bordering on the interface may be written down according to the Crank-Nicholson method as follows. For layer 1

$$u_{m,j+1} - u_{m,j} = \beta_1(u_{p,j+1/2} - 2\,u_{m,j+1/2} + u_{m-1,j+1/2}) \qquad (A.24)$$

and for layer 2

$$u_{m,j+1} - u_{m,j} = \beta_2(u_{m+1,j+1/2} - u_{m,j+1/2} + u_{q,j+1/2}) \qquad (A.25)$$

where p and q are two fictional nodes introduced as shown in Fig. A.1.

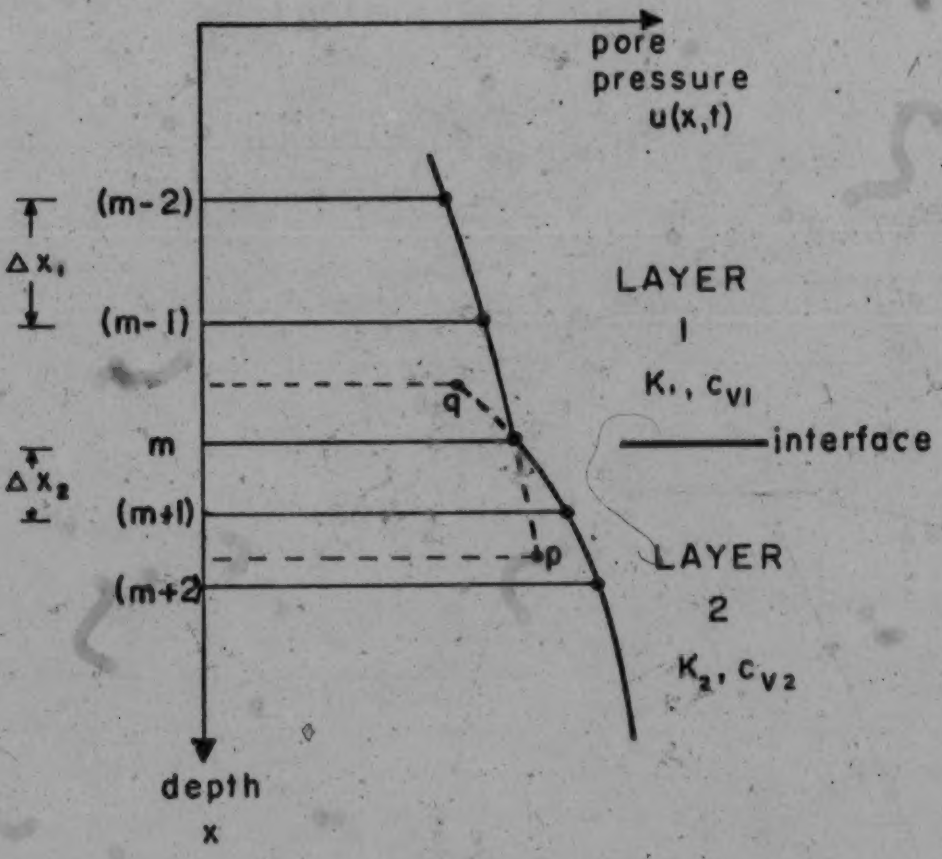

Fig. A.1 Finite Difference Grid at the Interface Between Two Soil Layers

We must now satisfy the continuity of pore fluids at the interface. In order to be consistent with the Crank-Nicholson difference method, central difference operators must be used to approximate the first order derivatives in the continuity equation, and this requires the presence of the nodes p and q. As central difference operators are applied, the discretization error of the Crank-Nicholson method $(\Delta x)^2$ is preserved. At the time level j+1/2, we have therefore

$$K_1 \left.\frac{\partial u}{\partial x}\right|_{m,j+1/2} \text{(in layer 1)} = K_2 \left.\frac{\partial u}{\partial x}\right|_{m,j+1/2} \text{(in layer 2)} \qquad \text{(A.26)}$$

In discrete form, eq. (A.26) becomes

$$K_1 \frac{u_{p,j+1/2} - u_{m-1,j+1/2}}{2\ \Delta x_1} = K_2 \frac{u_{m+1,j+1/2} - u_{q,j+1/2}}{2\ \Delta x_2} \qquad \text{(A.27)}$$

Equations (A.24), (A.25) and (A.27) now contain three unknown values of the excess pore pressure $u_{p,j+1/2}$, $u_{q,j+1/2}$ and $u_{m,j+1/2}$. Eliminating $u_{p,j+1/2}$ and $u_{q,j+1/2}$ from these equations, and setting

$$u_{i,j+1/2} = 1/2\ (u_{i,j+1} + u_{i,j})$$

for consistency with the Crank-Nicholson scheme, the following implicit finite difference equation is obtained for node m:

$$- u_{m-1,j+1} + (1+1/\beta_1+I_r/\beta_2+I_r)\ u_{m,j+1} - I_r\ u_{m+1,j+1}$$

$$= u_{m-1} + (1/\beta_1+I_r/\beta_2-1-I_r)\ u_{m,j} + I_r\ u_{m+1,j} \qquad \text{(A.28)}$$

where $I_r = \dfrac{K_2\ \Delta x_2}{K_1\ \Delta x_1}$

Hence the finite difference equations for the two layers are linked by another linear tridiagonal equation. The complete set of linear equations for the layered profile may now be written in matrix form, and solved by the method described in Appendix A.3.

A.6 Program Listing for Thaw-Consolidation in a Two-Layer Soil Profile

Purpose:- To determine the excess pore pressure distribution and degree of settlement in a thawing soil with a constant applied surface temperature. The soil profile is assumed to exhibit two distinct sets of thermal and geotechnical properties.

Description:- The rate of thaw and the resulting thaw-consolidation solution are well established for the thawing of the overlying layer, and this program determines the solution subsequent to the thaw plane entering the underlying layer. The rate of thaw through the lower layer is calculated using the simple Stefan-type relationship derived for a two layer system in Section 2.9. The program is set up to calculate the pore pressure distribution in the two layer system using a Crank-Nicholson finite difference procedure similar to that used in Appendix A.3. The major difference is that this routine must incorporate extra finite difference equations to satisfy the excess pore pressure conditions at the interface between the two soil strata.

Usage:- The program requires data on three cards as follows.

(i) In FORTRAN format (7F10.0) the necessary parameters in order are

$$\frac{k_2}{k_1} H, \ \frac{2\, k_2\, T_s}{L}, \ t_f, \ c_v, \ \Delta x, \ P_o, \ \gamma'$$

where k_1 and k_2 are the thermal conductivities of the upper and lower layers respectively,

H is the height of the upper layer,

T_s is the constant applied surface temperature,

L is the latent heat of the soil,

t_f is the termination time for the program,

c_v is the consolidation coefficient for the underlying layer,

Δx is the finite difference interval in the x-direction,

P_o and γ' are the surface loading and submerged unit weight of the soil.

(ii) The second data card requires the following data in order in format (5F10.0),

K_1, K_2, c_{v1}, α, H

where K_1 and K_2 are the permeabilities of the upper and lower layers,

c_{v1} is the consolidation coefficient for the upper layer,

and α is the alpha value for the upper layer.

(iii) The third data card requires the parameter NG in FORTRAN format (I3), and the description of this parameter is given in Appendix A.4.

Units:- A suggested set of units is lbs, feet and years.

Output:- The program prints out the thaw depth, time, time$^{1/2}$, degree of settlement and the normalised excess pore pressure profile, and this information is output two hundred times between $t = 0$; and $t = t_f$.

Example of data input:- For an example of 10 feet of fine-grained soil overlying a coarser material, a typical set of data is

$\frac{k_2}{k_1} H$ = 10 ft.

$\frac{2\ k_2 T_s}{L}$ = 100 ft/year$^{1/2}$

t_f = 16 years

c_v = 225 ft^2/year

Δx = 0.5 ft.

P_o = 0

γ' = 60 lbs/ft^2

K_1 = 1 ft/year

K_2 = 4 ft /year

c_{v1} = 25 ft^2/year

α = 10 ft/year$^{1/2}$

H = 10 ft.

NG = 50 (See overleaf for program listing.)

A.7 Finite Difference Scheme for Thaw-Consolidation with Sand-Drains

Writing eq. (6.5) and (6.6) in finite difference form according to the Crank-Nicholson scheme we obtain respectively

$$- \left(1 + \frac{\Delta r}{2r}\right) \beta_r V_{i,j+1} + (1 + 2\beta_r) V_{i,j} - \left(1 - \frac{\Delta r}{2r}\right) \beta_r V_{i,j-1}$$

$$= u_{i,j,k} \frac{\beta_z}{\alpha^2 t} \left\{ u_{i+1,j,k} - 2\ u_{i,j,k} + u_{i-1,j,k} \right.$$

$$\left. + \frac{\alpha^2\ z\ \Delta z}{4\ c_v} (u_{i+1,j,k} - u_{i-1,j,k}) \right\} \qquad \text{(A.29)}$$

```
C-----PROGRAM TO CALCULATE THE PORE PRESSURES IN A THAWING SOIL.
C-----THE PROGRAM USES THE CRANK-NICHOLSUN FINITE DIFFERENCE METHOD..
C-----IT IS A FIXED GRID. MOVING BOUNDARY SITUATION. AND THE SOIL IS
C-----ASSUMED HOMOGENEOUS...  ONE DIMENSIONAL FLOW IS PERMITTED. AND
C-----THE PROGRAM CAN INCORPERATE ANY SPECIFIED RATE OF THAW....
C-----
C-----THE PROGRAM IS NOW ADAPTED TO SOLVE A TWO-LAYER PROBLEM USING A RATE
C-----OF THAW CALCULATED FROM THE FORMULA GIVEN BY NIXON & MC.ROBERTS(1973)
C-----*****************************************************************
      REAL U(500).A(500).B(500).C(500).D(500)
      COMMON DX.PO.H
C------ENTER THE PARAMETERS NECESSARY FOR SOLUTION
  99  READ(5.101)CB,CN,TF,CV.DX.FO.GAMD
  101 FORMAT(7F10.0)
      WRITE(6.102)CB.CN.TF,CV.DX.PO.GAMD
  102 FORMAT('1','         DATA  INPUT:-'/'    THE RATE OF THAW IS GIVEN BY
     1:'/20X.'P     =',F8.2,'  Q=    ',F8.3/'THE SOLUTION WILL BE TERMINAT
     2ED AT TIME=',F10.3/'THE COEFFICIENT OF CONSOLIDATIUN IS',F10.5/
     3'THE GRID SPACING IN THE X-DIRECTION IS',F7.3/'THE APPLIED LOAD AT
     4 THE SURFACE IS',F10.4/'THE SUBMERGED UNIT WEIGHT OF THE SOIL IS',
     5F8.3)
      READ(5.35)PK1.PK2.CV1.ALPHA.H
  35  FORMAT(5F10.0)
      WRITE(6.36)PK1.PK2.CV1.ALPHA.H
  36  FORMAT('0','THE PERMEABILITY OF THE UPPER LAYER IS',F10.6/'THE PER
     1MEABILITY OF THE LOWER LAYER IS',F10.6/'THE COEFFICIENT OF CONSOLI
     2DATION FOR THE OVERLYING LAYER IS',F10.5,' FT**2/YEAR'/'THE ALPHA
     3VALUE FOR THE UPPER LAYER IS',F10.5,' FT/YR**0.5'/'THE HEIGHT OF
     4THE UPPER LAYER IS',F10.4 )
      READ(5.31)NG
  31  FORMAT(I3)
      W=PK2/PK1
      TOUT=TF/200.
      TOUTP=TOUT
      M=H/DX
      X0=1.1*DX
      T0=((X0+CB)*(X0+CB)-CB*CB)/CN
      TIME=T0
      DT=T0/20.
      X=X0
      DERIV=X/TIME
      CALL POSIT(X.DX.N,V.NP)
      N1=NP+M
      V1=V
      N=N1+1
C-----************************************
C-----CALCULATE THE INITIAL VALUES.....
C-----
      R=ALPHA/(2.*SQRT(CV1))
      RP=SQRT(3.14159J)
      AA=PO/(ERF(R)+EXP(-R*R)/(RP*R))
      BB=GAMD/(1.+1./(2.*R*R))
      DO 37 I=1.M
      ZI=I
      Z=ZI/N1
  37  U(I)=AA*ERF(R*Z)+BB*I*DX
      GRAD=PK1*(U(M)-U(M-1))/PK2
      U(M+1)=GRAD+U(M)
      U(M+2)=U(M+1)+GRAD*V1
      CALL OUTPUT(U.X.N1.V1.GAMD.TIME)
  25  TIME=TIME+DT
      IF(TIME.GT.TF)   GO TO 99
      BT1=CV1*DT/(DX*DX)
      BT2=CV*DT/(DX*DX)
      BT=BT1
C-----  STORE  X AND DX/DT AT THE JTH TIME STEP.....
      XJ=X
      DERJ=DERIV
```

```
C-----CALCULATE X AND DX/DT AT THE (J+1)TH TIME STEP.....
      CALL THAW(X.DERIV.TIME.CB.CN)
      XJ1=X
      DERJ1=DERIV
      CALL POSIT(X.DX.N2.V2.NP)
      N2=NP+M
      IREM=0
      IF(N2.EQ.N1)    GO TO 1
      IREM=N2-N1
      V2=V2+IREM
      MARK=1
    1 D(1)=2.*(1.-BT)*U(1)+BT*U(2)
      N=N1+1
      NL2=N-2
      DO 2 I=2.NL2
      BT=BT2
      IF(I.LT.M)    BT=BT1
    2 D(I)=BT*(U(I+1)+U(I-1))   +2.*(1.-BT)*U(I)
    4 D(N-1)=BT*V1*U(N-2)/(1.+V1) +(1.-BT)*U(N-1) + BT*U(N)/(1.+V1)
      DO 3 I=1.NL2
      BT=BT2
      IF(I.LT.M)    BT=BT1
      A(I)=2.*(1.+BT)
      B(I)=-BT
    3 C(I)=-BT
      C(1)=0.
      BT=BT2
      A(N-1)=1.+BT
      C(N-1)=-BT*V2/(1.+V2)
      B(N-1)=-BT/(1.+V2)
C-----CALCULATE THE COEFFICIENTS FOR THE FINITE DIFFERENCE EQUATION
C------AT THE BOUNDARY(NTH) NODE ......
      BJ=CV*DT/(V1*V1*DX*DX)
      BJ1=CV*DT/(V2*V2*DX*DX)
      PJ=P(P0.GAMD.XJ)
      PJ1=P(P0.GAMD.XJ1)
      CJ=V1*DX*DERJ/CV
      CJ1=V2*DX*DERJ1/CV
      A(N)=1.+BJ1*(1.+CJ1)
      C(N)=-BJ1
      B(N)=0.
      D(N)=(1.-BJ-BJ*CJ)*U(N)+BJ*U(N-1) +BJ1*CJ1*PJ1 +BJ*CJ*PJ
      A(M)=1.+1./BT1+W/BT2+W
      B(M)=-W
      C(M)=-1.
      D(M)=U(M-1)+(1./BT1+W/BT2-1.-W)*U(M) + W*U(M+1)
      CALL GAUSEL(A.B.C.D.N)
      DO 8 I=1.N
    8 U(I)=C(I)
      IF(MARK.EQ.0)    GO TO 10
      DIST=V2*DX
      GRAD=(U(N)-U(N1))/DIST
      UX=U(N)
      DO 5 I=N.N2
    5 U(I)=U(N1)+GRAD*(I-N1)*DX
      U(N2+1)=UX
   10 N1=N2
      V1=V2-IREM
      MARK=0
      DT=DX/(NG*DERIV)
      TIME2=TIME/2.
      IF(DT.LT.TIME2)     GO TO 30
      DT=TIME2
   30 IF(TIME.LT.TOUTP)    GO TO 25
      TOUTP=TOUTP+TOUT
      CALL OUTPUT(U.X.N1.V1.GAMD.TIME.QV)
      GO TO 25
      END
      SUBROUTINE GAUSEL(A.B.C.D.N)
C-----***************************************************************
C-----THIS SUBROUTINE SOLVES 'N' LINEAR SIMULTANEOUS TRIOIAGONAL
C-----EQUATIONS. AND STCRES THE FESULT IN THE ARRAY C(I).......
C-----***************************************************************
      REAL A(1).B(1).C(1).D(1)
      IF(N.GT.1)GO TO 8
      C(N)=D(N)/A(N)
      GO TO 6
C----- TO CHANGE TO UPPER TRIANGULAR FORM.
    8 DO 5 I=2.N
      A(I)=A(I)-B(I-1)*C(I)/A(I-1)
      D(I)=D(I)-D(I-1)*C(I)/A(I-1)
    5 C(I)=0.
C----- BACK SUBSTITUTICN..
      C(N+1)=0.
      I=N
    4 C(I)=(D(I)-B(I)*C(I+1))/A(I)
      IF(I.LE.1)GU TO 6
    7 I=I-1
      GO TO 4
    6 RETURN
      END


      SUBROUTINE OUTPUT(U.X.N1.V1.GAMD.TIME.CV)
      REAL U(1).UOUT(500)
      COMMON DX.PO.H
      NL1=N1-1
      Z=X+H
      SUM=0.
      DO 1 I=1.NL1
    1 SUM=SUM+2.*U(I)
      SUM=SUM+U(N1)
      SUM=SUM*0.5*DX
      SUM=SUM+0.5*V1*DX*(U(N1)+U(N1+1))
      SETEND=PO*Z+GAMD*0.5*Z*Z
      SET=SUM/SETEND
      SET=1.-SET
      TIMDAY=TIME
      RTDAY=SQRT(TIMDAY)
      WRITE(6.8)X.TIMDAY.RTDAY
    8 FORMAT('0'.'  THE DEPTH OF THAW IS'.F12.4.'AND T='.F10.4.' DAYS
     1  AND ROOT DAYS='.F10.4)
      TIMFAC=CV*TIME/(X*X)
      WRITE(6.2)TIMFAC.SET.N1.V1
    2 FORMAT('0'.'TIME FACTOR CV.T/X**2 ='.F14.8.'    DEGREE OF SETTLEMEN
     1T ='.F10.5/'N1='.I5.'     AND THE FRACTION IS'.F10.4)
      N=N1+1
      P=PO+GAMD*Z
      DO 4 I=1.N
    4 UOUT(I)=U(I)/P
      WRITE(6.3)(UOUT(I).I=1.N)
    3 FORMAT(' '.10F10.3)
      RETURN
      END
      SUBROUTINE THAW(X,DERIV,TIME,CB,CN)
C-----THIS.SUBROUTINE CALCULATES THE DEPTH OF THAW FROM THE FORMULA
C-----                     X(T) = B.T**N
C-----THE ROUTINE ALSO CALCULATES THE DERIVATIVE DX/DT....
C------***************************************************************
      X=SQRT(CB*CB+CN*TIME)-CB
      DERIV=CN/(2.*SQRT(CB*CB+CN*TIME))
      RETURN
      END


      SUBROUTINE POSIT(X,DX,N,V,NP)
C-----THIS ROUTINE GIVES THE POSITION OF THE FREEZE-THAW INTERFACE
C-----FROM THE RESULTS FROM SUBROUTINE*THAW* AND OUTPUTS A NODE AND
C-----THE FRACTION OF A NODE SPACING WHERE THE INTERFACE IS......
      NP=X/DX
      V=X/DX-NP
      N=NP+1
C-----  *N* IS THE NUMBER OF FINITE DIFFERENCE EQUATIONS FOR THE NEXT
C-----TIME STEP..........
      RETURN
      END


      REAL FUNCTION P(PO,GAMD,X)
C-----THIS FUNCTION CALCULATES THE EFFECTIVE OVERBURDEN STRESS
C-----AT THE FREEZE-THAW INTERFACE....
      COMMON DX,GG,H
      P=PO+GAMD*(X+H)
      RETURN
      END
```

where $i = 2, ---- n + 1$

$j = 2, ---- m + 1$

Boundaries

$$u_{i,m+2,k} = u_{i,m,k}; \qquad i = 2, n + 1$$

$$u_{i,1,k} = 0; \qquad i = 2, n + 1$$

and

$$- \frac{\beta_z}{\alpha^2 t} \left(1 + \frac{\alpha^2 z \, \Delta z}{4 \, c_v}\right) u_{i+1,j,k+1} + \left(1 + \frac{2\beta_z}{\alpha^2 t}\right) u_{i,j,k+1}$$

$$- \frac{\beta_z}{\alpha^2 t} \left(1 - \frac{\alpha^2 z \, \Delta z}{4 \, c_v}\right) u_{i-1,j,k+1}$$

$$= V_{i,j} + \beta_r \left\{ V_{i,j+1} - 2 \, V_{i,j} + V_{i,j-1} + \frac{\Delta r}{2r} (V_{i,j+1} - V_{i,j-1}) \right\} \quad (A.30)$$

$j = 2, ---- m + 1$

$i = 2, ---- n$

Boundaries

$$V_{i,j} = 0; \quad j = 2, m+1$$

where $m = \dfrac{b - a}{\Delta r}$

$n = \dfrac{1}{\Delta z}$

$\beta_r = \dfrac{c_v \Delta t}{(\Delta r)^2}$

and $\beta_z = \dfrac{c_v \Delta t}{(\Delta z)^2}$

The finite difference equations along the thaw line ($i = n+1$) are somewhat complicated, and are derived by combining the finite difference expressions for equations (6.5a) and (6.7). The final expression is

$$\left\{1 - \frac{2\beta_z}{\alpha^2 t} + \frac{\beta_z \, \Delta z}{c_v t}\left(1 + \frac{\alpha^2 \, z \, \Delta z}{4 \, c_v}\right)\right\} u_{n+1,\, j,k+1}$$

$$- \frac{2\beta_z}{\alpha^2 t} u_{n,j,k+1} = V_{i,j} + \beta_r \left\{ V_{i,j+1} - 2V_{i,j} + V_{i,j-1} \right.$$

$$\left. + \frac{\Delta r}{2r} \left(V_{i,j+1} - V_{i,j-1}\right)\right\} + \frac{\beta_z}{\alpha^2 t}\left(1 + \frac{\alpha^2 z \, \Delta z}{4 \, c_v}\right) \frac{\alpha^2 \Delta z}{c_v} \; P \qquad (A.31)$$

$$j = 2, \text{----} \; m + 1$$

where $P = P_o - \sigma'_o + \gamma' X$.

The complete set of finite difference equations has been programmed for solution and a listing of the program follows. The magnitude of the time step Δt is varied automatically to optimise the program processing time. The format statement for data input is self-explanatory, and the input parameters necessary are,in order;

$a, b, m, n, \alpha, c_v, (P_o - \sigma'_o), \gamma', t_f$

where t_f is the time at which the program will terminate execution. A suggested set of units are lbs., feet and years; or tonnes, metres and years.

A.8 Program Listing for Thaw-Consolidation With Sand Drains

Purpose:- To determine the excess pore pressures and degree of consolidation settlement in a thawing soil, when the rate of consolidation is accelerated by the presence of vertical sand-drains.

Description:- The program solves a two-dimensional consolidation problem in co-ordinates r (radius) and x (depth). The Terzaghi-Rendulic equation is solved by an ADI procedure, subject to the boundary condition on a thaw interface which moves according to the law:

$$X = \alpha\sqrt{t}$$

The consolidation equation is transformed in such a way as to place the co-ordinate system in motion, and the thaw plane is made stationary in the transformed co-ordinate system $z = x/X(t)$. Thus, there are a fixed number of finite difference nodes in the z direction spaced equally at Δz. The degree of consolidation is calculated by vertical integration of the excess pore pressures.

Usage:- The program requires nine parameters in FORTRAN format (2F8.0, 2I8, 5F8.0), in the following order

$a, b, m, n, \alpha, c_v, P_o, \gamma'$ and t_f

where a is the radius of the sand drain,

b is the effective radius of the sand drain (= 0.525 times the spacing),

m is the number of finite difference subdivisions in the r-direction,

n is the number of discrete intervals in the z direction,

α is the constant of proportionality between thaw depth and time$^{1/2}$,

c_v is the consolidation coefficient,

P_o is the surface applied loading,

γ' is the submerged unit weight of the soil,

and t_f is the termination time for the program.

Units:- A suggested set of units is lbs, feet and years.

Example of data input:-

$a = 0.5$ ft.

$b = 5.25$ ft.

$m = 10$

$n = 10$

$\alpha = 10$ ft/year$^{1/2}$

$c_v = 50$ ft^2/year

$P_o = 500$ lb/ft^2

$\gamma' = 50$ lb/ft^3

$t_f = 16$ years

```
      REAL A(50).B(50).C(50).D(50).U(50.50).V(50.50)
      COMMON M1.N1
    1 READ(5,2)AD.BD.M.N.ALF.CV.PO.GAMD.TF
    2 FORMAT(2F8.0.2I8.5F8.0)
      WRITE(6.3)AD.BD.M.N.ALF.CV.PO.GAMD.TF
    3 FORMAT('1','A=',F10.3,10X,'B=',F10.3,10X,'M=',I3,10X,'N=',I3/
     1'ALPHA=',F10.3,10X,'CV=',F10.3/'PO=',F10.3,10X,'GAMMA SUB.=',F10.3
     2/'THE FINAL TIME IS',F10.3)
      OUT=0.25
      XOUT=OUT
      NG=50
      X=BD/20.
      DX=X/N
      TIME=X*X/(ALF*ALF)
      DZ=1./N
      DR=(BD-AC)/M
      N1=N+1
      M1=M+1
      M2=M+2
C-----CALCULATE THE INITIAL PORE PRESSURES.....
      RR=ALF/(2.*SQRT(CV))
      SP=SQRT(3.141593)
      AA=PO/(ERF(RR)+EXP(-RR*RR)/(SP*RR))
      BB=GAMD/(1.+1./(2.*RR*RR))
      DO 4 I=2.N1
      XX=(I-1.)*X/N
      UX=AA*ERF(XX/(2.*SQRT(CV*TIME))) + BB*XX
      DO 4 J=1.M2
    4 U(I.J)=UX*(J-1.)/M
      CALL OUTPUT(U.DX.X.TIME.PO.GAMD)
      DT=0.5/(CV*(1./(DX*DX)+1./(DR*DR)))
C-----FORM THE BOUNDARY CONDITIONS.....
      DO 6 I=1.N1
      U(I.1)=0.
    6 V(I.1)=0.
      DO 7 J=1.M2
      U(1.J)=0.
    7 V(1.J)=0.
    5 BTZ=CV*DT/(DZ*DZ)
      BTR=CV*DT/(DR*DR)
C-----FORM THE L.H. BOUNDARY CONDITION....
      DO 8 I=1.N1
    8 U(I.M2)=U(I.M)
C
      DO 21 J=1.M1
   21 U(N+2.J)=ALF*ALF*DZ*(PO+GAMD*X-U(N1.J))/CV+U(N.J)
      DO 10 I=2.N1
      Z=(I-1.)*DZ
      DO 15 J=2.M1
      R=(J-1.)*DR+AC
      A(J-1)=1.+2.*BTR
      B(J-1)=-(1.+DR/(2.*R))*BTR
      C(J-1)=-(1.-DR/(2.*R))*BTR
   15 D(J-1)=U(I.J)+ (BTZ/(ALF*ALF*TIME))*(U(I+1.J)-2.*U(I.J)+U(I-1.J)
     1+0.25*ALF*ALF*Z*DZ*(U(I+1.J)-U(I-1.J))/CV)
```

```
      C(M)=-2.*BTR
      B(M)=0.
      D(1)=C(1)-C(1)*U(I,1)
      C(1)=0.
      CALL GAUSEL(A,B,C,D,M)
      DO 11 J=2,M1
   11 V(I,J)=C(J-1)
   10 CONTINUE
C-----
C-----INCREMENT THE TIME BY TWO HALF TIME STEPS.....
      TIME=TIME+2.*DT
      X=ALF*SQRT(TIME)
      CON=BTZ/(ALF*ALF*TIME)
C-----
C-----ALTERNATE THE INTEGRATION TO THE Z-DIRECTION.....
      DO 12 I=2,N1
   12 V(I,M2)=V(I,M)
      DO 13 J=2,M1
      R=(J-1.)*DR+AC
      DO 14 I=2,N1
      Z=(I-1.)*DZ
      A(I-1)=1.+2.*CON
      B(I-1)=-CON*(1.+0.25*ALF*ALF*Z*DZ/CV)
      C(I-1)=-CON*(1.-0.25*ALF*ALF*Z*DZ/CV)
   14 D(I-1)=V(I,J)+BTR*(V(I,J+1)-2.*V(I,J)+V(I,J-1)+ DR*(V(I,J+1)
     1-V(I,J-1))/(2.*R))
      A(N)=1.+2.*CON+BTZ*DZ* (1.+0.25*ALF*ALF*Z*DZ/CV)/(CV*TIME)
      B(N)=0.
      C(N)=-2.*CON
      D(N)=D(N)+CON*(1.+0.25*ALF*ALF*Z*DZ/CV)*ALF*ALF*DZ*(P0+GAMD*X)/CV
      C(1)=0.
      CALL GAUSEL(A,B,C,D,N)
      DO 16 I=2,N1
   16 U(I,J)=C(I-1)
   13 CONTINUE
      DX=X/N
      IF(X.LT.XOUT)   GO TO 19
      XOUT=XOUT+OUT
      CALL OUTPUT(U,DX,X,TIME,P0,GAMD)
   19 DT=5.0/(CV*(1./(DX*DX)+1./(DR*DR)))
      IF(TIME.LT.TF)   GO TO 5
      GO TO 1
      END
      SUBROUTINE OUTPUT(U.DX.X.TIME.P0.GAMD)
C-----THIS SUBROUTINE OUTPUTS THE NORMALISED EXCESS PORE PRESSURES
C-----THROUGHOUT THE SOIL MASS. AND COMPUTES THE DEGREE OF SETTLEMENT
C-----PROFILE ACROSS A DIAMETER BY VERTICAL LINE INTEGRATION....
C-----******************************************************************
      REAL U(50.1).W(50.50).SET(50)
      COMMON M1.N1
      WRITE(6.8)X.TIME.DX
    8 FORMAT('0'.'THE DEPTH OF THAW IS'.F10.3.'  AND THE TIME IS'.F10.4.
     1'     DX=',F10.5)
      DO 1 I=1.N1
      P=P0+GAMD*X
      IF(I.EQ.1)    P=1.
      DO 1 J=1.M1
    1 W(I.J)=U(I.J)/P
      WRITE(6.2)
    2 FORMAT('0'.'THE NORMALISED EXCESS PORE PRESSURES ARE:-')
      DO 3 I=1.N1
    3 WRITE(6.4)(W(I.J).J=1.M1)
    4 FORMAT(' '.12F10.3)
      DO 5 J=1.M1
      SUM=(W(1.J)+W(N1.J))/2.
      N=N1-1
      DO 6 I=2.N
    6 SUM=SUM+W(I.J)
    5 SET(J)=1.-SUM/N
      WRITE(6.7)(SET(J).J=1.M1)
    7 FORMAT(' './/'THE SETTLEMENT PROFILE IS'./12F10.3)
      RETURN
      END


      SUBROUTINE GAUSEL(A.B.C.D.N)
C-----******************************************************************
C-----THIS SUBROUTINE SOLVES 'N' LINEAR SIMULTANEOUS TRIDIAGONAL
C-----EQUATIONS. AND STORES THE RESULT IN THE ARRAY C(I).......
C-----******************************************************************
      REAL A(1).B(1).C(1).D(1)
      IF(N.GT.1)GO TO 8
      C(N)=D(N)/A(N)
      GO TO 6
C----- TO CHANGE TO UPPER TRIANGULAR FORM.
    8 DO 5 I=2.N
      A(I)=A(I)-B(I-1)*C(I)/A(I-1)
      D(I)=D(I)-D(I-1)*C(I)/A(I-1)
    5 C(I)=0.
C----- BACK SUBSTITUTION..
      C(N+1)=0.
      I=N
    4 C(I)=(D(I)-B(I)*C(I+1))/A(I)
      IF(I.LE.1)GO TO 6
    7 I=I-1
      GO TO 4
    6 RETURN
      END
```

APPENDIX B

LABORATORY RESULTS FOR THAW CONSOLIDATION TESTS

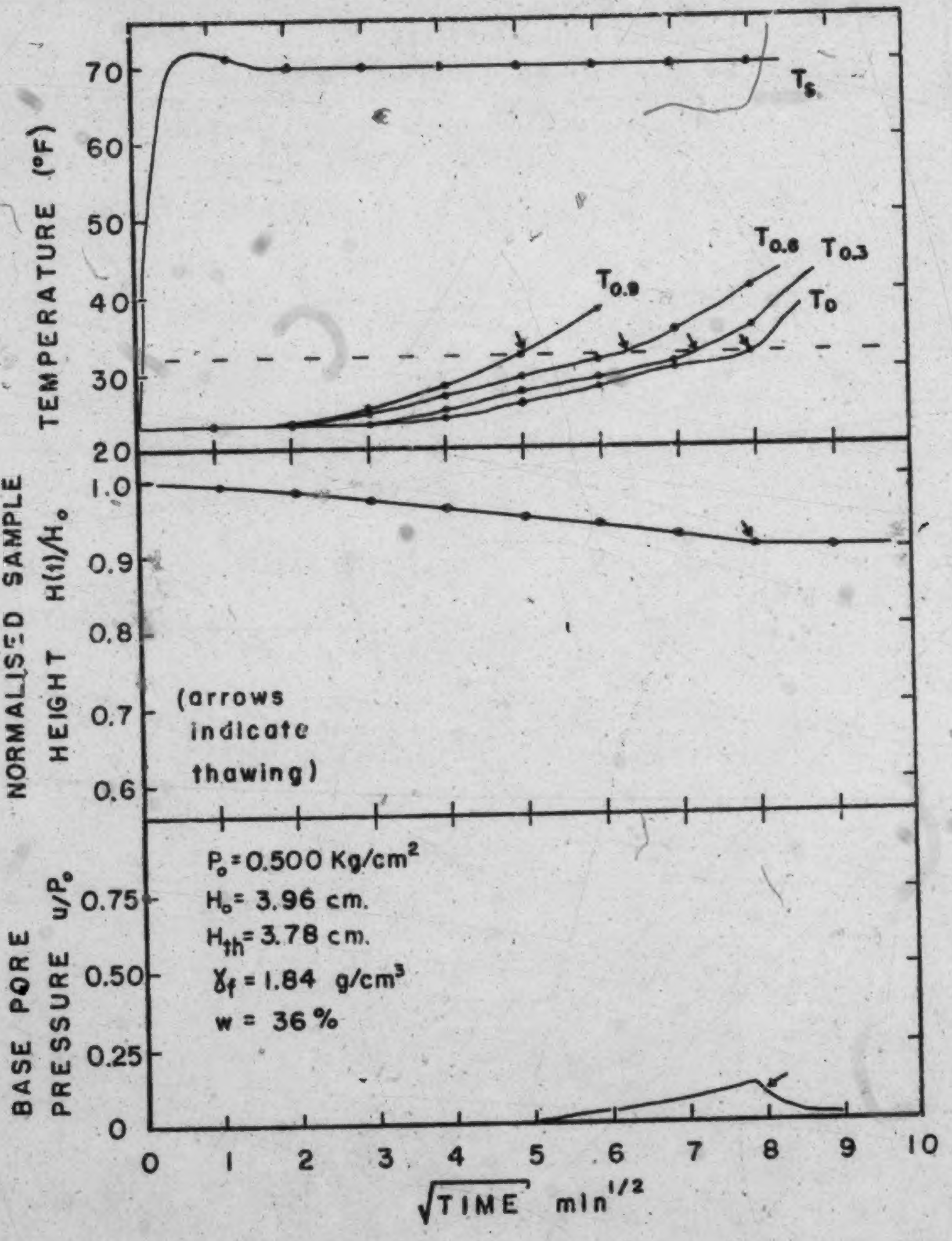

Fig. B.1 Test NWU-2

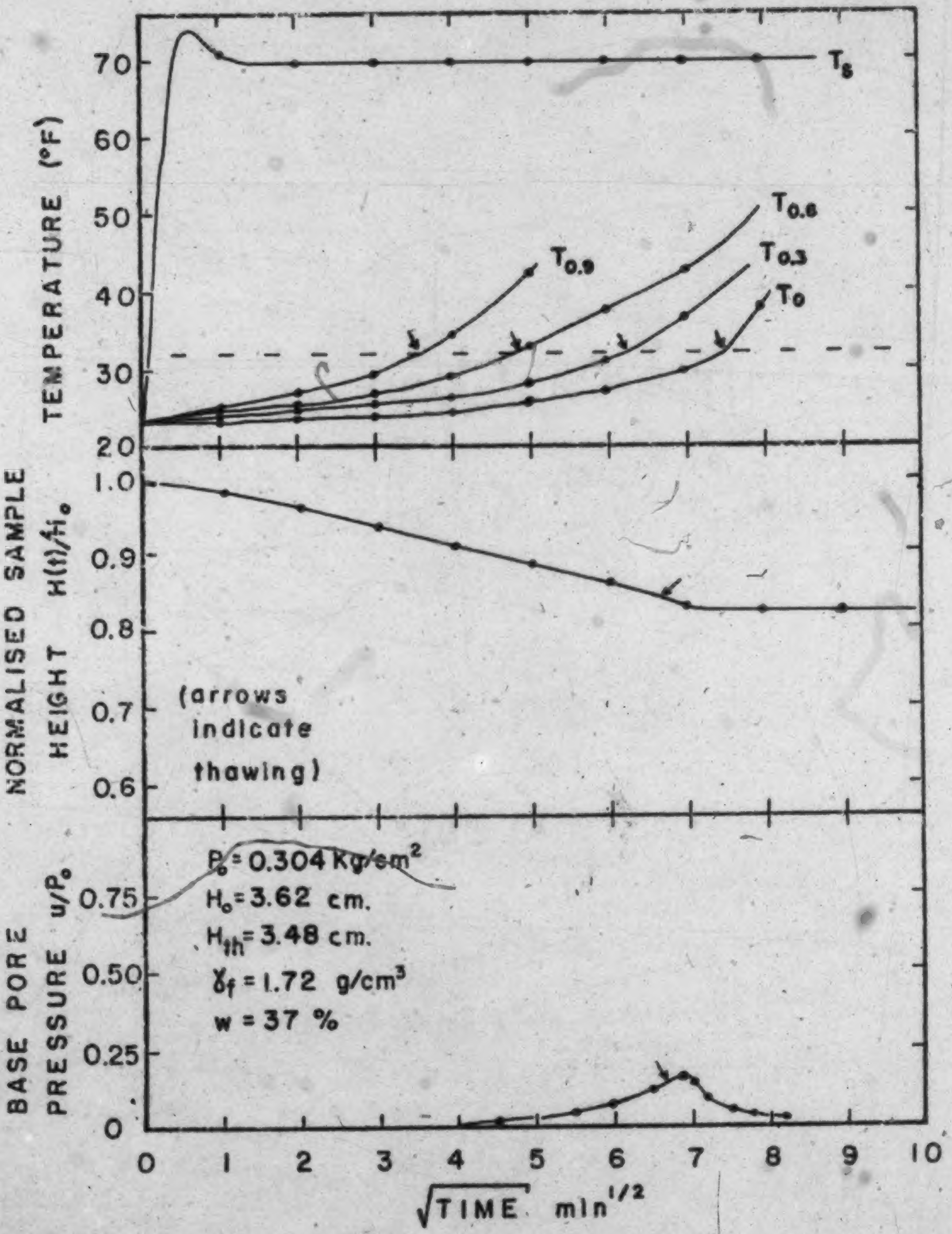

Fig. B.2 Test NWU-4

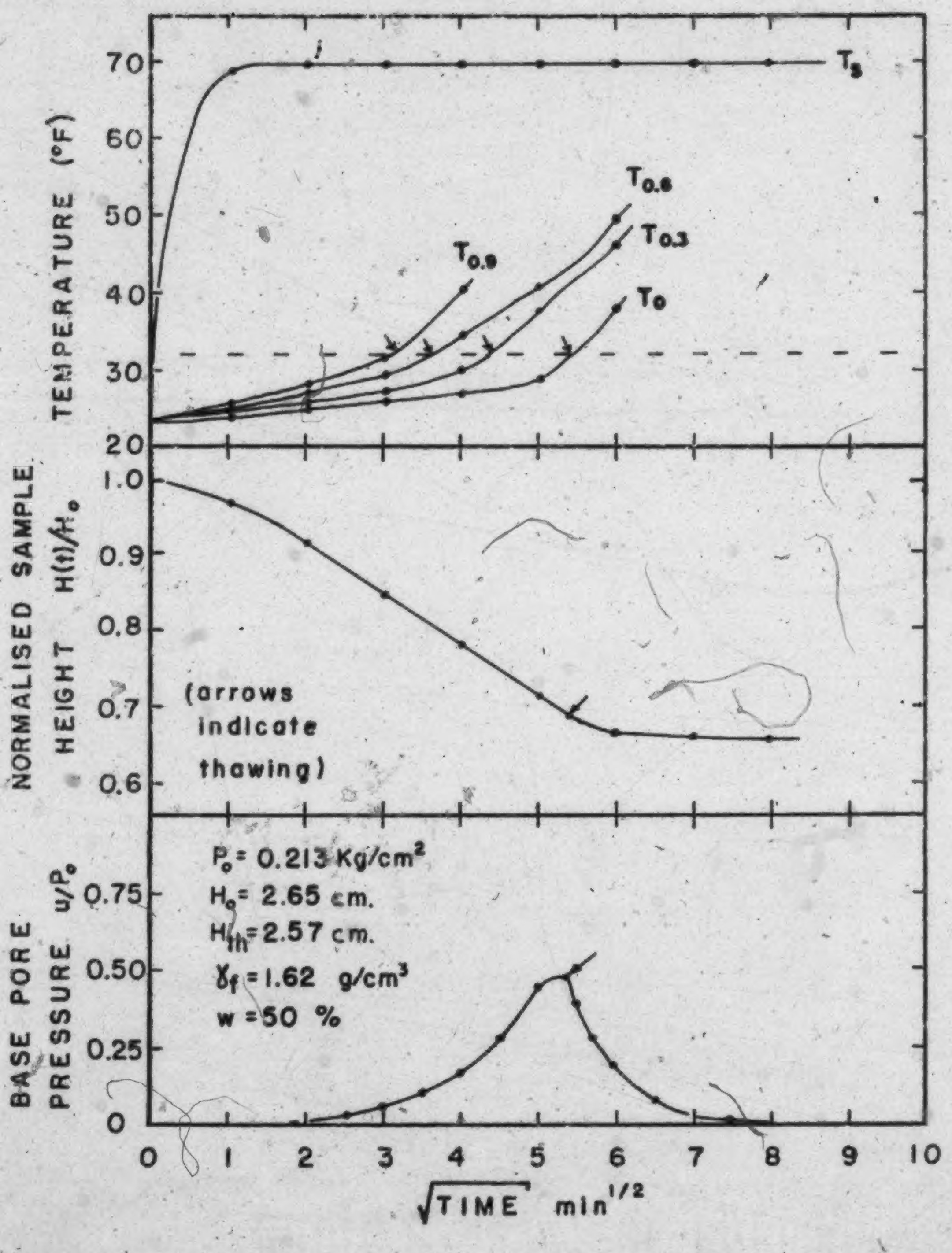

Fig. B.3 . Test NWU-9

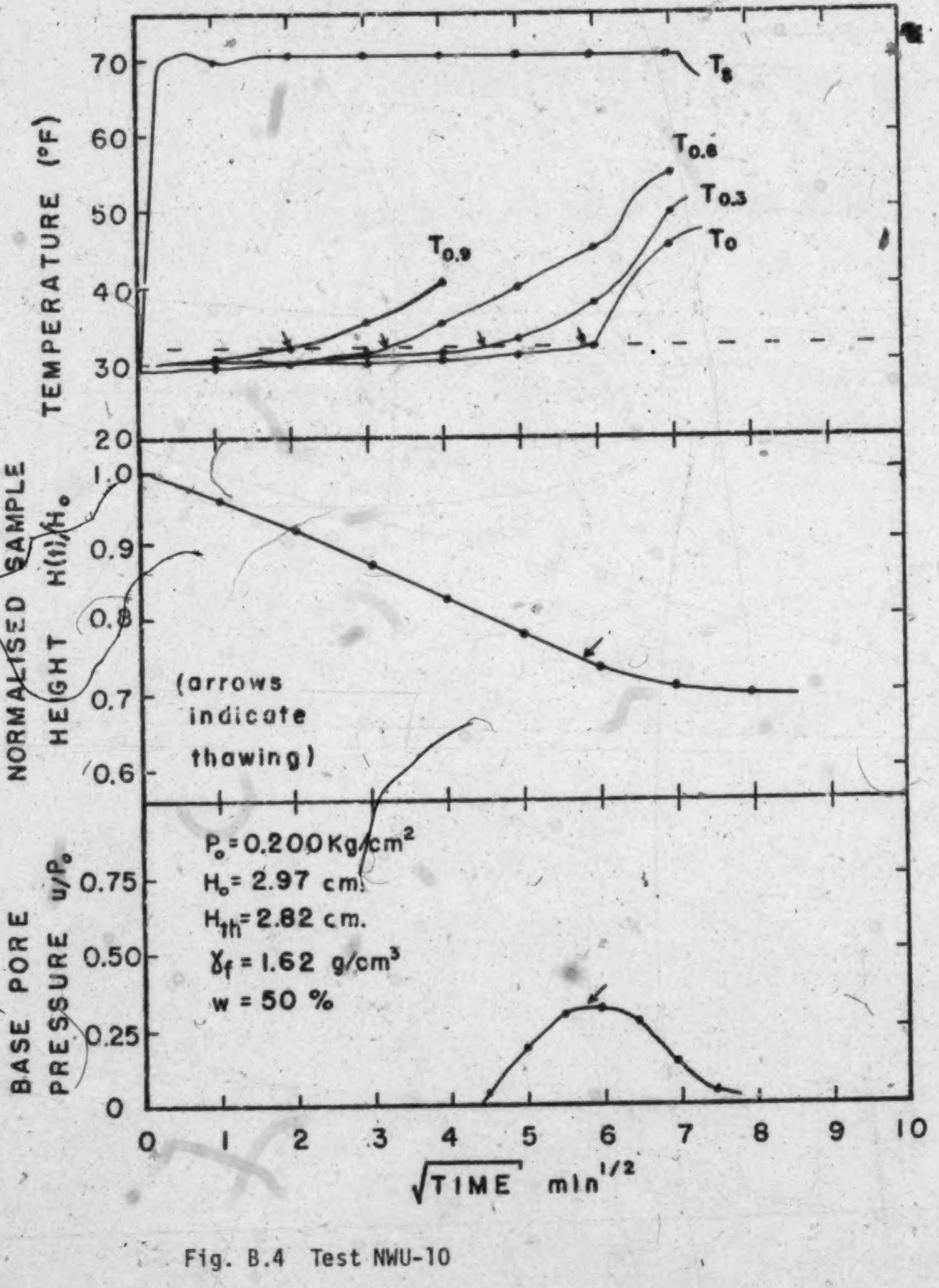

Fig. B.4 Test NWU-10

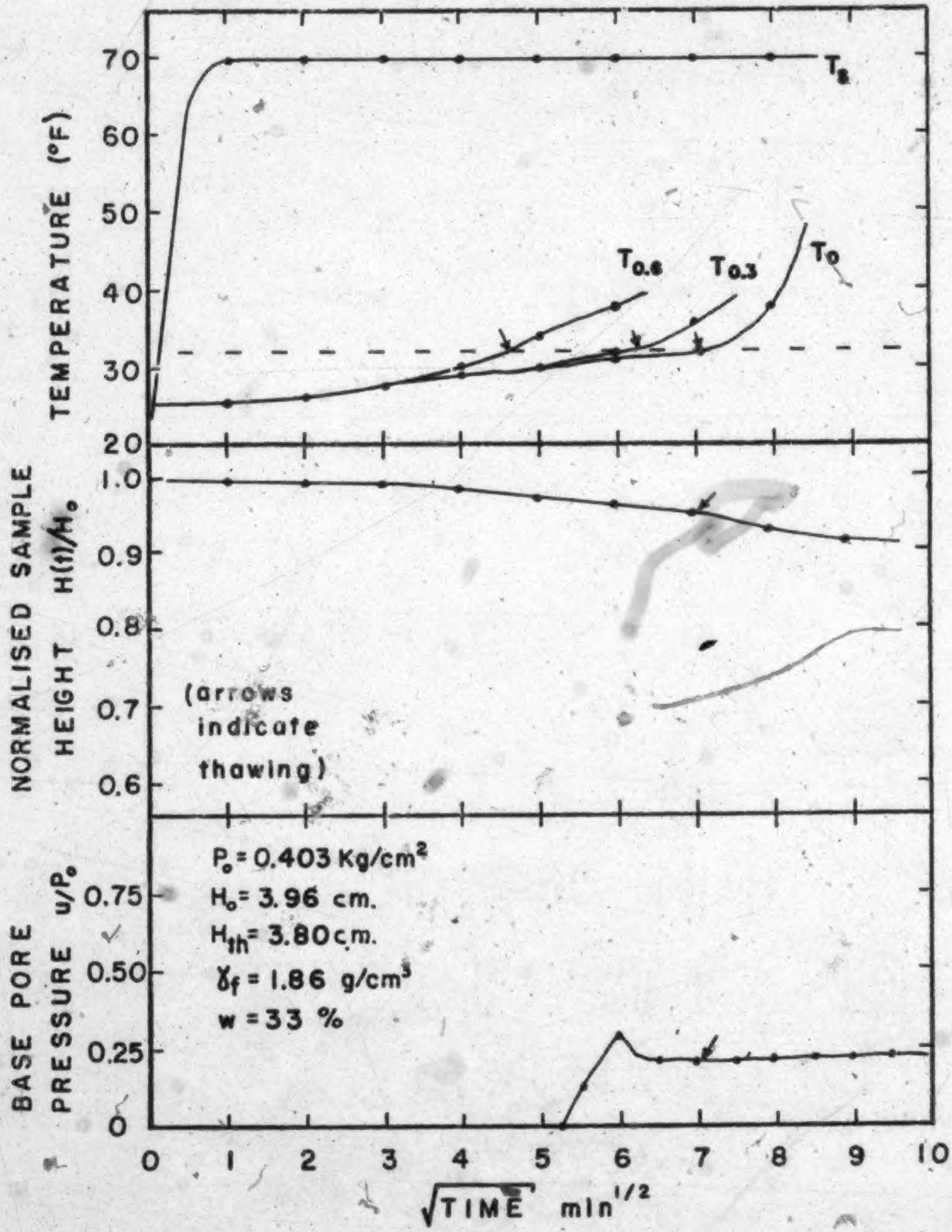

Fig. B.5 Test I-2

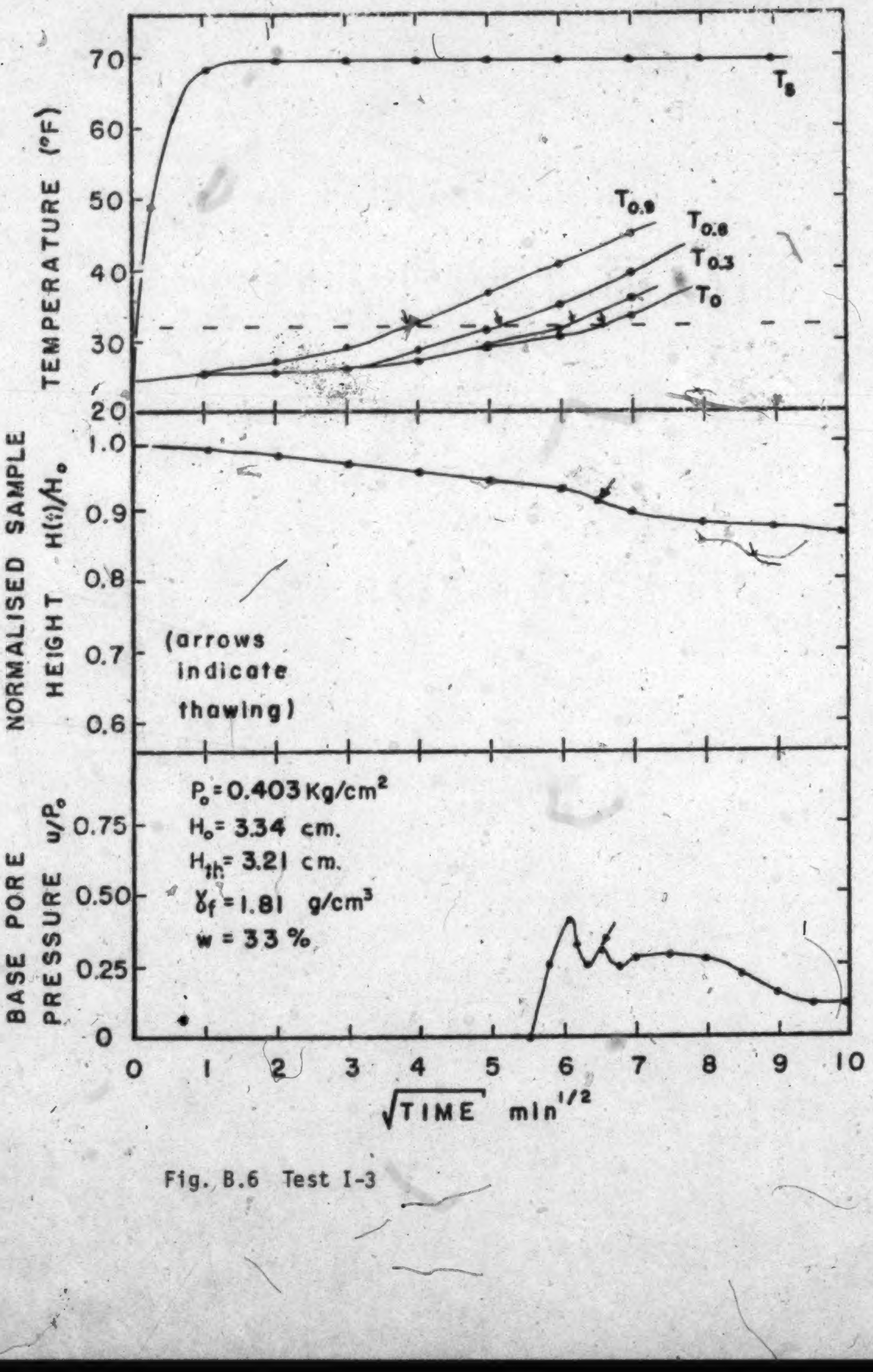

Fig. B.6 Test I-3

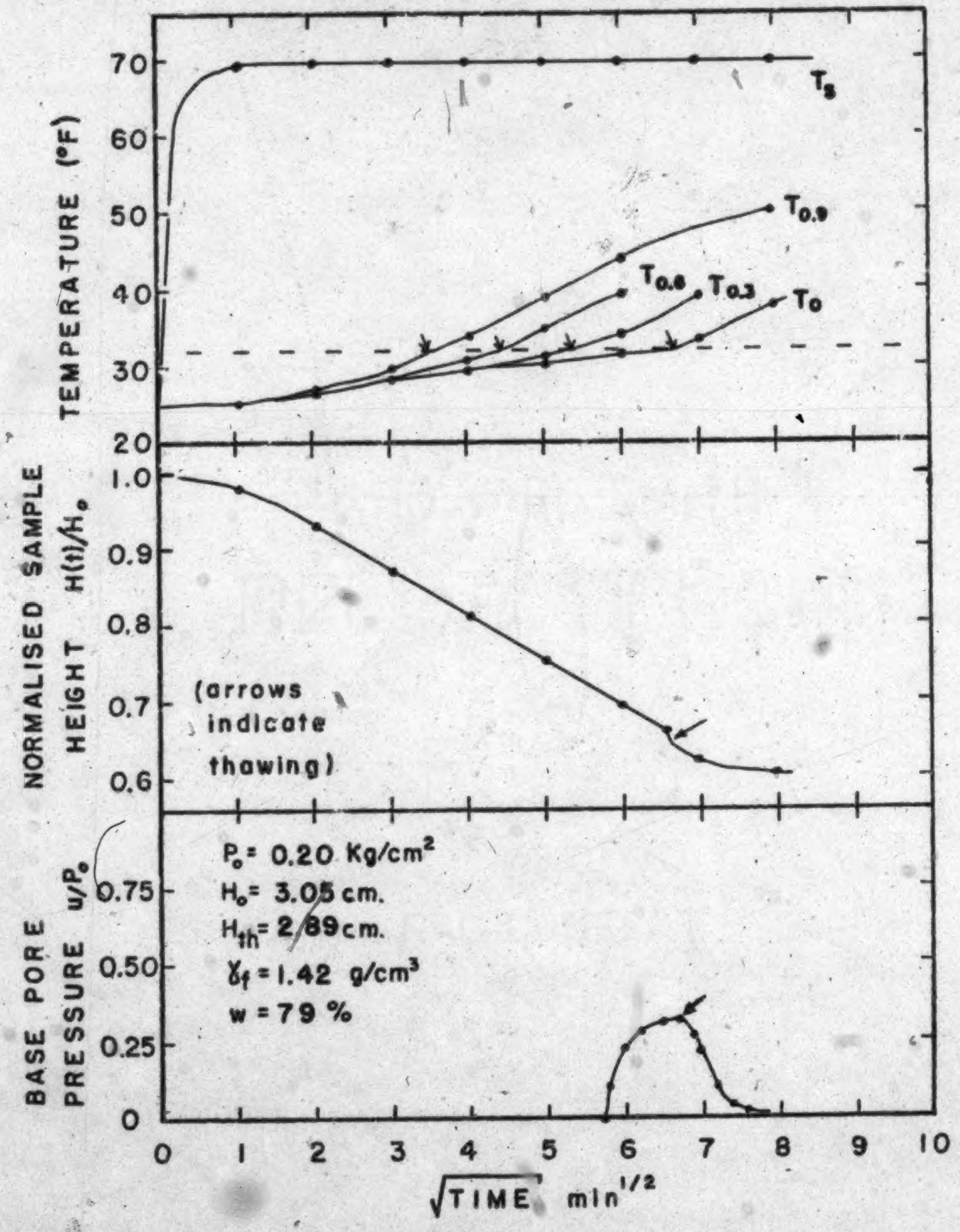

Fig. B.7 Test I-4

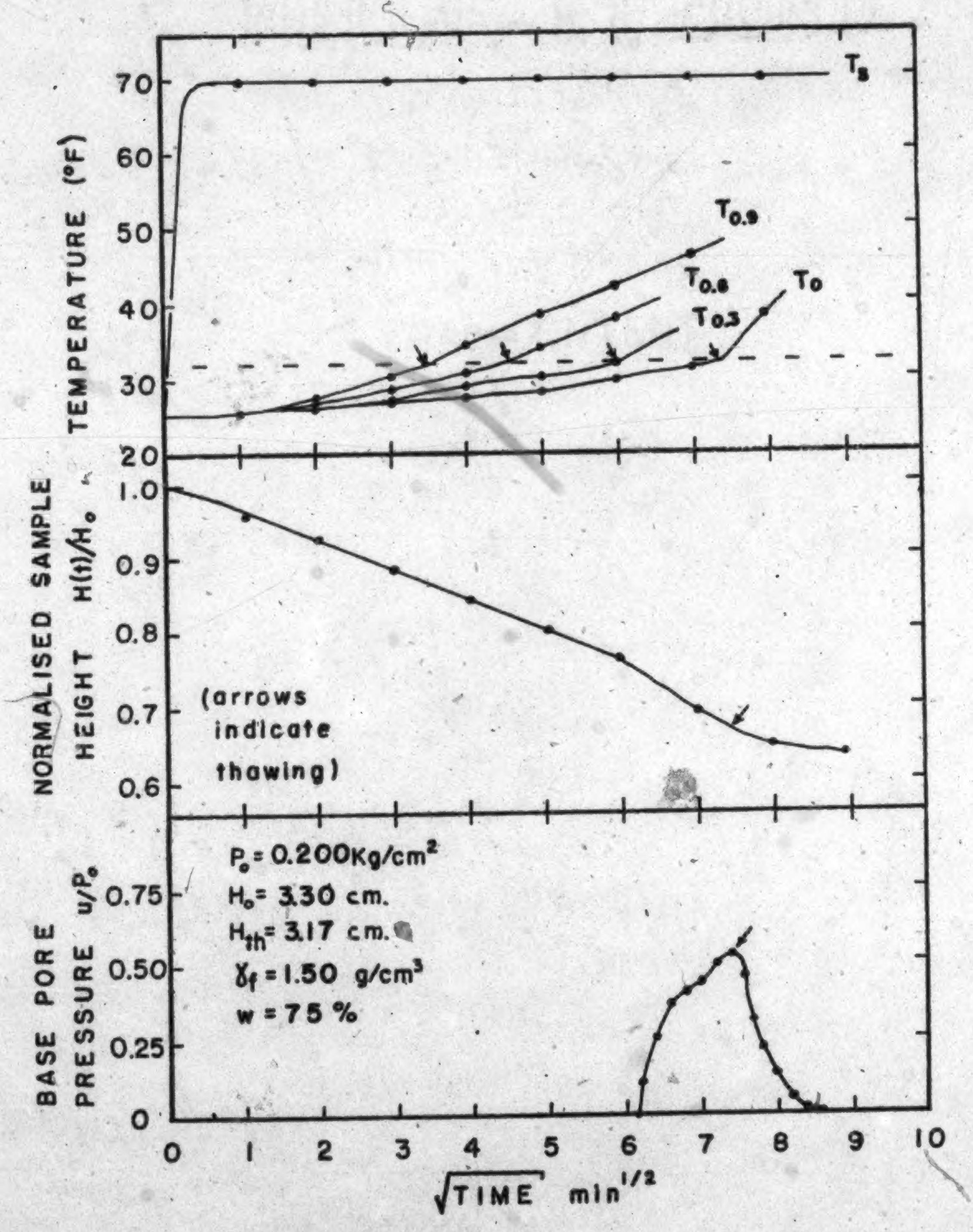

Fig. B.8 Test I-5

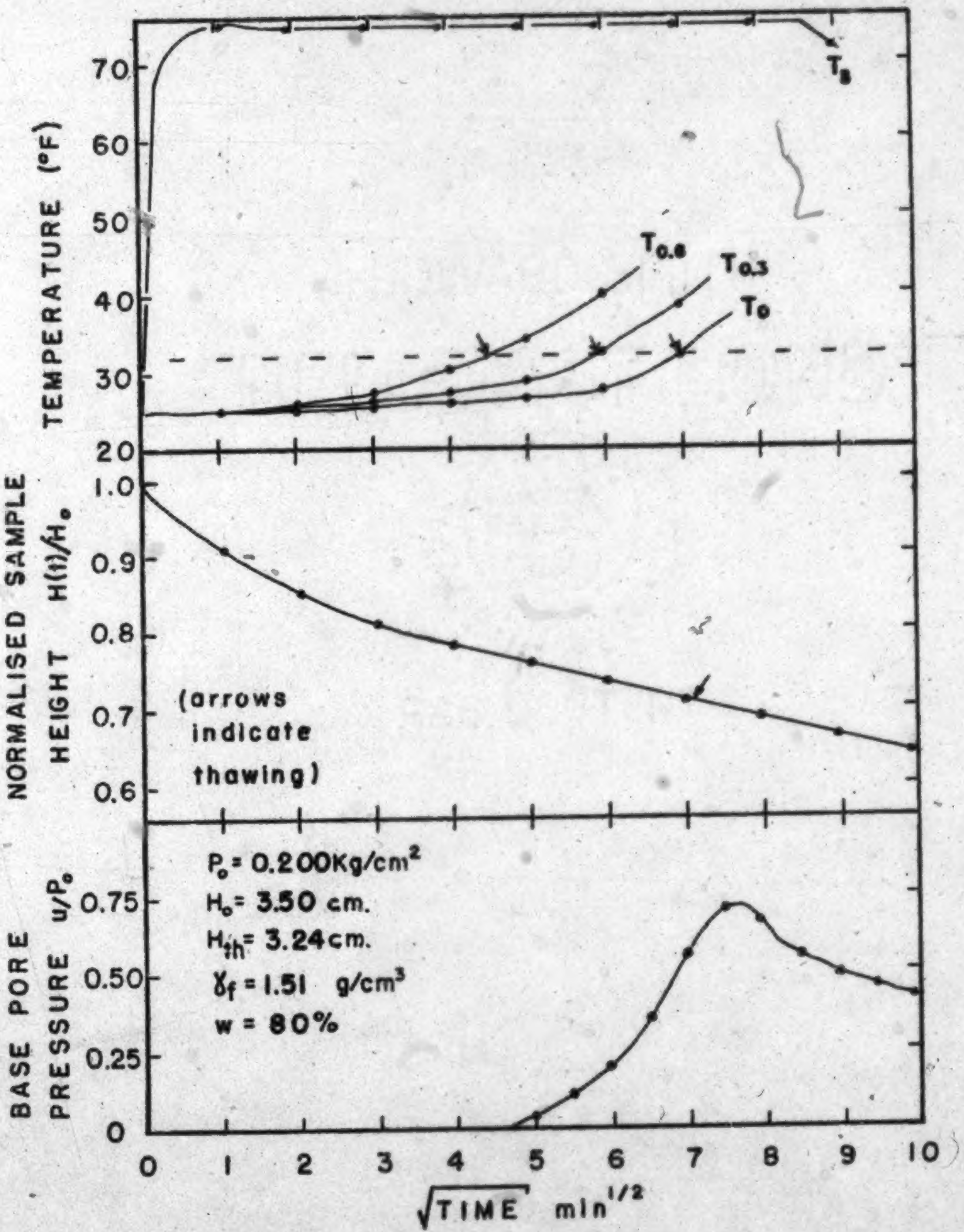

Fig. B.9 Test MR-1

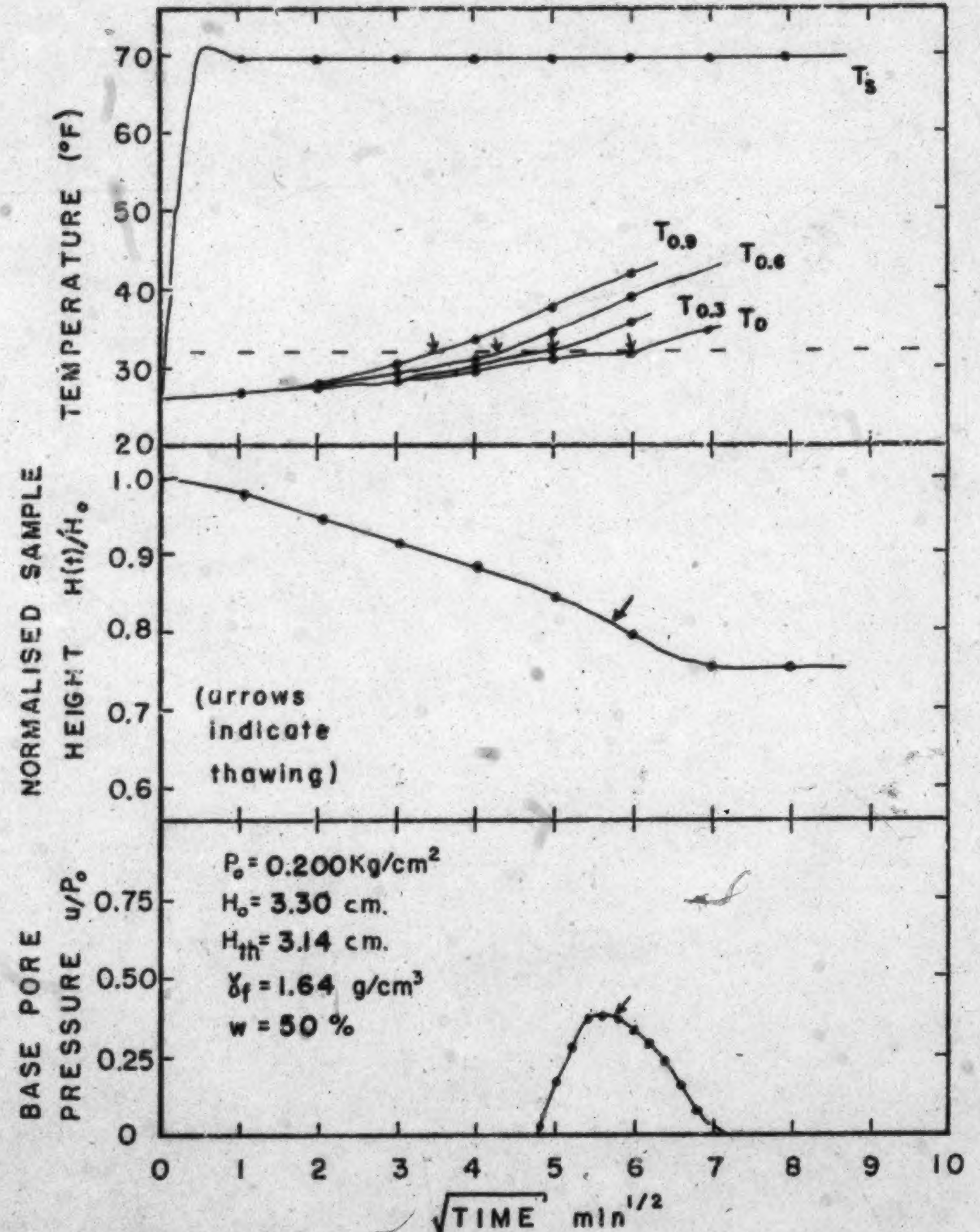

Fig. B.10 Test DS-1